



**HAL**  
open science

# Trace metals in estuarine and coastal waters: dynamics, speciation and bioavailability under various environmental conditions

Camille Gaulier

## ► To cite this version:

Camille Gaulier. Trace metals in estuarine and coastal waters: dynamics, speciation and bioavailability under various environmental conditions. Géotechnique. Université de Lille; Vrije universiteit Brussel (1970-..), 2020. English. NNT: 2020LILUR013 . tel-03772172

**HAL Id: tel-03772172**

**<https://theses.hal.science/tel-03772172v1>**

Submitted on 8 Sep 2022

**HAL** is a multi-disciplinary open access archive for the deposit and dissemination of scientific research documents, whether they are published or not. The documents may come from teaching and research institutions in France or abroad, or from public or private research centers.

L'archive ouverte pluridisciplinaire **HAL**, est destinée au dépôt et à la diffusion de documents scientifiques de niveau recherche, publiés ou non, émanant des établissements d'enseignement et de recherche français ou étrangers, des laboratoires publics ou privés.



# **Trace metals in estuarine and coastal waters: Dynamics, speciation and bioavailability under various environmental conditions**

**Camille Gaulier**

**Academic year: 2019-2020**

**Promotors: Prof. dr. Yue Gao & Prof. dr. Gabriel Billon**

A dissertation submitted to the Vrije Universiteit Brussel and the University of Lille, in partial fulfilment of the requirements for the double degree of Doctor of Science and Doctor in “Optique et Lasers – Physico-chimie – Atmosphère”.

# Examination Committee

<b>Promotors:</b>	Prof. dr. Yue Gao	AMGC, Vrije Universiteit Brussel
	Prof. dr. Gabriel Billon	LASIRE, University of Lille
<b>Other members:</b>	Prof. dr. ir. Marc Elskens <i>Chairman</i>	AMGC, Vrije Universiteit Brussel
	Dr. Pierre-Jean Superville <i>Secretary</i>	LASIRE, University of Lille
	Prof. dr. em. Willy Baeyens <i>Co-promotor</i>	AMGC, Vrije Universiteit Brussel
	Dr. Véronique Lenoble <i>External member</i>	MIO, University of Toulon
	Dr. Joël Knoery <i>External member</i>	LBCM, French Research Institute for the Exploitation of the Sea
	Dr. Patrick Roose <i>External member</i>	OD Nature, Royal Belgian Institute of Natural Sciences

Joint-PhD between the Vrije Universiteit Brussel and the University of Lille. The research presented in this thesis was funded by the Belgian Science Policy Office (BELSPO) through the NewSTHEPS project (BR/143/A2/NEWSTHEPS; FOD-12).

On the front cover, icons from Noun Project created by: M (crab, jellyfish, dead fish), Nook Fulloption (fish, shell), Agne Alesiute (coral - left), Yu Luck (coral – right, grey), Vectors Market (corals – right, blue), Pixels Studio (corals – bottom).

All rights reserved. No parts of this book may be reproduced or transmitted in any form or by any means, electronic, mechanical, photocopying, recording or otherwise, without the prior written permission of the author.

**UNIVERSITÉ DE LILLE**

Ecole Doctorale Sciences de la Matière, du Rayonnement et de l'Environnement  
LASIRE CNRS UMR 8516

**VRIJE UNIVERSITEIT BRUSSEL**

Doctoral School Natural Sciences and (Bioscience) Engineering  
AMGC Department

**THÈSE DE DOCTORAT EN COTUTELLE**

En vue de l'obtention du grade de

**DOCTEUR EN OPTIQUE ET LASERS, PHYSICO-CHIMIE ET  
ATMOSPHÈRE DE L'UNIVERSITÉ DE LILLE**

Et de

**DOCTOR OF SCIENCE DE LA VRIJE UNIVERSITEIT BRUSSEL**

**Les métaux traces en eaux côtières : étude de leur dynamique,  
spéciation et biodisponibilité dans des milieux variés**

*Trace metals in estuarine and coastal waters: dynamics, speciation  
and bioavailability under various environmental conditions*

Présentée par

**CAMILLE GAULIER**

Et soutenue le **16 Juillet 2020** à la Vrije Universiteit Brussel devant la commission  
d'examen composée de :

Prof. dr. Yue Gao	AMGC, Vrije Universiteit Brussel	Directrice de Thèse
Prof. dr. Gabriel Billon	LASIRE, Université de Lille	Directeur de Thèse
Prof. dr. ir. Marc Elskens	AMGC, Vrije Universiteit Brussel	Président du Jury
Dr. Pierre-Jean Superville	LASIRE, Université de Lille	Co-encadrant
Prof. dr. em. Willy Baeyens	AMGC, Vrije Universiteit Brussel	Co-encadrant
Dr. Véronique Lenoble	MIO, Université de Toulon	Examinatrice
Dr. Joël Knoery	LBCM, Institut français de recherche pour l'exploitation de la mer	Rapporteur
Dr. Patrick Roose	OD Nature, Institut Royal des Sciences Naturelles de Belgique	Rapporteur



# Table of contents

Acknowledgements.....	v
Summary.....	vi
Samenvatting.....	viii
Résumé.....	x
Notation index.....	xii

<b>Chapter 1</b>	General introduction Trace metals in estuarine and coastal environments	2
<b>Chapter 2</b>	Investigation on trace metal speciation and distribution in the Scheldt Estuary	50
<b>Chapter 3</b>	Trace metal speciation in North Sea coastal waters	92
<b>Chapter 4</b>	Dynamic transport of suspended particulate matter in the North Sea coastal zone	138
<b>Chapter 5</b>	Trace metal vertical distribution and speciation in Baltic Sea waters	180
<b>Chapter 6</b>	General conclusions and perspectives	222
<b>Annexes</b> .....		<b>230</b>
	Leaching of two Northern France slag heaps: influence on the surrounding aquatic environment.....	<b>232</b>
<b>References</b> .....		<b>266</b>
<b>Curriculum Vitae</b> .....		<b>308</b>



# Acknowledgements

**To each one of you, thank you.**

To be completely honest, if I really had to thank one by one all the people who helped me, gave their support from near or far, or who even simply supported me in the cool and less cool meanders of my life as a PhD student, it would take me as many pages and time as it took me to complete this thesis work. It is therefore to spare you another hundred pages to read (and for me, another hundred pages to write) that I would allow myself to be brief but truly sincere: thank you all from the bottom of my heart.

# Summary

Estuarine and coastal ecosystems provide multiple ecological, social and economic services. They are a source of food, income and are at the heart of marine trade, merchant shipping and sea transport. They therefore play a key role in our modern world and their conservation from an environmental point of view is today critical. Despite all the efforts done in environmental management, pollution associated with the rapid coastal development and intensive industrialization was certain and still remains one of the main threats towards marine ecosystems today. Specifically, trace metal contamination is of high concern as coastal areas are generally prone to accumulate them. Most trace metals exhibit a dual role in marine waters: they act as nutrients in low concentrations, yet rapidly have toxic effects in higher concentration ranges. Continuous monitoring of their concentrations in estuarine and coastal ecosystems is therefore needed to better understand their biogeochemical behavior in such marine environments. However, limited knowledge exists on their bioavailability towards marine organisms: especially as the toxicity of these metals is not only related to their concentration but also strongly linked with their speciation which shows both seasonal and spatial variations. Thus, the main objective of this PhD research was to investigate the biogeochemical cycles of various trace metals and unravel their speciation and bioavailability in various aquatic systems: from very dynamic mixing zones of the Scheldt estuary to coastal harbors and shallow seawaters of the North Sea, and even to deeper and anoxic regions of the Baltic Sea. Trace metal concentrations and speciation were explored seasonally and spatially along horizontal and vertical gradients, and a comparison of classic active samplings of dissolved trace metals with a passive sampling technique (Diffusive Gradients in Thin-films; DGT) was carried out. The DGT technique was successfully used for the *in-situ* measurement of labile metals and eventually constitutes a good surrogate

to the biomonitoring of trace elements (e.g. use of mussels, algae, etc.). This method offsets the lack of knowledge in terms of water quality monitoring and the results challenge the classic criteria which are used by international regulatory requirements (e.g. WFD, MSFD) and local commitments (e.g. OSPAR, HELCOM). Indeed, new criteria based on labile metal species instead of total dissolved species should be considered in the future. Such approach of trace metal speciation and assessment in aquatic systems could surely lead to a more integrated environmental management and improve our knowledge on anthropogenic impacts and pollutant fluxes. Moreover, it is eventually the main key to explain and predict bioavailability and potential toxicity of trace metals to the marine fauna and flora. This work therefore invites you to dive into a journey along our coasts, from urbanized areas to wild open seas, from their surface to their deepest waters.

# Samenvatting

Estuariene en kustecosystemen verlenen diverse ecologische, sociale en economische diensten. Zij zijn een bron van voedsel, inkomsten en zijn het hart van zeehandel, koopvaardij en zeeverkeer. Daarom spelen ze een sleutelrol in onze moderne wereld maar hun behoud vanuit milieuoogpunt is vandaag kritisch. Niettegenstaande alle inspanningen die gedaan werden op het vlak van milieumanagement, merken we dat de vervuiling geassocieerd met de snelle kustontwikkeling en intensieve industrialisatie onvermijdelijk bleek zodat het tot op vandaag één van de voornaamste bedreigingen van mariene ecosystemen blijft. Specifiek, verontreiniging veroorzaakt door sporemetalen is een grote bezorgdheid aangezien deze metalen zich in het algemeen ophopen in kustzones. De meeste sporemetalen spelen een dubbele rol in het marien milieu: zij gedragen zich als nutriënten bij lage concentratie maar worden toxisch bij hogere waarden. Continue monitoring van hun concentraties in estuariene en kustecosystemen is daarom noodzakelijk om hun biogeochemisch gedrag in zulke mariene milieus beter te begrijpen. Over hun biobeschikbaarheid voor mariene organismen is er echter slechts weinig geweten, in het bijzonder omdat de toxiciteit van deze sporeelementen niet met hun concentratie is gerelateerd maar integendeel met hun speciatie (de verschillende vormen waarin ze voorkomen) die bovendien variaties vertoont in tijd en ruimte. Daarom is de belangrijkste doelstelling van dit doctoraatsonderzoek, het bestuderen van de biogeochemische cycli van diverse sporemetalen en hun biobeschikbaarheid in diverse aquatische systemen: van zeer dynamische mengzones van het Schelde-estuarium tot kusthavens en ondiep zeewater van de Noordzee, en zelfs tot diepere en anoxische zones van de Baltische zee. Sporemetaalgradiënten werden tijds- en ruimteafhankelijk onderzocht en een vergelijking van de klassieke

staalnameprocedure voor opgeloste sporemetalen met de passieve staalnametechniek van DGT (Diffusieve Gradients in Dunne Films), werd uitgevoerd. De DGT techniek werd succesvol gebruikt voor *in-situ* metingen van labiele metalen en vormt als dusdanig een goed surrogaat voor de biomonitoring van sporemetalen (bijv. gebruik van mosselen, algen, etc.). Deze methode compenseert het gebrek aan kennis op het gebied van waterkwaliteitsbewaking en de resultaten dagen de klassieke criteria uit die worden gebruikt door de voorschriften (bijv. WFD, MSFD) en verplichtingen (bijv. OSPAR, HELCOM) van de internationale regelgeving te voldoen. In de toekomst zouden inderdaad nieuwe criteria op basis van labiele metaalsoorten in plaats van totaal opgeloste soorten moeten worden overwogen. Onze aanpak inzake speciatie en bepalingen van sporemetalen in aquatische systemen kan zeker leiden tot een meer geïntegreerd milieubeheer en een betere kennis van de pollutant fluxen. Bovendien is het de meest geschikte weg om de biobeschikbaarheid en de potentiële toxiciteit van sporemetalen voor mariene flora en fauna te kunnen verklaren. Dit werk is een uitstap langs onze kusten, van ge-urbanizeerde zones tot open zee, van hun oppervlakte tot de diepste water.

# Résumé

Les écosystèmes estuariens et côtiers assurent de multiples services écologiques, sociaux et économiques. Ils constituent une source de nourriture, de revenus et sont au cœur du commerce et du transport maritime. Ils jouent donc un rôle clé dans notre monde moderne et leur préservation d'un point de vue environnemental est aujourd'hui crucial. Malgré tous les efforts réalisés en matière de gestion de l'environnement, la pollution associée au développement économique rapide du littoral et à une industrialisation intensive était finalement inévitable et demeure encore aujourd'hui l'une des principales menaces pesant sur les écosystèmes marins. Plus précisément, la contamination par éléments-traces métalliques est particulièrement préoccupante, car les zones côtières sont généralement enclines à les accumuler. La plupart de ces éléments-traces métalliques jouent un double rôle dans les eaux de mer : ils agissent comme nutriments à de faibles concentrations, mais peuvent rapidement avoir des effets toxiques dans des gammes de concentrations plus élevées. Une surveillance continue de leurs concentrations dans les écosystèmes estuariens et côtiers est donc nécessaire, afin de mieux comprendre leur comportement biogéochimique dans de tels environnements. Cependant, peu d'informations existent sur leur biodisponibilité vis-à-vis des organismes marins, d'autant plus que la toxicité de ces éléments traces n'est pas seulement dépendante de leur concentration, mais est également fortement liée à leur spéciation qui montre de fortes variations saisonnières et spatiales. Ainsi, l'objectif principal de ce travail de thèse était d'étudier les cycles biogéochimiques de divers éléments-traces métalliques et de percer le mystère de leur spéciation et de leur biodisponibilité dans des systèmes aquatiques variés : des zones turbulentes et dynamiques de l'estuaire de l'Escaut aux ports côtiers et aux eaux superficielles de la mer du Nord, et même jusqu'à des régions plus profondes



et anoxiques de la mer Baltique. Les variations de concentration et de spéciation des éléments-traces métalliques ont été explorées dans le temps et dans l'espace, le long de gradients horizontaux et verticaux. En parallèle, une comparaison des techniques classiques d'échantillonnage des éléments-traces métalliques dissous a été réalisée avec une méthode d'échantillonnage passif (Diffusive Gradients in Thin-films ; DGT). La technique des DGT a été utilisée avec succès pour la mesure *in situ* de la fraction labile des éléments-traces métalliques et représente, en définitive, un substitut de qualité à la biosurveillance des éléments-traces (par exemple, en remplacement de l'utilisation de moules, d'algues, etc.). Cette méthode permet de compenser le manque de connaissances en termes de surveillance de la qualité de l'eau et les résultats remettent en cause les critères classiques utilisés par les exigences réglementaires internationales (par exemple WFD, MSFD) et les engagements locaux (par exemple OSPAR, HELCOM). En effet, de nouveaux critères basés sur les espèces métalliques labiles plutôt que sur les espèces totales dissoutes devraient être envisagés à l'avenir. Une telle approche de la spéciation et de l'évaluation des éléments-traces métalliques dans les systèmes aquatiques pourrait certainement, à termes, conduire à une gestion environnementale plus intégrée et parfaire nos connaissances sur les impacts anthropiques et les flux de polluants le long de nos côtes. En outre, c'est finalement la clé principale pour expliquer et prédire la biodisponibilité et la toxicité potentielle des éléments-traces métalliques à l'égard de la faune et de la flore marines. Ce travail vous invite donc à plonger dans un voyage le long de nos côtes, de zones peuplées et urbanisées au grand large sauvage, de la surface aux eaux les plus profondes.

# Notation index

## A

A	Exposure area of a DGT piston
AA	Annual Average
APS	Ammonium persulfate
ASV	Anodic Stripping Voltammetry

## B

BCZ	Belgian Coastal Zone
-----	----------------------

## C

$C_{DGT}$	Concentration measured by DGT
CRM	Certified Reference Materials

## D

D	Diffusion Coefficient
DBL	Diffusive Boundary Layer
$\Delta G$	Thickness of the diffusive domain
DGT	Diffusive Gradients in Thin-films

## E

EA-IRMS	Elemental Analysis-Isotope Ratio Mass Spectroscopy
EF	Enrichment Factor
EQS	Environmental Quality Standards

## G

GF	Glass Fibre
----	-------------

## H

HAC	Hierarchical Ascendant Classification
HELCOM	Baltic Marine Environment Protection Commission
HR-ICP-MS	High Resolution-Inductively Coupled Plasma-Mass Spectrometry

## K

$K_D$	Partition Coefficient
-------	-----------------------

**L**

LOD            Limit Of Detection

**M**

m              Mass

MAC           Maximum Allowable Concentration

MQ water     Milli-Q water

**N**

NewSTHEPS    New Strategies for monitoring and risk assessment of Hazardous chemicals in the marine Environment with Passive Samplers

**O**

OSPAR            Commission for the protection of the North-East Atlantic marine environment

**P**

PCA             Principal Component Analysis

PN               Particulate Nitrogen

ppm             Parts per million

POC             Particulate Organic Carbon

POM             Particulate Organic Matter

PSU             Practical Salinity Unit

PVDF            Polyvinylidene Difluoride

**R**

RSD             Relative Standard Deviation

**S**

SPE             Solid-Phase Extraction

SPM             Suspended Particulate Metal

**T**

t                 Deployment time

TEMED          Tetramethyl ethylenediamine

**W**

WFD             Water Framework Directive



# Chapter 1

## General introduction

### Trace metals in estuarine and coastal environments



Estuarine and coastal ecosystems provide multiple ecological, social and economic services, especially for the fishing, touristic and shipping sector (Kalaydjian and Girard, 2017). Despite all the efforts made in environmental management, the pollution associated with the intensive industrialization of coastal areas remains one of the main threats to marine ecosystems: changing and reforming littoral landscapes, the seabed, etc... Anthropogenic inputs transferring from the land to the sea increased a lot too. Due to the discharges coming from major industries, port refineries but also from urban sewage, marine environments currently suffer from intense pollution issues which need to be imperatively considered. Metal pollution is of particular concern because coastal areas are generally prone to accumulate them, not only in sediments but also in the overlying waters for some metals (Kennish, 1994; Ho et al., 2010). Recent studies have shown that particulate trace metal levels have globally decreased in aquatic environments, in the last 30 years (Zwolsman et al., 1996), following the implementation of European environmental policies and regulations aiming to lower pollutant emissions (see for example the Water Framework Directive). Despite these measures, it seems that the concentration of dissolved trace metals has increased since 2000 (Gao et al., 2013). The switch of metallic elements from a particulate phase to a dissolved phase is nowadays a big concern, because it could influence directly the bioavailability of trace metals (TM) towards marine fauna and flora.

## **1.1. General description of trace metals**

### **1.1.1. General definition**

Metals and metalloids, also widely known and wrongly popularized as heavy metals (Hodson, 2004), form one of the main element clusters in the periodic table (Sigg et al., 2014). Overall, they differ from other elements due to several distinctive features, but these characteristics often result in contradictory definitions based on density, atomic weight, atomic number or other element properties (Hodson, 2004). In environmental studies, relevant characteristics to define metals and metalloids would be not biodegradable (unlike organic contaminants), bioaccumulation ability, some act as nutrients, their toxicity is speciation dependent (Ali et al., 2019; Caruso and Montes-Bayon, 2003; Rainbow, 2002). The “heavy metal” designation being obsolete for several reasons (Nieboer and Richardson, 1980), and as they usually occur at relatively low concentrations in the environment, heavy metals are now - chemically speaking and as an alternative - designated as **trace metals**.

### **1.1.2. Biological relevance**

On one hand, most trace metals exhibit a dual role in marine waters, acting as nutrient at low concentrations and being toxic at high concentrations. This first group of elements is therefore defined as biological-essential trace metals, including elements such as Co, Cu, Fe, Mn, Ni and Zn. They are necessary nutrients for life and play the part of enzyme cofactors for many metabolism reactions (Andreini et al., 2008; Morel and Price, 2003; Shahzad et al., 2018), as well as having structural role for many proteins (Garg and Smith, 2017). All organisms (e.g. phytoplankton, fish, human, etc.) require essential metals in small amount, as a lack or an excessive concentration of the same trace metals can be harmful and lead to adverse effects at a cell-, organ- or body-level (Fig. 1.1 (a); see section 1.3.1) (Sigg et al., 2014). On the other hand,

another category of trace metal exists and is described as non-biological-essential elements such as Cd, Hg and Pb: organisms do not require them as nutrients, and even worse, they become rapidly toxic to life even at low concentrations in the environment (Fig. 1.1 (b); see section 1.3.1) (Rainbow, 2018). Their toxicity to organisms is high, leading to various adverse effects impacting the metabolism, the growth rate, or even the reproduction of one given individual.

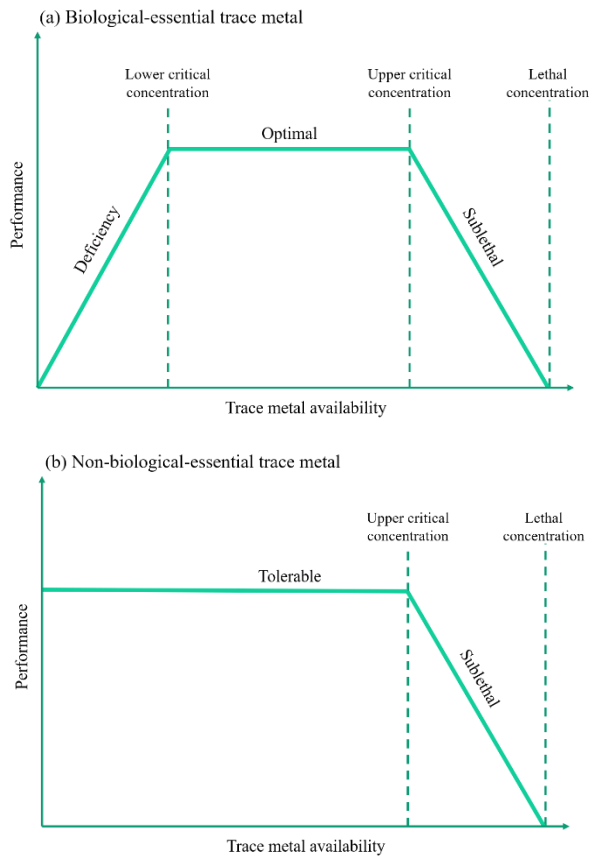


**Figure 1.1:** Effects of increasing availability of (a) biological-essential and (b) non-biological-essential trace metals on the organism performance (i.e. yield, growth, survival, reproduction) (adapted from Luoma and Rainbow, 2011)



In this study, focus has been made on essential elements: Co, Cr, Cu, Fe, Mn, Ni, and on non-essential element: Cd and Pb, as these trace metals are recognized either as hazardous substances of primary concern by legal frameworks and directives (Cd and Pb) or as compounds of possible concern (Cr, Co, Cu, Fe, Mn, Ni) (for further information, see 1.3.4). They are all recognized for their persistence in marine environments, their ability to be bioaccumulated and their potential toxicity. Moreover, they are known to be present at medium to high concentrations in the studied marine environments (*i.e.* the North and Baltic Sea, the Scheldt Estuary) and show cross-influenced behaviors. Also, the same methods and protocols can be performed for their measurement and analysis in the environment: making the sampling and the sample treatments more efficient and cost-effective. Despite their well-known toxicity to organisms, mercury as well as arsenic were not considered in this dissertation: their behaviors in aquatic environments are too different from the elements we studied here. In addition, their measurements and the assessment of their speciation required different methods which could not be applied in the present work.

## **1.2. Trace metals in marine environments**

### **1.2.1. Metallic sources, pathways and fate in marine environments**

Trace metal enrichment in aquatic systems is due to three kind of contributions as shown on Fig. 1.2: atmospheric inputs (particles, dust from various origins) riverine inputs (after weathering, leaching of inner lands, rock erosion) and deep-sea inputs (deep-sea volcanism, hydrothermalism). Enrichment from the atmosphere or waterways can result either from natural processes or come

from anthropogenic sources. Meanwhile, recent studies have shown the existence of freshwater inputs, coming from underground water sources called the Submarine Groundwater Discharge (de Souza Machado et al., 2016; Michael et al., 2005; Taniguchi et al., 2002). These contributions to marine environments can be substantial, even more than rivers. However, it seems that their pollution relevance has not been studied yet.

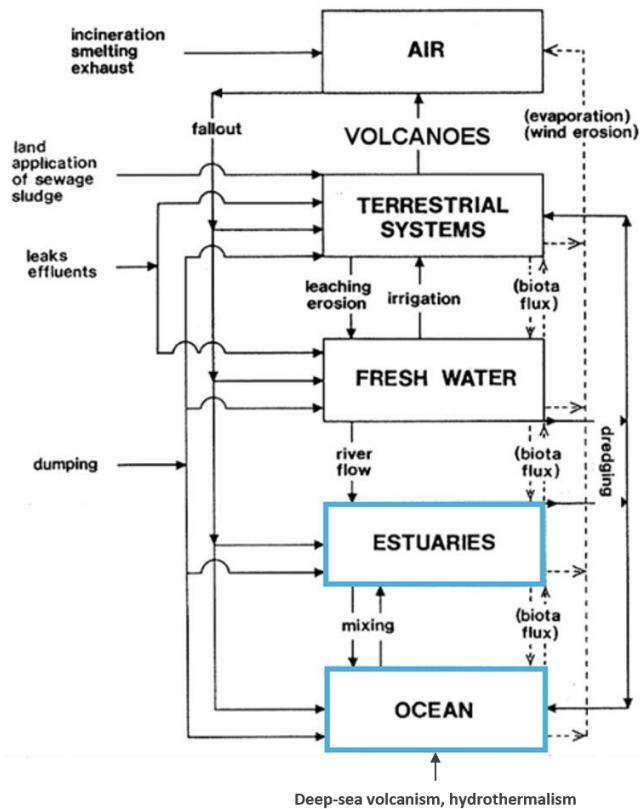


**Figure 1.2:** Sources and pathways of trace metals into the environment of interest (marine area, here in blue; Förstner and Wittmann, 2012)

First, natural source of trace metals is a consequence of their natural abundance in the continental Earth's crust (*i.e.* natural rock weathering,

terrestrial/deep-sea volcanisms, hydrothermalism). Then, diverse and numerous anthropogenic contributions were identified such as mining, refineries, fossil fuel combustion, agricultural activities, marine traffic, etc. Table 1.1 summarizes the main sources of trace metals discussed in this work. In conclusion, trace metals occur naturally on continental crust and are being occasionally eroded by natural processes, but the disturbance of the metal-enriched ores by mining and anthropogenic activities drastically accelerates the rate of trace metal introduction into the marine environment (Förstner and Wittmann, 2012).

**Table 1.1:** Natural and anthropogenic sources of trace metals to the marine environment, example of the studied elements

Element	Main ionic form in marine environments	Associated ores	Natural sources to the environment	Anthropogenic sources to the environment	References
Cadmium (Cd)	Cd <sup>2+</sup>	CdCO <sub>3</sub> , CdS, CdO	Erosion, forest fire, volcanism, soil	Mining, smelting, refining of zinc, fossil fuel combustion, stabilizer for plastic, fertilizers, battery, waste disposal, electroplating, pigmentation, photography	(OSPAR, 2002)
Cobalt (Co)	Co <sup>2+</sup>	CoS <sub>2</sub> , CoAs <sub>2</sub> , Co <sub>3</sub> S <sub>4</sub>	Erosion, forest fire, volcanism, soil	Metalworking industries, coal combustion, mining, plastic and rubber production, pigmentation, battery	(Lesven, 2008)
Chromium (Cr)	Cr <sup>3+</sup> , CrO <sub>4</sub> <sup>2-</sup> , Cr <sub>2</sub> O <sub>7</sub> <sup>2-</sup>	Fe <sub>2</sub> Cr <sub>2</sub> O <sub>4</sub>	Continental dust, erosion	Fossil fuel combustion, ore processing, chromate manufacture, electroplating, leather tanning, textile, waste disposal, metal plating, industrial dyes	(O'Connor, 1974)
Copper (Cu)	Cu <sup>2+</sup>	CuFeS <sub>2</sub> , Cu <sub>2</sub> S	Weathering, volcanism, soil	Fossil fuel combustion, wastewater, wood production, fertilizers, antifouling paint	(O'Connor, 1974)
Iron (Fe)	Fe <sup>2+</sup> , Fe <sup>3+</sup>		Erosion, soil	Mining, steel industry	(ATSDR, 2019)
Manganese (Mn)	Mn <sup>2+</sup> , Mn <sup>3+</sup>	MnO <sub>2</sub> , MnCO <sub>3</sub>	Erosion, volcanism	Fossil fuel combustion, metal production, fertilizers, glass industry	(ATSDR, 2019; Lesven, 2008)
Nickel (Ni)	Ni <sup>2+</sup>	NiS, Ni <sub>3</sub> S <sub>4</sub>	Erosion, forest fire, volcanism	Mining, smelting, refining, fuel combustion, waste incineration, manufacture of stainless steel, non-ferrous metal production	(ATSDR, 2019)
Lead (Pb)	Pb <sup>2+</sup>	PbS, PbO, PbCO <sub>3</sub> , PbSO <sub>4</sub>	Volcanism, continental dust, erosion	Non-ferrous metal production, mining, glass and ceramic production, offshore industry, waste incineration and disposal, fossil fuel combustion, battery; historically in gasoline, paint, pesticides	(O'Connor, 1974; OSPAR, 2002)

After entering estuaries and coastal zones, trace metals go through diverse biogeochemical cycles, inducing processes such as dilution and vertical transport from surface to deep waters. In addition, they undergo hydrodynamical forces, transporting and distributing the elements depending on surface- and deep-water circulations (Fig. 1.3; Frank, 2011).

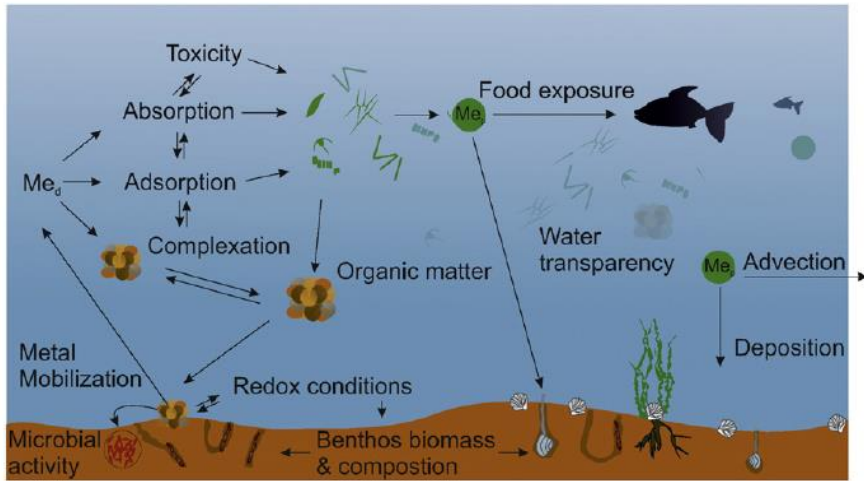


**Figure 1.3:** Conceptual model of the main biogeochemical trace metal cycles (dissolved  $Me_d$  and particulate  $Me_p$ ) in aquatic environments (from de Souza Machado et al., 2016)

Trace metals are stable in marine systems i.e. they do not degrade which generally favors their accumulation in the marine environment (Belgian Federal Science Policy Office, 2018). In the water itself, the metallic compounds can show a certain residence time, but they can also enter the food web through various exposure routes, or deposit and accumulate in the sediment. Often, they accumulate in coastal areas, usually close to densely industrialized and populated littorals (Elliott and Hemingway, 2002; Temara et al., 1998).

As depicted in section 1.1, trace metals constitute an important group: for their physiological relevance, but also for their possible toxic effects on organisms. In marine environments, their concentration range is not the only factor to consider: their speciation also plays a significant role and shows both seasonal and spatial variations.

### **1.2.2. Speciation in the water column**

Generally, aquatic environments consist of two compartments: the water column and the sediment, which can be further subdivided into four pools considering trace metal distribution: the Suspended Particulate Matter (SPM) and the sediment which form the solid particulate phase, and the water column and the sediment pore waters which form the dissolved phase. Strong interactions occur among these four compartments through physical and chemical processes leading to intense element transfers from one pool to another. Physicochemical reactions such as sedimentation, complexation, adsorption/desorption, biological uptake/release (in the water column as well as in sediment), sediment resuspension, etc. (Figure 1.4; Sigg et al., 2014) represent these transfers and consequently influence trace metal distribution and chemical speciation in the marine environments. They are also strongly linked with the aquatic biogeochemical cycles of trace metal, which were mentioned above (section 1.2.1). In this research, we focus on the water column and the SPM within, in order to investigate both dissolved and particulate phases of trace metals.

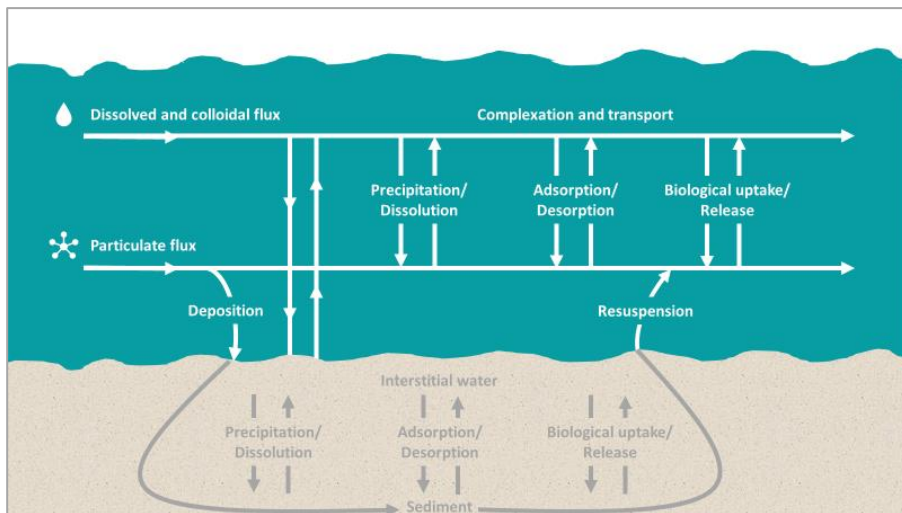


**Figure 1.4:** Biogeochemical interactions ruling trace metal transfers in aquatic environments (adapted from Morrison et al., 1989)

While an element is transferring from one aquatic pool to another (e.g. from SPM to the dissolved species of the water column), its physical and chemical form will also switch from one form to another (e.g. from precipitates to colloids, molecules and ions): this brings us to the concept of **speciation**. In simple words, the term speciation could be described as the distribution of a given trace metal regarding the physical and chemical forms it takes in the environment (Stumm and Morgan, 1996). This property has been shown as one of the main keys for understanding the biogeochemical behavior of trace metal and its impact on organisms; even more important than their actual total concentration (Gao et al., 2020; National Research Council (US) Commission on Natural Resources, 1977; Thanh et al., 2016). The speciation approach allows to differentiate several types of metal species, mainly based on the particle size (Stumm and Bilinski, 1973): a first distinction is made between the particulate and the dissolved phases of trace metals which can be separated

using a 0.45µm filtration (Hargreaves et al., 2017). However, this pore size limit has been questioned in the past (Danielsson, 1982) and it should be mentioned that several studies also conceded that using filters with a 0.20µm pore size may be accepted as well to distinguish the particulate from the dissolved phase (Dupré et al., 1999; Pinedo-Gonzalez et al., 2014; Takeda et al., 2000; Turetta et al., 2005; Viers et al., 2005). Nevertheless, the majority of studies has been performed using 0.45µm filters, which has become a standard procedure for the measurement of dissolved compounds. In addition, only 0.45µm filters were available for this work. Further distinctions between particulate and dissolved phases are described in Figure 1.5.

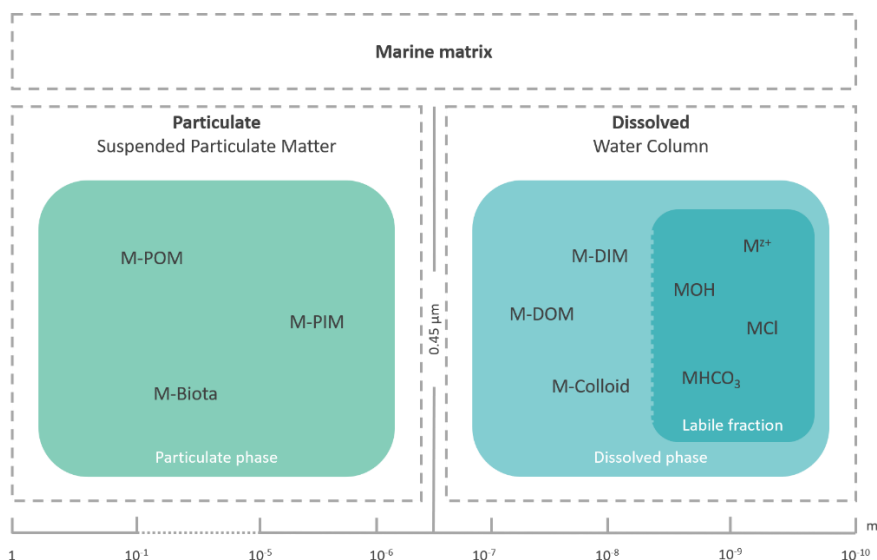


**Figure 1.5:** Conceptual diagram of trace metal speciation in seawater. M is a trace metal, POM stands for Particulate Organic Matter, PIM for Particulate Inorganic Matter, DOM for Dissolved Organic Matter and DIM for Dissolved Inorganic Matter.

The total dissolved fraction of trace metal is not entirely representative for the bioavailable metal fraction of interest here, which is a smaller part of this



dissolved phase. The bioavailability of elements is yet crucial to assess as it corresponds to a portion directly assimilable by the organisms. It is dependent on element mobility (usually related to diffusivity or internalization) and lability (*i.e.* ability of complexes to dissociate) (Baeyens et al., 2018a). Thus, the bioavailable fraction gives a strong correlation with the most labile trace metals (Baeyens et al., 2018a; Davison, 2016a; Simpson et al., 2012; Tessier and Turner, 1995). Labile elements include free metal ions, weak metal complexes with dissolved inorganic ligands (e.g. hydroxides) or organic ligands (e.g. fulvic complexes) (Davison, 2016a; Gao et al., 2019). Accordingly, in this research, focus has been made on the three following trace metal fractions (Figure 1.5): particulate ( $> 0.45\mu\text{m}$ ), dissolved ( $< 0.45\mu\text{m}$ ), and, within this dissolved fraction, labile (free ions, small and weakly bonded complexes). The recent progress of analytical techniques has made it possible to undertake advanced studies on the speciation of metallic elements in aquatic environments (Illuminati et al., 2019a). Particulate and dissolved metal concentrations are evidently investigated, because they both embody the two main forms taken by trace metals. Several studies have revealed the interest of studying the SPM, because of its enrichment in metals, but also because of its constitution in marine environments, which is mainly phytoplanktonic, demonstrating the biological importance of the particulate fraction (Paucot and Wollast, 1997). In addition, and in terms of total budget, the largest fraction of metals is particulate. Dissolved and even labile metal species are studied too, for their biological and ecological relevance.

The speciation will vary depending on the element and its physicochemical attributes but will also be significantly influenced by environmental conditions, such as (Prasad et al., 2005; Roberts et al., 2005):

- Physicochemical parameters: for instance, more acidic conditions tend to solubilize cationic trace metals, whereas alkaline

conditions favor their adsorption on SPM (Belgian Federal Science Policy Office, 2018). Temperature variations induce changes in kinetic and thermodynamic equilibrium of chemical reactions. For example, high temperatures generally disrupt complex stabilities (Byrne et al., 1988). The scarcity of oxygen also influences the reductive and oxidative state of trace elements (Jonnalagadda and Rao, 1993). In addition, the redox state of the solution (thermodynamic pE) also drives the speciation (Benjamin, 2014);

- Ligand type and concentration: organic SPM and ligands take time to adsorb/complex trace element, because the complexing sites are less accessible. However, once the complexes are formed, they show a strong stability. The complexation of metals with inorganic ligands is faster and easier, but generally less stable (except for instance (poly)sulfide ligands). In addition, the more inorganic and organic ligands, the more the metal have binding sites to associate to, and the more chemical complexes and colloids are formed. Finally, trace metal speciation is also widely influenced by interactions with marine organisms through complexation, primary production processes, biodegradation, exopolymerization, etc., and will be further detailed in the following part.

Due to the points listed above, trace metals are thus continuously switching from one phase to another. As described, the labile fraction is biologically interesting in the water column, because it reflects the ability of an element to interact with organisms (e.g. passage of biological membranes, bioaccumulation).

### **1.2.3. Uptake by marine organisms**

Trace metals entering the marine environment constantly change through various biogeochemical processes, also including the interaction with living marine organisms from nanoscopic and microscopic ones like phytoplankton to bigger ones such as fishes and marine mammals. Different kinds of uptake occur, at all the trophic levels, whether the element is essential or not. For higher organisms, trace metals can be incorporated through diet, through respiratory pathways or through the skin, via simple environmental exposure (Jakimska et al., 2011), and their body burdens will be influenced by many variables specific to the living being: its size, life stage (young, adults), species and its feeding habits (Wang, 1987). Then, the accumulated trace metal is bound to metal-binding proteins, and either gets stored in cells, tissues (metabolically available or stored) or are eliminated (excretion processes, feces, eggs, molts; Rumisha et al., 2017). The followed accumulation pattern is influenced by the organism physiology, by the type of element (some trace metals play a role in essential metabolic reactions, or some are to be excreted or stored, or some bind to certain biomolecules and thus give toxic effects). Figure 1.6 gives a schematic example of free ionic trace metals crossing the cell membrane of a phytoplankton, in the case of simple environmental exposure.

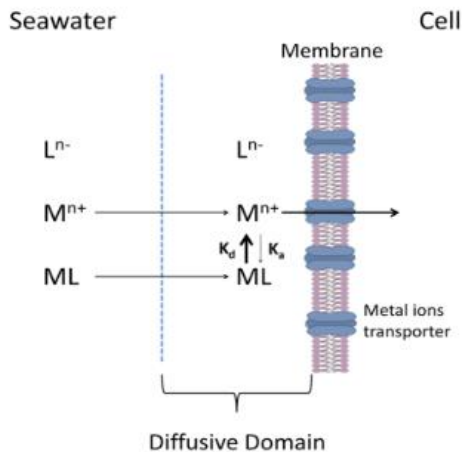


**Figure 1.6:** Internalization of free ions through the cell membrane of a phytoplankton, where M represents a metallic element and L a ligand (Baeyens et al., 2018a).

---

In estuarine and coastal environments, trace metals have real and direct interactions with living beings. Consequently, there is a wide range of uptake mechanisms of trace metals by marine organisms, leading to a wide range of body concentrations with various biological and ecological relevance (Rainbow, 2002). These relations may interact and play a part in the element biogeochemistry or, vice versa, with the organism metabolism. Figure 1.7 gives an example of mutual interactions between phytoplankton and trace metals: phytoplankton communities regulate the concentration, speciation and biogeochemical cycling of trace metals (biological uptake, mineralization, transport of biogenic particles), yet their productivity (biomass, growth) and the species composition and interactions are themselves controlled by the trace metals (inhibition/catalysis reactions) (Sunda, 2012).

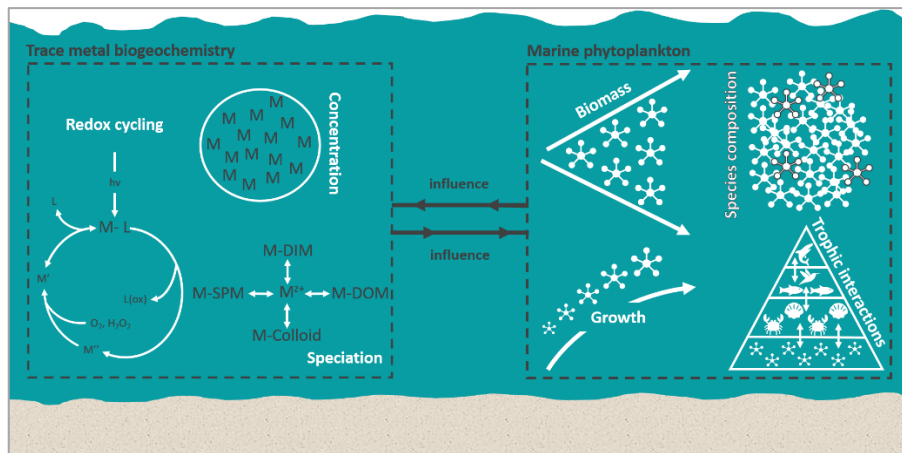


**Figure 1.7:** Conceptual diagram of mutual interactions between phytoplankton and trace metals (inspired by Sunda, 2012). M is a trace metal, L a ligand, SPM stands for Suspended Particulate Matter, DOM for Dissolved Organic Matter and DIM for Dissolved Inorganic Matter.

Trace metals are inherently not chemically biodegradable and can accumulate to a certain extent in the tissues of many marine species in a process called bioaccumulation. Once the metal concentration is above a given threshold in living organisms, the assimilated metal become toxic due to non-desired binding to crucial molecules, blocking their functioning and disrupting essential metabolic reactions (Belgian Federal Science Policy Office, 2018; Rainbow, 2002).

### 1.3. Trace metals as pollutants in marine environments

*“Contaminants are substances (i.e. chemical elements and compounds) or groups of substances that are toxic, persistent and liable to bio accumulate and other substances or groups of substances which give rise to an equivalent level of concern.”*

*Water Framework Directive, Article 2(29)*

The elements which can affect living being on a short- or long-term scale, by altering its growth rate, its metabolism, by interfering with its overall health, or even by altering its natural behavior, are considered as pollutant. (Park, 2007).

### **1.3.1. Toxicity, bioaccumulation and impact on marine ecosystems**

Anthropogenic inputs from various origins has been entering the aquatic environment by weathering and runoff from extractive industries, intensive agriculture, urbanized areas, etc. for decades. These pollutants such as trace metals are now a worldwide concern, specifically in coastal and industrialized environments. Trace metal pollution can damage the health of whole aquatic ecosystems and make aqueous products unsuitable for human consumption (Belgian Federal Science Policy Office, 2018). For example, the anthropogenic pressure on marine environments have disrupted the biogeochemical cycles of trace metals and consequently, increased their bioavailability towards marine organisms (Driscoll et al., 1994; Gaillardet et al., 2003). And as highlighted in section 1.1.2., trace metals may be toxic at excessive concentrations. For organisms, the toxicity of trace metals is actually linked to a threshold concentration of metabolically available (here, bioavailable) trace metal and not to a total dissolved metal concentration in the environment (Rainbow, 2002). Factors influencing trace metal toxicity in marine environments are:

- Trace metal speciation: toxicity is dependent on the physical and chemical form of metal compounds. The specific pollutant form decisively influences its adverse effects on marine organisms (Förstner and Wittmann, 2012), as discussed in 1.2.2. Environmental parameters which are speciation-related may therefore also influence

the organism physiology or trace metal toxicity: pH (low pH tend to solubilize cationic trace metals and render them easily bioavailable - see 1.2.2.; Belgian Federal Science Policy Office, 2018), temperature (higher temperatures disrupt thermodynamic equilibrium - see 1.2.2.; Byrne et al., 1988), alkalinity and hardness (both involved in metal detoxification processes), dissolved oxygen (toxicity increases in case of dissolved oxygen depletion), light (only poorly studied, but the biological uptake seems to decrease with decreasing lighting; Gorbi et al., 2001), salinity (protective effect of high salinity) (Barletta et al., 2019; Kahlon et al., 2018; Nordberg, 1978; Wang, 1987);

- Presence of other trace metals: metal mixture toxicity, possible cumulative, synergic or antagonism effects (Nordberg, 1978);
- The affected species: stage, size, sex, feeding habits, adaptation behavior. Some species or populations are more tolerant than others (Kennish, 1998). For instance, it has been shown that, in historically known contaminated coastal areas, marine populations display more tolerance than their fellows from unpolluted zones, for the same trace metal levels (Clark et al., 1997).

Overall, trace metal exposure or uptake at toxic concentrations can lead to different kinds of damage and inhibition in marine organism functioning. Table 1.2 summarizes them, for the elements of concern in this study.

**Table 1.2:** Toxic effects of trace metals on marine organisms, example of the studied elements. Here, and depending on the cited reference, we tried to consider a broad range of living being developing in the water column such as invertebrates (mollusks, crustaceans, echinoderms) and vertebrates (marine fish, marine tetrapod).

Element	Essential needs	Toxic effects	Cross-influence / Cross-toxicity	References
Cadmium (Cd)	none	Embryotoxic, teratogenic effects; DNA damages and carcinogenic; peroxidation of lipids and formation of DNA adducts; affect DNA, RNA, ribosome synthesis, deactivate systemic enzymes; disrupt reproductive processes (estrogenic, anti-estrogenic and endocrine)	Toxicity and accumulation of Cd increase due to Zn deficiency; Cd uptake increases as a result of Cu deficit; Cd and Cr interact synergistically	(Jakimska et al., 2011; OSPAR, 2002; Solomon, 2008; W.-C. Wang et al., 2014)
Cobalt (Co)	Carbon and hydrogen transfer reactions, N <sub>2</sub> fixation, component of vitamin B12	Growth inhibition, damage reproductive and respiratory system	Co absorption increases in case of Fe deficiency	(Kim et al., 2006; Sunda, 1989)
Chromium (Cr)	Required for carbohydrate metabolism	Inhibits growth	Cr and Cd interact synergistically	(Solomon, 2008)
Copper (Cu)	Takes part in many life processes (reproduction, growth); regulated metabolically; constituent of many enzymes, hemocyanin and respiratory pigments	Embryotoxic, teratogenic effects; DNA damage and carcinogenic; affects enzymatic activity; peroxidation of lipids and formation of DNA adducts		(Jakimska et al., 2011; W.-C. Wang et al., 2014)
Iron (Fe)	Takes part in many life processes (reproduction, growth); electron transport in respiration and photosynthesis, in nitrogen fixation	Growth inhibition, damages reproductive system		(Grimwood and Dixon, 1997; Sunda, 1989)
Manganese (Mn)	Constituent of many enzymes, metalloenzymes and respiratory pigment	Growth inhibition, chlorophyll inhibition, neurotoxic	Mn can induce Fe deficiency; influence on Cd, Cu and Zn toxicity	(Howe et al., 2004; Jakimska et al., 2011)
Nickel (Ni)	Constituent of many enzymes, role in the urease and hydrogenase metabolisms	Causes mortality; restrains the rate of growth, behavioral and endocrine disturbances	Ni toxicity increases in the presence of Cu	(Jakimska et al., 2011; Muysen et al., 2004)
Lead (Pb)	none	Embryotoxic, teratogenic effects; DNA damage and carcinogenic; blood-related diseases, damage to the immune system; affects reproductive processes (decreased sperm amount, motility, estrogenic effects); causes behavioral disturbances; affects survival, growth and metabolism; inhibits photosynthesis, gill		(Jakimska et al., 2011; OSPAR, 2009; W.-C. Wang et al., 2014)



As mentioned in 1.2.3, detoxifying processes exist, involving for instance metallothionein molecules (W.-C. Wang et al., 2014), adenochroms, basal, digestive or excretory cells (Penicaud et al., 2017). However, if the trace metal levels in the environment are excessive, these mechanisms are not satisfying enough to neutralize the exceeding amount of pollutant, leading to adverse metabolic effects (Mason, 2013). In any cases, the elements of concern in this study (Cd, Co, Cr, Cu, Fe, Mn, Ni and Pb) can bioaccumulate in marine organisms (Jakimska et al., 2011; OSPAR, 1996), but they do not show biomagnifying mechanism through the food chain, in marine ecosystems (Barwick and Maher, 2003; Elliott and Hemingway, 2002).

### **1.3.2. Marine pollution status in Europe**

In Europe, no fewer than 70 000 km of coastline boards the marine environment. European littoral zones gather 40% of its total inhabitants and represent as well 40% of its economy (Belgian Federal Science Policy Office, 2018), highlighting its importance as a human resource. Scientists even predicted that, as the world's population increased, 60% of people would live close to the coasts by 2050 (Elliott et al., 2019; Kummu et al., 2016). It will necessarily result in increasing industrial and agricultural activities and, as a consequence, to more anthropogenic pressures on marine coastal environments (Belgian Federal Science Policy Office, 2018). Today, the major threats to European coastal zones are water pollution and eutrophication, urban development, loss of biodiversity, landscape degradation and coastal erosion (European Environment Agency, 2008). To understand and prevent from future challenges in Europe, many surveys and environmental policies have taken the lead to draw up a review of European marine areas.

### **1.3.2.1. Legal frameworks and directives**

In response to the growing scientific and public concern about pollution status of our aquatic environments, European environmental policies and regulations have settled on different directives regarding trace metal level in waters. The first policies which were implemented to protect aquatic environments date from the early 1970s: the Oslo Convention in 1972 and the Paris Convention in 1974, which later gave rise to the OSPAR Convention in 1992 (Convention for the Protection of the Marine Environment of the North-East Atlantic; OSPAR, 2019). Meanwhile in 1992, another regional convention was signed under the acronym HELCOM (Baltic Marine Environment Protection Convention – also known as the Helsinki Convention; Baltic Marine Environment Protection Commission, 2019). The OSPAR and HELCOM Commissions are both governing bodies for the protection of marine environment (of the North-East Atlantic and the Baltic Sea areas, respectively), resulting from intergovernmental cooperation.

More recently, in 2000, Europe adopted the Water Framework Directive (European Environment Agency, 2008) which has been supplemented by numerous daughter-directives: especially in 2008, with the adoption of the Marine Strategy Framework Directive (MSFD). Overall, the main objectives were (i) to promote aquatic ecosystem management in its entirety and to set targets for a suitable use of the environment, (ii) to assess and regulate the ecological status of fresh-, transitional and coastal waters, taking into account nutrient pressures, biological, chemical and hydrodynamical characteristics, and (iii) to set out Environmental Quality Standards (EQS; Directive 2008/105/EC) for substances or groups of substances identified as priority pollutants and listed in the Annex X of the WFD, because of the significant risk they pose to the aquatic life (European Environment Agency, 2008; European Parliament and of the Council, 2008). The EQS are defined on the

lowest acute toxic effect observed on individual standard aquatic organisms during laboratory tests (Green, 2003). In practice, chemical and ecological monitoring stations are defined in water bodies by national Water Agencies, Environmental Directorates and partner institutions. At these stations, regular monitoring is undertaken with a maximum time-interval of one month (Bhurtun, 2018). In littoral zones, two categories of aquatic systems are identified: the coastal zone corresponding to the maritime domain off the coastline (up to 1 nautical mile from the shore – 12 nautical miles for the assessment of the chemical status), and the transitional waters such as estuaries, located near river mouths (Water Agency Artois-Picardie, 2017a).

In terms of environmental policy, the WFD is certainly the most important piece of legislation ever implemented across Europe, providing a standardized framework for a global community policy in the area of water management (Carvalho et al., 2019; Hering et al., 2010; Voulvoulis et al., 2017). However, the implementation of such directives was eventually more time-consuming than expected, and the procedures were more intricate to apply (Hering et al., 2010). In addition, the global objective of reaching good status of all European aquatic bodies by 2027 seems quite ambitious and challenging (Carvalho et al., 2019). Although the environmental monitoring has guaranteed a good observation of aquatic systems over time and allowed highlighting the areas at risk, this screening mainly had a regulatory purpose and did not allow a deep understanding of the overall functioning and dynamics of the ecosystem and water network (Bhurtun, 2018). In the same way, the monitoring data are only poorly obtainable outside the WFD sphere, even though these are abundant and strongly valuable (Hering et al., 2010). Moreover, the WFD and the MSFD are nowadays facing some challenges as they do not consider labile fraction of elements yet, due to very low concentrations (but not necessarily harmless) of pollutants or to insufficient

standardized analytical techniques (low-frequency, low resolution, spot sampling, etc.) (Brack et al., 2017). Applying innovative monitoring methods is thus needed for the enhancement of pollution management and mitigation, as well as the implementation of new EQS based on lability and bioavailability of elements of concern in the water.

Another European legal framework which also played a part in reaching a better environmental status is the Registration, Evaluation, Authorization and Restriction of Chemical substances Regulation (EU REACH Regulation). Adopted in 2007, the purpose of the REACH Regulation is to ensure human health and environment protection through a better identification of the chemical properties, such as their environmental toxicity. Hazardous substances and their characteristics are registered and gathered in the REACH system, and their progressive replacement to possible and suitable alternatives is then established (Official Journal of the European Union, 2006).

Table 1.3 gives an overview of the legal frameworks and directives listing and ruling trace metals in aquatic environments. The listed elements are also ranked as A, B and C category based on their classification by the European legal frameworks and directives. This table demonstrates that all directives and frameworks agreed on giving a priority concern to Cd, but also on a lesser extent to Pb and Ni. Cr, Co, Cu and Mn are not recognized as hazardous substances by the OSPAR and HELCOM Convention and the WFD, but they are identified as toxic substances for aquatic life (Cu and Mn) or as highly concerning substances (Co and Cr) in the REACH Program. No information was found for Fe since it is not recognized as a pollutant yet and as its relatively low level in marine waters does not give rise to adverse effects on the environment.

**Table 1.3:** Overview of European legal frameworks and directives for trace metals in marine matrices

Element	Oslo and Paris Commission (OSPAR) <sup>1</sup>	Helsinki Commission (HELCOM) <sup>2</sup>	Water Framework Directive (WFD) <sup>3</sup>	Registration, Evaluation, Authorization and Restriction of Chemicals (REACH) <sup>4</sup>
Cadmium (Cd)	A	A	A	A
Cobalt (Co)			B	A
Chromium (Cr)			B	A
Copper (Cu)			B	B
Iron (Fe)				
Manganese (Mn)				C
Nickel (Ni)			B	C
Lead (Pb)	A	A	B	A

<sup>1</sup>A: substance for priority action

<sup>2</sup>A: hazardous substance

<sup>3</sup>A: priority substance and priority hazardous substance, B: priority substance, but not priority hazardous substance

<sup>4</sup>A: substance of very high concern, B: recognized as very toxic to aquatic life, C: recognized as toxic to aquatic life

For the years to come and while pursuing the regulation of the ecological status of marine environments, the main challenge of these directives would be to guarantee the sustainability of coastal developments, from an environmental appreciation. Moreover, this should encompass all the policy domains related to water, nature, pollution, fisheries, climate change and land management (European Environment Agency, 2008).

### **1.3.2.2. Trace metal concentrations along European coasts**

In Europe, there are four main marine basins: the Mediterranean, Black and Baltic seas and the North Atlantic Ocean, which also includes the North Sea (European Environment Agency, 2008). Trace metal distribution along their coasts has been studied for decades until now (e.g. Baeyens et al., 1987; Ebling and Landing, 2015; Gelting, 2006; Laslett, 1995). Figure 1.8 gathers quantitative data published so far in the environments of interest in this study (*i.e.* North Sea, Scheldt Estuary and Baltic Sea) and gives an overview of trace metal concentrations in these coastal and transitional environments. This zonal but comprehensive literature survey synthesizes results from various studies since 1981 but shows a decrease in frequency of metal studies in more recent years. Figure 1.8 also provides evidence of a lack of knowledge and monitoring on the labile form of trace metal (specifically for the North Sea and the Scheldt Estuary), yet the most bioavailable (*i.e.* likely to come into contact and accumulate in organisms) and potentially hazardous fraction (*i.e.* bioavailable concentration at toxic levels for organisms). The most frequently reported trace metal fractions are particulate or total dissolved forms. Moreover, the concentrations of trace metals such as Cr, Co, Fe and Mn in the water column are not well documented neither by the scientific community. In addition, it seems that sediment is a better-investigated compartment than the water column. Thus, to achieve a better understanding of the bioavailable levels of trace metals in the water column, the labile concentrations of trace metals should be investigated as well. To compensate such lack, this research work focuses on the assessment of labile, total dissolved and particulate trace metals in estuarine and marine waters.

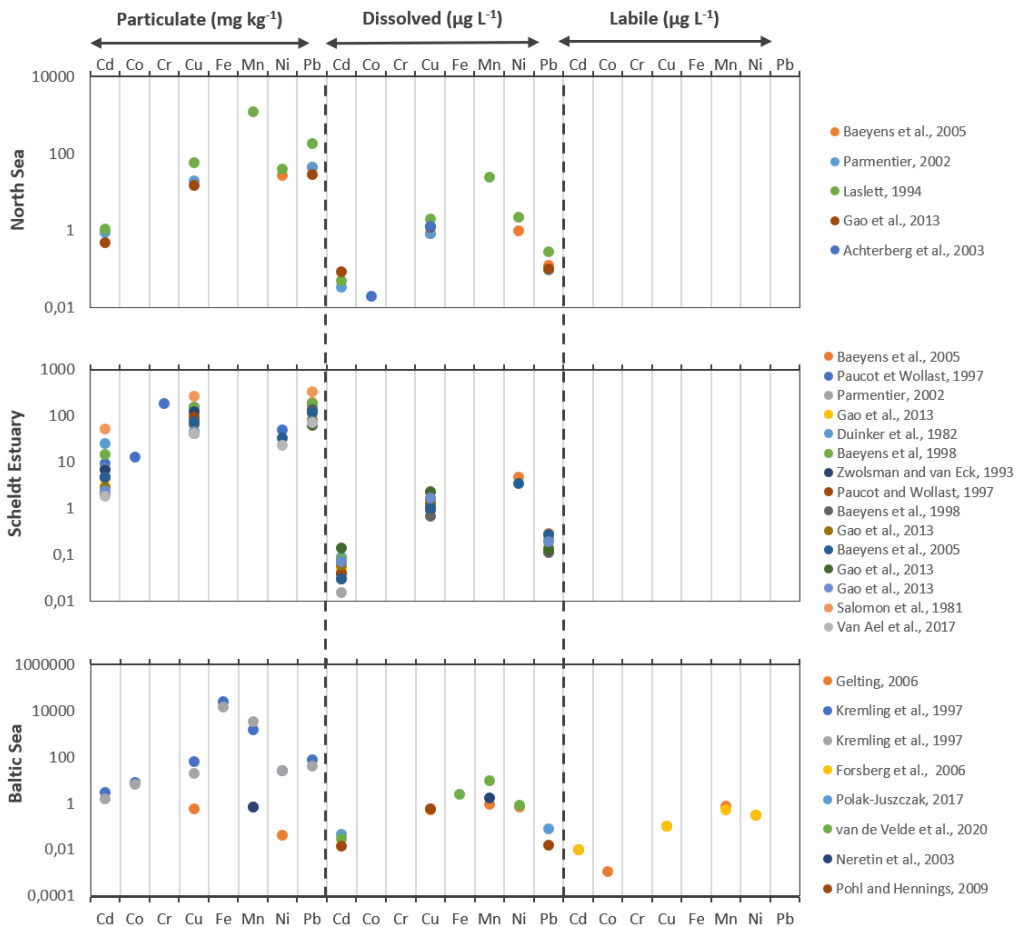


**Figure 1.8:** Summary of trace metal levels in the North and Baltic sea, and in the Scheldt Estuary, as these zones are investigated in this research work. Distinction is made between particulate, dissolved and labile values. The data come from scientific studies published between 1981 and 2020, with measurements made in the water column.

#### **1.4. Sampling and chemical analysis of trace metals and their speciation in marine environments**

For a comprehensive examination of aquatic environments, a wide range of methods and instruments can be used for the sampling and analysis of trace metals in all the compartments (water column, sediment). Today, these techniques need to allow both direct evaluation of the fate and level of pollutants, and the evaluation of their toxicity and impact towards ecosystems (Zabiegała et al., 2010). However, and due to specificities of seawater matrices, the determination of trace metal concentrations in the water column can be a very challenging task. Firstly, their concentration is relatively low in marine environments (W. Baeyens et al., 1998): making their detection by most analytical instruments quite difficult. To get around this issue, techniques in analytical chemistry endeavored to develop instruments of higher precision (lowering the detection limit), or novel methods of sampling and measurements which would isolate the species of interest and preconcentrate them (Huysman, 2019; Komjarova and Blust, 2006). Secondly, the complexity of the seawater matrix is often another source of troubles: for instance, the salt matrix increases the risk of chemical interferences during measurement. It also increases the risk of crystallization and clogging of instrument tubing, eventually damaging some parts of the analytical device. To overcome this second issue, the samples can be diluted, but only to a certain extent as the concentration of dissolved trace metals might be already low. Commonly, preconcentration systems are therefore used for their capacity to simultaneously remove the salt matrix as they isolate the targeted analytes.

Direct dilution of the samples is still foreseeable when the salinity is low and when the analytical instrument used provides high-resolution measurements. In any other case, advances made in analytical chemistry have allowed various



techniques to emerge: sample pretreatment methods like preconcentration (liquid-liquid extraction, solid-phase extraction) and coprecipitation, or passive sampling methods, or analytical methods (electrochemistry, mass spectrometry), or even biomonitoring methods (*i.e.* the use of organisms to assess the environmental contamination) (Menegário et al., 2017; Gao et al., 2019; Holmes et al., 2019; Jacks and Nystrand, 2019; Richir, 2016; Companys et al., 2017). All these techniques have made a significant contribution to the understanding of trace metal biogeochemistry in aquatic environments, unraveling many mysteries around trace metal distribution and speciation in seawater.

However, as many techniques exist, it often becomes a maze to select the most appropriate one. Liquid-liquid extraction technique are more and more neglected, because they often involve environmentally unsafe reagents. Whereas, solid-phase extraction using cation-exchange principle like resins are ever more preferred for the determination of dissolved trace metal in water, in the same way as electrochemistry (*i.e.* voltammetry). In addition, innovative tools like passive samplers are more and more used in the field, to assess labile concentrations of trace metals and highlight their speciation. Thanks to research progress, analytical advancements and increasing public concern, trace metals have been widely and steadily studied, and the quality of their measurement improved. The detection limits of many analytical methods have, for instance, been first extended to the  $\mu\text{g L}^{-1}$  level (Batley and Gardner, 1977) and further to the  $\text{ng L}^{-1}$  (Ali and Aboul-Enein, 2006; Mirzaei et al., 2011). The following part presents the most commonly used sampling, pretreatment and analytical techniques for measuring trace metals in marine environments, including the ones applied in this work.

### 1.4.1. Sampling procedures

Sampling is one of the most sensitive steps of the whole measurement procedure, in terms of sample contamination risks. In environmental monitoring, two kinds of sampling approaches coexist: the active and the passive sampling. On the one hand, the active sampling, also known as spot or grab sampling, is the conventional method (Mills and Gravell, 2015): based on a sample collection at one point in space and in time, this approach thereby provides a “snapshot” of information. On the other hand, the passive sampling technique results from the *in situ* deployment of a device accumulating chemical pollutants from the aquatic environment over time and provides a time-weighted average information (Górecki and Namieśnik, 2002; Zabiegała et al., 2010).

#### 1.4.1.1. Active sampling

**Active sampling** allows to capture the dissolved species as well as the mass of analytes associated with suspended particulate matter including colloidal organic matter (Supowit et al., 2016). It offers the advantage of brief sampling durations, much shorter than those required by passive sampling techniques which rely, for most of them, on deployment strategies for days (Supowit et al., 2016). The main drawback of such sampling is linked to the “snapshot” information gained on the pollutant level which could induce misunderstanding if the concentration fluctuates a lot (Mills and Gravell, 2015). In practice, clean bottles (e.g. Go-Flo, Niskin-X) are usually used to sample the seawater, which is then filtered in order to separate the dissolved and particulate phases. The filtration is commonly undertaken using membrane filters (0.45 µm pore size). The filtered seawater can be stored in clean PE or Teflon bottles at 4°C, acidified with 0.2% distilled HNO<sub>3</sub> and further used for total dissolved concentration assessment (see 1.4.2.1 and

1.4.3; Batley and Gardner, 1977; Colombo et al., 2019; Elderfield et al., 2006; Gillain et al., 1979). Finally, filters can be stored at -20 °C before treatment for particulate concentration measurements (see 1.4.2.2).

### **1.4.1.2. Passive sampling**

#### **1.4.1.2.1. Generalities on passive samplers**

**Passive sampling** techniques are becoming more and more popular in environmental monitoring, mainly thanks to their ability to (i) preconcentrate trace elements and eliminate most of the matrix; (ii) produce time-averaged concentrations instead of spot concentrations (*i.e.* active sampling); and (iii) enable *in situ* preconcentration. Indeed, passive samplers allow to combine sampling, trace metal extraction and preconcentration into a single step (Górecki and Namieśnik, 2002). In addition to active sampling techniques described in 1.4.1.1, passive samplers permit a more comprehensive understanding of trace metal speciation. They rely on the free flow or diffusion of analytes from the solution to the receiving phase (*i.e.* binding phase inside of the passive sampler), via a diffusion barrier or a membrane (Zabiegała et al., 2010). The targeted compounds accumulate on the device over time due to a concentration gradient, which finally gives a time-weighted average concentration in the environment (Amato et al., 2018; Charriau et al., 2016; Huysman, 2019; Salim and Górecki, 2019). The passive samplers can be either directly deployed in the water column and retrieved later or deployed in snapshot samples (e.g. liters collected during fieldwork and brought back to the laboratory). Table 1.4 gives an overview of existing passive sampling techniques in aquatic environment monitoring.

**Table 1.4:** Comparison of different passive samplers that have been used for sampling trace metals in aquatic matrices (adapted from Vrana et al., 2005)

	Diffusing and receiving phase	Measurable elements	Sampling purpose	Deployment time	Sample treatment for chemical analysis
Chemcatcher	Immobilized chelating acceptor resin on a PTFE base, cellulose acetate membrane filter acting as a thin diffusion layer	Cd, Cu, Ni, Pb and Zn	<i>in situ</i> sampling, integrative, speciation	14 days to 1 month	acid extraction
Diffusive Gradients in Thin-films (DGT)	2 layers of acrylamide gel in a holder device, one is an acceptor phase, the other is a diffusion layer	55 metallic elements	Integrative, speciation, screening, imitating biological uptake	days to weeks	acid extraction
Permeation Liquid Membrane (PLM)	Microporous hydrophobic support separating test solution from receiving solution	Cu, Pb	Bioavailable metal species	hours	solvent extraction
Supported Liquid Membrane (SLM)	Strip solution with strong complexing agent separated from the test solution by a macro-porous hydrophobic membrane	Doubly charged cations	Integrative, preconcentration, imitating biological membranes	days	solvent extraction
Stabilized Liquid Membrane Device (SLMD)	LDPE lay-flat tubing containing an acidic solution with high affinity for the target elements	Divalent metal ions	Preconcentration, <i>in situ</i> sampling, determination of labile metals in grab samples	days to weeks	acid extraction

Most of passive sampler calibration necessitates equilibrium or linear uptake isotherms, which is often enhanced by the use of Performance Reference Compounds (PRC) for quality control (Supowit et al., 2016), besides the hydrogel technique of Diffusive Gradients in Thin-films (DGT) used in this study.

#### **1.4.1.2.2. Diffusive Gradients in Thin-films (DGT)**

The DGT technique turns out to be a relevant tool for environmental studies, mainly thanks to its use as a proxy for assessing element bioavailability (Davison, 2016a; Li et al., 2019; Slaveykova et al., 2009; Zhang et al., 2014). Placed *in situ* (here, in the water column; Baeyens et al., 2011; Zhang and Davison, 1995), this passive sampler relies on the controlled diffusive transport of the targeted analytes and results in the measurement of labile fractions of trace metals (free or weakly complexed ions), an ecologically relevant fraction (see 1.2.2). However, just like bioavailability and toxicity are species-dependent (see 1.3.1), the assessed labile concentrations are technique-dependent. Thus, the DGT technique allows the measurement of a DGT-labile concentration of trace metals, which, for simplicity, will be designated as labile concentrations in the further chapters. DGTs have several advantages over conventional monitoring methods, and labile concentrations determined by DGTs are recognized to provide a better scientific basis for risk assessment (Davison, 2016a; Väänänen et al., 2018; Wang et al., 2018; Xu et al., 2019).

In practice, the device is composed of a filter and two hydrogel layers: a diffusive hydrogel that is backed up by a second one containing the metal-selective accumulative resin (figure 1.9a).

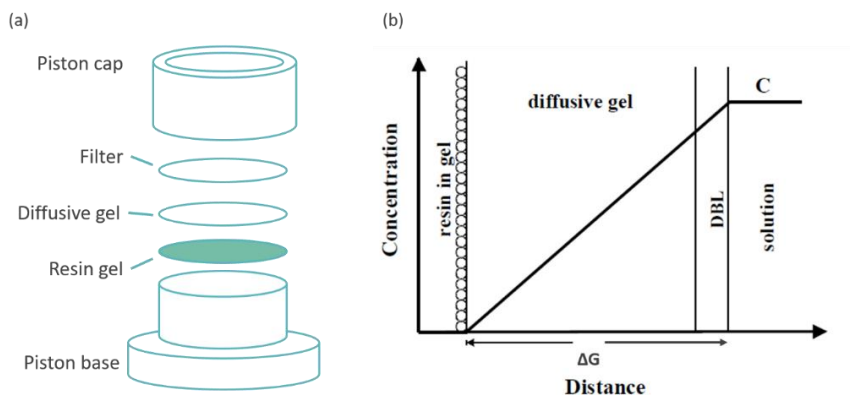


**Figure 1.9:** Diffusive Gradients in Thin-films (DGT) device (a), and schematic cross-section when deployed (b), showing the steady-state concentration gradient. The diffusive layer is shown as a single layer of gel but contains a diffusive hydrogel layer and a filter (adapted from Zhang and Davison, 1995).

The DGT piston (DGT research<sup>®</sup>) consists of a round plastic molding (a cap and a piston base, both assembled), holding together successive layers, which are, for most cationic trace metals: a 0.45  $\mu\text{m}$  pore size cellulose acetate membrane filter (0.125 mm thick), a polyacrylamide diffusive hydrogel (0.8 mm thick) and finally a binding Chelex<sup>®</sup>-100 resin gel (0.4 mm thick). From the total mass of accumulated metal on the resin during deployment, the average DGT-labile trace metal concentration can be calculated following Fick's law (Eqn 1.1), assuming perfect sink conditions (*i.e.* all metal ions arriving at the interface between the diffusive hydrogel and the resin gel are immediately bound to the resin):

$$C_{DGT} = \frac{m \times \Delta G}{D \times A \times t} \quad \text{Equation 1.1}$$

where  $C_{DGT}$  is the DGT-labile metal concentration in the seawater in  $\mu\text{g L}^{-1}$ ,  $m$  is the trace metal mass accumulated on the resin gel in  $\mu\text{g}$ ,  $\Delta G$  is the total thickness of the diffusive domain in cm [diffusive gel, membrane filter,

Diffusive Boundary Layer (DBL; fig. 1.9b)],  $D$  is the diffusion coefficient of the trace metal in  $\text{E}^{-6} \text{cm}^2 \text{s}^{-1}$ ,  $A$  is the DGT piston window area in  $\text{cm}^2$  and  $t$  is the deployment time of the piston in s.

With the development of Diffusive Gradients in Thin-films probes (DGT), the estimation of trace metal bioavailability in natural waters became possible, thanks to its pore size limitation, the diffusive layer and the selective resin (Davison, 2016a; Estrada et al., 2017; Paller et al., 2019; Pelcová et al., 2018). At a wider scale, their use in the future would be ideal to adapt the existing environmental quality standards of the WFD. Passive sampling techniques succeeded in establishing themselves in environmental research, as they greatly simplified sample collection and treatments and as they are now considered as a powerful tool for speciation analysis, risk assessment or even bioavailability forecast in the case of DGT (Supowit et al., 2016; van Leeuwen et al., 2005). Using passive samplers offers non-negligible advantages as a low-tech and cost-effective monitoring systems. Indeed, they do not require power (i.e. electricity), significantly reducing the cost of analyses, and it ensures the protection of samples against degradation during transport, storage, and treatment (Namieśnik et al., 2005; Zabiegała et al., 2010). In addition, it helps to avoid visiting the sampling sites multiple times to collect representative samples (Zabiegała et al., 2010). Last but not least, passive samplers like DGT allow the detection of labile fractions at very low concentrations in aquatic environments (Namieśnik et al., 2005). In conclusion, passive sampling shows three main interests: preconcentration (analytical relevance), temporal variation determination (environmental relevance), speciation investigation (both analytical and environmental relevance). However, few drawbacks need to be considered when using such sampling techniques in aquatic environments: biofouling (i.e. accumulation of microorganisms, plants, algae, or animals on the sampling device surfaces)

usually happens after two weeks of deployments in waters and may cause a bias in calculations (Mills and Gravell, 2015; Uher et al., 2012). In addition, it is necessary to assess the Diffusive Boundary Layer (DBL) forming in front of the DGT device, which can have significant impact on the final results in less dynamic environments (*i.e.* low flow conditions; Uher et al., 2013). Moreover, the deployment time might be limited depending on the binding phase capacity and the trace metal concentrations in the studied environment (*i.e.* saturation) (Brumbaugh et al., 2002). On the field, specific attention must be paid to the complete submersion of the device during the whole deployment time, especially in tidal environments. Finally, longer deployment time could increase the risk of losing the samplers, which is quite usual in turbulent areas. At last, active and passive sampling techniques are complementary and enable to obtain comprehensive information on trace metal speciation in the marine environment (Huysman, 2019; Schintu et al., 2008; Uher et al., 2018).

## **1.4.2. Pretreatment methods**

### **1.4.2.1. Solid-Phase Extraction (SPE)**

**Solid-Phase Extraction (SPE)** is nowadays widely used for extraction of dissolved trace metals in complex aquatic matrices and is a good example of preconcentration methods following an active sampling (see 1.4.1.1; Giakissikli et al., 2016; Granado-Castro et al., 2018; He et al., 2017; Huysman, 2019; Parham et al., 2009; Poole, 2002; Simpson, 2000; Thurman and Mills, 1998; Tuzen et al., 2005; Zhu et al., 2016). In order to cope with seawater features, SPE is used to simultaneously preconcentrate the analytes and remove the salt matrix (Figure 1.10; Stockdale, 2005; Watkinson, 2008), using an appropriate sorbent phase to which dissolved trace metals from a filtered and acidified seawater sample will bind.



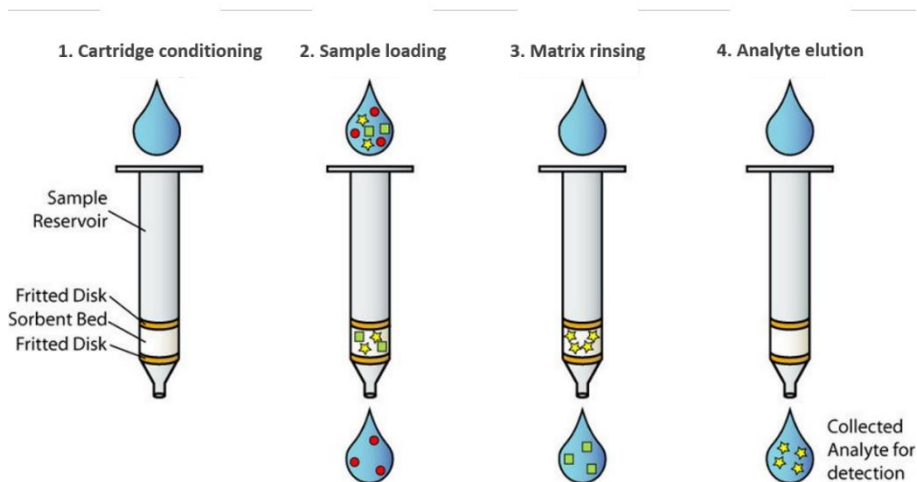


**Figure 1.10:** Schematic steps of a SPE procedure (adapted from Watkinson, 2008)

In most cases, cation-exchange resins are used as a sorbent phase (i.e. Chelex<sup>®</sup>-100, 8-Hydroxyquinoline, etc.) to which dissolved trace metals can be bound (Orians and Boyle, 1993; Soylak, 2004; Stockdale, 2005). Such SPE is then often followed by analyses with Inductively Coupled Plasma-Atomic Emission Spectrometry (ICP-AES; Abbasse et al., 2003; Liang et al., 2004; Rao et al., 2006), or with Inductively Coupled Plasma-Mass Spectrometry (ICP-MS, see 1.4.3.1; AlSuhaimi et al., 2019; Dierssen et al., 2001; Wang et al., 2014a).

#### 1.4.2.2. Acidic digestion of SPM

As mentioned in 1.4.1.1., the filters used in the filtration allow to collect Suspended Particulate Matter (SPM) from the water samples and can further be used to measure particulate trace metal concentrations. The filters are generally weighed before the filtration and rinsed with Milli-Q water after the filtration to remove the salt. They are then dried under a laminar flow hood or

in an oven at 60 °C for 12 hours and weighed again to obtain the amounts of SPM (Loring and Rantala, 1992). Various procedures exist for the treatment of the filters and their SPM deposits, and they all aim at decomposing the SPM retained on the filters by digestion processes. The **total digestion** method consists in using a mixture of strong acids (HF, HCl, HNO<sub>3</sub> and HBO<sub>3</sub>). A similar digestion can be carried out, only using Aqua Regia (HNO<sub>3</sub> and HCl). During these both digestion procedures, the filters do not decompose (polyvinylidene fluoride membrane, hydrophilic), but only SPM is digested (Yeats and Dalziel, 1987). The resulting solutions are finally stored, further diluted and analyzed using flame or graphite furnace AAS, ICP-AES or ICP-MS (see 1.4.3.1), depending on the compounds of interest and the demanding limits of detection (Akçay et al., 2003; dos Passos et al., 2018; Fick et al., 2018; Loring and Rantala, 1992; Sandroni et al., 2003; Santoro et al., 2017).

### **1.4.3. Analytical techniques**

#### **1.4.3.1. Instrumental analysis by Inductively Coupled Plasma-Mass Spectrometry**

Inductively Coupled Plasma-Mass Spectrometry (ICP-MS) has become a pillar instrument in trace metal research. This powerful tool gathers a good sensitivity, low detection limits, high analysis rate, low sample consumption, wide range of concentrations and multi-element capability (Ray et al., 2004). It has been already successfully applied to the simultaneous determination of various metallic elements in water (Arslan et al., 2018; Dundar and Altundag, 2018; Gaillardet et al., 2003; Sekhar et al., 2003; Warnken et al., 1999; Xing et al., 2019). The following sections give an overview of its principle and basic functioning.

#### **1.4.3.1.1. Sample and standard preparation**

Nowadays, sample introduction systems for the analysis of gaseous, liquid and solid samples have been developed (Komjarova, 2009), but as it is the case for most ICP-MS applications and for this research work in particular, only the principle for liquid samples will be described here. Before their introduction in the ICP-MS, the samples must be in a liquid form: either from digested solid samples, or eluted samples, filtered and acidified samples, etc. Depending on the expected concentrations of the elements of concern and/or the chemical composition and concentration of eluents (for instance, very acidified samples), the liquid samples can be diluted prior to analysis, in order to protect the instrument tubings and/or to be consistent with the calibration range. Meanwhile, various points should be taken into consideration regarding sample handling and preparation. First, and as only few mL of samples will be used by the ICP-MS, care must be taken to ensure that the collected samples are all representative of the bulk material (Raja and Barron, 2019). In addition, contamination prior to measurements by ICP-MS constitutes a serious concern: especially, when the targeted analytes are expected to be present at very low concentrations in the samples. Thus, the samples should be prepared as close as possible to the ICP-MS, under a laminar flow hood of a clean room (Raja and Barron, 2019; United States Department of Agriculture, 2018). For instance, and even with these precautions, it has not been possible to consider Zn in this work.

Concerning the standard preparation, they can be obtained by direct dissolution of the targeted metal or metal salt, in an appropriate acid solution. Another way was followed here: acidified multi-standards solutions were purchased commercially and diluted to different desired concentration levels. The latter were further used to make a calibration curve. The more standard with different concentrations (in the range of the sample concentrations), the

more accurate the measurements will be (Raja and Barron, 2019). Additional quality controls can be carried out by measuring certified reference materials such as SLRS-6 (river water; National Research Council Canada), MESS-3 (marine sediment; National Research Council Canada), IAEA-405 (estuarine sediment; International Atomic Energy Agency), etc.

#### 1.4.3.1.2. Overall functioning

ICP-MS gathers an ion-generating argon plasma source with the sensitive detection limit of mass spectrometry detection (Raja and Barron, 2019). Overall, the instrument encompasses six components: a sample introduction system, an ion source represented by the plasma torch, an interface, ion optics, a mass/charge separator and a detector (Figure 1.11; Komjarova, 2009).

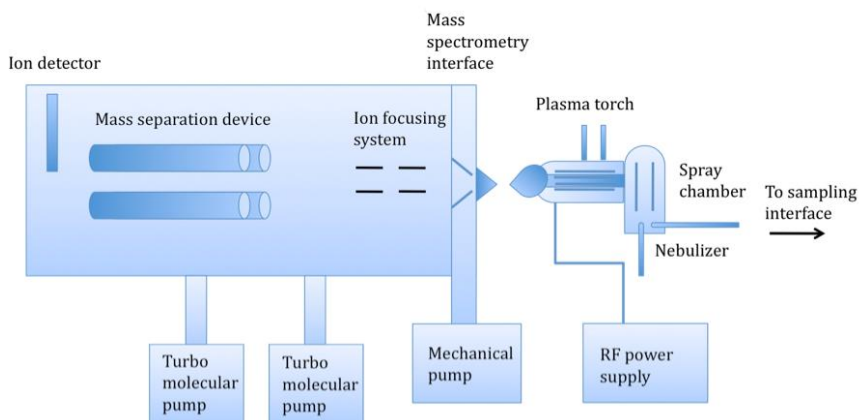


**Figure 1.11:** Schematic representation of basic ICP-MS components (adapted from Thomas, 2013)

In practice, the sample of interest is pumped at 1 mL/min with a peristaltic pump into a nebulizer, where it is converted into a fine aerosol thanks to argon gas supply at about 1 L/min (Thomas, 2004). This is the sample introduction

system. Next, the droplets of the formed aerosol are separated into smaller and larger ones in the spray chamber, where only the small droplets are retained in the aerosol which is then transported to the plasma torch via an injector (Thomas, 2004). Through the plasma torch, the fine aerosol is ionized by a high-temperature plasma induced by an electromagnetic field and generates ions (Komjarova, 2009; Thomas, 2004). Once formed, the ions are transported to the mass spectrometer through a first interface composed of two sequential cones: the sampler and the skimmer which enable the transport of ions to the ion optics and the mass separation device, from atmospheric pressure at around 8000K to vacuum at room temperature (Thomas, 2004). The ions are then transported across a sequence of electrostatic lens: the ion optics, which allow the separation and isolation of cations from photons, particulate, negatively charged and neutral species. Thus, only the cations will reach the mass analyzer where they are divided according to their mass-to-charge ratio (Komjarova, 2009; Thomas, 2004). In this study, measurements were made with a High-Resolution ICP-MS (HR-ICP-MS, Thermo Finnigan Element II). Thus, the mass analyzer used is a double focusing magnetic sector (not shown on Figure 1.14). The very last step involves an ion detector (e.g. Faraday cup, discrete dynode electron multiplier), counting individual ions exiting the quadrupole and converting the ions into electrical pulses. The intensity of the latter are recorded and correspond to the ion amount present in the original sample (Thomas, 2004).

#### **1.4.3.2. Electrochemical voltammetry**

Electrochemical **voltammetry** is another method that can be used for measuring trace metals in aquatic environments. Numerous voltammetric techniques have been applied for measuring dissolved trace metals in aquatic matrices and for metal speciation analyses (Achterberg and Braungardt, 1999; Bruland et al., 1985; Colombo and van den Berg, 1997; Maity et al., 2017;

van Leeuwen et al., 2005). These are sensitive and rapid methods based on the measurement of a current, resulting from the reduction or oxidation of compounds present in solution under the effect of controlled variations of the potential between two specific electrodes (Bedioui, 1999). A voltammetric device consists of two components: a cell equipped with a set of three electrodes (1 working electrode, 1 counter electrode and 1 reference electrode, Figure 1.12), and an electronic circuit called potienstat-galvanostat, which allows to control or measure the current and potential.

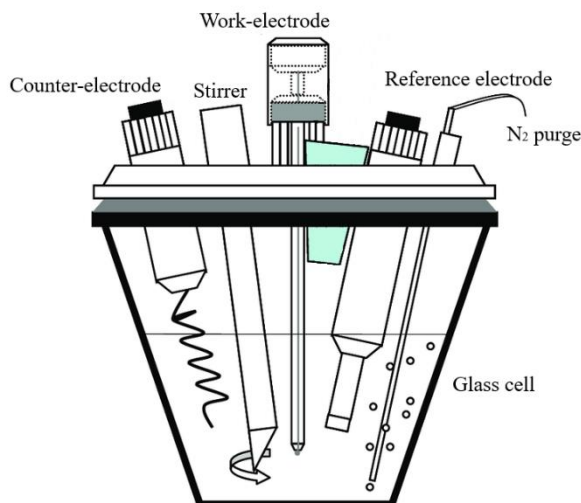


**Figure 1.12:** Schematic voltammetric cell (adapted from Louis, 2008)

---

In the case of Anodic or Cathodic Stripping Voltammetry (ASV or CSV, respectively), the trace metal of interest is pre-concentrated for several minutes by electro-deposition on a working electrode, such as on a mercury drop or film electrode (Figure 1.13; Farghaly et al., 2014). The quantification is finally performed by anodic or cathodic redissolution (van Leeuwen et al., 2005) and a standard addition calibration curve is often chosen for such

techniques. In addition, the selectivity is ensured by electrochemical reactions located at known potentials.

Even though electrochemistry can in certain cases allow simultaneous determination of trace metals, voltammetric determinations are often labor intensive (Komjarova, 2009).

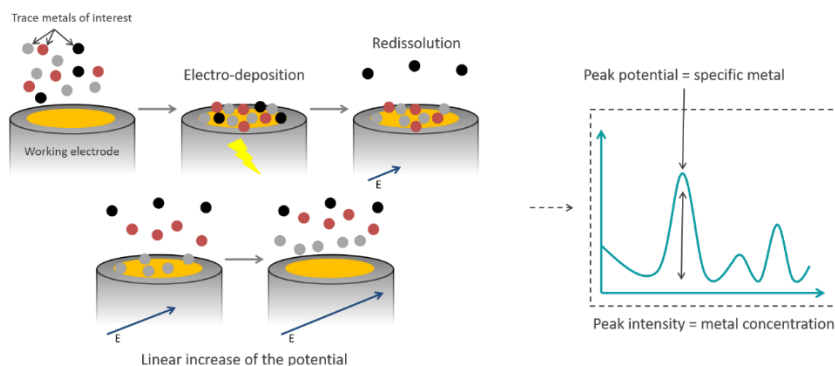


**Figure 1.13:** Scheme of Anodic Stripping Voltammetry (retrieved from Palmsens BV). After accumulation, during the stripping phase, every element oxidizes on the electrode surface at a specific potential. Every time an element is oxidized, an electrical current is measured by the potentiostat.

## 1.5. Objectives of the PhD research work

### 1.5.1. Research plan

This work fits directly into the application of the Water Framework Directive "Strategy for marine environments" which aims to limit the impact of pollutants on the environment. This PhD research is devoted to a monitoring improvement of our seas and oceans, and, above all, to establish a picture of coastal marine ecosystems regarding the presence of different metallic pollutants. Specifically, contamination of marine systems by some trace metals (Cd, Co, Cr, Cu, Fe, Mn, Ni, Pb), their speciation and bioavailability

are the main contents of this research. In the water column, the bioavailability of trace elements is well represented by the labile concentration which constitutes a part of the dissolved fraction of trace metals (Baeyens et al., 2018a). So far, numerous coastal studies were only focused on the measurement of particulate and dissolved trace metals (Gao et al., 2013; Scoullou et al., 2007; Tankere and Statham, 1996). In addition, the 2013 EQS Directive (2013/39/EU) which defines the EQS, only considers dissolved concentrations of trace metals. They do not consider the chemical speciation of elements, yet as important as their actual concentrations in the environment. Thus, a need of new EQS is pertinent, because toxicity depends on the speciation of element as well and not only on their concentrations and because defining new standards will improve our understanding of the whole functioning of aquatic ecosystems. Providing advanced data on their labile concentrations could ideally help building new EQS based on their potential bioavailability, and not only on their total dissolved fractions. However, there are only few studies on labile trace metal assessment in transitional and coastal environments. This research work endeavors to fill this gap.

To investigate the geochemical behavior of trace metals in marine environments using the DGT technique, many field campaigns have been organized: notably in the North Sea and on the Scheldt estuary, but also in the Baltic Sea, aboard scientific vessels equipped with laboratories and sampling equipment. In addition, a study has also been done only on particulate metal behavior depending on tidal cycles. Concurrently and for some campaigns, SPM has been characterized to better understand particulate trace metal behavior, and its origin has been traced back by measuring its stable isotope content (C and N), as organic matter of natural and anthropogenic origins shows different isotopic signatures.



### **1.5.2. Scope, novelty and research impact**

In this research work, approaches based on passive samplers are developed: for chemical exposure (monitoring) as well as for the evaluation of the biological risk. Particulate and total dissolved concentrations, but also the labile (i.e. bioavailable) fraction of trace metals are determined, providing a better understanding of trace metal speciation in marine environments and a better prediction of ecological risk. This innovative approach enables (i) to improve measurements of metallic contamination in marine environments by taking into account their concentrations and speciation (ii) to assess anthropogenic chemical pressures on coastal and transitional ecosystems and (iii) to participate in the development of new European assessment criteria for aquatic environments under the Marine Strategy Framework Directive. This work also participates in developing a toolbox for monitoring anthropogenic pressures on estuarine and coastal ecosystems, since these water bodies are relevant to the WFD. It assists in the development and validation of extensive and integrated procedures for aquatic monitoring and risk assessment at a European level; vital levers to meet European regulatory requirements (WFD, MSFD) and regional commitments (OSPAR, HELCOM Convention).

### **1.5.3. Thesis structure**

Pollutants such as trace metals transferring to the environment from different anthropogenic activities are of worldwide concern. Their accumulation and biogeochemical behavior in the water column of different estuarine and coastal environments were thoroughly investigated to evaluate their fate and potential risks. Figure 1.14 summarizes the thesis structure.

Located between Belgium and the Netherlands, the Scheldt estuary is a semi-enclosed embayment with fresh river water coming from the inland and saline water entering from the North Sea. In the last decade, only few research

studies focused on trace metal speciation along this transitional environment. **Chapter 2** fills this gap of knowledge and additionally explores the application of passive sampling techniques to assess trace metal availability along a horizontal transect. Estuaries are the typical interface between inland waters and marine environments. Whether they are subject to tide influences or not, the future of elements transported by the rivers will be determined at their level. Wide variations of physicochemical parameters are usually observed in these interfaces, and consequently strongly influence the distribution of trace metals between the dissolved and the particulate phase. Concentration gradients of bioavailable, dissolved and particulate trace metals were investigated (from the upper part of the estuary to its mouth) and compared through a timeline from the early 80's.

**Chapter 3** extends the work done in Chapter 2 by offering an overview of trace metal speciation along the Belgian Coastal Zone (BCZ). Located offshore of the Scheldt estuary, the BCZ is an interesting place to study trace metals, because of the variety of anthropogenic inputs influencing the water composition (atmospheric deposition, direct wastewater discharge from coastal industries and the Scheldt estuary). The idea, here, was to define the chemical anthropogenic pressure on Belgian coastal environments by monitoring the trace metal levels, by studying their speciation and also by tracing the SPM towards their origin, using isotopic measurements of carbon. Chapter 3 is an adaptation of the paper named "Trace Metal Speciation in North Sea Coastal Waters", published in Science of the Total Environment in November 2019 (Gaulier et al., 2019a).

Not only in estuaries but also along the coasts, tidal cycles strongly influence SPM transport, trace metal distribution and physicochemical parameters such as pH, salinity, turbidity, etc. **Chapter 4** presents a specific research work on the behavior and transport of particulate trace metals and SPM, regarding

monthly tidal cycles over the Belgian Coastal Zone. Like initiated in Chapter 3, the SPM composition is thoroughly described by measuring their carbon and nitrogen contents, along with their stable isotope ratio.

Leaving the Belgian waters, **Chapter 5** offers a focus on the Baltic Sea through a study on trace metal speciation regarding depth and redox gradients. The deep and anoxic waters of the Eastern Gotland Basin generate large variations of physicochemical parameters from the surface to the bottom, influencing trace metal distribution and speciation. Concentration gradients of bioavailable, dissolved and particulate trace metals were investigated, from surface-oxygenated waters to deep-anoxic ones, on both Swedish and Latvian waters.

Finally, **Chapter 6** serves as a general conclusion of the previous chapters and offers further discussions and research perspectives.

At the time of writing, only Chapter 3 was been published. However, all the chapters are currently in preparation for submission in international journals as well.

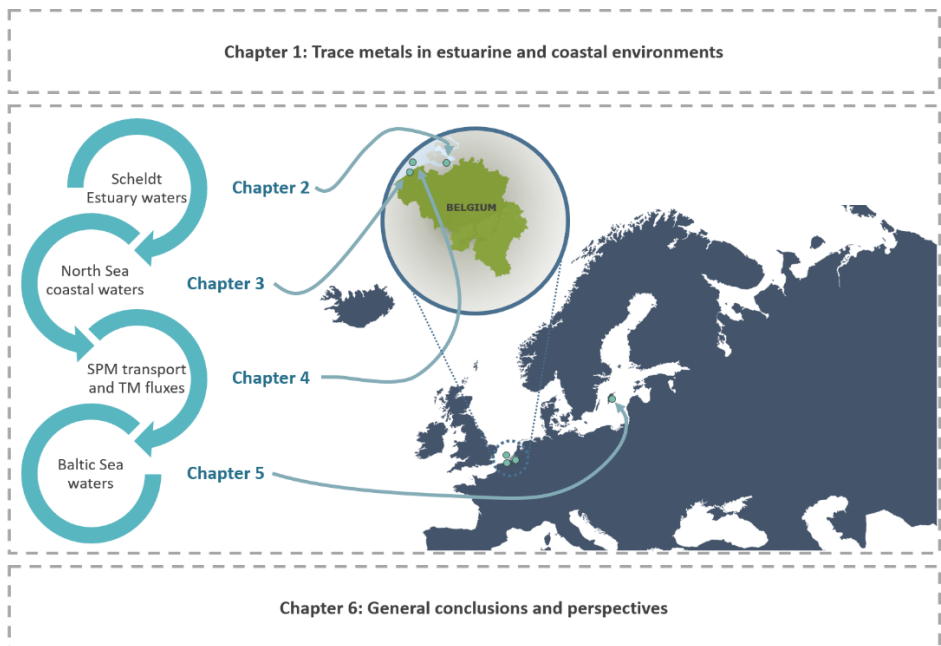
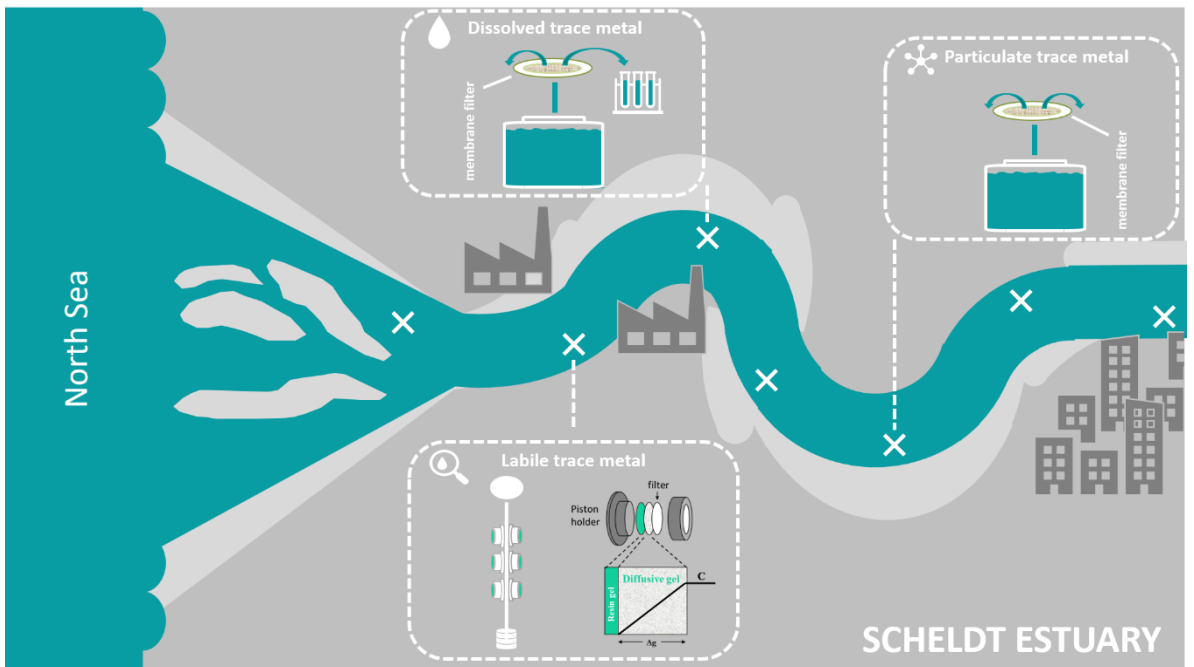


**Figure 1.14:** Conceptual framework of this research work

# Chapter 2

## Investigation on trace metal speciation and distribution in the Scheldt Estuary



# **Investigation on trace metal speciation and distribution in the Scheldt Estuary**

*Gaulier C., Zhou C., Gao Y., Guo W., Reichstädter M., Ma T., Baeyens W., Billon G. In preparation for Science of the Total Environment..*

## **Abstract**

In this research work, the biogeochemical behavior of Cd, Co, Cr, Cu, Ni and Pb along the historically polluted Scheldt Estuary (Belgium - The Netherlands) was investigated. As never studied before in this area, labile trace metals were measured using innovative DGT passive samplers, while the total dissolved and particulate trace metal concentrations were assessed using classic active sampling techniques. This dual approach allowed us to highlight the variations of trace metal speciation and distribution in the estuarine surface waters, considering environmental and physicochemical gradients along the transect. The large data set obtained was then compared to literature data from historical measurements along the Scheldt (from 1980 until today), but also from other estuaries. As emphasized by our results, trace metal mobility and partitioning along the Scheldt Estuary is mainly driven by biogeochemical gradients. Hence, all species of trace metals display a non-conservative behavior. More precisely, dissolved labile fractions of trace metals show higher levels in the middle estuary, where many solubilization and remobilization processes occur due to turbulent mixing mechanisms. Our study confirms the decreasing trend historically observed for particulate metals along the Scheldt, as well as the rising concentrations recorded for dissolved trace metals which might also lead to an increase of their labile fraction. Finally, these first results suggest that a more regular monitoring of labile metallic levels along the Scheldt Estuary is essential to have a deep understanding of trace metal speciation and to review bioavailability of trace metals within estuarine ecosystems.

**Keywords: Trace metals, Speciation, DGT, Scheldt Estuary, Biogeochemistry**

## 2.1. Introduction

In Europe, no fewer than 70 000 km of coastline boards marine environments. European littoral zones gather 40% of its total inhabitants and represent as well 40% of its economy (European Environment Agency, 2013), highlighting its importance as a human resource. Estuaries often stride along these coasts and form ecotones: connecting land and ocean, freshwater and seawater (Hobbie, 2000; Meire et al., 2005). Whether they are subject to strong tide influences or not, they are highly productive systems and are homes to an important biome (Meire et al., 2005). Moreover, they play an important role in determining the future and fate of many elements transported by rivers. Historically, estuaries have been major sites for the development of strong anthropogenic activities, driven by industry, agriculture, fishery and tourism as well (European Environment Agency, 2008; Förstner and Wittmann, 2012). Discharges of chemical compounds such as trace metals (transported by rivers and tributaries, but also metal-rich effluents along estuary shores) pass, deposit and accumulate in the water column and sediments of estuaries (Förstner and Wittmann, 2012), where they eventually take various forms (free ions, labile or complexed, associated with particles, colloids, etc.) (Diop et al., 2014; Gonzalez et al., 2007; Illuminati et al., 2019a). They can deposit via sedimentation and accumulate along the estuarine bed (da Silva et al., 2017). They can also enter the water column either by surface processes (atmospheric deposition, flow from rivers) or by sediment resuspension (tides, marine traffic and dredging activities) leading to the remobilization of metallic contaminants (Peres et al., 2016). Along estuaries, the natural modification of physicochemical parameters (pH, turbidity, oxygen, salinity, etc.) and biological processes also influence the mobility and bioavailability of these trace metals in the estuarine ecosystem (Bianchi, 2007; Du Laing et al., 2009; Folens and Du Laing, 2017).

At the European scale, the Scheldt Estuary drains a watershed considered as highly industrialized and going through major urban and harbor areas like Antwerp, Ghent (Belgium) and the Netherlands. The total Scheldt river basin actually forms one of the most heavily populated regions of Europe (W. F. J. Baeyens, 1998) with one of the highest economic activity but also one of the highest biological value (Meire et al., 2005). Past and present wastewater discharge and historical metal pollution from industries and refineries have strongly affected the environmental quality of this coastal ecosystem (Baeyens et al., 2005; Deycard et al., 2014). Historically, many surveys endeavored to measure dissolved and particulate trace metal spread along the Scheldt Estuary and further along the Belgian coasts (Baeyens, 1997; Baeyens et al., 2005, 1998, 1987; Duinker et al., 1982; Gao et al., 2013; Regnier and Wollast, 1993; Teuchies et al., 2013; etc.). However, to our knowledge, none of them attempted to report the labile contents of trace metals in the Scheldt Estuary, yet the most bioavailable and hazardous fraction in the water column (Gao et al., 2019; Linnik et al., 2018; Simonsen et al., 2019; Tusseau-Vuillemin et al., 2007). Moreover, dissolved and particulate trace metal levels have been indeed investigated for a long time in the Scheldt, but a monitoring gap seems to appear since 2010 (because of a lack of project proposals and funding). To fulfill such lack of knowledge and to achieve an advanced investigation of trace metal speciation and distribution along the Scheldt Estuary, this work assessed labile, dissolved and particulate trace metals in surface estuarine waters. Especially as trace metal bioavailability and consequently toxicity mainly depend on their speciation rather than on their total concentration only (Allen and Hansen, 1996; Landner and Reuther, 2004; Elskens et al., 2014; Aldana et al., 2018).

In a nutshell, this study focuses on the distribution, transport and partitioning of six trace metals (Cd, Co, Cr, Cu, Ni, Pb) in the highly urbanized Scheldt



Estuary. The objectives of this research are (i) to assess the metallic contamination and fluxes released into the Scheldt Estuary, (ii) to discuss the speciation and potential fate of this trace elements along the estuarine system, regarding various biogeochemical gradients and (iii) to project our results over a timeline from the early 80's and on a European scale.

## **2.2. Material and methods**

### **2.2.1. Chemicals and materials**

For the material cleaning and preparation (Glass, PE and Teflon bottles, Teflon and glass plates), nitric acid ( $\text{HNO}_3$ ; Fisher, Trace Metal Grade, 65%), distilled nitric acid (distilled in the laboratory), Milli Q water (Millipore) were used. For DGT preparation, Chelex<sup>®</sup>-100 (Bio-Rad, 200-400 mesh size), cross-linker (DGT Research, Lancaster), acrylamime (40%, Merck), ammonium persulfate (APS; Merck), tetramethylethylenediamine (TEMED; Merck, >99%), DGT pistons (caps and bases, DGT research, Lancaster), 0.45  $\mu\text{m}$ -pore size filter membranes (Merck Millipore, Durapore<sup>®</sup>, 0.45  $\mu\text{m}$  PVDF Membrane, HVLP grade) and NaCl (Merck, Suprapur) were used. For DGT treatment, 1M  $\text{HNO}_3$  was prepared by diluting 63 mL  $\text{HNO}_3$  (Fisher, Trace Metal Grade, 65%) into 937 mL Milli Q water. For sample treatments, distilled nitric acid ( $\text{HNO}_3$ ; Fisher, Trace Metal Grade, 65%; distilled in the laboratory), Milli Q water (Millipore), HCl (Fisher, Trace Metal Grade, 37%), HF (Fisher, Trace Metal Grade, 40%) and  $\text{H}_3\text{BO}_3$  (Fisher, Trace Metal Grade, 4% w/v) were used.

### **2.2.2. Study sites**

The Scheldt estuary is formed by the rivers Rhine, Meuse, and Scheldt (Wollast, 1988), ends up in the North Sea and is one of the European estuaries where the tidal strength has the most influence (Vlaams Instituut voor de Zee,

2012). It starts from the city of Vlissingen (km 0: mouth, the Netherlands) and extends to the city of Ghent (km 160: upper part, Belgium), with a mean depth of 10 m and a funnel shape (Figure 2.1). It is a typical tide-dominated estuary (Scanes et al., 2017). More precisely, it exhibits an intricate morphology composed of flood- and ebb-channels, large intertidal flats and salt marshes (Meire et al., 2005). The estuarine zone is defined by the water salinity (brackish to seawater) and also by the significance of tidal influences. In Ghent, a series of locks limiting the tide influence are considered as the boundary with the upper-Scheldt river. The longitudinal gradient of salinity in the estuary is mostly determined by the importance of the river discharges. As the Scheldt estuary is a relatively shallow and well-mixed system, vertical salinity gradients are minor or insignificant (Soetaert et al., 2006; Van Damme et al., 2005). In this mixing zone, pollutant transport is widely controlled by the long residence time of the water masses. This entails a high stagnancy of contaminants in the water column and consequently accentuates their accumulation in sediments (de Souza Machado et al., 2016). In parallel, strong variations of biogeochemical parameters and bioavailable fractions of chemical compounds have been observed in the estuarine area (Wollast, 1988).

As previously suggested by Baeyens (1998), the Scheldt Estuary can be divided in two main zones, regarding their hydrodynamical and physicochemical properties (Figure 2.1). The first one goes from 1 to 10 PSU and usually shows lower salinity, high turbidity, high sedimentation and lower water oxygenation. This zone is also called the geochemical filter as trace metal speciation is controlled by various geochemical processes (redox, adsorption/desorption, complexation, etc.). Downstream, trace metal distribution is rather controlled by biological processes like phytoplankton activity (incorporation, scavenging), thanks to a better oxygenation and a

lower turbidity of the environment. This second zone is also called the biological filter. Overall, the metallic contamination along the Scheldt has been widely influenced by large inputs of trace metals and other physicochemical factors resulting in oxygen depletion, high turbidity and high sedimentation (Baeyens et al., 1998).

For this study, seven stations designated as S01, S04, S07, S09, S12, S15, S22 (Figure 1) were sampled from the city of Antwerp (Belgium) to the mouth of the Scheldt Estuary in Vlissingen (The Netherlands). The sampling expedition was performed onboard of the R.V. Belgica in March 2019. Early Spring constitutes a key-season in such aquatic environment and an ideal period to investigate trace metal bioavailability since the biomass (*e.g.* phytoplankton) expands and grows again in this period. Surface water sampling and *in situ* passive measurements were carried out from a Zodiac, in order to avoid contamination of the research vessel. The information on water tide and water flow was recorded during the sampling and is presented in Table 2.1.



**Figure 2.1:** Location of the sampling sites along the Scheldt Estuary (adapted from Vlaams-Nederlandse Scheldecommissie, 2018). Two distinct zones were defined, according to the work of Baeyens (1998).

**Table 2.1:** Water tide and flow during the sampling campaign along the Scheldt Estuary (retrieved from Vlaamse Milieumaatschappij, Waterbouwkundig Laboratorium, Maritieme Dienstverlening & Kust en De Vlaamse Waterweg NV, internal communication).

Date	City	Tides	
		High tide	Low tide
19 <sup>th</sup> March 2019	Vlissingen	00:21	06:51
		12:44	19:12
	Antwerp	02:21	09:06
		14:34	21:27
20 <sup>th</sup> March 2019	Vlissingen	01:09	07:42
		13:30	19:58
	Antwerp	03:01	10:01
		15:46	10:34
Average flow (m <sup>3</sup> s <sup>-1</sup> )			
19 <sup>th</sup> - 20 <sup>th</sup> March	Melle (Zeeschelde)	44.82	
March 2019	Melle (Zeeschelde)	48.30	
Year 2019	Melle (Zeeschelde)	17.94	

### 2.2.3. *In situ* measurements

Temperature, pH, salinity and dissolved oxygen saturation were measured *in situ* at each station with a multi-meter (VWR International bvba, Multimeter MU 6100 H set 2) and using electrodes previously calibrated. To measure pH, combined glass and Ag/AgCl/KCl electrodes (VWR, pHenomenal<sup>®</sup> 111) were used; dissolved oxygen and temperature were measured using a membrane covered galvanic sensor (VWR, pHenomenal<sup>®</sup> Oxy 11-3); and salinity by a 2-pole graphite sensor (VWR, pHenomenal<sup>®</sup> Co 11). Measurements were conducted in freshwaters, brackish waters as well as in seawaters, following a salinity gradient: a correction of the pH and dissolved oxygen recordings was therefore made according to the method of Aminot and K erouel (2004). The

measurements were taken twice: at DGT deployment and once again at DGT removal (see 2.2.4.1).

## **2.2.4. Trace metals in the surface waters**

### **2.2.4.1. DGT sampling and analysis**

The DGT technique relies on a controlled diffusive transport of the analyte and is either applied in the water column (e.g. Baeyens et al., 2011; Zhang and Davison, 1995) to assess labile trace metal fractions or inserted vertically in sediments (e.g. Gao et al., 2006, 2015; Zhang et al., 2002) to determine high-resolution profiles of trace element concentrations and/or fluxes at the sediment-water interface (SWI). The DGT technique allows to assess a time integrated concentration of the labile trace metal fraction, which is a good indicator of the element bioavailability in an aquatic system (Bade et al., 2012; Baeyens et al., 2018a; Davison, 2016b; Roig et al., 2011; Sierra et al., 2017; Simpson et al., 2012). The DGT piston is composed of a round plastic molding (a cap and a piston base, both assembled), holding together three successive layers, which are: a membrane filter (0.45  $\mu\text{m}$  pore size cellulose acetate – 0.125 mm thick), a diffusive hydrogel (polyacrylamide hydrogel – 0.8 mm thick) backed up by a resin gel (binding Chelex®-100 resin – 0.4 mm thick). In this study, the DGT samplers were deployed in the water column of each selected sampling point.

The diffusive and the resin gels were prepared according to the method reported by Zhang and Davison (Zhang and Davison, 1995) and the assembly of DGT probes is described in Gaulier et al. (2019). All procedures above were carried out in an analytical clean laboratory. At each sampling station, 6 DGT pistons were enclosed for  $\pm 24$  hours in a plastic cage which was held with a 2 m nylon rope below the water surface, anchored to the seabed using a weight and lifted to the surface with the help of a buoy. The exact time and water

temperature at DGT deployment and removal were recorded at each station and further used for DGT concentration calculations. Six procedural blanks were treated in the same way (except for the deployment step).

After deployment, the labile trace metals, accumulated on the resin gel, were eluted in 1 mL of 1M HNO<sub>3</sub> for at least 24 hours. The eluents were then diluted five times with MQ-water, prior to their analysis. Using the mass of the accumulated metals on the resin gel, the labile metal concentration was then calculated based on the Fick's first law in a steady state, as described in Gaulier et al. (2019), assuming a perfect sink condition (*i.e.* all metal ions arriving at the interface between the diffusive hydrogel and the resin gel are immediately bound to the resin).

#### **2.2.4.2. Sampling and sample treatment for dissolved and particulate metals**

##### **2.2.4.2.1. Dissolved metal phase**

At the same time DGT pistons were deployed and retrieved, seawater samples were taken below the surface in two replicates, using clean glass bottles. Prior to use, these bottles were cleaned with 10% HNO<sub>3</sub>, rinsed three times with Milli-Q water in the laboratory and with seawater in the field. 500 mL of seawater samples were then filtered using 0.45 µm pre-weighted filter membranes (Merck Millipore, Durapore<sup>®</sup>, HVLP grade), under a clean laminar flow hood in a clean laboratory onboard. The filtrate was acidified with 0.2% distilled HNO<sub>3</sub> and then stored in a clean Teflon bottle, at 4 °C. The filters were stored at -18 °C and later treated for the analysis of suspended particulate metal phase. The acidified filtrates (seawater samples) were finally diluted 10 times with MQ water, prior to analysis.

#### **2.2.4.2.2. Suspended Particulate metal phase**

The filters used for seawater sample filtration were dried under a laminar flow hood for 2 days and weighted again. The mass difference of the filters was recorded for the calculation of particulate metal concentrations and for the determination of the Suspended Particulate Matter (SPM) amount. The filters were digested by concentrated HF (40%), concentrated HCl (37%), concentrated HNO<sub>3</sub> (65%) and H<sub>3</sub>BO<sub>3</sub> (4%), as described in Gaulier et al. (2019). To validate this digestion method, the certified reference material IAEA-405 (CRM; estuarine sediment, International Atomic Energy Agency) was treated in the same way as the filter samples. The results of the CRM were within the range of certified values and are displayed in the supporting information section.

#### **2.2.4.3. Analysis and validation**

In all sample solutions, trace metals (Cd, Co, Cr, Cu, Ni, Pb and Al) were determined using a High Resolution-Inductively Coupled Plasma Mass Spectrometer instrument (HR-ICP-MS, Thermo Finnigan Element II). The calibration was carried out with appropriate dilutions of a multi-element stock solution (Merck, ICP-MS standard XIII) and indium (1 µg L<sup>-1</sup>) was used as an internal standard. Limits of detection (LOD) were 0.004 µg L<sup>-1</sup> for Cd, 0.004 µg L<sup>-1</sup> for Co, 0.029 µg L<sup>-1</sup> for Cr, 0.32 µg L<sup>-1</sup> for Cu, 0.18 µg L<sup>-1</sup> for Ni and 0.015 µg L<sup>-1</sup> for Pb. The relative standard deviation (RSD) was lower than 9.8% for all metal species. An additional CRM (SLRS-6; river water, National Research Council Canada) was also analyzed, the results were within the range of certified values and are displayed in the supporting information section.

## 2.3. Results

### 2.3.1. Physicochemical parameters and SPM amount

The physicochemical parameters of all stations are presented in Figure 2.2. Initially, the salinity shows a typical longitudinal gradient along the Estuary with low values in the inner area (zone 1; freshwater dominant, close to urbanized zones and to the city of Antwerp) and gradually increases seawards (zone 2; seawater dominant, at the mouth). Overall, salinity varies from 1 PSU at station S22 to 26 PSU at station S01.

The water temperature varies from 7.95 to 8.90 °C and displays a reverse trend than salinity: a significant negative relationship is observed between these two parameters (correlation factor of -0.92,  $p < 0.005$ ; see the Supplementary Information for the complete correlation and associated p-value matrices). Even though it remains in a narrow range of values, the higher temperatures are found at low salinities, while colder ones appear at the mouth.

Regarding dissolved oxygen, its saturation varies between 84 and 117 % from the low salinity zone to the well-oxygenated seawaters. The dissolved oxygen saturation remains around 115 % in the second zone. The water column oxygenation is significantly and positively correlated to the salinity along the estuary (correlation factor of 0.90,  $p < 0.005$ ), while it is negatively correlated with the temperature (correlation factor of -0.81,  $p < 0.05$ ). The pH varies from 7.88 to 8.05 and shows a similar longitudinal profile to that of dissolved oxygen with an increase seaward [correlation factor of 0.90 ( $p < 0.01$ )].

The total amount of SPM ( $> 0.45 \mu\text{m}$ ) is 185 mg L<sup>-1</sup> at station S22 (~ 1 PSU) indicating that the SPM levels in the inner zone of the estuary is consistent with the relatively high flow of the Scheldt recorded during the campaign (see Table 1), bringing more suspended materials resulting from increasing erosion



and resuspension processes. Then, it steeply decreases to  $49 \text{ mg L}^{-1}$  and remains at values below  $75 \text{ mg L}^{-1}$ , oscillating seaward.

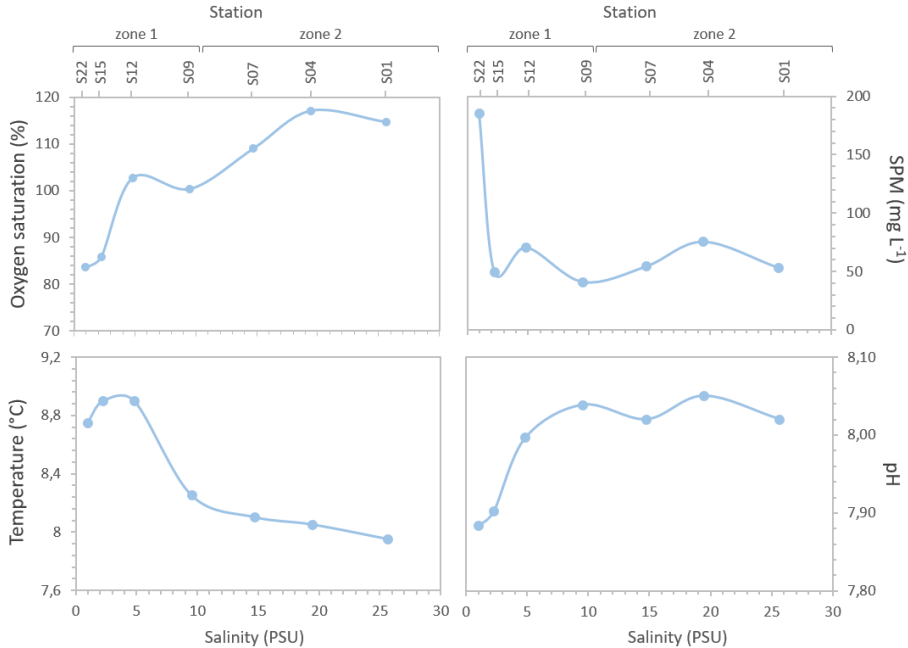


**Figure 2.2:** Hydrographic records and SPM amount along the Scheldt Estuary as a function of salinity.

## 2.3.2. Dissolved trace metal fractions

### 2.3.2.1. Labile trace metals

Along the estuary, the labile trace metal content varies with the salinity gradient and follows fluctuating trends (Figure 2.3). Generally, the labile concentration of Cd, Co, Cu and Ni is decreasing from the most upper estuarine station (S22) to the one (S01) close to the sea, while labile fractions of Cr and Pb present a fluctuated trend. However, labile Cd and Cu start to decrease sharply by a factor 2 from station S22 to S15, before another increase until station S09 in the middle estuary. The estuarine fraction from S22 to S09

(zone 1) is the most dynamic zone, with the most fluctuations in terms of trace metal distribution. Then in the last kilometers to the sea, labile Cd and Cu finally decrease again reaching their lowest concentrations of the whole estuary.

Labile Pb and Cr concentrations increase progressively in zone 1, until the middle estuary. This concentration peak appears at the same point where elevations of labile Cd and Cu appeared too. Seaward, their concentration levels drop to reach minimum values of  $0.06 \mu\text{g L}^{-1}$  for Pb and of  $0.12 \mu\text{g L}^{-1}$  for Cr. At station S01, their labile concentrations eventually reach similar values as at station S22 (the upper estuary).

Along the whole estuary, labile Co and Ni show simple dilution trends with a decrease from  $0.25$  to  $0.07 \mu\text{g L}^{-1}$  for Co, and from  $1.51$  to  $0.78 \mu\text{g L}^{-1}$  for Ni. Both elements reach a plateau in the middle estuary, between 5 and 10 PSU, before their labile concentrations progressively decrease seaward.

### **2.3.2.2. Total dissolved trace metals**

The dissolved trace metal concentration also varies with the salinity gradient and follows different trends (Figure 2.3). On one hand, dissolved Cd shows a general increasing tendency seaward and its concentrations range between  $0.05 \mu\text{g L}^{-1}$  and  $0.15 \mu\text{g L}^{-1}$ . In zone 1, the dissolved Cd content almost rises threefold, before stabilizing in zone 2.

Conversely, Co, Cu, Ni and Pb display clear decreasing trends seaward. The dissolved concentration ranges of these trace metals are  $0.12 - 0.53 \mu\text{g L}^{-1}$  for Co,  $1.78 - 4.58 \mu\text{g L}^{-1}$  for Cu,  $0.44 - 2.77 \mu\text{g L}^{-1}$  for Ni and  $0.10 - 0.28 \mu\text{g L}^{-1}$  for Pb. While Cu and Ni exhibits a concentration decrease as a function of salinity, dissolved Co and Pb initially show a sharp decline in the first 10 km

of the estuary and then, with less intensity, they progressively decrease to the sea.

Finally, the longitudinal variations of dissolved Cr are more variable along the transect: the concentration is quite constant (around  $0.25 \mu\text{g L}^{-1}$ ) excepted for station S04 ( $\sim 20$  PSU) where a maximum is clearly identified ( $0.42 \mu\text{g L}^{-1}$ ).

However, the labile Cd concentration is higher than its total dissolved concentration at station S22 and the labile Cr and Pb concentrations are higher than their total dissolved concentrations at station S09, which can be explained by the difference in sampling methods used for these two fractions. The labile fraction is assessed through a passive sampling technique (DGT) giving a time-weighted average concentration, while the total dissolved fraction is measured through an active sampling technique providing a “snapshot”, at one given time, of the actual dissolved concentration.

### **2.3.3. Particulate trace metal**

The particulate trace metals in the water column present similar profiles for all the studied elements (Figure 2.3), with a clear decreasing trend from the upper estuary towards the sea. The values range are  $3.5 - 0.52 \mu\text{g g}^{-1}$  for Cd,  $193 - 59 \mu\text{g g}^{-1}$  for Cr,  $25 - 6 \mu\text{g g}^{-1}$  for Co,  $74 - 13 \mu\text{g g}^{-1}$  for Cu,  $60 - 22 \mu\text{g g}^{-1}$  for Ni and  $109 - 24 \mu\text{g g}^{-1}$  for Pb. These particulate metals initially show a significant increase in the first 10 km of the estuary, with the exception of Cd which remains stable in this area. Then, all of them progressively decrease to the sea, over 60 km.

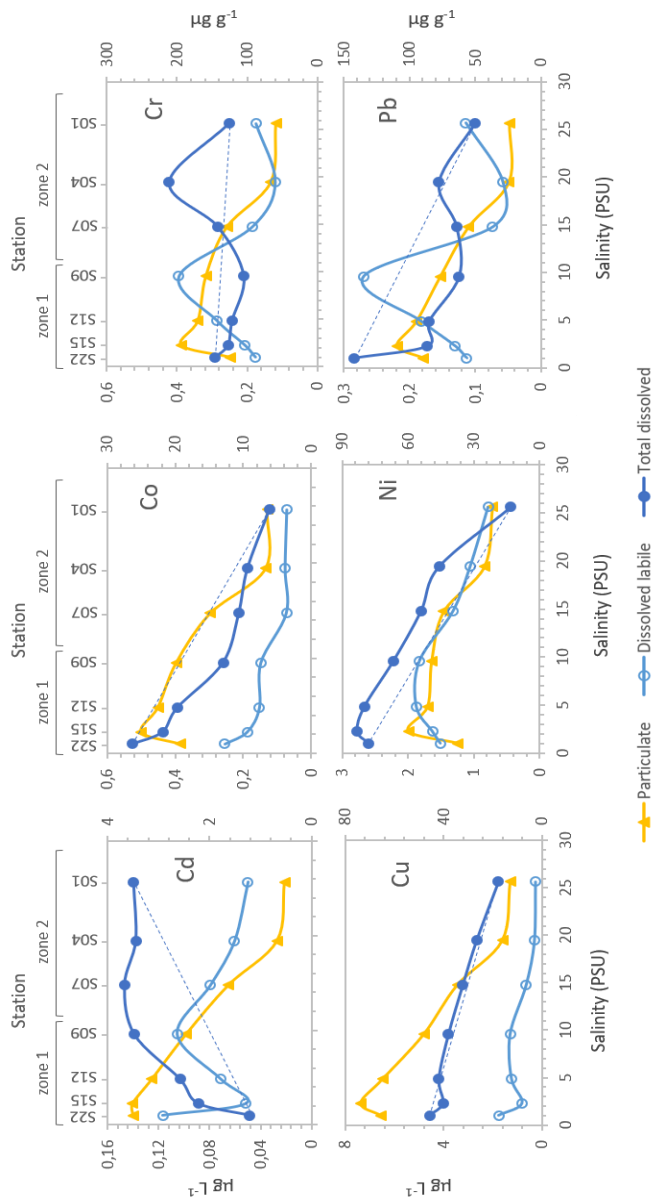


**Figure 2.3:** Longitudinal profiles of trace metals along the Scheldt Estuary waters. Particulate concentrations are given in  $\mu\text{g g}^{-1}$  (yellow; right y-axis), dissolved ones in  $\mu\text{g L}^{-1}$  (dark blue; left y-axis) and labile ones in  $\mu\text{g L}^{-1}$  (light blue; left y-axis). The Theoretical Dilution Line (TDL) of the total dissolved compounds is shown by the dark blue dash-line.

### **2.3.4. Partitioning of trace metals between solid and dissolved phases**

Trace element speciation significantly changes along the estuary. Figure 2.4 reports the longitudinal distribution of the different metal fractions. Three trace metal pools have been considered in the water column: a dissolved labile metal fraction, a dissolved non-labile metal fraction and a particulate metal fraction. Pb and Cr show similar partitioning along the estuary: their particulate fraction accounts for more than 90% of the total concentration. As the dissolved labile concentrations of Cr and Pb show high variabilities, the comparison with the total dissolved concentrations was, in this case not relevant and is therefore not included in the figure. Thus, only the total dissolved fraction is shown on Figure 2.4. It has a small contribution for both elements and only shows a slight increase seaward.

Ni and Co follow the same longitudinal pattern as Cr and Pb, yet for Ni the particulate fraction is less pronounced and the labile fraction accounts for 18 to 45% of total Ni. However, most of Co is in the particulate fraction (> 70%) and an equal partitioning is found between labile Co and non-labile Co.

Cd and Cu behave differently along the estuary. First, Cd shows a clear partitioning pattern: in zone 1 (< 10 PSU), particulate Cd is the most important fraction and accounts for ~ 72% of the total content. However, it progressively decreases seaward, handing over to dissolved Cd. The junction between particulate and dissolved fraction is especially marked in the middle estuary, between station S12 and S09 (~ 5 and ~ 10 PSU, respectively). The labile phase of Cd is dominant in the first zone and then decreases to finally be balanced with the non-labile phase, from the middle estuary to the sea.

Cu is dominated by the dissolved fraction (accounting for 55% of the total on average) which gradually increases along the salinity gradient. The dissolved non-labile fraction accounts for most of the dissolved concentration and labile Cu remains below 22% of the total content and below 39% of the dissolved fraction.

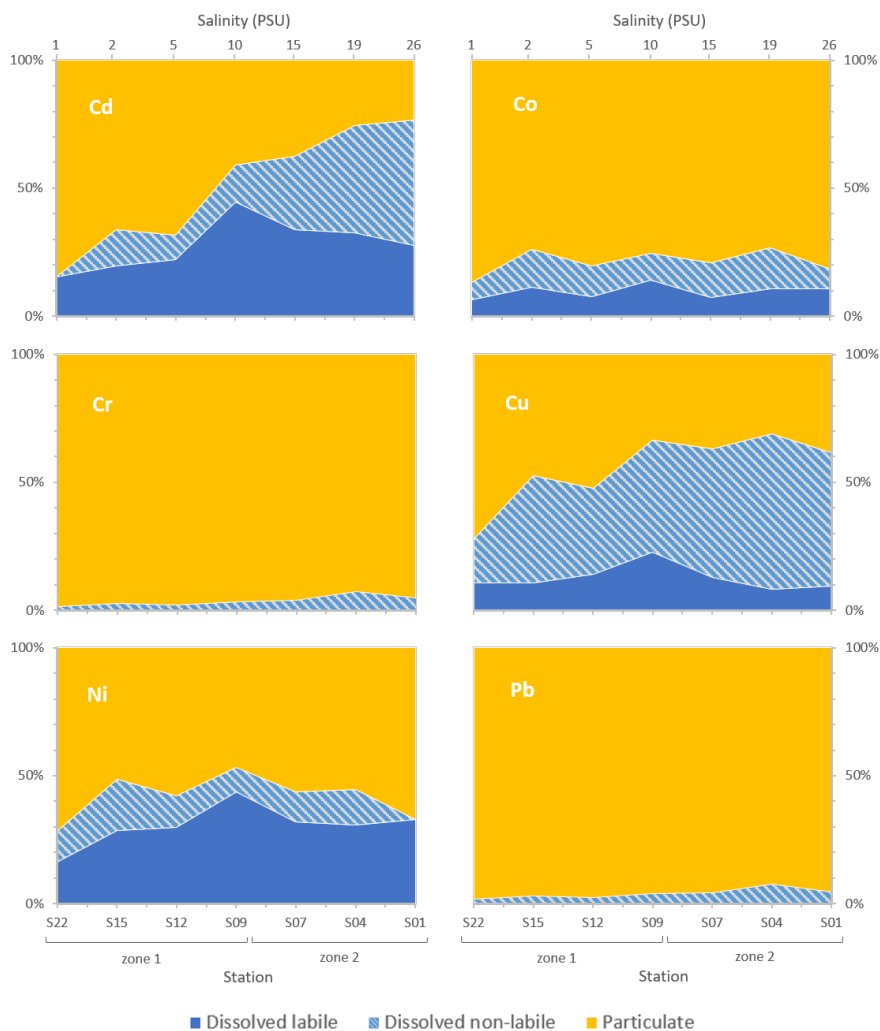


**Figure 2.4:** Longitudinal profiles of trace metal speciation along the Scheldt Estuary waters. The total metal load in the water column is illustrated by the 100% value. The particulate fraction is depicted in yellow (the particulate fraction is converted to  $\mu\text{g L}^{-1}$  taking into account the SPM concentration in the water column) and the dissolved fraction is split into two distinct phases: the dissolved labile elements (free ions or weak dissolved complexes, dynamic form) given in dark blue, and the dissolved non-labile elements (colloidal, non-dynamic) given in light blue and resulting from the subtraction between total dissolved and labile concentrations. For Cr and Pb, only the total dissolved fraction is depicted.

## **2.4. Discussion**

### **2.4.1. Environmental forces and processes along a salinity gradient**

The salinity gradient allows a division of the estuary in two zones: zone 1 (1 to 10 PSU) and zone 2 (10 to 26 PSU), and can be easily related to those defined and studied by Baeyens (1998; see 2.4.3.2 for further comparisons). Zone 1 (comprising stations S09, S12, S15 and S22) appears like a mesohaline area, where the river discharge occurs. Zone 2 (comprising stations S01, S04 and S07) forms the polyhaline area of the estuary. First, Baeyens (1998) has shown that zone 1 has often the most variable SPM concentrations due to variety of sources involved. In March 2019, the Scheldt Estuary was likely in flood (Table 2.1). This indicates that the freshwater discharge and forces might had a greater influence in the upper part of the estuary during the sampling campaign, as likely indicated by the reduced salinity and higher SPM content at station S22 (Figure 2.2). There, the river discharge influence is clearly observed: the temperature and the SPM amount are high, while the available oxygen and the pH are lower than in the rest of the estuary. This state remains quite short, as a steep decrease of SPM amount occurs: SPM are rapidly reduced and/or quickly settle down to the bottom. This flocculation is usually generated by an increase of salinity, which balances the negatively charged surface of freshwater particles (*i.e.* Van der Waals forces; Sholkovitz, 1978). Further on, dissolved oxygen, pH, and SPM slightly increase, due to various mixing forces between freshwater and seawater. Higher SPM concentrations at stations S04, S12 and S22 are suggested to be linked with higher disturbance of the estuarine bed (for S04 and S12) due the occurrence of new source of water discharge and stronger mixing zones, and with an amplified erosion of the upstream banks (for S22). The elevated amount of



carbonate compounds brought by the increasing salinity results in a pH rise seaward (de Souza Machado et al., 2016).

Ultimately, the obvious salinity gradient is one of the first typical aspects occurring in an estuary and is the root of various physicochemical changes and processes, including non-conservative behavior of trace metals (de Souza Machado et al., 2016; Drexler et al., 2003), as observed here (Fig. 2.3). By changing the water density and physicochemical properties (dissolved oxygen, pH, SPM, etc.), the salinity influences trace element mobilization, availability and potential toxicity (Du Laing et al., 2008; Iglesias et al., 2020; Valenta et al., 1986).

## **2.4.2. Trace metal speciation along the Scheldt Estuary**

### **2.4.2.1. Influence of estuarine features on trace metal speciation**

The river discharge is the main driver for the speciation of elements in the estuary. Thus, in the first zone (< 10 PSU), turbidity and SPM amount are high, and the particulate fraction of trace metals is the highest of the whole transect. More specifically, the maximum turbidity is observed at station S22, which is a classic feature of estuaries, where high amount of SPM and metal complexes are found, flowing from surrounding rivers, bottom sediments and usually accentuated by physical forces such as tides, mixing forces, etc. (Hobbie, 2000; Robert et al., 2004). Upstream, the high quantity of SPM results in higher trace metal adsorption and precipitation on particles (i.e. effect of the ionic strength which neutralizes colloids) (Baeyens, 1998; Gonzalez et al., 2007), explaining the highest particulate trace metals found at this station. Further, higher ionic strength and the presence of anions and cations tend to desorb the trace elements from particles. Thus, the metallic

contamination mainly comes from the upper streams and rivers and a combination of particulate dilution and mixing with less contaminated downstream waters makes the particulate metal contents decrease when the salinity is higher than 2 PSU.

The trace metals of interest in this study are not only influenced by conservative dilution mechanisms. The non-conservative pattern are indeed recorded for all the dissolved elements (to less extent for Cu and Ni, after station S15) implies a removal of these elements during the estuarine mixing, via flocculation and sedimentation processes. The longitudinal profiles (Fig. 2.3) suggest a removal of Co, Cr and Pb during the estuarine mixing via flocculation and sedimentation processes which are particularly important in zone 1. Dissolved Cu and Ni are less affected by such mechanisms than the other elements and shows a near-conservative behavior, even unreactive. This could most likely imply higher residence time in the estuary water column and later in the sea, compared to other elements which get more easily trapped in the sediment (Turner et al., 1998).

Around 5 PSU (station S12), a slight local maximum in particulate metal concentrations suggests a potential addition of these elements in the environment, via other riverine inputs or sediment resuspension (Fig. 2.3). As there is no water discharge here and given the increase of SPM in this area, the remobilization of particles from sediments (at this station and from tidal flats located around) would be the main reason (de Souza Machado et al., 2016; Teuchies et al., 2013).

At the end of the transect (i.e. close to the sea mouth), Co, Cu and Ni show stabilizing particulate concentrations, while their dissolved concentrations keep on decreasing. In this area where the estuary is strongly influenced by the sea fluxes, marine phytoplankton may play a role in trace metal

mobilization: a biological uptake could indeed lead to a transfer of Co, Cu and Ni from the dissolved pool to the particulate one (Paquin et al., 2003). This hypothesis could also be supported by the fact that marine phytoplankton (mostly diatoms) only thrive until the limit with brackish waters and usually show a first Spring bloom at the end of March, when the sampling was done. Freshwater phytoplankton appear much later, in Summer (Naithani et al., 2016). To confirm this assumption, a measurement of the total organic carbon content of the water could be performed.

The evolution of labile trace metals along the estuary seems more variable: several fluctuations appear along the transect, including a peak at 10 PSU for all elements (Figure 2.3). This mid-estuary peak is co-registered with the appearance of a strong mixing-zone (between zone 1 and zone 2). This has been interpreted as due to the desorption of labile elements from particles, which were locally and tidally resuspended into the water column (Martino et al., 2004, Baeyens et al., 1998). Several labile metals (Cd, Co and Ni) constitute a non-negligible fraction of the dissolved pool all along the estuary. One explanation could be large riverine inputs of labile elements due to the high river flow (Chester, 1990), coupled with the release from decomposing organic matter in the benthic zone (Braungardt et al., 2011; Waeles et al., 2009) and from dissolved humic substances (Balch and Guéguen, 2015; Mangal et al., 2016). Overall, the bioavailability of trace metals seems to fluctuate significantly in the estuary, given the variations of labile concentrations: organisms might therefore be subject to different degrees of exposure if they move along the estuarine zones (Iglesias et al., 2020; Vicente-Martorell et al., 2009): especially, station S09 and S22 often show the highest labile concentrations.

The constant increase of the dissolved Cd fraction along the estuary (Figure 2.4) is mainly linked to its desorption from SPM due to the increasing salinity.

Cd indeed tends to form stable and dissolved complexes with chloride and sulfate (Bingham et al., 1984; Lefèvre et al., 2009), but also with low-molecular-weight organic ligands (Waeles et al., 2008). Thus, the estuarine water column is enriched in dissolved Cd mainly stemming from upstream particles. In the seaward direction, a shift towards dissolved non-labile phases of Cd appears, in contrast to the zone 1 where the labile contribution is clearly dominant. Thus, the formation of labile chloro- and/or sulfato-complexes might be more effective until a salinity of 10 PSU, labile species being more available upstream. While dissolved Cd organic complexes are formed later along the estuary (zone 2), resulting from SPM desorption (Waeles et al., 2005). The same speciation pattern was also observed earlier in the Scheldt estuary by Baeyens et al. (1998), elsewhere in the Po river plume by Illuminati et al. (2019) and in the Venice lagoon by Morabito et al. (2018). As suggested by Illuminati et al. (2019), the colloidal Cd (*i.e.* dissolved non-labile) forming from 10 PSU to the sea might result from the adsorption and/or uptake of Cd on/in nanoplanktons (small algal cells like Coccolithophorids or Dinoflagellates) or with phytoplankton exudates. Such association can be enhanced by high concentrations of calcium in the water (Perfus-Barbeoch et al., 2002).

Co and Ni are little influenced by sorption processes, even unreactive to estuarine mixing because both elements only show very small variations of their distribution along the transect. The contribution of particulate Co is slightly more important than particulate Ni. In the dissolved fractions, labile Ni is dominant while a more balanced distribution between the non-labile and the labile phases is observed for Co. In a study carried out in English estuaries, Turner et al. (1998) and later Martino et al. (2004) have also shown a low biogeochemical reactivity of Ni in the estuarine waters, emphasized by its low particle-affinity and by the presence of specific dissolved organic ligands.

In the Scheldt estuarine waters, Cr and Pb speciation is undoubtedly dominated by their particulate fractions. They do not seem to be heavily affected by desorption processes and keep their particle-reactive character all along the estuary (Illuminati et al., 2019a; Santschi et al., 1980; Schulz-Baldes et al., 1983). The high daily discharge at the time of sampling (Table 2.1) could explain the higher contribution of the particulate fraction over the area, and also the intense sedimentation in the upper estuary. Regarding the dissolved pool of Cr and Pb, their labile concentrations (indicative of bioavailability) seem highly variable (Fig. 2.3). Both elements only show a slight increase of their total dissolved fraction in the direction of the sea: with increasing salinity, free ions like  $\text{Ca}^{2+}$  and  $\text{Na}^{2+}$  can indeed feebly replace bound trace elements from particles as demonstrated by Fairbrother et al. (2007). The distribution of Pb between the particulate and the dissolved pools is in agreement with previous studies (Braungardt et al., 2011; Illuminati et al., 2019a). Regarding Cr, Cr(III) might be the most represented one along the estuary given its affinity to the particulate pool in aquatic environments (Gustafsson et al., 2014; Pađan et al., 2019). Thus, the dissolved pool may be mainly composed of stable dissolved Cr(VI) oxo-complexes, as investigated by Pađan et al. (2019) in Krka Estuary (Croatia).

As observed for Cd, the dissolved fraction of Cu keeps increasing seaward as well. However, Cu distribution within the dissolved fraction is different from that of Cd, as the transfer of Cu is made towards non-labile species all along the transect. A continuous solubilization of Cu is therefore noticed, from the upper estuary to its mouth. The resulting dissolved Cu species are strongly bound to dissolved organic ligands, reducing the amount of free Cu ions which can accumulate on the DGT samplers. The strong complexation of Cu with dissolved organic matter also limits the process of biosorption in organisms, in contrast with Cd (see above). The same observations were obtained by

Zitoun (2019) in New Zealand estuaries and by Ndungu et al. (2005) in the bay of San Francisco. Both studies revealed that non-labile Cu accounted for more than 97% of the dissolved Cu and highlighted the role of dissolved organic compounds in regulating Cu speciation.

#### **2.4.2.2. Identification of critical zones**

As no labile reference value yet exists, our labile metal concentrations have been compared with Environmental Quality Standards (EQS) for dissolved trace metal concentrations in seawater (Directive 2000/60/CE and 2008/105/CE; Maycock et al., 2011). In this condition, labile levels are all below the EQS-yearly average values (EQS-YA). In the same way, they are all below the Acute Water Quality Criteria (WQC; Durán and Beiras, 2013), except labile Cu whose concentrations at stations S09, S12 and S22 exceed the recommended probabilistic value of  $1.39 \mu\text{g L}^{-1}$ . Dissolved concentrations of all studied metals are also below the EQS-yearly average values (EQS-YA). However, the dissolved Cd concentration measured at S07 is relatively close to its EQS-YA value of  $0.2 \mu\text{g L}^{-1}$ . In addition, they are all below the WQC, except for dissolved Cu exceeding the recommended probabilistic value of  $1.39 \mu\text{g L}^{-1}$  at all stations.

To get a better insight on the toxicity degree of the measured labile and dissolved concentrations, the results of Cd, Cu, Ni and Pb were also compared to Predicted No-Effect Concentrations (PNEC) proposed by Källqvist (2007). Our concentrations for labile and dissolved Pb are all below the PNEC of  $2.49 \mu\text{g L}^{-1}$ , irregardless of the sampling point. The concentrations obtained for Cd remain rather close to the PNEC value of  $0.18 \mu\text{g L}^{-1}$ , especially at stations S22 and S09 (for labile Cd) and from the mid-estuary (S09) to the sea (for dissolved Cd), but do not exceed it. However, the dissolved concentrations of

Cu (as well as labile, except at station S01 and S04) exceed the PNEC defined for Cu ( $0.64 \mu\text{g L}^{-1}$ ). In the same way, dissolved concentrations measured for Ni at all stations (except S01, the closest to the sea) and labile ones at S09, S12 and S15 are higher than the PNEC proposed by Källqvist (2007;  $1.53 \mu\text{g L}^{-1}$ ).

Particulate Cd, Co (except values found at station S04 and S01), Cr, Cu (except values found at station S01), Ni and Pb (except values found at station S04 and S01) are above the pedogeochemical references defined in the region (Sterckeman et al., 2007). In order to draw a parallel between the level of particulate metals along the estuary and the actual contamination level of suspended particles, an enrichment factor was calculated for each element, as follows (Eq. 2.1):

$$EF(Me) = \left(\frac{Me}{Al}\right)_{sample} / \left(\frac{Me}{Al}\right)_{background}$$

Equation 2.1

Where EF is the enrichment factor, Me is a trace metal,  $\left(\frac{Me}{Al}\right)_{sample}$  is the ratio of the particulate metal and Al concentration in the sample, and  $\left(\frac{Me}{Al}\right)_{background}$  is the ratio of the background metal and Al concentration (natural median levels in earth's crust). EF values are ranked into five categories ranging from low ( $EF < 2$ ) to extremely high enrichment ( $EF > 40$ ) (Barbieri, 2016). EF values of Co, Cu, Cr and Ni are  $\leq 2$ , which is equivalent to a minimal enrichment (Figure 2.5). Upstream (between station S22 and S12), the estuarine SPM show a significant enrichment in Pb and a very high enrichment in Cd. From S09 ( $\sim 10$  PSU) to the sea, the EF decreases to a moderate enrichment in Pb and to a significant enrichment in Cd.

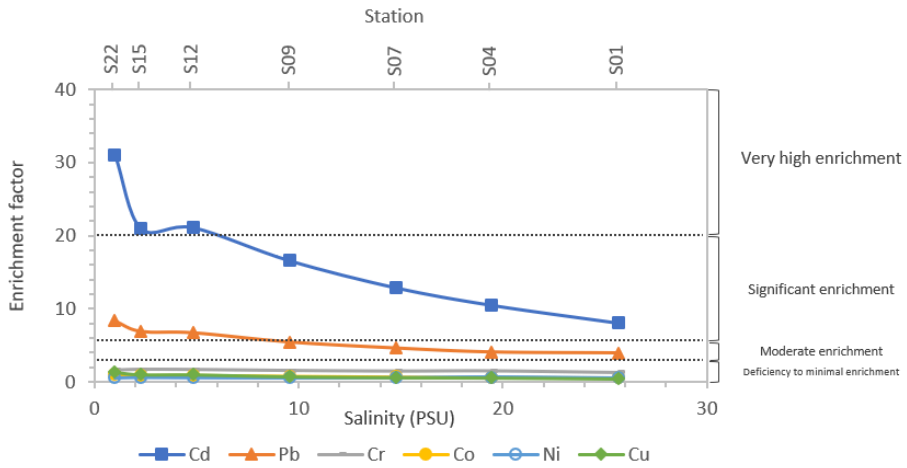


**Figure 2.5:** Enrichment factor of suspended particles trace metals, along the Scheldt Estuary.

In terms of contamination, the most critical areas are located in the upper part of the estuary where the highest concentrations and enrichments are found: this is especially true for Cd and Pb, yet they are considered as substances of priority concern by the OSPAR Convention (OSPAR, 2009, 2002). SPM are less and less contaminated along the estuary, but a large quantity of SPM is also lost at the beginning of the estuary towards the estuarine bed, due to sedimentation. The dissolved pool seems less worrying than the particulate one, but specific attention needs to be made on dissolved Cd (station S07), Cu (all stations) and Ni (all stations except S01) for future monitoring surveys. Concerns around an increasing use of copper-based antifouling paints on boats are nowadays rising, because they might increase the release of dissolved Cu concentrations in aquatic environments (Matthiessen et al., 1999; Warnken et al., 1999; Elskens et al., 2014; Lagerström et al., 2020). However, a direct impact of Cu on the estuarine ecosystem cannot be fully confirmed here, as an



important fraction of dissolved Cu is strongly bound with dissolved organic matter and thus, remains non-labile (i.e. less accessible to organisms).

### **2.4.3. The Scheldt Estuary situation in Europe and in time**

#### **2.4.3.1. Temporal evolution of the metallic loads in the Scheldt Estuary**

In answer to the growing scientific and public concern around pollution status and contamination of aquatic environments, European environmental policies and regulations have settled on different directives regarding trace metal level in water (Water Framework Directive, Marine Strategy Framework Directive; European Parliament and of the Council, 2000). In comparison with the research previously done by Baeyens (1998; Table 2.2), the total dissolved and particulate profiles of Cd, Cu, Ni and Pb recorded in the present study follow the same general trends as those recorded in the 80's and in the 90's in the Scheldt Estuary. However, particulate trace metal concentrations in the Scheldt Estuary have largely decreased between 1978 and 1988 following the implementation of regulation policies regarding atmospheric emissions and direct wastewater discharges, and kept on decreasing until 2010 with less intensities, as highlighted by Gao et al. (2013). Our results of particulate Cd, Cu and Pb are in good agreement with this decreasing trend, at the fluvial and marine endmembers but also in the middle estuary. In the same study, Gao et al. have simultaneously shown that total dissolved trace metal concentrations of Cd, Cu and Pb tend to increase in the Scheldt from 1990 on, highlighting a shift from the particulate to the dissolved phase. Our measurements are also in line with this observation. Along the same lines, the logarithm of the partition coefficient  $K_D$  is calculated (Gaulier et al., 2019 for the calculation details) and compared with those of previous studies on the Scheldt (Table

2.2): the average  $K_D$  ranking obtained in this study is in good agreement with the past measurements, *i.e.*  $Cr > Pb > Co > Ni > Cd > Cu$ . Overall, Cr and Pb clearly shows a higher affinity for the particulate phase than the other elements, while Cu is the most soluble element. In this study, all the  $K_D$  values are lower than those obtained in the last decades, except for Ni for which insufficient data for comparison was reported in previous work. This difference is even higher in the fluvial and marine endmembers than in the middle estuary. Moreover, the  $K_D$  decrease seems stronger for Cd and Cu than for Pb. This demonstrates the lesser affinity of Cd, Cu and Pb for the particulate phase over time, and might increase the concern around dissolved harmful compounds in the Scheldt Estuary (Baeyens et al., 2005; Gao et al., 2013).

If considering an alternative “labile”  $K_D$  using labile concentrations of trace metals instead of total dissolved ones, the average  $K_D$  ranking would be slightly different in the Scheldt Estuary, *i.e.*  $Cr > Pb > Co > Cu > Ni > Cd$ . In this new pattern, Cd and Ni show more concern than the other elements, as they tend to be more bioavailable, while Cr and Pb are less worrying, as shown with the “classic”  $K_D$ .

**Table 2.2:** Evolution of the average dissolved and particulate metal concentrations in the Scheldt Estuary, from 1978 until today (no former data was found on Cr and Co measurements).

	Year	Cd			Cu			Ni			Pb			References	
		<i>Flu.</i>	<i>Mid.</i>	<i>Mar.</i>	<i>Flu.</i>	<i>Mid.</i>	<i>Mar.</i>	<i>Flu.</i>	<i>Mid.</i>	<i>Mar.</i>	<i>Flu.</i>	<i>Mid.</i>	<i>Mar.</i>		
Dissolved	1978	0.06		0.12										Duinker et al., 1982	
$\mu\text{g L}^{-1}$	1981-1983	0.09		0.07	1.0		1.1				0.23	0.18		Baeyens et al., 1998	
	1987-1988	0.02		0.05	1.0		1.0							Zwolsman and Van Eck, 1993	
	1991-1994	0.02		0.07	1.6		1.0							Paucot and Wollast, 1997	
	1995	0.02		0.05	0.7		0.7				0.17	0.05		Baeyens et al., 1998	
	1995-1997		0.07	0.04		2.3	0.9				0.14	0.13		Gao et al., 2013	
	1995-1998	0.02	0.05	0.03	1.3	1.0	0.8	4.7	4.9	1.0	0.26	0.47	0.10		Baeyens et al., 2005
	2009-2010		0.21	0.06		3.0	1.7				0.14	0.11			Gao et al., 2013
	2010	0.05		0.09	2.2		1.2				0.27	0.10			Gao et al., 2013
	2019	0.05	0.10	0.14	4.6	4.2	1.8	2.6	2.7	0.4	0.28	0.17	0.10		This study
Particulate	1978	45.0		5.0										Duinker et al., 1982	
$\text{mg kg}^{-1}$	1979	52.0			271						334			Salomon et al., 1981	
	1981-1983	27.9		1.8	278		31				288	83		Baeyens et al., 1998	
	1987-1988	12.2		1.2	213		29				207	63		Zwolsman and van Eck, 1993	
	1991-1994	8.3		1.3	159		32							Paucot and Wollast, 1997	
	1995	8.8		0.8	112		17				214	45		Baeyens et al., 1998	
	1995-1997		5.1	0.8		73	20				118	49		Gao et al., 2013	
	1995-1998	7.2	6.4	0.9	104	100	20	40	35	23	166	149	44		Baeyens et al., 2005
	2009-2010		3.5	0.5		65	19					85	41		Gao et al., 2013
	2010	4.3		0.5	77		15				120		28		Gao et al., 2013
	2010-2011	3.4	2.1	<LOD	58	46	24	27	22	20	105	72	39		Van Ael et al., 2017
2019	3.5	3.1	0.5	66	65	13	37	51	22	89	95	24		This study	
Log $K_D$	1978	5.91		4.62										Duinker et al., 1982	
	1981-1983	5.51		4.41	5.44		4.45				6.10	5.66		Baeyens et al., 1998	
	1987-1988	5.79		4.38	5.35		4.48							Zwolsman and van Eck, 1993	
	1991-1994	5.64		4.30	5.01		4.49							Paucot and Wollast, 1997	
	1995	5.64		4.24	5.22		4.38				6.10	5.95		Baeyens et al., 1998	
	1995-1997		4.86	4.31		4.50	4.36				5.93	5.58		Gao et al., 2013	
	1995-1998	5.68	5.11	4.42	4.92	5.00	4.38	3.93	3.85	4.37	5.81	5.50	5.66		Baeyens et al., 2005
	2009-2010		4.22	3.92		4.34	4.06				5.78	5.57			Gao et al., 2013
	2010	4.93		3.75	4.54		4.10				5.65	5.45			Gao et al., 2013
	2019	4.85	4.49	3.55	4.16	4.19	3.86	4.15	4.28	4.70	5.50	5.75	5.38		This study
Log $K_D$ "labile"	2019	4.48	4.64	4.02	4.57	4.72	4.68	4.39	4.44	4.44	5.90	5.72	5.33		This study

*Flu.* (Fluvial) = S22; *Mid.* (Middle) = S12; *Mar.* (Marine) = S01

One of the main reasons for the increase of dissolved concentrations would be the recent (2006) implementation of a wastewater treatment system in Brussels and Antwerp (Belgium) urban areas, which has widely changed the Scheldt water composition and therefore influenced the dissolved oxygen concentration and the speciation of trace elements (Meire et al., 2005). A different composition of particles linked with a higher amount of dissolved organic complexes could also be another explanation for the change in affinity of trace metals regarding the dissolved or particulate phase (Gao et al., 2013). At a larger scale, the switch observed from particulate to dissolved phases could also be linked to a global acidification of marine environments due to the climate change. But even if the decline in pH estimated or observed in the North Atlantic Ocean or in the North Sea (Blackford and Gilbert, 2007; Lauvset and Gruber, 2014; Ríos et al., 2015; Vázquez-Rodríguez et al., 2012 - for instance, -0.1 pH units since pre-industrial times in the North Sea) could match relatively well with the increase of dissolved trace metals, it is hard to predict how significant this relation is or will be in the Scheldt Estuary, and how acidification may disturb interactions and processes of marine biogeochemical cycles (Blackford and Gilbert, 2007). For future monitoring, it is suggested that pH should be systematically measured during sampling for speciation studies.

Unfortunately, and to our knowledge, research surveys attempting to measure labile concentrations of trace elements in estuaries are few and far between, even nonexistent here, in the Scheldt Estuary. In order to overcome this issue, and because labile concentrations of compounds should be a good indicator of their bioavailability, our results are compared to several measurements of trace metals which accumulated in various estuarine species along the Scheldt Estuary. For most of them, the selected sampling location are similar to the ones studied here. Thus, a comparison could be made between concentrations

found in biota and labile levels recorded at a same location. First and for instance, Van Ael et al. (2017) reported Cd and Ni concentrations in shrimp muscle and in shore crab hepatopancreas which appear to show the same variations along the Scheldt as the labile values obtained in our study. The same was also observed for Pb in *Oligochaeta* and in European flounder gills. Cr and Cd in shrimp hepatopancreas and, to a lesser extent Cu, were also in good agreement with our data. In De Wolf et al. (2000), the author measured different trace elements bioaccumulated in soft body parts and shells of the periwinkle *Littorina littorea*: Cd, Ni and Pb show the same peak of concentration as the labile ones measured here (at ~ 10 PSU). Finally, Co and Cd concentrations measured along the Scheldt Estuary in *Mytilus edulis* by Wepener et al. (2008) seem to follow the same trend as their labile levels, assessed in this study.

#### **2.4.3.2. Comparison with other European estuaries**

The concentrations of three metal species considered in this study (particulate, dissolved and labile) are compared to literature data of the Belgian Coastal Zone (BCZ; where the Scheldt Estuary flows) and of different estuarine systems in Europe (Table 2.3). Both dissolved and particulate values recorded in the BCZ are in the same order of magnitude as those measured in this study (Gaulier et al., 2019). More precisely, they are really similar to the results found at the estuary mouth (station S01, ~ 26 PSU). The only exception is particulate Cu which is higher in harbors of the BCZ than along the estuary, most likely due to the intense boat traffics in harbors coupled with the use of antifouling paints for boat which are copper-based (Gaulier et al., 2019b; Jones and Bolam, 2007). Furthermore, labile trace metals in the Scheldt Estuary show two- or three-times higher concentrations than those found in

the BCZ. Regarding their speciation, dissolved Cd is the dominant species in both systems and, while particulate Pb is the main one (Gaulier et al., 2019b). In the same way, Cu and Ni total contents are dominated by their dissolved fraction as shown in the same studies (except at offshore stations, located further away in the North Sea). Same speciation patterns have been shown in previous studies in the same areas (Baeyens et al., 1987). Yet, the surroundings have changed a lot since 1987 when the latter study was performed (more inhabitants, different human activities but also different regulations regarding emissions and discharges of pollutants, new wastewater treatment system, etc.). This eventually indicates that the nature and composition of water inputs might have evolved with time, but the general speciation pattern remains most likely the same.

Further, and within the dissolved fraction, non-labile Cd is the dominant species in the BCZ, which eventually fits with the increase of the Cd non-labile phase which was observed seaward. Finally, Co shows the same speciation pattern in the Scheldt Estuary as the one observed in the industrial harbor of Zeebrugge, a city located 10 km away from the Scheldt Estuary mouth (Gaulier et al., 2019b). The concentrations of dissolved Cd, Cu and Pb in the Atlantic Ocean (Aparicio-González et al., 2012) were all lower than those in the Scheldt estuary.

Moreover, dissolved Cd and Pb concentrations are, on average, higher than those measured in other European estuaries listed on table 2.3 (dissolved values from 0.002 to 0.09  $\mu\text{g L}^{-1}$ ) and remain in the same range of values as in the Arno, the Ebro and the Seine estuaries. Dissolved levels of Cu and Ni are in good agreement with measurements described in the literature (from 0.4 to 5.0  $\mu\text{g L}^{-1}$  on average for Cu, 1.32  $\mu\text{g L}^{-1}$  measured in Acheloos for Ni). Only the Severn estuary (UK) shows higher range of dissolved variations for Cd, Cu and Pb at least (0.11 - 0.40  $\mu\text{g L}^{-1}$ , 4.0 - 5.0  $\mu\text{g L}^{-1}$  and 0.39  $\mu\text{g L}^{-1}$ ,

respectively). Particulate Cd, Cu, Ni and Pb are all higher in the Scheldt Estuary than in other European estuaries of France, Italy, Croatia and Greece. Compared to most of the estuaries depicted in table 2.3, the Scheldt Estuary shows a higher population density, as well as more industrial and agricultural activities around its shore: this could easily explain the higher concentrations of trace metals observed.

In a nutshell, the level of trace metals measured in the BCZ shows a good link with the Scheldt Estuary content. The Scheldt Estuary seems to be more contaminated than other estuaries in Europe (for dissolved and particulate Cd, particulate Cu and particulate Ni, at least), after the Severn Estuary which drains a heavily industrialized and urbanized mining region and shows either comparable or higher concentrations of trace metals than in the Scheldt Estuary.

**Table 2.3:** Overview of trace metal concentrations around the Scheldt Estuary's mouth and along various estuaries in Europe.

Site	Labile (L; $\mu\text{g L}^{-1}$ ), Dissolved (D; $\mu\text{g L}^{-1}$ ) and Particulate (P; $\mu\text{g L}^{-1}$ ) concentrations						References
	Cd	Co	Cr	Cu	Ni	Pb	
Scheldt Estuary	0.05-0.12 (L), 0.05-0.15 (D), 0.04-0.64 (P)	0.07-0.25 (L), 0.12-0.53 (D), 0.52-3.44 (P)	0.12-0.39 (L), 0.21-0.42 (D), 4.9-21.9 (P)	0.27-1.76 (L), 1.78-4.58 (D), 1.1-11.8 (P)	0.78-1.87 (L), 0.44-2.77 (D), 1.6-6.6 (P)	0.06-0.27 (L), 0.10-0.28 (D), 1.9-16.1 (P)	This study
Belgian Coastal Zone	0.02 (L), 0.12 (D), 0.03 (P)	0.08 (L), 0.14 (D), 0.21 (P)	0.04 (L)	0.24 (L), 1.44 (D), 2.28 (P)	0.43 (L), 0.98 (D), 0.68 (P)	0.04 (L), 0.12 (D), 1.0 (P)	Gaulier et al., 2019
Atlantic Ocean	0.01 (D)			0.1 (D)		0.02 (D)	Aparicio-González et al., 2012
European Estuaries							
Severn, UK	0.11-0.40 (D)			4.0-5.0 (D)		0.39 (D)	Harper, 1991
Tay, UK	0.01 (D)			0.8 (D)		0.13 (D)	Owens and Balls, 1997
Aber Wrac'h, FR	0.04 (D), 0.01 (P)			0.4-0.6 (D), 0.29 (P)			L'Her Roux et al, 1998
Gironde, FR	0.004-0.09 (D)			0.1-1.3 (D)			Michel et al., 2000
Huveaunne, FR	0.01 (D)			1.7 (D)		0.13 (D)	Oursel et al., 2013
Jarret, FR	0.01 (D)			1.8 (D)		0.08 (D)	Oursel et al., 2013
Loire, FR	0.01-0.03 (D)			0.5-1.3 (D)			Waelles et al., 2004
Rhône, FR				2.1 (D)		0.07 (D)	Ollivier et al, 2011
Seine, FR	0.03-0.20 (D)			0.76-2.29 (D)			Chiffolleau et al, 1994
Ebro, SP	0.12 (D)			1.0 (D)		0.16 (D)	Dorten et al., 1991
Marche estuaries, IT	0.01-0.020 (D), 0.01-0.02 (P)			0.4-1.97 (D), 0.1-1.0 (P)		0.07-0.15 (D), 0.03-1.86 (P)	Annibaldi et al., 2015
Arno, IT	0.1 (D)			1.7 (D)		0.2 (D)	Dorten et al., 1991
Krka, CR	0.002 (D), 0.001 (P)			0.28 (D), 0.39 (P)		0.01 (D), 0.02 (P)	Cindrić et al., 2015
Acheloos, GR				0.68 (D), 0.31 (P)	1.32 (D), 2.76 (P)	0.23 (D), 0.25 (P)	Dassenakis et al., 1997

## 2.5. Conclusion

The biogeochemical behavior of Cd, Co, Cr, Cu, Ni and Pb was studied along the strongly urbanized Scheldt Estuary. For the first time, labile trace metal concentrations were measured *in-situ* in the estuary using the DGT passive sampling technique, giving an insight into their bioavailability towards the estuarine ecosystem over a specific time period. The dissolved and particulate



trace metal concentrations were assessed as well, using classic active sampling techniques. This highlighted the variations of trace metal speciation and their partitioning coefficients in the estuarine surface waters, considering environmental and physicochemical gradients. Despite their high ecological values, estuaries are constantly changing environments, which greatly influence biogeochemical cycles of trace metals including their availability towards estuarine ecosystems. In the Scheldt Estuary for instance, dissolved trace metals show a non-conservative behavior due to the influence of various environmental gradients, such as salinity, dissolved oxygen content, etc. and due to local mechanisms, such as sediment resuspension, runoffs along the shore, etc. Moreover, different zones could be drawn, based on trace metal changes in concentration and partitioning mainly influenced by physicochemical processes of adsorption/desorption. Thus, all metals eventually display an increase in their lability in the mid-estuary zone, while they are mainly bound to particles when entering the estuary. Metals like Co, Cr, Ni and Pb mainly remain under an unreactive particulate form, while others like Cd, Cu undergo several desorption and solubilization processes throughout the whole estuary. Furthermore, from the SPM and particulate concentrations measured, we supposed that the sediment constitutes an important reservoir for metallic compounds in the upper part of the estuary, while it can also be an additional source further along the Scheldt, where the salinity varies a lot.

The comparison with literature data allowed to redraw the continuum of trace metals from the Scheldt estuary to the North Sea and further, highlighting the importance of the estuary as a major source of material. In Europe, the Scheldt Estuary remains one of the most contaminated inlets: Cd, Cu and Ni being the most concerning elements which will surely need more monitoring. Moreover, the trace metal loads have widely and interestingly evolved from the 80's until

today: showing decreasing particulate trace metal concentrations, while the dissolved ones tend to rise. Such pattern will also require an extensive monitoring in the years to come. If the population growth and the input of dissolved organic matter due to the new wastewater treatment plant keep rising, it might lead to an increase of the labile metal concentrations, which could be a major concern in a near future. Indeed, the higher the labile fraction, the more the element is bioavailable and the larger the threat for the marine ecosystem (Baeyens et al., 2018a; Simpson et al., 2012). Thus, future research should focus more on the monitoring of this labile phase and on its correlation with changing conditions such as tidal cycles, rising temperatures and seawater levels, changes in estuarine water circulation.

In addition, and for the years to come, the intense development of the marine, agriculture and tourism sectors is expected to continue. While pursuing the regulation of the ecological status of marine environments, the main challenge of future water-related directives would therefore be to guarantee the sustainability of this development, from an environmental appreciation. Concurrently, the sea level is also expected to increase, bringing along even more concerns: it might affect various estuarine components directly related to biogeochemical cycles of trace metals, like the freshwater discharge, the remobilization of elements from upper soil (which the water could not reach before), etc. (Meire et al., 2005). The seawater rise will most likely involve a rising of the salinity gradient within the estuary: its impact on upstream environment which are more polluted will need a better follow-up in the future, concurrently with a reinforcement of trace metal monitoring in their most concerning phase (*i.e.* labile). Finally, further studies should be carried out on the effects of higher river discharges (during flood, extremely rainy periods, snow melt etc.) on trace metal speciation as it seems to influence the proportion of labile trace metals brought from the river to the estuary.

## **Acknowledgement**

The authors would like to thank the funding bodies from the NewSTHEPS project (BR/143/A2/NEWTHEPS, FOD12, BELSPO), the VUB SPR2 and the Chinese Scholar Council (PhD fellowship 201606190219). The RV Belgica crew members, the scientific vessel of the Belgian government, are thanked for the sampling campaign.

## 2.6. Supplementary Information

The Supplementary Information includes 2 tables.

**Table S2.1:** Use of reference materials for the measurement of particulate trace metals (IAEA-405; estuarine sediment, International Atomic Energy Agency) and for the analysis of trace metals by HR-ICP-MS.

		Cd	Pb	Cr	Co	Ni	Cu
		<i>mg/kg</i>	<i>mg/kg</i>	<i>mg/kg</i>	<i>mg/kg</i>	<i>mg/kg</i>	<i>mg/kg</i>
IAEA-405	measured	0.798	73.6	95	15.3	27.4	44.2
	certified	0.73	74.8	84	13.7	32.5	47.7
	recovery	109%	98%	113%	112%	84%	93%
SLRS-6	measured	0.0085	0.17	0.253	0.043	0.585	29.1
	certified	0.0063	0.17	0.252	0.053	0.616	23.9
	recovery	135%	100%	100%	81%	95%	122%

**Table S2.2:** Correlation and associated p-value matrices for the physicochemical measurements.

### Correlation matrix

	<i>conductivity</i>	<i>salinity</i>	<i>temperature</i>	<i>pH</i>	<i>O2</i>	<i>% saturation</i>	<i>SPM</i>
conductivity	1						
salinity	1,00	1					
temperature	-0,92	-0,92	1				
pH	0,76	0,74	-0,76	1			
O2	0,76	0,75	-0,68	0,93	1		
% saturation	0,91	0,90	-0,81	0,90	0,96	1	
SPM	-0,46	-0,43	0,35	-0,63	-0,51	-0,50	1

*Salinity measures the amount of salts in water. Salinity and conductivity show a very good correlation, because dissolved ions increase salinity as well as conductivity.*

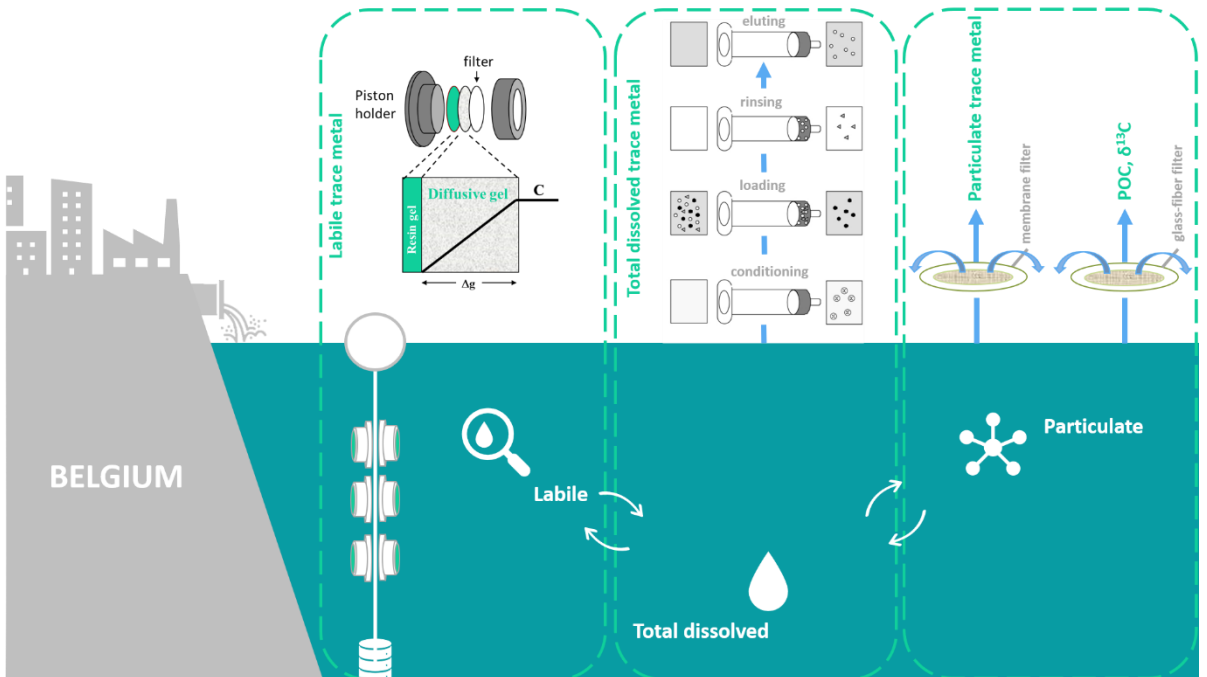
**p-values**

	<i>conductivity</i>	<i>salinity</i>	<i>temperature</i>	<i>pH</i>	<i>O2</i>	<i>% saturation</i>	<i>SPM</i>
conductivity	0						
salinity	0,0001	0					
temperature	0,013	0,004	0				
pH	0,050	0,056	0,049	0			
O2	0,047	0,053	0,090	0,00 2	0		
% saturation	0,004	0,005	0,026	0,00 6	0,00 1	0	
SPM	0,344	0,334	0,436	0,12 9	0,24 1	0,249	0



# Chapter 3

## Trace metal speciation in North Sea coastal waters



## Trace metal speciation in North Sea coastal waters

*Adapted from Gaulier C., Zhou C., Guo W., Bratkic A., Superville P.-J., Billon G., Baeyens W., Gao Y. (2019). Science of The Total Environment 692, 701–712. doi: 10.1016/j.scitotenv.2019.07.314*

### Abstract

Most trace metals exhibit a dual role in marine waters, acting as nutrients at low concentration and being toxic at high concentration. But besides concentration range, speciation is also an important factor. They both show both seasonal and spatial variations. A thorough comparison between total dissolved and particulate concentrations estimated from manual sampling and an assessment of the bioavailability using Diffusive Gradients in Thin Films (DGT) has been performed in this work for Cd, Co, Cu, Ni and Pb, at several sampling points of the Belgian Coastal Zone (BCZ). Additional information to trace back the origin and identify the anthropogenic fingerprint of Suspended Particulate Matter (SPM) was measured using stable carbon isotope measurements in particulate organic matter. Our results show that: (i) particulate and total dissolved metal concentrations are higher at two stations, one in the harbor of Oostende and one offshore; (ii) dissolved and particulate trace metal concentrations do not correlate with the dissolved labile fractions; and (iii) SPM in the harbor zone is likely from allochthonous sources, while in the offshore station marine origin has been evidenced. Our results indicate that, even though contamination is higher in the harbor zones, the trace metal toxicity, which is linked to the metal bioavailability, is most likely not higher than in the open sea. However, with increasing acidification of the ocean, a shift from particulate to dissolved phase might lead to increasing adverse effects on the coastal environment.

**Keywords:** Diffusive Gradients in Thin-films, Trace metals, Lability, Coastal Environment, Belgian Coastal Zone



### **3.1. Introduction**

Anthropogenic pressures and pollution issues are nowadays difficult topics to avoid when discussing about environmental research. Humans have certainly seriously changed and reformed the environment. During the XIX century, at the beginning of the industrial era, mines, plastic or fertilizer producers and refineries appeared on our landscape releasing tons of pollutants. These organic and inorganic contaminants have been emitted for decades and by entering aquatic environments in various ways, they display adverse effects on these ecosystems today. The Belgian Coastal Zone (BCZ) is an example of an historically polluted area via metallic inputs from atmospheric deposition, direct wastewater discharge from coastal industries and the Scheldt Estuary which is enriched in trace metals from the industrial site of Antwerp (W. Baeyens, 1998; Paucot and Wollast, 1997; Van Ael et al., 2017; Zwolsman et al., 1996). The BCZ constitutes a transition area between the heavily polluted Scheldt estuary and the clean Atlantic waters entering the North Sea through the English Channel. Thus, the BCZ is an interesting area to study trace metal behavior, because of the variety of anthropogenic inputs (W. Baeyens et al., 1998).

Even if European environmental policies and regulations have taken actions to lower pollutant emissions (see for example the Water Framework Directive), their effect on the contamination level in marine systems is sometimes still surprising. While particulate trace metal levels decreased in the BCZ (Zwolsman et al., 1996), the dissolved trace metal concentrations increased in the last decade (Gao et al., 2013). The change in metal species from particulate to dissolved phase is nowadays a big concern because it could influence more directly the bioavailability of trace metals (TM) towards marine fauna and flora in the North Sea.

Our research is part of the NewSTHEPS project (New Strategies To assess Hazardous chemicals in the Environment using Passive Samplers, Belgian Science Policy Office) and aims at developing new monitoring systems and models for pollutants in the Belgian Coastal Zone, and eventually assessing the resulting anthropogenic pressure on the marine environment ([www.newstheps.be](http://www.newstheps.be)). In this project, trace metal speciation, in which particulate and dissolved phases were separated using 0.45µm filtration, was investigated in the water column. However, the total dissolved trace metal concentration is not representative for the bioavailable metal fraction, the toxicity potential and the impact on the marine ecosystem: therefore, labile fractions of trace metal complexes were studied using the passive sampling technique of Diffusive Gradients in Thin-films (DGT; Davison, 2016). It has been shown that the bioavailable fraction corresponds to free metal ions and the most labile trace metal complexes (e.g. Baeyens et al., 2018; Simpson et al., 2012; Tessier and Turner, 1995).

Besides the assessment of metal pollutant levels, it is also interesting to obtain information about the origin of those pollutants. Carbon and nitrogen contents and their isotopic signatures in Suspended Particulate Matter (SPM) will help us to determine the origin (autochthonous or allochthonous) of the particulate organic matter (Raymond and Bauer, 2001). The objectives of the study presented here are (i) to explore the lability of trace metals in the water column of the Belgian North Sea coastal zone using DGT probes; this is also the first time that DGT samplers are deployed *in situ* in the water column of the BCZ, for studying the speciation of dissolved pollutants. (ii) to characterize the environmental status of this specific aquatic environment; (iii) to compare the trace metal behavior in Belgian coastal harbors with an offshore location; and finally (iv) to assess the anthropogenic pressure on coastal ecosystems by tracing back the origin of the Suspended Particulate Matter (SPM).

## **3.2. Material and methods**

### **3.2.1. Chemicals and materials**

For the material cleaning and preparation (Niskin and Teflon bottles, Teflon and glass plates), nitric acid ( $\text{HNO}_3$ ; Fisher, Trace Metal Grade, 65%), distilled nitric acid (distilled in the laboratory), Milli Q water (Millipore) were used. For DGT preparation, Chelex<sup>®</sup>-100 (Bio-Rad, 200-400 mesh size), cross-linker (DGT Research, Lancaster), acrylamide (40%, Merck), ammonium persulfate (APS; Merck), tetramethylethylenediamine (TEMED; Merck, >99%), DGT pistons (caps and bases, DGT research, Lancaster), 0.45  $\mu\text{m}$ -pore size filter membranes and NaCl (Merck, Suprapur) were used. For DGT treatment, 1M  $\text{HNO}_3$  was prepared by diluting 63 mL  $\text{HNO}_3$  (Fisher, Trace Metal Grade, 65%) to 937 mL Milli Q water. For sample treatments, distilled nitric acid ( $\text{HNO}_3$ ; Fisher, Trace Metal Grade, 65%; distilled in the laboratory), Milli Q water (Millipore), ammonia ( $\text{NH}_3$ ; Merck, Suprapur, 25%), glacial acetic acid ( $\text{CH}_3\text{COOH}$ ; Fisher, Trace Metal Grade, >99%), HCl (Fisher, Trace Metal Grade, 37%), HF (Fischer, Trace Metal Grade, 40%) and  $\text{H}_3\text{BO}_3$  (Fischer, Trace Metal Grade, 4%) were used.

### **3.2.2. Study sites**

The BCZ is a shallow marine environment as the water depth varies between 15 and 30 meters. This part of the North Sea is also particular for its high turbidity and low salinity due to the mixing of estuarine water with seawater and to strong tidal currents. The outflow of the Scheldt estuary creates a gyre in front of the Belgian coast which strongly increases the residence time of solutes and particles in this area (W. Baeyens et al., 1998; Nihoul and Hecq, 1984; Paucot and Wollast, 1997).

In this study, five stations were selected and sampled during sampling campaigns in Spring and Autumn (in April and October 2017, in March and October 2018). Four stations are located in two harbors along the Belgian coast: HO-1 and HO-2 in Oostende, HZ-1 and HZ-2 in Zeebrugge. The fifth station OZ-MOW1 is located in the North Sea, about 5 km away from the coastline (Figure 3.1). The coordinates of each station are mentioned in the Supplementary Information (SI). Oostende and Zeebrugge harbors have both hosted a variety of industrial harbor activities for several decades and are therefore good candidates for the study of marine sites polluted by high metal loads. Strong tidal currents at station OZ-MOW1, which is an offshore station resulted in loss of passive samplers. Therefore, no DGT data are available for this station in 2018.



**Figure 3.1:** Location of the sampling sites on the Belgian Coastal Zone (BCZ; adapted from Chemical Oceanography Unit, University of Liège, 2008)

### 3.2.3. DGT sampling and analysis

The DGT technique relies on controlled diffusive transport of the analyte and is either used in the water column (e.g. Baeyens et al., 2011; Zhang and Davison, 1995) to assess labile trace metal fractions or inserted vertically in sediments (e.g. Gao et al., 2006, 2015; Zhang et al., 2002) to determine high-resolution profiles of trace element concentrations and/or fluxes at the water-sediment interface. It is generally composed of two hydrogel layers: a polyacrylamide hydrogel that is backed up by a second polyacrylamide hydrogel layer containing the metal-selective Chelex®-100 accumulative resin. DGT samplers allow us to obtain a time integrated concentration of the labile trace metal fractions in an aquatic system (Davison, 2016b). The labile metal concentrations obtained from DGT measurement are good indicators of the element bioavailability in the environment (Bade et al., 2012; Roig et al., 2011; Sierra et al., 2017; Simpson et al., 2012), i.e. as a general case, the bioavailability is dependent on the labile metal concentration, estimated by  $C_{DGT}$  in our work (Baeyens et al., 2018b). The DGT piston consists of a round plastic molding (a cap and a piston base, both assembled), holding together three successive layers, which are, from the cap to the bottom piston: a membrane filter (0.45  $\mu\text{m}$  pore size cellulose acetate – 0.125 mm thick), a diffusive hydrogel (polyacrylamide hydrogel – 0.8 mm thick) and finally a resin gel (binding Chelex®-100 resin – 0.4 mm thick).

The diffusive hydrogel, the resin gel and DGT probes were prepared and handled under a laminar flow hood in a clean laboratory room before each campaign and according to the method reported by Zhang and Davison (Zhang and Davison, 1995) and described in the Supplementary Information (SI). At each sampling station, 6 DGT pistons were enclosed in a plastic cage which was held with a nylon rope 2 m below the water surface, anchored to the seabed using a weight and lifted to the surface with the help of a buoy. The

deployment time and temperature at each station were recorded during the campaigns and were further used for DGT concentration calculations.

After deployment and recovery of the DGT devices in the field, the labile trace metals, accumulated on the resin gel, were eluted in 1 mL of 1M HNO<sub>3</sub> for at least 24 hours. The eluents were then diluted ten times with MQ-water prior to their analysis. From the total mass of accumulated metal, the average labile trace metal concentration was calculated following Fick's law (Eqn 3.1), assuming perfect sink conditions (*i.e.* all metal ions arriving at the interface between the diffusive hydrogel and the resin gel are immediately bound to the resin):

$$C_{DGT} = \frac{m \times \Delta G}{D \times A \times t} \quad \text{Equation 3.1}$$

where  $C_{DGT}$  is the labile metal concentration in the seawater in  $\mu\text{g L}^{-1}$ ,  $m$  is the trace metal mass accumulated on the resin gel,  $\Delta G$  is the total thickness of the diffusive domain in cm [diffusive gel, membrane filter, Diffusive Boundary Layer (DBL, 0.2 mm; see SI for details)],  $D$  is the diffusion coefficient of the trace metal in  $\text{E}^{-6} \text{cm}^2 \text{s}^{-1}$ ,  $A$  is the DGT piston window area in  $\text{cm}^2$  and  $t$  is the deployment time of the piston in s.

### **3.2.4. Sampling and sample treatment for metals**

#### **3.2.4.1. Total dissolved trace metals**

At the same time DGTs were deployed, seawater samples were taken 2 m below the surface using HDPE Niskin bottles. Prior to use, these bottles were cleaned with 10% HNO<sub>3</sub>, rinsed three times with Milli-Q water in the laboratory and with seawater in the field. 500 mL of seawater samples were then filtered using 0.45  $\mu\text{m}$  pre-weighted filter membranes (Durapore<sup>®</sup>, HVLP grade). The solution was acidified with 0.2% distilled HNO<sub>3</sub> and then stored in clean Teflon bottles. The filters were later treated for the analysis of

particulate compounds. As dissolved trace metals are generally present in the BCZ at  $\text{ng L}^{-1}$  levels (W. Baeyens et al., 1998), their concentrations are often close to the detection limit of most analytical instruments. Moreover, the complexity of the seawater matrix represents a second challenging issue for ICP-MS analysis. The salt matrix can crystallize and cause clogging of instrument tubing and nebulizer, and even damage some parts of the instrument. In order to avoid these analytical problems, a pre-concentration method using a solid-phase extraction (SPE) of the trace element from the seawater sample with a cation-exchange resin (Chelex<sup>®</sup>-100, 200-400 mesh size), is proposed.

To 100 mL of filtered and acidified seawater, 2.5 mL of concentrated ammonium acetate buffer were added to reach a sample pH of 5. Next, a succession of treatments was carried out on the Chelex-100 resin all at a flow rate of  $4 \text{ mL min}^{-1}$ : (1) the pre-conditioning of the home-made column with 10 mL 2M  $\text{HNO}_3$  / 1M HCl, 10 mL Milli-Q-water, 10 mL diluted  $\text{NH}_4\text{Ac}$  (pH 5) and 10 mL Milli-Q-water; (2) loading of the samples on the column, with retention of the metals on the resin; (3) rinsing of the column with 10 mL of diluted  $\text{NH}_4\text{Ac}$  (pH 5) and 10 mL Milli-Q-water, in order to remove the salt matrix and also other interfering elements from the resin; (4) elution of the trace metals from the column using 2M  $\text{HNO}_3$  as eluting agent. The reagent preparations are described in the SI. The acidic eluent resulting from this last step was stored at  $4^\circ\text{C}$  prior to analysis. In order to validate the method, a multi-element standard solution (Merck, ICP-MS standard XIII, 1ppm; including Cd, Cu, Pb, Ni, Co) was used as a spike in North Sea samples, reaching a concentration of  $10 \mu\text{g L}^{-1}$  and then introduced into the SPE system before testing the real seawater samples. The recovery of Cd, Cu, Pb, Ni, Co was respectively 90, 95, 86, 96, and 96%.

#### **3.2.4.2. Particulate metals**

The filters used for seawater sample filtration were dried under a laminar flow hood for 2 days and weighted again. The mass difference of the filters was recorded for the calculation of particulate metal concentrations. The filters were then introduced into clean Teflon tubes where 3mL of concentrated HF (40%), 3mL of concentrated HCl (37%) and 1mL of concentrated HNO<sub>3</sub> (65%) were added. The solution was heated at 70°C overnight and finally after cooling down, 20 mL of H<sub>3</sub>BO<sub>3</sub> (4%) were added to the Teflon bottles. This solution was then heated at 70°C for three hours. Once the solution was cooled down again, it was transferred to PE vessels and further diluted for analysis. To validate the process, two certified reference materials MESS-3 (marine sediment, National Research Council Canada) and IAEA-405 (estuarine sediment, International Atomic Energy Agency) were treated in the same way as samples. All reference sample results were within the range of the certified values.

#### **3.2.5. Sampling and sample treatment for organic matter**

500 mL of seawater samples were collected in a similar way as for metals, then filtered using 0.70 µm pre-treated (*i.e.* heated at 500 °C for 2 hours) and pre-weighted glass-microfiber filters (Sartorius Stedim Biotech, 0.70 µm pore size, MGF grade). For each station, three replicates were carried out. After filtration, the glass-microfiber filters were dried in the oven at 50°C overnight and weighted again. The filters were then used for particulate carbon concentrations (POC) and isotope ratio determinations. A subsample of each filter was placed for 24 hours in an acid-fume chamber (HCl fumes) to remove the carbonate fraction and therefore only organic carbon content was obtained. The acidified subsamples were then heated to 50 °C during at least two hours, folded, enclosed in tin cups and analyzed. Another subsample of each filter



was also folded, enclosed in tin cups without any additional treatment and analyzed, in order to measure its total carbon (inorganic and organic) content.

### **3.2.6. Analysis and validation**

#### **3.2.6.1. Trace metal analysis**

In the final solutions, trace metals (Cd, Cu, Pb, Ni, Co and Al) were determined using a High Resolution-Inductively Coupled Plasma Mass Spectrometer instrument (HR-ICP-MS, Thermo Finnigan Element II). Calibration was carried out with appropriate dilutions of an acidified multi-element stock solution (Merck, ICP-MS standard XIII). Indium was used as an internal standard. Limits of detection (LOD) were around 0.002  $\mu\text{g L}^{-1}$  for Cd, 0.05  $\mu\text{g L}^{-1}$  for Cu, 0.011  $\mu\text{g L}^{-1}$  for Pb, 0.005  $\mu\text{g L}^{-1}$  for Co, 0.033  $\mu\text{g L}^{-1}$  for Ni and 6.8  $\mu\text{g L}^{-1}$  for Al. The relative standard deviation (RSD) was about 10% for all metal species.

#### **3.2.6.2. Carbon and stable isotope ratio analysis**

The amount of POC and the stable isotope ratio of the samples were determined using an Elemental Analyzer coupled with an Isotope Ratio Mass Spectrometry (EA-IRMS instrument, Flash EA112, Delta V Plus, Thermo Scientific). Isotope ratios are here reported in the conventional isotope terminology and calculated following the formula (Eqn 3.2):

$$\delta(\text{‰}) = \frac{R_{\text{sample}}}{R_{\text{standard}}} \times 1000 \quad \text{Equation 3.2}$$

where  $\delta$  stands for  $\delta^{13}\text{C}$  and  $R_{\text{sample}}$  and  $R_{\text{standard}}$  are the  $^{13}\text{C}/^{12}\text{C}$  ratios of the sample and the standard, respectively. For carbon measurements, the certified reference material IAEA-CH6 sucrose was used as internal standard. The RSD of the measurements was below 7%.

### **3.2.7. Statistical analysis**

Statistical analyses were performed based on a Principal Component Analysis (PCA) and a Hierarchical Ascending Classification method (HAC) using the R data processing software ([www.r-project.org](http://www.r-project.org)). Two packages were used in this study: corrplot and FactoMineR. These multidimensional exploratory statistics allowed individuals (here, the sampling points) to be divided into groups, called clusters, so that similar individuals are in the same group. In a nutshell, the aim is to build homogeneous groups depending on the results obtained for each sampling point. For the parameters, the aim is to search for correlations between the labile, total dissolved and particulate trace metals.

## **3.3. Results**

### **3.3.1. Suspended Particulate Matter**

#### **3.3.1.1. Particulate carbon concentrations and stable isotope ratios**

SPM amount at station OZ-MOW1 is much higher than at the harbor stations and reaches its highest peak in October 2017 ( $304 \text{ mg L}^{-1}$ ; Figure 3.2). Tidal currents at the offshore station are usually stronger than in the coastal harbors, causing much higher resuspension of bottom sediments and higher SPM concentrations. Conversely, station HO-1 shows the lowest amount of SPM in October 2017, below  $50 \text{ mg L}^{-1}$ . In most cases, the carbon content of SPM is dominated by  $C_{\text{org}}$  with percentages ranging between 45 and 100% of total C, but stations OZ-MOW1 and HZ-2 also show a high amount of inorganic C (respectively 44% and 36% of total C in average). No particular seasonal trend is noticed at our scale of monitoring. In terms of concentration, POC contents are higher at OZ-MOW1 than in the harbors reaching a maximum value of  $275 \text{ }\mu\text{M}$  in October 2017. At OZ-MOW1, the POC concentration varies

around 1.5-3.6 mg L<sup>-1</sup> of carbon. Compared to the 200-300 mg L<sup>-1</sup> of SPM, the organic fraction is very small. This is typical for a shallow sea with sandy sediments and strong tidal currents. Conversely, the values are the lowest in Zeebrugge harbor; it varies from 14 to 106 μM at HZ-1 and from 17 to 85 μM at HZ-2. Moreover, POC contents in the harbor stations exhibit the highest values in Springtime, with the maximum concentration found at HO-2 (164 μM). δ<sup>13</sup>C isotopic ratios fluctuate over a wide range: between -41 and 3.4‰. At the harbor stations, δ<sup>13</sup>C isotopic ratios increase from Spring to Autumn in both years (Fig. 3.2). In contrast, δ<sup>13</sup>C values remain stable at around -20‰, at the marine station OZ-MOW1.

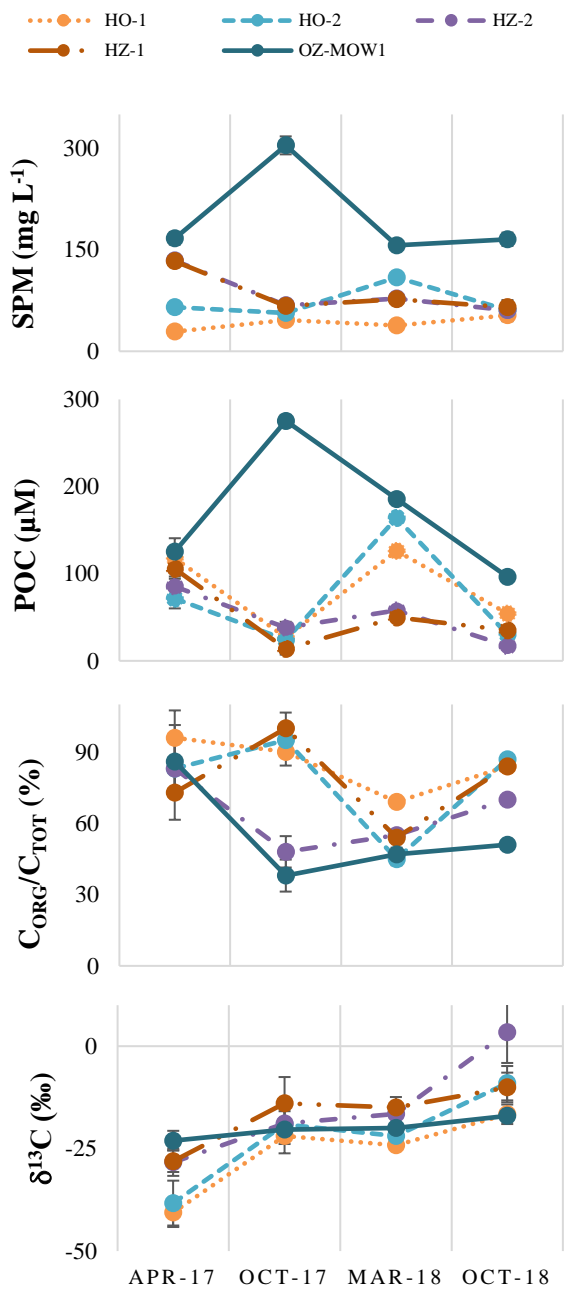


**Figure 3.2:** Seasonal variations of the SPM composition in the BCZ water column

### **3.3.1.2. Particulate metals**

Particulate trace metal values have been normalized to those of aluminum, as this element is the major component of fine-grained aluminosilicates which are strongly associated with trace metals. Aluminum is commonly used as a reference element when studying metal contents in marine SPM (Dehairs et al., 1989; Regnier and Wollast, 1993). The range of particulate normalized ( $\times 10^4$ ) concentrations is 1-3 for Co, 2-67 for Cu, <0.2-35 for Ni, 0.1-2.5 for Cd, 4-217 for Pb (Table 3.1).

**Table 3.1:** Seasonal and spatial variations of particulate trace metal concentrations in the BCZ water column, normalized to Al x10<sup>4</sup>

<i>Element</i>	<i>Station</i>	min. - max.	Average	Median	EQS* particulate (mg kg <sup>-1</sup> )	BRCs* particulate
Cd	HO-1	0.1 - 2.4	0.9	0.6		
	HO-2	0.1 - 2.5	0.9	0.5		
	HZ-2	0.2 - 2	0.7	0.3	2.5	0.018
	HZ-1	0.1 - 1.1	0.5	0.3		
	OZ-MOW1	0.1 - 0.3	0.1	0.1		
Pb	HO-1	11 - 217	66	18		
	HO-2	6 - 17	10	9		
	HZ-2	4 - 8	6	6	53.4	1.7
	HZ-1	4 - 8	6	6		
	OZ-MOW1	4 - 12	7	5		
Co	HO-1	2 - 3	2	2		
	HO-2	1 - 2	2	2		
	HZ-2	1 - 2	2	2	-	3
	HZ-1	1 - 2	2	2		
	OZ-MOW1	2 - 3	2	2		
Ni	HO-1	4 - 35	16	12		
	HO-2	0.3 - 6	3	3		
	HZ-2	<0.2 - 5	3	4	4.3	10.6
	HZ-1	2 - 13	6	4		
	OZ-MOW1	4 - 15	8	6		
Cu	HO-1	15 - 56	35	34		
	HO-2	6 - 16	10	9		
	HZ-2	10 - 15	13	12	-	7.8
	HZ-1	4 - 12	8	9		
	OZ-MOW1	2 - 67	19	4		

\*Environmental Quality Standard (EQS); Background/Reference Concentrations (BRCs; reference in Earth's crust, normalized to Al x10<sup>4</sup>)

These broad ranges highlight spatially and temporally concentration differences. For particulate Cd, all stations follow the same trend: the concentrations increase from 2017 to 2018 (+ 0.2 offshore and + 1.5 in the harbors), and values are higher for Oostende harbor stations. For the other elements, the temporal trends seem to be station and element dependent. Particulate Co concentrations remain steady over the whole year and at all stations, with average values of 2. SPM is most enriched in Cd, Cu, Ni, Pb, and Co at station HO-1 (Table 3.1), despite its low amount. Station OZ-MOW1, which is supposedly less influenced by anthropogenic activities as it is situated further away from the coastline, is the second most contaminated in particulate trace metals, only for Cd and Pb station HO-2 shows higher levels. Conversely, Zeebrugge harbor stations (HZ-1 and HZ-2) show the lowest values for all elements.

Regarding Water Quality Standards for particulate trace metals in seawater (Bass et al., 2008; Grimwood and Dixon, 1997), particulate concentrations of Cd and Pb are below the threshold values of the Environmental Quality Standard (EQS), except for Pb at station HO-1 where the EQS value (53.4 mg kg<sup>-1</sup>) is exceeded (66 mg kg<sup>-1</sup>). Particulate concentrations measured for Ni are above the EQS value of 4.3 mg kg<sup>-1</sup>, except for stations HO-2 and HZ-2. The particulate concentrations of Cd, Cu and Pb are all above the Background/Reference Concentrations (BRCs) and those of Co and Ni are all below the BRCs, except for particulate Ni found at HO-1.

The enrichment factor (EF) is determined for each trace metal as follows (Eqn 3.3):

$$EF(Me) = \left(\frac{Me}{Al}\right)_{sample} / \left(\frac{Me}{Al}\right)_{background} \quad \text{Equation 3.3}$$

Where  $EF$  is the enrichment factor,  $Me$  is a trace metal,  $\left(\frac{Me}{Al}\right)_{sample}$  is the ratio of the particulate metal and Al concentration in the sample, and  $\left(\frac{Me}{Al}\right)_{background}$  is the ratio of the background metal and Al concentration (natural median levels in earth's crust).  $EF$  values are ranked into five categories ranging from low ( $EF < 2$ ) to high enrichment ( $EF > 40$ ) (Barbieri, 2016) and are given in SI. Overall, SPM shows a wide range of enrichment for all trace metals and at all stations.  $EF$  values of Co and Ni are  $\leq 2$ , which is equivalent to a minimal enrichment. The same is true for Cu, at the Zeebrugge harbor stations and HO-2. Moderate enrichments are observed for Cu (HO-1 and OZ-MOW1), and Pb (Zeebrugge harbor stations and OZ-MOW1). Finally, very high enrichments are found for particulate Pb (Oostende harbor stations) and Cd (all stations). Regardless of the element, the highest enrichment is always found at station HO-1, while the lowest ones are found at HZ-1 for Pb and Cu, at HZ-2 for Ni and Co and at OZ-MOW1 for Cd. In average, particulate Cd displays the highest  $EF$  values.

### **3.3.2. Trace metals in the dissolved fraction**

#### **3.3.2.1. Total dissolved trace metals**

The range of dissolved trace metal concentrations investigated in our study is 0.03-0.40  $\mu\text{g L}^{-1}$  for Co, 0.4-10.1  $\mu\text{g L}^{-1}$  for Cu, 0.49-2.83  $\mu\text{g L}^{-1}$  for Ni, 0.08-0.19  $\mu\text{g L}^{-1}$  for Cd, <0.011-0.54  $\mu\text{g L}^{-1}$  for Pb (Table 3.2).



**Table 3.2:** Seasonal and spatial variations of dissolved trace metal concentrations in the BCZ water column

<i>Element</i>	Station	min. - max. ( $\mu\text{g L}^{-1}$ )	Average ( $\mu\text{g L}^{-1}$ )	Median ( $\mu\text{g L}^{-1}$ )	EQS* dissolved		BRCs* dissolved
					YA*	MAC*	
Cd	HO-1	0.08 - 0.19	0.11	0.09			
	HO-2	0.09 - 0.16	0.11	0.10			
	HZ-2	0.10 - 0.15	0.11	0.11	0.2	0.45	0.004 - 0.009
	HZ-1	0.10 - 0.14	0.12	0.12			
	OZ-MOW1	0.09 - 0.19	0.13	0.12			
Pb	HO-1	0.08 - 0.54	0.28	0.26			
	HO-2	0.04 - 0.15	0.09	0.09			
	HZ-2	<0.011 - 0.015	0.01	0.01	1.3	14	0.033
	HZ-1	<0.011 - 0.13	0.04	0.02			
	OZ-MOW1	0.02 - 0.53	0.19	0.10			
Co	HO-1	0.10 - 0.40	0.26	0.26			
	HO-2	0.06 - 0.29	0.17	0.16			
	HZ-2	0.05 - 0.13	0.09	0.09	-	19	0.0035
	HZ-1	0.06 - 0.13	0.09	0.09			
	OZ-MOW1	0.03 - 0.14	0.07	0.06			
Ni	HO-1	0.27 - 2.83	1.78	2.01			
	HO-2	0.62 - 1.91	1.20	1.13			
	HZ-2	0.49 - 0.61	0.54	0.53	8.6	34	0.140
	HZ-1	0.61 - 0.63	0.62	0.63			
	OZ-MOW1	0.61 - 1.01	0.77	0.73			
Cu	HO-1	1.40 - 2.18	1.64	1.49			
	HO-2	0.67 - 1.04	0.88	0.90			
	HZ-2	0.60 - 1.60	0.87	0.65	-	10	0.070
	HZ-1	0.44 - 1.02	0.83	0.94			
	OZ-MOW1	0.32 - 10.1	2.99	0.79			

\**Environmental Quality Standard (EQS); Yearly Average (YA); Maximum Acceptable Concentration (MAC); Background/Reference Concentrations (BRCs)*

Highest concentrations (average) of Pb, Co and Ni are recorded at HO-1 while those of Cd and Cu at OZ-MOW1. The 2 stations of Zeebrugge harbor show similar concentration ranges for all elements, while this is not the case for Oostende harbor. Higher Co and Ni concentrations are observed in Springtime than in Autumn at stations HO-1 and HO-2. At HZ-1, HZ-2 and OZ-MOW1, no particular trend is recorded over the year whatever the metal considered. Regarding dissolved Pb, higher concentrations are observed for the stations HZ-1 and OZ-MOW1 in October 2017, while they are more or less constant at the other stations for the rest of the year. At station HO-1 higher dissolved Pb concentrations occurred in October 2018.

Dissolved concentrations of Ni and Pb are all below the Water Quality Standards (EQS-yearly averages) for dissolved trace metals in seawater (Journal Officiel de la République Française, 2018; Maycock et al., 2011), while dissolved Cd is slightly lower than the EQS-yearly average value of  $0.2 \mu\text{g L}^{-1}$ . At the offshore station OZ-MOW1, a very high Cu concentration has been surprisingly measured in October 2017: up to  $10 \mu\text{g L}^{-1}$ , which is equal to the Maximum Acceptable Concentration value (MAC).

### **3.3.2.2. Labile trace metals**

Labile metal concentrations range between  $0.02\text{-}0.22 \mu\text{g L}^{-1}$  for Co,  $0.09\text{-}0.60 \mu\text{g L}^{-1}$  for Cu,  $0.25\text{-}0.64 \mu\text{g L}^{-1}$  for Ni,  $0.003\text{-}0.049 \mu\text{g L}^{-1}$  for Cd,  $<0.011\text{-}0.23 \mu\text{g L}^{-1}$  for Pb (Table 3.3).

**Table 3.3:** Seasonal and spatial variations of labile trace metal concentrations in the BCZ water column

Element	Station	min. - max. ( $\mu\text{g L}^{-1}$ )	Average ( $\mu\text{g L}^{-1}$ )	Median ( $\mu\text{g L}^{-1}$ )	EQS** dissolved		BRCs** dissolved
					YA**	MAC**	
Cd	HO-1	0.005 - 0.037	0.018	0.015			
	HO-2	0.003 - 0.049	0.021	0.017			
	HZ-2	0.010 - 0.028	0.018	0.016	0.2	0.45	0.004 - 0.009
	HZ-1	0.014 - 0.036	0.022	0.018			
	OZ-MOW1*	0.027 - 0.029	0.028	0.028			
Pb	HO-1	0.015 - 0.024	0.019	0.018			
	HO-2	0.014 - 0.024	0.017	0.015			
	HZ-2	<0.011 - 0.020	0.014	0.014	1.3	14	0.033
	HZ-1	0.019 - 0.024	0.021	0.021			
	OZ-MOW1*	0.017 - 0.234	0.126	0.126			
Co	HO-1	0.055 - 0.087	0.071	0.071			
	HO-2	0.053 - 0.081	0.065	0.063			
	HZ-2	0.045 - 0.100	0.067	0.062	-	19	0.0035
	HZ-1	0.018 - 0.112	0.061	0.057			
	OZ-MOW1*	0.028 - 0.221	0.125	0.125			
Ni	HO-1	0.43 - 0.59	0.49	0.47			
	HO-2	0.35 - 0.55	0.42	0.39			
	HZ-2	0.27 - 0.45	0.36	0.35	8.6	34	0.140
	HZ-1	0.25 - 0.45	0.37	0.40			
	OZ-MOW1*	0.40 - 0.64	0.52	0.52			
Cu	HO-1	0.10 - 0.46	0.25	0.22			
	HO-2	0.10 - 0.28	0.17	0.16			
	HZ-2	0.21 - 0.60	0.41	0.42	-	10	0.070
	HZ-1	0.17 - 0.28	0.22	0.21			
	OZ-MOW1*	0.09 - 0.26	0.17	0.17			

\*for OZ-MOW1, only the samples from April and October 2017 are taken into account

\*\*Environmental Quality Standard (EQS); Yearly Average (YA); Maximum Acceptable Concentration (MAC); Background/Reference Concentrations (BRCs)

On average, highest labile concentrations are found at station OZ-MOW1 for all elements, except for Cu whose average concentration is higher at HZ-2 reaching  $0.41 \mu\text{g L}^{-1}$ . Labile trace metal concentrations at the harbor stations do not differ significantly (except Cu at HZ-2): using average values, they range between  $0.018$  and  $0.022 \mu\text{g L}^{-1}$  for Cd,  $0.014$ - $0.21 \mu\text{g L}^{-1}$  for Pb,  $0.06$ - $0.07 \mu\text{g L}^{-1}$  for Co,  $0.36$ - $0.49 \mu\text{g L}^{-1}$  for Ni,  $0.17$ - $0.25 \mu\text{g L}^{-1}$  for Cu. Temporal trends are observed for Cd and Cu: for Cu, the concentrations are higher in Autumn at stations HZ-2 and HO-1 (respectively,  $0.6$  and  $0.4 \mu\text{g L}^{-1}$  in Autumn,  $0.2$  and  $0.1 \mu\text{g L}^{-1}$  in Spring), while for Cd it is the opposite (respectively,  $0.012$  and  $0.010 \mu\text{g L}^{-1}$  in Autumn,  $0.023$  and  $0.026 \mu\text{g L}^{-1}$  in Spring).

As no labile reference values yet exist, our labile metal concentrations are compared with Water Quality Standards for total dissolved trace metal concentrations in seawater (Journal Officiel de la République Française, 2018; Maycock et al., 2011): labile levels are all below the EQS-yearly average values.

### **3.3.3. Partitioning of trace metals between the solid and the liquid phases**

Three trace metal pools in seawater have been considered: dissolved labile metal complexes, dissolved non-labile metal complexes and particulate metals (Figure 3.3). Average values over one-year sampling at each station were used.

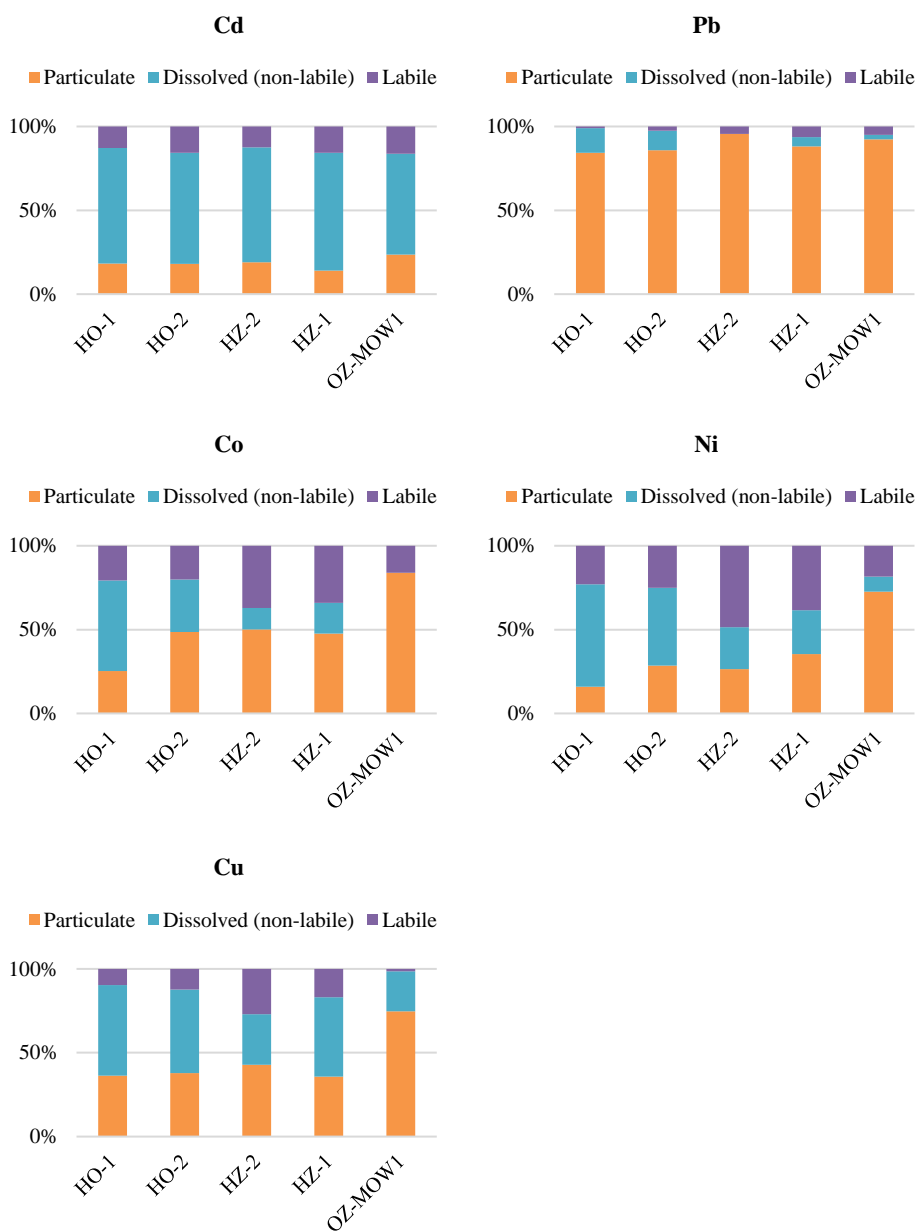


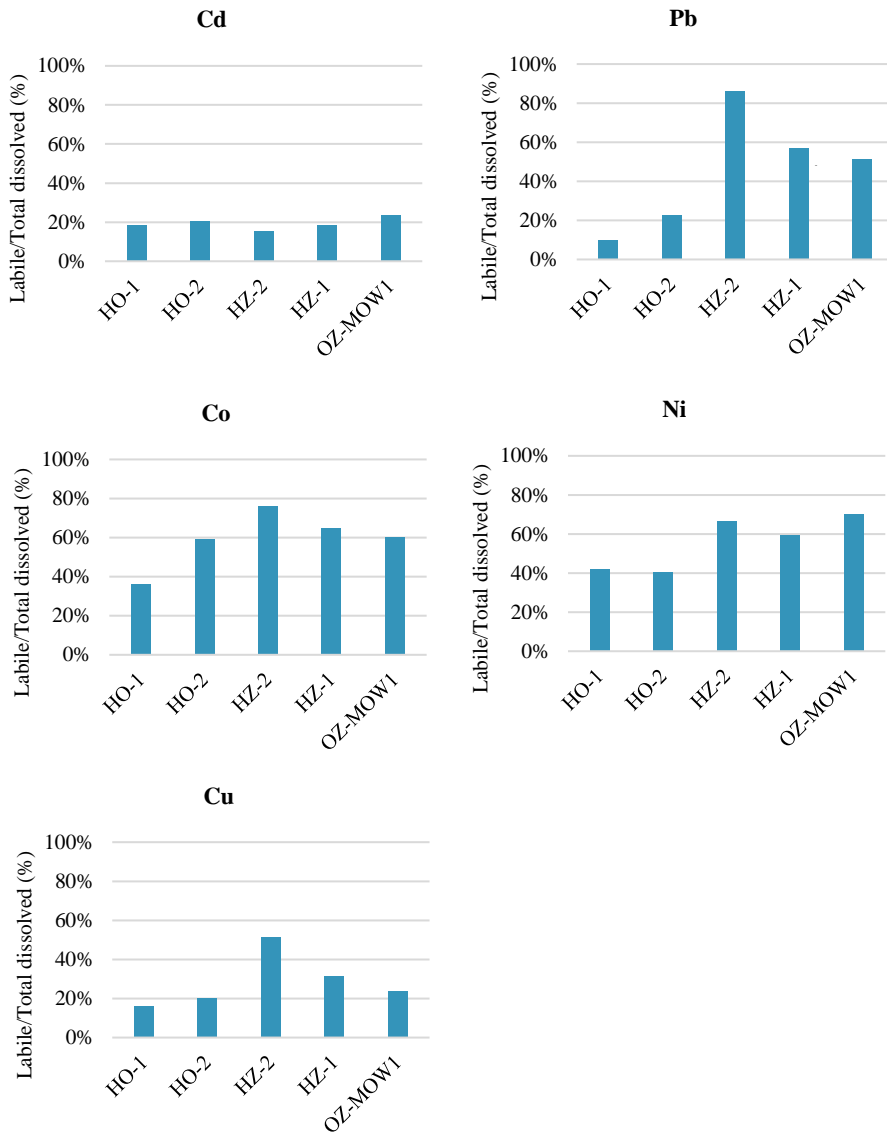
**Figure 3.3:** Trace metal distribution between particulate, dissolved and labile forms, in the BCZ water column

Three metals show a clear pattern: for Cd, the dissolved non-labile fraction seems to be dominant while for Pb and Co (except at HO-1), the particulate one is dominant. For the other metals, there is no clear pattern: for Ni, the dissolved non-labile fraction seems to be more important at Oostende harbor, while the labile one dominates at Zeebrugge harbor and the particulate fraction is higher at the marine station OZ-MOW1. For Cu, the particulate fraction is dominant at OZ-MOW1, the dissolved non-labile fraction is slightly higher than the particulate one at Oostende harbor and HZ-1, while the three fractions are more or less equilibrated at station HZ-2.

Moreover, the ratio of labile to total dissolved concentrations was determined for each element according to the following formula (Eqn 3.4):

$$\text{Lability} = \frac{[\text{TM}]_{\text{labile}}}{[\text{TM}]_{\text{dissolved}}} \times 100 \quad \text{Equation 3.4}$$

Where [TM] is the trace metal concentration, either for the labile fraction or for the total dissolved amount (both in  $\mu\text{g L}^{-1}$ ). The results are presented in Figure 3.4.



\*for total dissolved and therefore labile Pb at HZ-2, 3 values out of 4 were below the LOD. The bar chart only represents the ratio measured in October 2017.

\*\* for total dissolved and therefore labile Pb at HZ-1, 2 values out of 4 were below the LOD. The bar chart represents the average of the ratios measured in October 2017 and March 2018.

**Figure 3.4:** Trace metal lability, in the BCZ water column. The lability ratios result from an average of all the measurements.

The higher the labile fraction, the more the metal is bioavailable and the greater the threat for the marine ecosystem (Baeyens et al., 2018b; Simpson et al., 2012). Based on Figure 3.4, the lability of Cd varies from 15 to 24%, showing the lowest lability values of all elements. Annual averages are similar at all stations, except that a slightly higher lability is observed at station OZ-MOW1. The maximum lability is observed in Springtime for Cd. The lability of Pb varies between 10 to 52% (the largest range of all metals), with the highest value found at the marine station OZ-MOW1 and the lowest at HO-1. Cobalt displays the highest lability with values varying from 36 (HO-1) to 76% (HZ-2). The lability of Ni fluctuates from 41 to 70%, station HO-2 showing the minimum value and OZ-MOW1 the maximum one. Labile Cu varies from 16 to 52%. The highest average value for Cu is found at station HZ-2 and the lowest at HO-1.

To estimate the affinity of each trace metal for the dissolved or particulate phase, the partition coefficients  $K_D$  were calculated according to Equation 3.5:

$$K_D = \frac{[TM]_{\text{particulate}}}{[TM]_{\text{dissolved}}} \quad \text{Equation 3.5}$$

Where [TM] is the total trace metal concentrations, either in its dissolved (in  $\mu\text{g kg}^{-1}$  water) or particulate phase (in  $\mu\text{g kg}^{-1}$  suspended matter). The logarithm of  $K_D$  is presented in SI.  $\log K_D^{\text{Cd}}$  and  $\log K_D^{\text{Co}}$  respectively vary from 2.7 to 4.3 and from 3.5 to 5.3. Cd and Co have the largest  $K_D$  ranges, compared to the other elements.  $\log K_D^{\text{Pb}}$  varies from 4.6 to 6.0 and has, compared to the other elements, the highest  $K_D$  values.  $\log K_D^{\text{Ni}}$  fluctuates from  $< 2.4$  to 4.7, with the maximum value at station HO-1. Looking at the annual average values, the differences between stations are small, except for Pb at HZ-2 and Co at OZ-MOW1.



### 3.3.4. Statistical analysis

#### 3.3.4.1. Principal Component Analysis and parameter correlations

Labile and particulate Cr(III), Fe and Mn concentrations have been added to the data set to gain more insight on trace metal behavior in the water column (labile Cr(III), Fe and Mn were obtained by DGT measurements as described in 3.2.3, while particulate fractions were obtained with filter digestions as described in 3.2.4.2). As shown in Figure 3.5, the parameter correlogram help us to visualize correlations between variables in the water column.

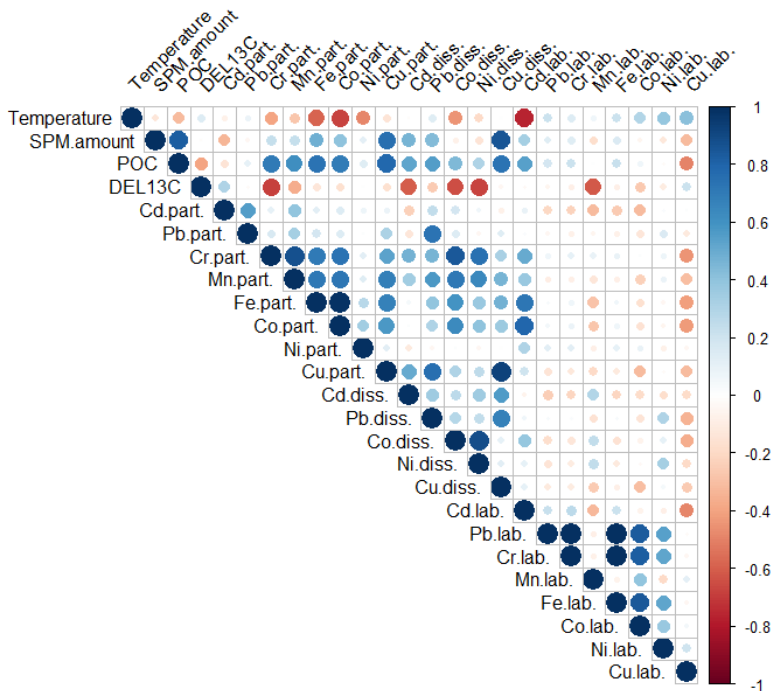


**Figure 3.5:** Correlogram of the parameters. The blue circles indicate positive correlations; the red circles indicate negative correlations. The size of the circles and the intensity of their color are proportional to the strength of the correlation. The legend indicates the link between colors and coefficients.

Labile and particulate concentrations of Cr (III), Fe and Mn have been added to the data set to gain more insight on parameter correlations (labile Cr(III), Fe and Mn were obtained by DGT measurements as described in 3.2.3, while particulate fractions were obtained with filter digestions as described in 3.2.4.2).

---

For most of the trace metals, the dissolved and particulate concentrations are grouped together and show positive correlation factors (Fig. 3.5). According to the correlogram and the associated p-values (available in the SI), particulate Co, Ni and Fe are negatively correlated with the temperature ( $p < 0.05$ ). The same significant negative correlation is observed between labile Cd and the temperature.

Furthermore, the SPM amount and its POC content are also grouped together with the dissolved and particulate elements. Moreover, the POC content displays a significant ( $p < 0.05$ ) negative correlation with labile concentrations of Cu. Labile trace metals are grouped separately from the dissolved and particulate ones and do not show significant correlation with them (Fig. 3.5;  $p > 0.05$ ).  $\delta^{13}\text{C}$  values are negatively related with the concentrations of labile Mn, dissolved Cd, Co, Ni, and particulate Cr ( $p < 0.05$ ).

### 3.3.4.2. Hierarchical Ascending Classification

The HAC plot (Figure 3.6) distributes our data set in five different clusters.

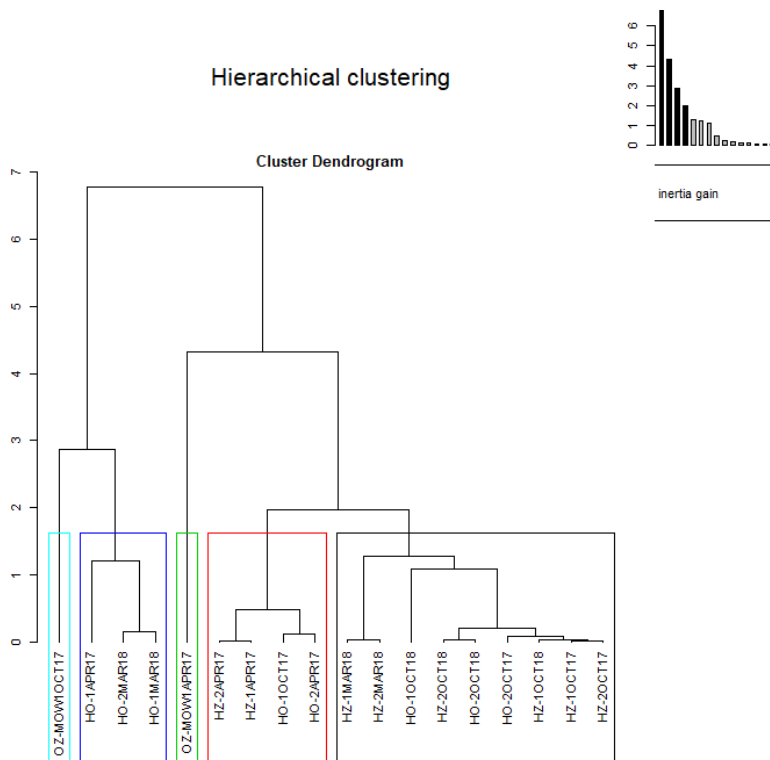


**Figure 3.6:** Dendrogram of the samples from all the campaigns, resulting from a HAC analysis

Cluster 1, which is the biggest group, contains all the harbor stations sampled in October 2018, all the harbor stations (except HO-1) sampled in October 2017 and the samples taken in Zeebrugge harbor in March 2018. These samples are characterized by higher particulate Cd and higher  $\delta^{13}\text{C}$  values, lower contents of POC, labile Mn, dissolved Co, dissolved Ni and particulate Cr. Cluster 2 gathers all the harbor samples from April 2017 (except HO-1)

and the HO-1 sample from October 2017. These samples are characterized by higher labile Mn, while they show lower values for labile Cd, particulate Cd and Mn. Cluster 3 only contains station OZ-MOW1 sampled in April 2017, which has higher concentrations of labile Co, Cr(III), Fe, Ni and Pb. Cluster 4 gathers the samples from Oostende harbor (HO-1 ad HO-2) in March 2018 and HO-1 from April 2017. These samples are characterized by higher concentrations of labile Cd, dissolved Co, Ni and particulate Co, Cr, Fe, Mn. Finally, cluster 5 only comprises the sample from OZ-MOW1 taken in October 2017, which shows higher contents of SPM and POC and higher concentrations of dissolved Cd, Cu, Pb and particulate Cu.

### **3.4. Discussion**

#### **3.4.1. Organic matter origin**

The change of  $\delta^{13}\text{C}$  values in the harbors stations indicates a change in the SPM origin. The results from April 2017 (-20 to -40‰) are in the harbors the lowest of the 4 campaigns and correspond to the range of  $\delta^{13}\text{C}$  values observed in POC of the Scheldt estuary (De Brabandere et al., 2002). These results thus clearly indicate a dominance of allochthonous SPM in the harbors in April 2017, coming from terrestrial sources (especially for HO-1 and HO-2). In the 3 other sampling periods, the isotopic C signature of the POC ranges from -10 to -20‰ indicating its autochthonous, marine origin.

In October 2018 at station HZ-2,  $\delta^{13}\text{C}$  shows an exceptional high positive value, 3.4‰, which is even close to the inorganic carbon isotope values in shallow marine environments (Trumbore and Druffel, 1995). Although we follow the analytical procedures in a stringent way, it cannot be excluded that all carbonate material in the SPM of the HZ-2 sample was eliminated when  $\delta^{13}\text{C}$  was determined in the organic matter. This could have led to the high

$\delta^{13}\text{C}$  result we found. At marine station OZ-MOW1, the particulate carbon source seems to remain almost constant during the monitoring period. The range and average values of  $\delta^{13}\text{C}$  suggest that autochthonous, marine organic matter prevailed in the SPM at this offshore station for all sampling periods. We can conclude that, in general, the POC in BCZ is of autochthonous origin even if the Scheldt Estuary constitutes one of the major freshwater sources. However, several factors influence its impact on the BCZ water composition such as the increase of salinity, dilution with the marine water mass and mixing processes with bottom sediments. Moreover, other smaller freshwater sources around or inside the harbors can also change the SPM composition and nature.

### **3.4.2. Labile versus total dissolved concentrations**

Regarding total dissolved levels in the BCZ, our results display higher concentrations than in the 80's for Cu and Cd, and in the same range for Pb (Baeyens et al., 1987). Total dissolved concentrations measured in our study are also higher than in 2010 for Cd and Cu, while the concentration levels are in the same range for Pb (Gao et al., 2013). In the BCZ no labile trace metals were previously measured but our labile Cd results are in the same order of magnitude as those measured in Mediterranean and Black Sea coastal areas (Schintu et al., 2008; Slaveykova et al., 2009), while labile Cu, Ni and Pb show higher values in the BCZ.

In the BCZ, Cd complexes are highly stable, while those of Co and Ni are mainly labile. The harbor station HO-1 shows the lowest lability for Pb, Co and Cu at their highest dissolved and particulate concentrations (i.e. the highest contamination level). On the other hand, Cd, Pb and Ni form the weakest complexes at the marine station OZ-MOW1, while Co and Cu form

the weakest ones at the harbor station HZ-2. A marina with a yacht refit and repair facility is located nearby station HZ-2. This infrastructure is used to take small boats out of the water and repair or restore them, using different kind of coatings and paints like copper-based boat paint. The later could explain high labile Cu concentrations measured at this station.

Labile and total dissolved concentrations do not correlate well as shown in Figure 3.5. Moreover, it seems that when dissolved Co and Ni concentrations are lower, the labile fraction is higher and vice versa. Considering the ratio of labile-total dissolved concentrations at each station, different rankings can be observed:

HO-1: Ni>Co>Cd>Cu>Pb  
HO-2: Co>Ni>Pb>Cd>Cu  
HZ-1: Co>Ni>(Pb>) Cu>Cd  
HZ-2: (Pb>) Co>Ni>Cu >Cd  
OZ-MOW1: Ni>Co>Pb>Cd=Cu

The ratio varies between stations, but both stations located in Zeebrugge harbor show the same ranking of metal lability, highlighting again similarities between these two stations. Considering all stations, Co and Ni show the highest lability capacity, indicating that their complexes are more labile than for the other elements. There is no clear trend for Pb, Cu and Cd, but they have a tendency to form complexes with lower lability. These lability ratios in the BCZ reflect less lability for Cd complexes than those recently measured by voltammetric techniques in the Northern Adriatic Sea, while ratios found for Cu and Pb are in the same range as those in the BCZ (Illuminati et al., 2019b).

### 3.4.3. Partitioning of trace metals

While total dissolved trace metals were not correlated to their labile fraction, more similarities are found with their particulate fraction. This highlights that high dissolved or particulate trace metal concentrations do not necessarily imply high labile concentrations. As for the dissolved fraction, our results exhibit an important particulate trace metal contamination, especially for Cd.

$K_D$  values reveal the affinity of a trace metal for either the particulate or the dissolved phase in the water column and vary depending on the element, the season and the location. Overall, our  $K_D^{Cd}$  values are slightly lower than those found in other studies in the BCZ (W. Baeyens, 1998; Parmentier, 2002; Valenta et al., 1986), revealing less affinity for Cd for the particulate phase than during the last decades. For the other elements, their  $K_D$ 's are within the range found in other studies (W. Baeyens, 1998; Parmentier, 2002; Valenta et al., 1986). All trace metals, except Cd, show higher solubility at HO-2 than at other stations. In general,  $\log K_D$  is highest for Pb, followed by Co, Cu, Ni and Cd:

$$\begin{aligned} \text{HO-1: } K_D^{\text{Pb}} &> K_D^{\text{Cu}} > K_D^{\text{Co}} > K_D^{\text{Ni}} > K_D^{\text{Cd}} \\ \text{HO-2: } K_D^{\text{Pb}} &> K_D^{\text{Co}} > K_D^{\text{Cu}} > K_D^{\text{Cd}} > K_D^{\text{Ni}} \\ \text{HZ-1: } K_D^{\text{Pb}} &> K_D^{\text{Co}} > K_D^{\text{Cu}} > K_D^{\text{Ni}} > K_D^{\text{Cd}} \\ \text{HZ-2: } K_D^{\text{Pb}} &> K_D^{\text{Co}} > K_D^{\text{Cu}} > K_D^{\text{Cd}} = K_D^{\text{Ni}} \\ \text{OZ-MOW1: } K_D^{\text{Pb}} &> K_D^{\text{Co}} > K_D^{\text{Ni}} > K_D^{\text{Cu}} > K_D^{\text{Cd}} \end{aligned}$$

These rankings are in good agreement with results obtained at the mouth of the Scheldt estuary (Baeyens, 1998 - Pb>Zn>Cu>Cd). The high  $K_D^{\text{Pb}}$  values are also in agreement with observations made by Valenta (1986), Baeyens (1998) and Parmentier (2002) in the BCZ. Stations from Zeebrugge harbor and HO-2 show similar rankings of partition coefficients.

The concentrations of the three pools in the water column (dissolved labile, dissolved non-labile and particulate - Fig. 3.3) were compared to other studies: in the BCZ, dissolved non-labile Cd is the largest pool of the total Cd content while particulate Pb dominates the total Pb content, as in the Northern Adriatic Sea (Illuminati et al., 2019b) or as shown in a previous study on the BCZ and along the Scheldt Estuary (Baeyens et al., 1987). Cu content is dominated by the dissolved fraction as shown by Baeyens et al. (1987) and Illuminati et al. (2019) (except at OZ-MOW1 where the particulate fraction is dominant), but does not account for 100% of the total Cu content as it was found in the Northern Adriatic Sea (Illuminati et al., 2019b).

#### **3.4.4. Parameter correlations and influences**

Figure 3.5 clearly shows that a correlation exists between dissolved and particulate trace metals in the water column. However, the graph also confirms our previous observations: the labile fraction seems not correlated to dissolved and particulate trace metal concentrations. Furthermore, the SPM amount and its POC content seem to vary in the same way as the dissolved and the particulate metals. The POC content is also inversely proportional to labile concentrations of Cu. The impact of temperature variations is visible on particulate Co, Ni, Fe and labile Cd concentrations as they are negatively correlated, meaning that when temperature increases, particulate concentrations of Co, Ni, Fe and labile Cd decrease. This observation points out future possible effects of climate changes and resulting temperature rises of oceans and seas on the solubility of particulate metals and their lability potentials. On one hand and regarding  $\delta^{13}\text{C}$  values, the more autochthonous the organic matter is, the lower the concentrations of labile Mn, dissolved Cd, Co, Ni, and particulate Cr, meaning the less contaminated the suspended



matter will be for these elements. If we look at our entire data set, it can be pointed out that particulate metal concentrations follow the same trend as total dissolved metal concentrations. However, particulate and total dissolved trace metal fractions do not correlate well with their labile and hence bioavailable fractions. These results highlight differences in the behavior of dissolved labile, dissolved non-labile and particulate metals.

### **3.4.5. Seasonality**

Our data set can be aggregated in five different clusters (Figure 3.6), which are strongly associated with seasonal variations. The two Zeebrugge harbor stations look similar to each other with low trace metal concentrations in Autumn and in Spring. In both Autumn seasons, all harbor stations show similar water compositions with the exception of HO-1 in October 2017 when low trace metal levels, a high concentration of particulate Cd and more autochthonous SPM are observed. Generally, station HO-1 shows more seasonal variabilities with lower trace metal levels in Autumn and higher trace metal levels in Spring. Offshore station OZ-MOW1 shows variability between Spring and Autumn too: in Spring, higher labile concentrations for Co, Cr(III), Fe, Ni and Pb are measured, while in Autumn the dissolved and particulate metal levels are the highest. Differences in trace metal behavior between the marine and harbor stations are consequently highlighted. Even if the marine station is only located 5 km away from the coast, stronger currents and wind intensities most likely influence OZ-MOW1 more than the harbor stations.

### **3.5. Conclusion**

This study focused on three main objectives: (1) assessing trace metal concentrations in different forms in the water column (i.e. labile, dissolved, particulate), in various seasons of the year and at various sites at the BCZ; (2) comparing the labile fraction, which is the most dangerous for the ecosystem, with the other trace metal pools; and (3) tracing back the origin of the Suspended Particulate Matter.

Regarding the first objective we observed higher particulate and dissolved metal concentrations in the Oostende harbor station HO-1 (mostly in Spring) and at the offshore station OZ-MOW1 in Autumn. Higher labile metal concentrations were measured for Co, Ni and Pb at the offshore station OZ-MOW1 and for Cd at the harbor station HO-1 in Spring. Regarding the second objective we could show that a classic comparison between dissolved and particulate trace metal concentrations is not enough to highlight the eventual impact on the marine ecosystems, as the labile fraction of trace metals does not correlate well with its particulate and dissolved concentrations. Because labile and bioavailable trace metal fractions are closely linked to each other in aquatic systems, measuring labile trace metals is important to make a risk assessment for the ecosystem. The labile fractions of trace elements measured by the DGT samplers do not differ significantly between sampling sites, however the offshore station OZ-MOW1 shows sometimes unexpected high trace metal levels in Springtime. Further campaigns will help us to characterize the time-evolution of trace metal concentrations and speciation in the BCZ. On a larger scale, this research can help us to foresee and explain pollutant bioaccumulation in marine organisms, and to build toxicity models for them. In a global warming context, increased acidification of the ocean in a near future may shift the trace metal partitioning between particulate towards the dissolved phase, even increasing the labile metal fractions, and might thus

lead to increased adverse effects on coastal ecosystems. Lastly, the results of POC and  $\delta^{13}\text{C}$  analysis clearly indicate a dominance of allochthonous SPM in the harbors (especially for HO-1 and HO-2) in April 2017, coming from terrestrial sources. In the 3 other sampling periods, the isotopic C signature of the POC ranges from -10 to -20‰ indicating its autochthonous, marine origin. At marine station OZ-MOW1, the particulate carbon remains almost constant during the monitoring period. The range and average values of  $\delta^{13}\text{C}$  suggest that autochthonous organic matter prevailed in the SPM at this offshore station.

## **Acknowledgement**

The authors would like to thank the Belgian Science Policy Office (BELSPO) for funding the NewSTHEPS project (BR/143/A2/NEWSTHEPS) and supporting Gaulier C. (FOD-12) and Guo W. (FOD-18). Zhou C. is supported by the Chinese Scholar Council (PhD fellowship 201606190219). The authors would like to thank the FWO research grant 1529016N. The RV Belgica crew members, the scientific vessel of the Belgian government, the Zeetijger crew members and the OD Nature staff (RBINS) are thanked for the sampling campaigns. Leermakers M., Verstraeten D. and Brion N. are also thanked for the analysis.

### 3.6. Supplementary Information

The Supplementary Information includes 5 tables and extra details regarding DGT and SPE protocols and can be found in the online version.

#### 3.6.1. Material and methods

##### 3.6.1.1. Study sites

**Table S3.1:** Sampling stations

Coastal location	Sampling Stations	Sampling Code	Coordinates DMS
Harbors	Oostende	HO-1	51°13'34.68"N ; 2°56'8.00" O
		HO-2	51°14'30.29"N ; 2°55'36.24"O
	Zeebrugge	HZ-1	51°20'25.68"N ; 3°12'12.11"O
		HZ-2	51°19'51.97"N ; 3°11'58.09"O
Offshore	MOW1	OZ-MOW1	51°21'37.78"N ; 3°6'49.01"O

##### 3.6.1.2. DGT preparation

To prepare the Chelex<sup>®</sup>-100 resin gel, 2 mL gel solution (0.75 mL acrylamide 40%, 0.32 mL DGT cross-linker, 0.95 mL Milli Q) was mixed with 0.8 g of Chelex<sup>®</sup>-100 powder. Sequentially, 12  $\mu$ L of 10% ammonium persulfate (APS, Merck) and 3  $\mu$ L tetramethylethylenediamine (TEMED, > 99%, Merck) were added and mixed well. Following mixing, the mixture was immediately cast between glass plates separated by a 0.25  $\mu$ m plastic spacer, resulting in a 0.4 mm-thick resin gel after hydration. The resin gels were kept in 0.03 M NaCl (Suprapur, Merck) solution before their application. The same protocol was followed for preparing the diffusive gel, without adding the Chelex<sup>®</sup>-100 powder and using a 0.50  $\mu$ m plastic spacer resulting in a 0.8 mm-thick diffusive gel.

### 3.6.1.3. DBL

In addition to the 6 DGT pistons deployed per station and per sampling event, additional DGT devices with different thicknesses of diffusion layers (0.4 and 1.2 mm) were deployed at station HO-1, to assess the DBL. According to these experiments and to the calculation reported by W. Davison and H. Zhang (2016; Chapter 2 of the book), a DBL of 0.20 mm was calculated. During previous studies of our team, DBL values in the range 0.10 to 0.23 mm were observed in turbulent aquatic environments (Guo et al., 2019). Hence, a DBL of 0.20 mm was used for all sampling points in the Belgian coastal area because these aquatic environments correspond to turbulent systems. The impact of a 25% change of the DBL on the final result is small: assuming a DBL of 0.15 mm instead of 0.20 mm, the bulk concentration will decrease with less than 5%.

The diffusive domain for a DBL of 0.20 mm equals 1.13 mm and for a DBL of 0.15 mm, 1.08 mm. Hence the change of the bulk concentration C-bulk(1) to C-bulk(2), using Fick's law and keeping all other parameters the same, is:

$$C\text{-bulk}(1) = \text{Constant} * (0.2 + 0.13 + 0.8) = 1.13 * \text{constant}$$

$$C\text{-bulk}(2) = \text{Constant} * (0.15 + 0.13 + 0.8) = 1.08 * \text{constant}$$

The difference between both is less than 5%.

### 3.6.1.4. Reagent preparation for the SPE

For total dissolved trace metal measurement, an ammonium acetate buffer was prepared by diluting 22.5 mL ammonia (NH<sub>3</sub>; Merck, Suprapur, 25%) and 11.8 mL glacial acetic acid (CH<sub>3</sub>COOH; Fisher, Trace Metal Grade, >99%) to 100 mL Milli Q water (Millipore) in a FEP bottle. A 2M HNO<sub>3</sub>/1M HCl mixture was prepared by diluting a solution of 126 mL HNO<sub>3</sub> (Fisher, Trace

Metal Grade, 65%) and 83 mL HCl (Fisher, Trace Metal Grade, 37%) to 791 mL Milli Q water.

### 3.6.2. Results

#### 3.6.2.1. Particulate metals

**Table S3.2:** Enrichment factor for particulate trace metal concentrations over the year sampling in the BCZ water column

<i>Element</i>	<i>Station</i>	min. - max. (EF)	Average (EF)	Median (EF)	SPM quality in average
Cd	HO-1	6 - 133	52	35	extremely high enrichment
	HO-2	5 - 139	51	29	
	HZ-2	10 - 109	39	19	very high enrichment
	HZ-1	5 - 64	25	16	
	OZ-MOW1	4 - 14	8	7	
Pb	HO-1	6 - 127	39	11	very high enrichment
	HO-2	4 - 10	6	5	significant enrichment
	HZ-2	2 - 5	4	4	moderate enrichment
	HZ-1	3 - 4	3	3	
	OZ-MOW1	2 - 7	4	3	
Co	HO-1	0.7 - 0.9	0.8	0.7	deficiency to minimal enrichment
	HO-2	0.4 - 0.6	0.6	0.6	
	HZ-2	0.4 - 0.7	0.5	0.5	
	HZ-1	0.5 - 0.6	0.6	0.6	
	OZ-MOW1	0.6 - 0.9	0.7	0.7	
Ni	HO-1	0.41 - 1.69	1.5	1.1	deficiency to minimal enrichment
	HO-2	0.03 - 0.58	0.3	0.3	
	HZ-2	<0.02 - 0.46	0.3	0.4	
	HZ-1	0.16 - 1.25	0.5	0.4	
	OZ-MOW1	0.37 - 1.39	0.7	0.6	
Cu	HO-1	2 - 7	4.5	4.4	moderate enrichment
	HO-2	1 - 2	1.3	1.2	deficiency to minimal enrichment
	HZ-2	1 - 2	1.6	1.6	
	HZ-1	0.5 - 2	1.1	1.1	
	OZ-MOW1	0.3 - 9	2.5	0.5	moderate enrichment



### 3.6.2.2. Partitioning of trace metals between the solid and the liquid phases

**Table S3.3:** Partition coefficient  $K_d$  of trace metals observed in the BCZ water column over one year

<i>Element</i>	<i>Station</i>	<i>min. - max. Log <math>K_d</math></i>	<i>Average Log <math>K_d</math></i>
Cd	HO-1	2.8 - 4.3	3.8
	HO-2	2.7 - 4.1	3.5
	HZ-2	2.8 - 4.2	3.6
	HZ-1	2.8 - 4.0	3.4
	OZ-MOW1	3.1 - 3.9	3.5
Pb	HO-1	5.0 - 5.5	5.2
	HO-2	4.7 - 5.4	5.0
	HZ-2	5.4 - 6.0	5.7
	HZ-1	4.6 - 5.9	5.4
	OZ-MOW1	4.7 - 5.9	5.2
Co	HO-1	3.9 - 4.3	4.1
	HO-2	3.5 - 4.4	4.0
	HZ-2	3.8 - 4.7	4.3
	HZ-1	4.1 - 4.6	4.3
	OZ-MOW1	4.6 - 5.3	4.9
Ni	HO-1	3.5 - 4.7	4.0
	HO-2	<2.4 - 4.2	3.5
	HZ-2	<2.5 - 4.2	4.0
	HZ-1	3.5 - 4.4	3.8
	OZ-MOW1	4.3 - 4.6	4.4
Cu	HO-1	4.1 - 4.6	4.4
	HO-2	3.7 - 4.3	3.9
	HZ-2	3.8 - 4.6	4.2
	HZ-1	3.4 - 4.5	4.0
	OZ-MOW1	4.0 - 4.4	4.2

### 3.6.2.3. Principal Component Analysis and parameter correlations

**Table S3.4:** Correlation matrix (column to be continued in next page)

	Temperature	Cd labile	Pb labile	Cr labile	Mn labile	Fe labile	Co labile	Ni labile	Cu labile	Cd total dissolved	Pb total dissolved	Co total dissolved	Ni total dissolved	Cu total dissolved	Cd particulate	Pb particulate	Cr particulate	Mn particulate
Temperature	1,00	-0.761	0.211	0.147	0.064	0.21	0.292	0.384	0.419	-0.017	0.138	-0.449	-0.198	0.004	-0.071	0.086	-0.399	-0.279
Cd labile	-0.761	1,00	0.223	0.262	-0.329	0.211	-0.065	-0.082	-0.487	-0.062	0.063	0.388	0.106	0.105	0.093	0.022	0.5	0.373
Pb labile	0.211	0.223	1,00	0.993	-0.087	0.995	0.831	0.542	-0.027	-0.245	0.038	-0.179	-0.144	-0.114	-0.209	-0.043	0.069	-0.095
Cr labile	0.147	0.262	0.993	1,00	-0.08	0.994	0.822	0.525	-0.047	-0.216	0.02	-0.134	-0.105	-0.106	-0.221	-0.08	0.104	-0.083
Mn labile	0.064	-0.329	-0.087	-0.08	1,00	-0.066	0.398	-0.194	0.115	0.294	-0.157	0.242	0.24	-0.258	-0.319	-0.058	0.096	-0.135
Fe labile	0.21	0.211	0.995	0.994	-0.066	1,00	0.843	0.524	-0.041	-0.219	0.037	-0.154	-0.113	-0.086	-0.254	-0.078	0.093	-0.086
Co labile	0.292	-0.065	0.831	0.822	0.398	0.843	1,00	0.373	0.056	-0.189	-0.15	-0.067	-0.037	-0.31	-0.319	-0.14	0.01	-0.234
Ni labile	0.384	-0.082	0.542	0.525	-0.194	0.524	0.373	1,00	0.203	-0.176	0.305	0.107	0.333	0.04	0.024	0.159	0.079	0.084
Cu labile	0.419	-0.487	-0.027	-0.047	0.115	-0.041	0.056	0.203	1,00	-0.188	-0.35	-0.365	-0.198	-0.259	0.014	-0.114	-0.442	-0.304
Cd total dissolved	-0.017	-0.062	-0.245	-0.216	0.294	-0.219	-0.189	-0.176	-0.188	1,00	0.351	0.263	0.356	0.564	-0.238	-0.134	0.47	0.349
Pb total dissolved	0.138	0.063	0.038	0.02	-0.157	0.037	-0.15	0.305	-0.35	0.351	1,00	0.286	0.241	0.677	0.24	0.731	0.466	0.572
Co total dissolved	-0.449	0.388	-0.179	-0.134	0.242	-0.154	-0.067	0.107	-0.365	0.263	0.286	1,00	0.887	0.1	0.183	0.141	0.841	0.71
Ni total dissolved	-0.198	0.106	-0.144	-0.105	0.24	-0.113	-0.037	0.333	-0.198	0.356	0.241	0.887	1,00	0.128	0.06	-0.043	0.747	0.645
Cu total dissolved	0.004	0.105	-0.114	-0.106	-0.258	-0.086	-0.31	0.04	-0.259	0.564	0.677	0.1	0.128	1,00	-0.076	0.132	0.326	0.465
Cd particulate	-0.071	0.093	-0.209	-0.221	-0.319	-0.254	-0.319	0.024	0.014	-0.238	0.24	0.183	0.06	-0.076	1,00	0.554	0.101	0.394
Pb particulate	0.086	0.022	-0.043	-0.08	-0.058	-0.078	-0.14	0.159	-0.114	-0.134	0.731	0.141	-0.043	0.132	0.554	1,00	0.168	0.339
Cr particulate	-0.399	0.5	0.069	0.104	0.096	0.093	0.01	0.079	-0.442	0.47	0.466	0.841	0.747	0.326	0.101	0.168	1,00	0.878
Mn particulate	-0.279	0.373	-0.095	-0.083	-0.135	-0.086	-0.234	0.084	-0.304	0.349	0.572	0.71	0.645	0.465	0.394	0.339	0.878	1,00
Fe particulate	-0.582	0.724	0.037	0.068	-0.286	0.061	-0.165	-0.042	-0.419	0.049	0.39	0.595	0.371	0.475	0.124	0.181	0.705	0.719
Co particulate	-0.677	0.791	0.05	0.087	-0.272	0.069	-0.152	-0.054	-0.429	0.015	0.302	0.634	0.404	0.365	0.146	0.14	0.732	0.724
Ni particulate	-0.489	0.309	0.127	0.12	-0.088	0.105	0.093	-0.075	-0.049	-0.112	-0.047	0.018	-0.048	-0.01	0.071	0.01	0.125	0.133
Cu particulate	-0.144	0.206	-0.142	-0.13	-0.195	-0.114	-0.311	-0.029	-0.315	0.506	0.755	0.309	0.259	0.924	0.082	0.315	0.538	0.683
SPM amount	-0.132	0.334	0.131	0.139	-0.175	0.16	-0.056	-0.128	-0.313	0.465	0.435	-0.072	-0.145	0.853	-0.331	-0.042	0.235	0.235
POC	-0.32	0.541	0.186	0.213	0.006	0.221	0.066	-0.03	-0.491	0.524	0.555	0.442	0.301	0.733	-0.145	0.108	0.703	0.611
DEL13C	0.149	-0.038	-0.053	-0.09	-0.613	-0.086	-0.269	-0.107	0.215	-0.61	-0.251	-0.646	-0.672	-0.041	0.306	-0.026	-0.685	-0.366

**Table S3.4:** Correlation matrix (continued)

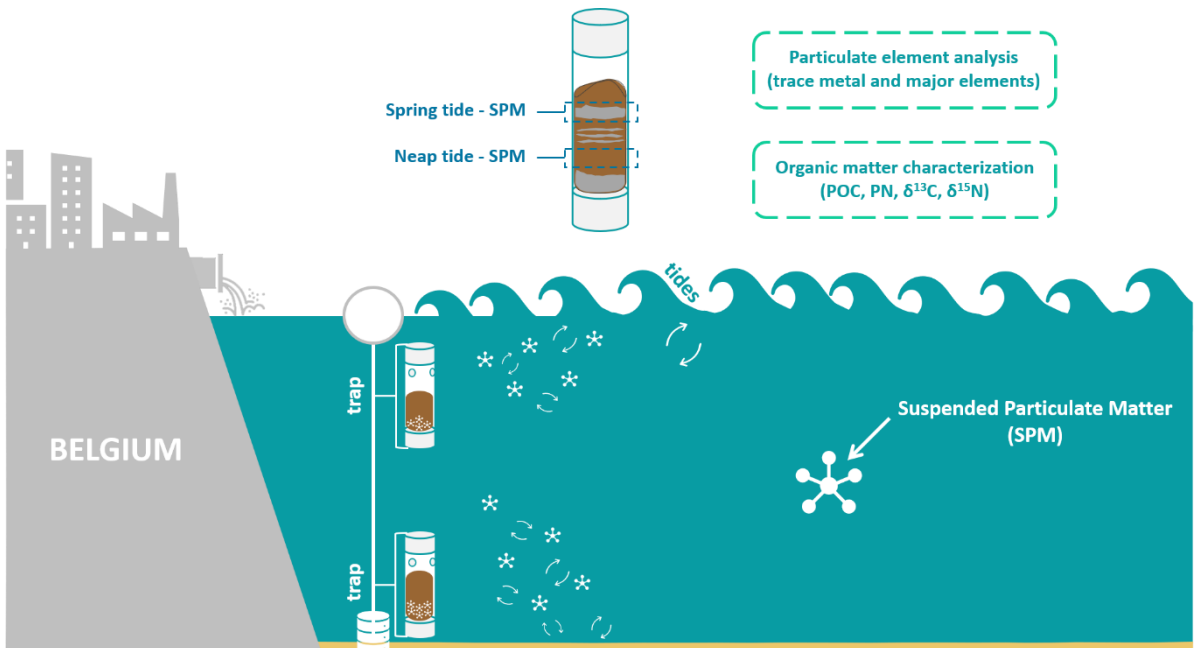
	Fe particulate	Co particulate	Ni particulate	Cu particulate	SPM amount	POC	DEL13C
Temperature	-0.582	-0.677	-0.489	-0.144	-0.132	-0.32	0.149
Cd labile	0.724	0.791	0.309	0.206	0.334	0.541	-0.038
Pb labile	0.037	0.05	0.127	-0.142	0.131	0.186	-0.053
Cr labile	0.068	0.087	0.12	-0.13	0.139	0.213	-0.09
Mn labile	-0.286	-0.272	-0.088	-0.195	-0.175	0.006	-0.613
Fe labile	0.061	0.069	0.105	-0.114	0.16	0.221	-0.086
Co labile	-0.165	-0.152	0.093	-0.311	-0.056	0.066	-0.269
Ni labile	-0.042	-0.054	-0.075	-0.029	-0.128	-0.03	-0.107
Cu labile	-0.419	-0.429	-0.049	-0.315	-0.313	-0.491	0.215
Cd total dissolved	0.049	0.015	-0.112	0.506	0.465	0.524	-0.61
Pb total dissolved	0.39	0.302	-0.047	0.755	0.435	0.555	-0.251
Co total dissolved	0.595	0.634	0.018	0.309	-0.072	0.442	-0.646
Ni total dissolved	0.371	0.404	-0.048	0.259	-0.145	0.301	-0.672
Cu total dissolved	0.475	0.365	-0.01	0.924	0.853	0.733	-0.041
Cd particulate	0.124	0.146	0.071	0.082	-0.331	-0.145	0.306
Pb particulate	0.181	0.14	0.01	0.315	-0.042	0.108	-0.026
Cr particulate	0.705	0.732	0.125	0.538	0.235	0.703	-0.685
Mn particulate	0.719	0.724	0.133	0.683	0.235	0.611	-0.366
Fe particulate	1,00	0.984	0.276	0.675	0.488	0.738	-0.14
Co particulate	0.984	1,00	0.342	0.578	0.4	0.69	-0.166
Ni particulate	0.276	0.342	1,00	0.122	0.115	0.136	0.004
Cu particulate	0.675	0.578	0.122	1,00	0.751	0.787	-0.163
SPM amount	0.488	0.4	0.115	0.751	1,00	0.826	-0.012
POC	0.738	0.69	0.136	0.787	0.826	1,00	-0.4
DEL13C	-0.14	-0.166	0.004	-0.163	-0.012	-0.4	1,00

**Table S3.5:** P-values < 0.05 related to the correlation matrix

	Temperature	Cd labile	Pb labile	Cr labile	Mn labile	Fe labile	Cu labile	Cd total dissolved	Pb total dissolved	Co total dissolved	Ni total dissolved	Cu total dissolved	Cd particulate	Cr particulate	Mn particulate	Fe particulate	Co particulate	Cu particulate	SPM amount	
Cd labile	0,0002																			
Cr labile			0,0000																	
Mn labile																				
Fe labile			0,0000	0,0000																
Co labile			0,0000	0,0000		0,0000														
Ni labile			0,0202	0,0252		0,0256														
Cu labile		0,0406																		
Ni diss.										0,0000										
Cu diss.								0,0148	0,0020											
Cd part.																				
Pb part.									0,0006				0,0170							
Cr part.		0,0347						0,0490		0,0000	0,0004									
Mn part.									0,0130	0,0010	0,0038			0,0000						
Fe part.	0,0112	0,0007								0,0092		0,0462		0,0011	0,0008					
Co part.	0,0020	0,0000								0,0047				0,0005	0,0007	0,0000				
Ni part.	0,0394																			
Cu part.								0,0320	0,0003			0,0000		0,0213	0,0018	0,0021	0,0119			
SPM amount												0,0000				0,0401			0,0003	
POC		0,0203					0,0387	0,0256	0,0169			0,0005		0,0011	0,0070	0,0005	0,0015	0,0001	0,00	
DEL13C				0,0069				0,0071		0,0038	0,0023			0,0017						

# Chapter 4

## Dynamic transport of suspended particulate matter in the North Sea coastal zone



## Dynamic transport of suspended particulate matter in the North Sea coastal zone

*Gaulier C., Adamopoulou A., De Winter N., Fettweis M., Baeye M., Parmentier K., Superville P.-J., Billon G., Baeyens W., Gao Y. In preparation for Science of the Total Environment.*

### Abstract

To investigate the biogeochemical transport of trace metals (Cd, Co, Cr, Cu, Mn, Ni, Pb) and the influence of Suspended Particulate Matter (SPM), major element cycles (Al, Ca, Fe, S and Si) and tidal forces, two SPM traps were deployed at two different depths in the turbid and turbulent Belgian Coastal Zone (BCZ) for one month. After removal, both traps revealed a recurrent layering of fine and thick SPM, which could be further linked with tidal cycles. The collected SPM were then subsampled and separately analyzed for (i) major and trace element contents using  $\mu$ XRF and HR-ICP-MS techniques; (ii) Particulate Organic Carbon (POC), Particulate Nitrogen (PN); and (iii) their stable isotope ( $\delta^{13}\text{C}$ ,  $\delta^{15}\text{N}$ ) compositions using EA-IRMS. The traps gathered a mixture of suspended carbon-rich organic and inorganic matter, biogenic particles and carbon-poor particles occasionally resuspended from the sediment, evolving in the water column as a function of tides and coastal currents. Particulate trace metals followed similar variation patterns along the SPM traps and were also strongly correlated with Fe- and Mn-oxides and POM. Lower concentrations during spring tides than neap tides were observed, mainly due to dilution effects of sedimentary material resuspension. The enrichment factor calculation shows the significant contribution of anthropogenic activities to the particulate concentrations of Cd and Pb, and an equivalent enrichment at spring and neap tides for every trace metal. In addition, the resuspension of historically contaminated sediments seems to contribute to a greater metal enrichment of SPM near the bottom. The SPM likely originate from both marine and terrestrial sources. Such sampling design is an interesting approach to improve our understanding of both SPM and pollutant transports in macro-tidal coastal environments.

**Keywords:** Suspended particulate matter, Trace metals, Organic matter, Belgian coastal zone

#### **4.1. Introduction**

Coastal ecosystems provide multiple ecological, social and economic services (Lau et al., 2019; Lau, 2013; Martínez et al., 2007). Geomorphologically, they also constitute large transition zones, where freshwaters meet and enter saline waters, and are driven back and forth by the ocean currents and tides (Wedding et al., 2018). Often, various chemical compounds and materials are brought into the coastal environment by the freshwater discharges, resulting from natural erosion processes occurring upstream (Förstner and Salomons, 1980; Helgen and Moore, 1996; Garneau et al., 2017; Kerr and Cooke, 2017), as well as from anthropogenic activities triggered by intensive coastal industrialization and urbanization (Phillips, 1977; Rumisha et al., 2012; Cloern et al., 2016; Andersen et al., 2020). The fate and the potential risks of such compounds are nowadays investigated intensively, especially in areas where seafood is harvested (Rumisha et al., 2017; Türk Çulha et al., 2017; van Leeuwen et al., 2005), which makes their partition into different environmental compartments (water column, sediment, biota) better understood (Balls, 1988; Barrett et al., 2018; Violintzis et al., 2009). For instance, these compounds are usually transported from the rivers down to the sea in suspended particle matters (SPM). These SPM either flocculate and deposit to the seabed where they become part of the sediment (Fettweis and Baeye, 2015; Violintzis et al., 2009; Wheatland et al., 2017), or are dissociated after a certain residence time by dilution and dissolution (Eisma and Irion, 1988; Fettweis et al., 2006; Fettweis and Baeye, 2015; Maerz et al., 2016). These SPM are complex materials gathering various types of particles with different compositions and configurations: from inorganic element like mineral particles to organic matter in various stages of decomposition, or even a combination of both types (Barrett et al., 2018; Chapalain et al., 2019; Fettweis et al., 2019, 2012; Fettweis and Lee, 2017). Furthermore,

microorganisms (*e.g.* phyto- and zooplankton) are also part of the SPM pool and can, for instance, be the dominant fraction during algal bloom (Bukaveckas et al., 2019; Cloern, 1996). Then certainly, all these particles carry along diverse pollutants like trace metals, organic contaminants, etc. (Balls, 1988; Bibby and Webster-Brown, 2006; Kerr and Cooke, 2017; Pourabadehei and Mulligan, 2016; Violintzis et al., 2009). In this way, the SPM composition often turns to be a good indicator of natural and anthropogenic fingerprint (Adriaens et al., 2018; Violintzis et al., 2009).

The distribution and biogeochemical composition of SPM (and by extension of particulate contaminants) is regulated by many external biotic and abiotic factors in the water column such as the biomass activity (*e.g.* phytoplankton bloom), salinity, pH, oxygen availability, temperature, currents, turbulence and physical mixing. (Chapalain et al., 2019; de Souza Machado et al., 2016; Fettweis et al., 2019, 2012; Hatje, 2003; Premier et al., 2019; Türk Çulha et al., 2017; Uncles et al., 2000). Along the Belgian coasts for instance, tides are quite strong and intense, varying on daily-scales and monthly-scales (Baeye et al., 2011; Brand, 2019; Fettweis et al., 2006; Strypsteen et al., 2017): this leads to large inputs of SPM from the Scheldt Estuary, sedimentary and coastal erosion, and other surrounding rivers (Rhine, Meuse) and widely increases the turbidity in this area (Adriaens et al., 2018; Baeye et al., 2011; Fettweis et al., 2012; Nolting and Eisma, 1988; Strypsteen et al., 2017; van der Zee et al., 2007).

In the framework of the NewSTHEPS project (New Strategies To assess Hazardous chemicals in the Environment using Passive Samplers; [www.newstheps.be](http://www.newstheps.be)) which aims to develop new monitoring system and modeling for pollutants in the Belgian Coastal Zone (BCZ), researches have been undertaken to investigate the influence of tides on size and composition of SPM in the water column, near the coasts of Belgium. For this purpose,



SPM were continuously sampled during one month in 2016 using two SPM traps. Thanks to a combination of hydrodynamical information, the tidal cycles were reconstructed as well (Adamopoulou et al., 2020 – *to be published*). The stronger the hydrodynamic action (i.e. spring tide), the higher the concentration of sand particles in the water column and thus the higher amount being trapped. Moreover, X-ray Computed Tomography (CT scan) performed on the traps nicely revealed darker and brighter sections (see the supplementary information): for instance, during spring tides (stronger currents than average), more sand in suspension resulted in a brighter section on the CT scans. The grainsize analysis also confirmed this observation. Such sampling approach was never attempted before in the BCZ and constitutes the main originality of the study.

From these preliminary results, the present study thoroughly investigates the chemical composition of these particles in the two traps. More precisely, the two main objectives were to (i) investigate the composition, provenance and dynamics of suspended organic matter based on their C and N content, as well as on the distribution of major elements (Al, Ca, Fe, S and Si); and (ii) assess the concentrations of various trace metals (Cd, Co, Cr, Cu, Mn, Ni and Pb) in the SPM and explain their variations according to biogeochemical processes.

## **4.2. Material and Methods**

### **4.2.1. Study site and sampling procedure**

The BCZ is a shallow and macro-tidal zone with a high turbidity, strong horizontal currents and increasing residence time of dissolved substances and particles (Gaulier et al., 2019b). As shown on Figure 4.1, the seabed vary from sandy to muddy sediments (Verfaillie et al., 2006; Fettweis et al., 2012; Baeye et al., 2011; Lourino-Cabana et al., 2014; Adriaens et al., 2018; Bockelmann

et al., 2018). The amount of SPM along the coastal zone varies between 0.02 and 0.07 g L<sup>-1</sup> in the surface waters, while the concentration ranges between 0.1 and 3 g L<sup>-1</sup> close to the seabed (Fettweis et al., 2012).

Sampling occurred between April and May 2016 in the Southern Bight of the North Sea, at a Belgian marine station MOW1 (51.3597°N; 3.11383°E; Fig. 4.1) where the water depth fluctuates between 15 and 20 m. Located about 5 km away from the coastline, MOW1 is in a maximum turbidity zone (Fettweis et al., 2006; Fettweis and Lee, 2017) where strong tidal currents often take place with a mean tidal range of 2.8 m during Neap Tide (NT) (current velocity of 0.2 to 0.6 m s<sup>-1</sup>) and 4.3 m during Spring Time (ST) (current velocity of 0.2 to 1.5 m s<sup>-1</sup>; Fettweis, 2012). A 2m-high benthic tripod was equipped with two stainless steel cages (50 cm height) and deployed on the seabed at an approximate water depth of 15 meters. One SPM trap was attached to each cage. The traps were made of a cylindrical plastic molding (50 cm length and 8 cm diameter). They were closed with plastic caps at the extremities and five sampling holes of 2 cm diameter were drilled on the sides of the top part of each trap, in order to collect SPM from horizontal currents. One trap was attached on the top of the tripod (1.5 m above the seabed), while the other one was fixed at the bottom (close to the seabed). After one-month deployment, the traps containing the collected SPM were scanned in an X-ray Computed Tomography (CT scan) and analyzed for grainsize hydrodynamic features (Adamopoulou et al., 2020 – *to be published*).

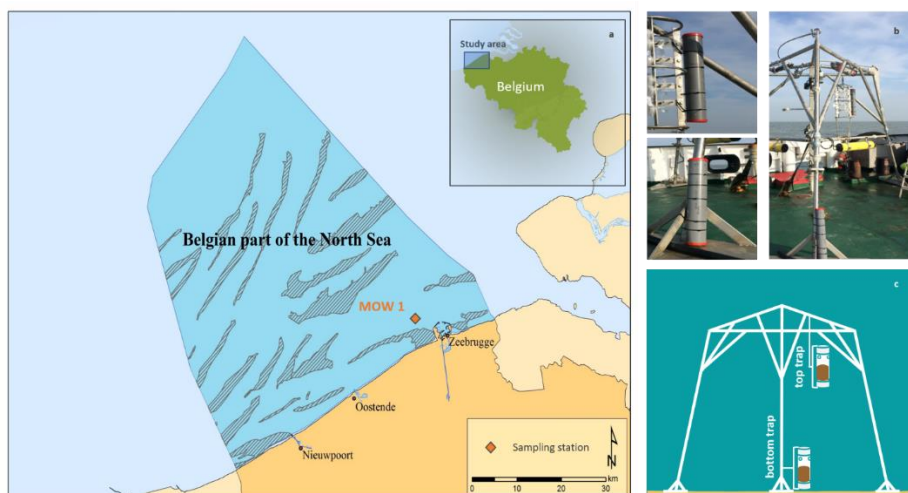


**Figure 4.1:** (a) Location of the marine station OZ-MOW1 (adapted from Vandepitte et al., 2010)). Hatched zones give the position of sandbanks. (b) Pictures on field of the sampling set-up (personal photographs). (c) Simplified diagram of the tripod and the SPM-trap deployment.

## 4.2.2. Elemental analysis

### 4.2.2.1. Micro-X-ray fluorescence spectrometry ( $\mu$ XRF)

The SPM traps were longitudinally sliced into two parts (see Adamopoulou et al., 2020 for further details) and subsampled with a U-Channel for Micro-X-ray Fluorescence ( $\mu$ XRF) spectrometry. The U-Channel (2.5 cm x 30 cm) was pressed into the part of interest for about 2 cm depth. It was then carefully lifted out, covered with plastic foil and stored at 2 °C to avoid dehydration. Multi-elements (Al, Ca, Cr, Cu, Fe, Mn, Ni, Pb, S and Si) were analyzed in this U-channel using an energy-dispersive Bruker M4 Tornado  $\mu$ XRF scanner (Bruker nano GmbH, Berlin, Germany). The Bruker M4 was equipped with a 30 W (50 kV, 800  $\mu$ A) Rh metal-ceramic X-ray tube. The source X-ray photons were focused on a 25  $\mu$ m wide (calibrated for Mo-K $\alpha$  radiation) circular spot on the sample surface using polycapillary optics. Fluorescent X-

rays returning from the sample were captured using 2 XFlash 430 Silicon Drift Detectors positioned such that the incident and outgoing X-Ray beams describe a 90° angle at the sample surface for optimal count statistics. Details on the setup and methodology of the M4 Tornado  $\mu$ XRF scanner can be found in de Winter and Claeys (2017). XRF line scans were produced at 500  $\mu$ m resolution by allowing the X-Ray spot to remain focused on each spot for 60 seconds. This time of analysis yielded the optimal compromise between measurement time and signal-to-noise ratio and was enough to reach the Time of Stable Accuracy and Time of Stable Reproducibility (see de Winter et al., 2017). XRF line scans were positioned perpendicular to the dominant lamination in the core (vertical) and spanned the full depth of the SPM accumulation. Due to the complexity of the sample matrix, well defined matrix-matched reference materials were not available to fully quantify the line scan results by means of multi-standard calibration. Instead, semi-quantitative results of Al, Ca, Cr, Cu, Fe, Mn, Ni, Pb, S and Si were produced using the built-in Fundamental Parameters (FP) quantification of the M4 Tornado calibrated to an obsidian reference material (one-standard calibration), assuming all elements were present in oxidized state.

Subsamples were taken from the U-Channels for particulate trace metal analysis (see 4.2.2.2), and measurements of Particulate Organic Carbon (POC), Particulate organic Nitrogen (PN) and their stable isotopes (see 4.2.3). These subsamples were freeze-dried using a freeze dryer (Lyovapor<sup>TM</sup> L-200, Büchi) and then homogenized using a clean ceramic mortar grinder.

#### **4.2.2.2. Trace metal extraction**

To measure the trace metal concentrations in each subsample, nitric acid (HNO<sub>3</sub>; Fisher, Trace Metal Grade, 65%), HCl (Fisher, Trace Metal Grade, 37%), HF (Fischer, Trace Metal Grade, 40%) and H<sub>3</sub>BO<sub>3</sub> (Fischer, Trace

Metal Grade, 4%) were used. Each subsample was weighed and introduced in a clean Teflon digestion tube where 4mL HF (40%), 2mL HCl (37%) and 6mL HNO<sub>3</sub> (65%) were added. The solution was heated by a microwave digestion system (Anton Paar Multiwave Go) for 9.5 minutes at 180 °C after a heating ramp of 10 min. After cooling down, 30mL of H<sub>3</sub>BO<sub>3</sub> (4%) was added to the Teflon tubes. This solution was then heated again for 5 minutes at 120°C with a heating ramp of 10 min, using the same microwave digestion system. Once the solutions cooled down again, they were transferred to clean PE vessels for analysis.

In the final treated sampling solutions, major and trace metals (Al, Cd, Co, Cr, Cu, Fe, Mn, Ni, Pb) were determined using an HR-ICP-MS (High Resolution-Inductively Coupled Plasma Mass Spectrometer, Thermo Finnigan Element II). Calibration was carried out with appropriate dilutions of an acidified multi-element stock solution (Merck, ICPMS standard XIII). Indium was used as an internal standard. To validate the whole process, two certified reference materials MESS-3 (marine sediment, National Research Council Canada) and IAEA-405 (estuarine sediment, International Atomic Energy Agency) were treated in the same way as samples. The results of all reference materials were within the range of the certified values (Table 4.1). Limits of detection (LOD) were 2.8 µg kg<sup>-1</sup> for Cd, 0.05 mg kg<sup>-1</sup> for Cr, 0.10 mg kg<sup>-1</sup> for Cu, 9.3 µg kg<sup>-1</sup> for Pb, 3.4 µg kg<sup>-1</sup> for Co, 0.10 mg kg<sup>-1</sup> for Ni, 0.35 mg kg<sup>-1</sup> for Mn, 2.1 mg kg<sup>-1</sup> for Fe and 2.5 mg kg<sup>-1</sup> for Al.

**Table 4.1:** Use of reference materials for the measurement of trace metals.

		Cd <i>mg kg<sup>-1</sup></i>	Pb <i>mg kg<sup>-1</sup></i>	Al <i>mg kg<sup>-1</sup></i>	Cr <i>mg kg<sup>-1</sup></i>	Mn <i>mg kg<sup>-1</sup></i>	Fe <i>mg kg<sup>-1</sup></i>	Co <i>mg kg<sup>-1</sup></i>	Ni <i>mg kg<sup>-1</sup></i>	Cu <i>mg kg<sup>-1</sup></i>
IAEA-405	measured	0.79	71.6	89288	94	545	47839	14.6	38.6	47.7
	certified	0.73	74.8	77900	84	495	37400	13.7	32.5	47.7
	recovery	108%	96%	115%	112%	110%	128%	106%	119%	100%
MESS-3	measured	0,27	20,2	96562	120	340	54401	14,9	51,6	32,5
	certified	0,24	21,1	85900	105	324	43400	14,4	46,9	33,9
	recovery	111%	96%	112%	114%	105%	125%	103%	110%	96%

### 4.2.3. Organic Matter (OM) characterization

Half of the remaining subsamples was weighed, put in silver cups and finally acidified with one drop of HCl (Fisher, 5%), in order to remove the carbonate fraction. The silver cups were then heated up to 50°C for at least four hours. This step (acidification and heating) has been repeated until all carbonates were removed (*i.e.* until there is no more visual reaction when adding the acid). Prior to analyses, the silver cups were folded and closed. The other half of the remaining subsamples was directly folded and enclosed in tin cups without any additional treatment, in order to measure the total carbon content.

The POC and PN amount and their stable isotope ratio contents (<sup>13</sup>C/<sup>12</sup>C and <sup>15</sup>N/<sup>14</sup>N) of all the subsamples were determined using an Elemental Analyzer coupled with an Isotope Ratio Mass Spectrometer (EA-IRMS instrument, Flash EA112, Delta V Plus, Thermo Scientific). Isotope ratios are calculated using the following formula (Eq. 4.1):

$$\delta(\text{‰}) = \frac{R_{\text{sample}}}{R_{\text{standard}}} \times 1000 \quad \text{Equation 4.1}$$

where  $\delta$  stands for  $\delta^{13}\text{C}$  or  $\delta^{15}\text{N}$  and  $R_{\text{sample}}$  and  $R_{\text{standard}}$  are the <sup>13</sup>C/<sup>12</sup>C or <sup>15</sup>N/<sup>14</sup>N ratios of the sample and the standard, respectively. For carbon and

nitrogen calibration curves, the certified reference materials IAEA-CH6 sucrose and IAEA-N2 ammonium sulfate were respectively used as standards. Limits of detection (LOD) were around 0.05 mg g<sup>-1</sup> for POC and 0.01 mg g<sup>-1</sup> for PN. The standard deviation (SD) of the measurements resulting from duplicates was below 0.51 and 0.12 mg g<sup>-1</sup>, respectively. For  $\delta^{13}\text{C}$  or  $\delta^{15}\text{N}$ , the SD was below 1.7 and 3.5%, respectively.

### **4.3. Results**

#### **4.3.1. Major and trace elements**

##### **4.3.1.1. Vertical profiles of elements using the $\mu\text{XRF}$ line scans**

The vertical profiles of major and trace elements (Al, Ca, Cr, Cu, Fe, Mn, Ni, Pb, S and Si) measured by  $\mu\text{XRF}$  are shown on Figure 4.2. These vertical profiles give a first overview of relative elemental composition in the SPM traps. In order to avoid bias caused by “edge effects” on the scans, the first and last 0.3 cm of the graphs were not considered.

The relative variations in elemental abundance vary up to 15% for Fe, 16% for S, 11% for Al, 46% for Si and 67% for Ca. On the other hand, the abundance of Cr, Mn, Ni, Cu and Pb is generally low and below an usable signal/noise ratio (< 2%), but few localized concentration peaks can be observed along the profiles especially around -4 cm, indicating the SPM deposit after the ST, and around -8 cm indicating the SPM deposit between the ST and NT.

Overall, Ca and Si significantly display opposite trends along the traps (correlation factor of -0.80,  $p < 0.001$ ; see the supplementary information for further details). In the same way, Si is negatively correlated to Al, Fe, Mn, S

(correlation  $< -0.37$ ;  $p < 0.001$ ) and, with less intensity, to Cr and Pb ( $-0.1$ ;  $p < 0.05$ ). Regarding the metallic elements only, the results show positive correlations between Fe and Al ( $0.47$ ;  $p < 0.001$ ), while Mn is rather proportional to Fe, Cu and Pb (correlation  $> 0.21$ ;  $p < 0.001$ ). Ni is correlated to Pb ( $0.26$ ;  $p < 0.001$ ) and seems to vary quite independently of the other elements.



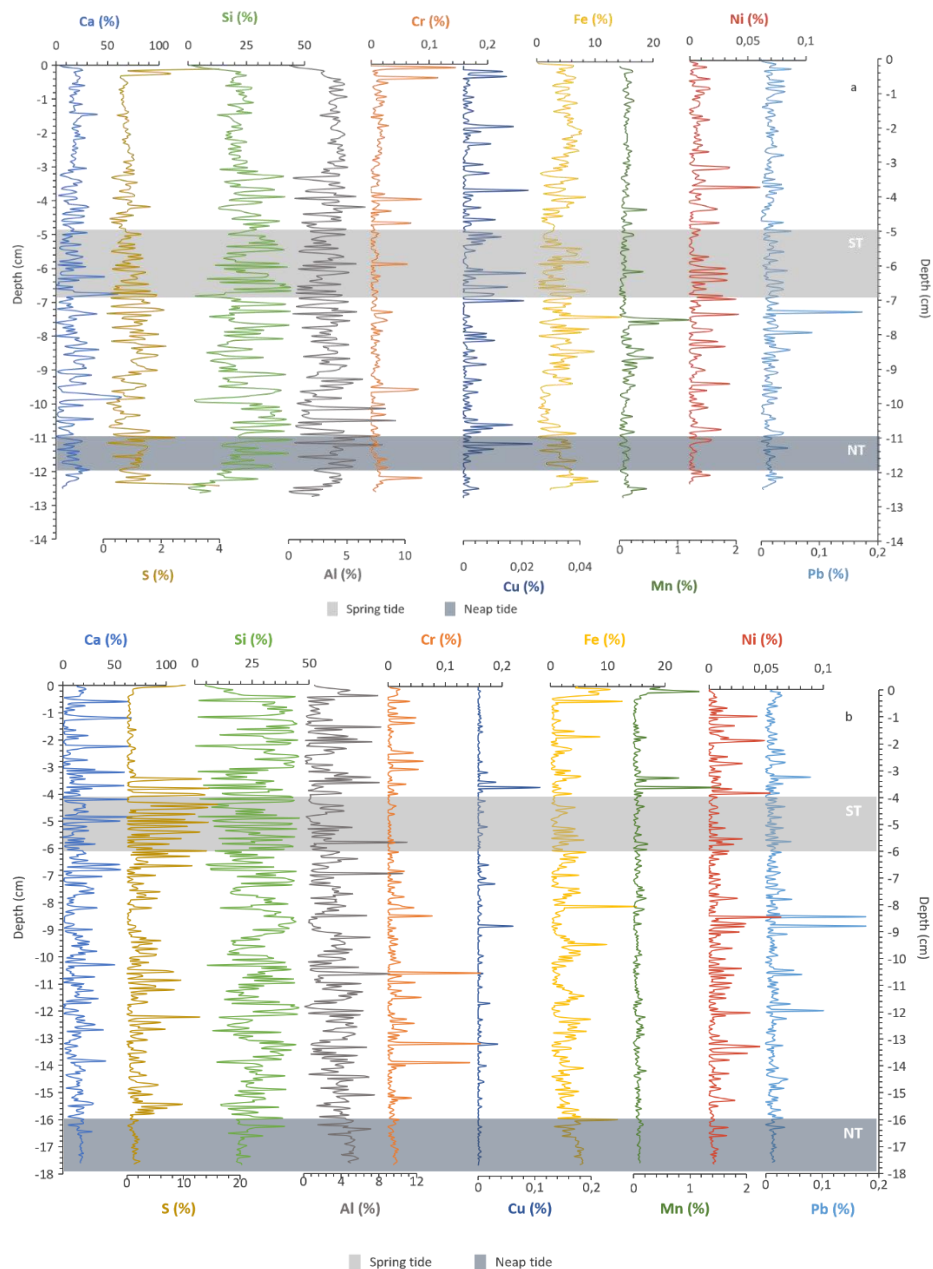


**Figure 4.2:** Micro-X-ray fluorescence spectrometry ( $\mu$ XRF) line scans of the (a) top and (b) bottom traps. On the x-axis, 0 cm corresponds to freshest SPM deposit (*i.e.* the top of the traps), while (a) 14 cm and (b) 18 cm indicate the oldest SPM deposit (*i.e.* the bottom of the traps).

For most of the elements measured in the top trap, the relative concentrations remain stable in the first 3 cm of samples (*i.e.* last SPM deposit in time) and show more variation peaks in the following sections. On the other hand, concentrations measured in the bottom trap undergo stronger fluctuations for S, Ca, Si and Al all along the scan. In the bottom trap for instance, the ST event results in a strong increase and fluctuation of S, Ca and Si. Regarding the other elements, their abundance and variations remain similar between the traps.

#### **4.3.1.2. Major and trace metal concentrations using the HR-ICP-MS**

The particulate trace metal concentrations vary from 0.17 to 0.26 mg kg<sup>-1</sup> for Cd, 16 to 29 mg kg<sup>-1</sup> for Pb, 28 to 61 mg kg<sup>-1</sup> for Cr, 0.25 to 0.49 g kg<sup>-1</sup> for Mn, 14.3 to 24.5 g kg<sup>-1</sup> for Fe, 4.3 to 10.5 mg kg<sup>-1</sup> for Cu, 3.7 to 7.0 mg kg<sup>-1</sup> for Co, 9 to 19 mg kg<sup>-1</sup> for Ni and 12.0 to 24.4 g kg<sup>-1</sup> for Al (Figure 4.3).

In average, the concentrations are always higher in the bottom trap, except for Al. In addition, all trace metals except Al follow very similar variations (correlation factor > 0.83,  $p < 0.001$ ; see the SI). Generally, they reach their lowest concentration at 6 cm deep (*i.e.* at ST). The highest concentrations in the top trap and bottom trap are found close to and during the NT, respectively. The concentration differences between the ST and NT in the top trap are less relevant than in the bottom trap. At the surface of both traps and after the ST event, the trace metal concentrations seem to rise again for all elements.

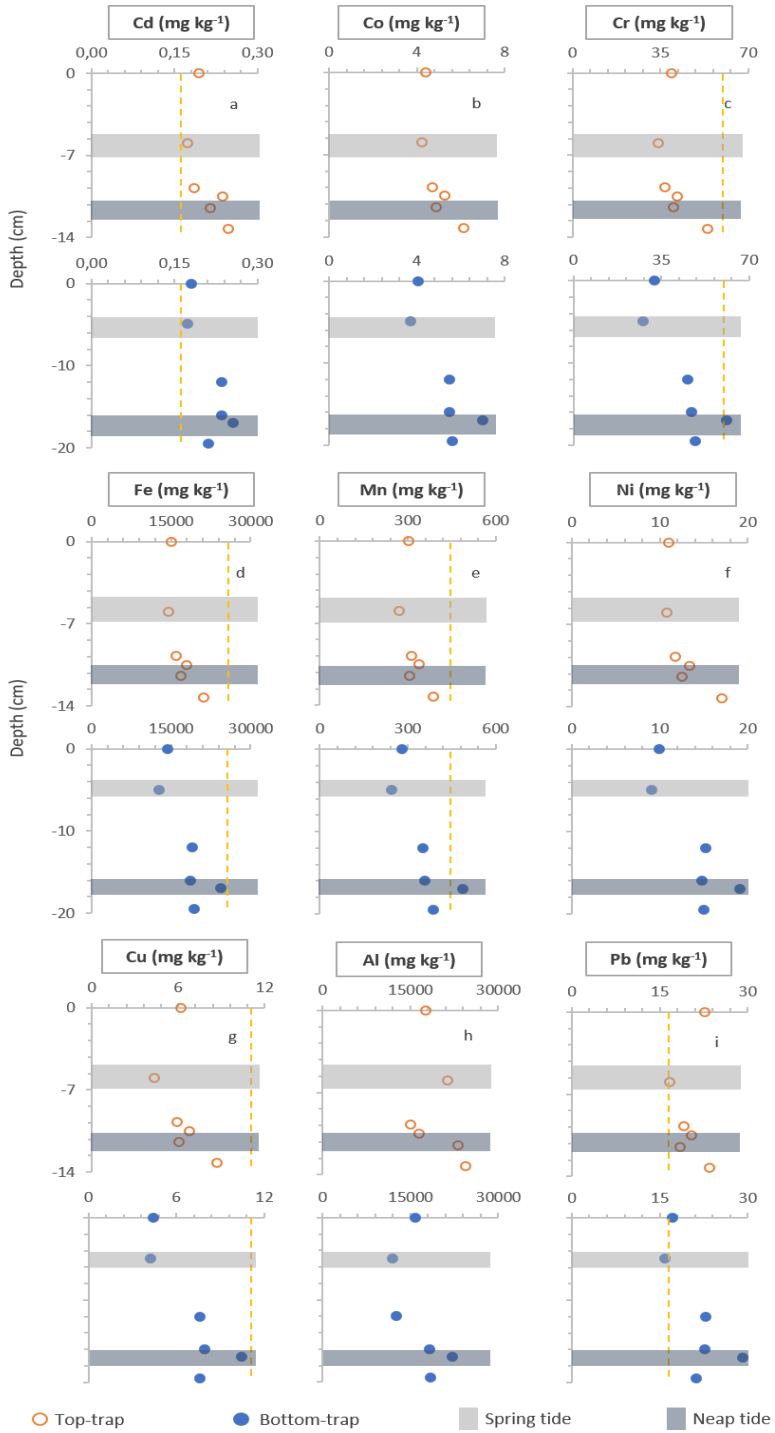


**Figure 4.3:** Particulate trace metal composition of each trap, where orange empty circles describe the top trap and blue full circles the bottom one. The y-axis represents the successive SPM deposit layers within the SPM trap (i.e. the depth within the SPM trap); the x-axis gives the concentration of each trace metal in mg kg<sup>-1</sup>. The light-grey zones represent the ST event, while the dark-grey ones are the NT event. For each element, a yellow dash-line indicates the background pedogeochemical references defined in the region (Sterckeman et al., 2007), in mg kg<sup>-1</sup>. The background reference is not indicated when out of scale (e.g. 42.3 g kg<sup>-1</sup> for Al, 11.3 mg kg<sup>-1</sup> for Co and 27.3 mg kg<sup>-1</sup> for Ni).

---

Further, the trace metal values have been normalized to those of aluminum, as this element is a major component of fine-grained aluminosilicates which usually shows minor anthropogenic input and is not affected by redox potential changes (Dehairs et al., 1989; Regnier and Wollast, 1993; Remeikaitė-Nikienė et al., 2018). And in order to link the concentrations of trace metal measured in the traps to the actual contamination level of SPM, an enrichment factor was calculated for each element, as follows (Eq. 4.2; Remeikaitė-Nikienė et al., 2018):

$$EF(Me) = \left(\frac{Me}{Al}\right)_{sample} / \left(\frac{Me}{Al}\right)_{background} \quad \text{Equation 4.2}$$

Where  $EF$  is the enrichment factor,  $Me$  is a trace metal,  $\left(\frac{Me}{Al}\right)_{sample}$  is the ratio of the particulate concentration of the metal and Al in the sample, and  $\left(\frac{Me}{Al}\right)_{background}$  is the ratio of the background concentration of the metal and Al in the study area (Sterckeman et al., 2007). The background reference concentration used here corresponds to an uncontaminated background level, assessed in the area of interest.  $EF$  values are ranked into five categories ranging from low ( $EF < 2$ ) to high enrichment ( $EF > 40$ ) (Barbieri, 2016) and are given in table 4.2.

**Table 4.2:** Enrichment factor for particulate trace metal concentrations in each SPM-trap, normalized to Al. ST stands for Spring Tides, NT for Neap Tides.

Enrichment factor (Al-based)					
Element	Station	min. - max.	average	ST-NT	SPM quality in average (Barbieri, 2016)
Cd	Top trap	2.1 – 3.8	2.9	2.1 - 2.5	moderate enrichment
	Bottom trap	3.0 – 4.9	3.6	3.9 - 3.1	
Pb	Top trap	2.0 – 3.4	2.8	2.0 - 2.1	moderate enrichment
	Bottom trap	2.8 – 4.7	3.5	3.5 - 3.4	
Cr	Top trap	1.1 - 1.8	1.5	1.1 - 1.2	
	Bottom trap	1.4 - 2.5	1.9	1.6 - 1.9	
Mn	Top trap	1.2 - 2.0	1.6	1.2 - 1.3	
	Bottom trap	1.7 - 2.7	2.0	2.0 - 2.1	
Fe	Top trap	1.1 - 1.8	1.4	1.1 - 1.2	deficiency to minimal enrichment
	Bottom trap	1.5 - 2.4	1.8	1.7 - 1.8	
Co	Top trap	0.7 - 1.2	1.0	0.7 - 0.8	
	Bottom trap	1.0 - 1.6	1.2	1.2 - 1.2	
Ni	Top trap	0.8 - 1.3	1.0	0.8 - 0.8	
	Bottom trap	1.0 - 1.9	1.3	1.2 - 1.3	
Cu	Top trap	0.8 - 1.5	1.2	0.8 - 1.0	
	Bottom trap	1.0 - 2.2	1.6	1.3 - 1.7	

For all the trace metals, the trapped SPM show various levels of enrichment. The average EF values of Co, Cr, Cu, Ni, Fe and Mn are  $\leq 2$ , which indicates no significant metal enrichment in SPM. On the other hand, moderate enrichments are observed for Cd and Pb with maximum values of 3.8 and 3.4 in the top trap and 4.9 and 4.7 in the bottom one, respectively. On average, the enrichment is always higher in the bottom trap. Moreover, the EF of every

element during ST and NT are in the same order of magnitude, indicating that the enrichment of SPM is similar during ST and NT events.

Although Fe is redox sensitive and less stable than Al in minerals, this element was also evaluated as a normalizing element, because of its suitability for normalizing trace metal concentrations in marine environment as well (Birch, 2020; Turner and Millward, 2000). Thus, an alternative enrichment factor was calculated for each element, using Fe to replace Al in Equation 4.2.

**Table 4.3:** Enrichment factor for particulate trace metal concentrations in each SPM-trap, normalized to Fe. ST stands for Spring Tides, NT for Neap Tides.

Enrichment factor (Fe-based)					
Element	Station	min. - max.	average	ST-NT	SPM quality in average
Cd	Top trap	1.9 - 2.2	2.0	1.9 - 2.1	moderate enrichment
	Bottom trap	1.7 - 2.2	2.0	2.2 - 1.7	
Pb	Top trap	1.8 - 2.4	1.9	1.9 - 1.8	moderate enrichment
	Bottom trap	1.8 - 2.0	1.9	2.0 - 1.9	
Cr	Top trap	1.0 - 1.1	1.1	1.0 - 1.0	
	Bottom trap	1.0 - 1.1	1.0	1.0 - 1.1	
Mn	Top trap	1.1 - 1.2	1.1	1.1 - 1.1	
	Bottom trap	1.1 - 1.2	1.1	1.1 - 1.2	
Co	Top trap	0.7 - 0.7	0.7	0.7 - 0.7	deficiency to minimal enrichment
	Bottom trap	0.7 - 0.7	0.7	0.7 - 0.7	
Ni	Top trap	0.7 - 0.8	0.7	0.7 - 0.7	
	Bottom trap	0.7 - 0.8	0.7	0.7 - 0.7	
Cu	Top trap	0.7 - 0.9	0.9	0.7 - 0.8	
	Bottom trap	0.7 - 1.0	0.9	0.8 - 1.0	

Compared to Al-normalized EFs, the EFs based on Fe concentrations (Table 4.3) are slightly lower but show a similar trend: with moderate enrichments in Cd and Pb, while the other metals rather display minimal enrichments. In addition, the Fe-normalized EFs values remain relatively stable over the SPM deposits (*i.e.* time).

### **4.3.2. Organic matter (OM) characterization**

#### **4.3.2.1. POC and PN contents**

In each SPM trap, the POC and PN variations follow the same trend (Figure 4.4a, b; correlation factor of 1.0,  $p < 0.001$ ). In terms of concentrations, POC varies from 6.7 to 13.1 mg g<sup>-1</sup> in the top trap, and from 4.7 to 17.1 mg g<sup>-1</sup> in the bottom one. The PN contents are lower than POC and range from 1.0 to 2.2 mg g<sup>-1</sup> in the top trap, and from 0.7 to 2.9 mg g<sup>-1</sup> in the bottom one. The maximum values are reached at -13 cm in the top trap and at -17 cm in the bottom trap: respectively right before and during the NT event. The lowest values are found during the ST for both traps. A general increasing trend of POC and PN amount is also noticed from the top to the bottom of each SPM trap, which indicates a decrease of POC and PN content when considering the chronological scale of SPM deposits from the NT to the ST event. In addition, when comparing the two traps, the POC and PN concentrations follow the same trend as well, but the range of variation from an extreme value to another is higher in the bottom trap.

The carbon content of SPM (fig. 4.4d) is rather dominated by inorganic C, as C<sub>org</sub> percentages range between 17 and 35% of the total C content (with slightly higher values in the bottom trap than in the top trap). The highest proportion of C<sub>org</sub> is measured during the Neap Tide (NT) event, for both traps (30% for the top trap, 35% for the bottom one). The lowest value is found at

the surface of the traps *i.e.* after the ST (23% for the top, 17% for the bottom trap). For the both SPM traps, the C/N ratio (fig. 4.4c) remains in the same narrow range of values: between 7.1 and 7.7 in the top trap, and between 6.8 and 7.7 close to the seabed.

As highlighted by the correlation analysis (see the SI), the trace metals measured from the acid digestion are strongly and positively correlated with the variations of POC, PN and POC/PC ratios (correlation factor  $< 0.86$ ;  $p < 0.001$ ). Al is proportional to these parameters as well, but with less intensity (correlation factor around 0.60;  $p < 0.05$ ).



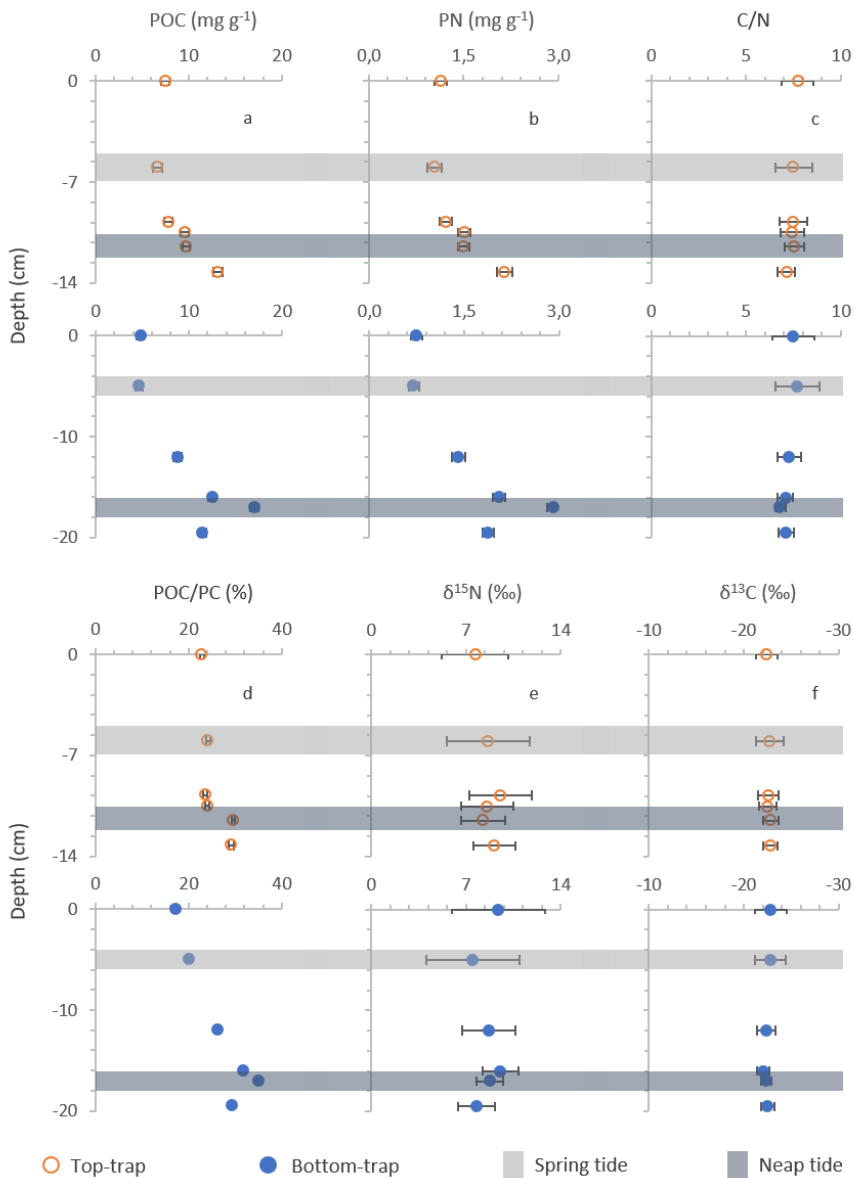


**Figure 4.4:** (a) Particulate Organic Carbon (POC), (b) Particulate Organic Nitrogen (PN), (c) C/N ratio, (d) POC/Total Particulate Carbon (PC) ratio, (e)  $\delta^{15}\text{N}$  composition and (f)  $\delta^{13}\text{C}$  of each SPM-trap, where orange empty circles describe the top trap and blue full circles the bottom one. The y-axis represents the successive SPM deposit layers within the SPM trap (i.e. the depth within

the SPM trap). The light-grey zones represent the ST events, while the dark-grey ones are the NT events.

---

#### **4.3.2.2. Stable isotope composition**

$\delta^{13}\text{C}$  and  $\delta^{15}\text{N}$  vary in a narrow range of values (fig. 4.4e, f). Values for  $\delta^{13}\text{C}$  exhibit range between  $-22.4 (\pm 1.2)$  to  $-22.8 (\pm 0.8)$  ‰ in the top trap and  $-22.1 (\pm 0.7)$  to  $-22.8 (\pm 1.7)$  ‰ in the bottom trap. The  $\delta^{15}\text{N}$  signature ranges between  $7.7 (\pm 2.5)$  to  $9.5 (\pm 2.3)$  ‰ at the top and  $7.5 (\pm 3.4)$  to  $9.5 (\pm 1.3)$  ‰ close to the seabed. These variations are not significant enough to depict any trend, indicating that the stable isotope signatures are rather stable along the traps and along a monthly tidal cycle. Moreover, the results do not show any difference between the two traps.

### **4.4. Discussion**

#### **4.4.1 Input of organic matter in the SPM traps**

In the trapped SPM, the POC and PN concentrations follow the same variations, showing a good consistency with previous studies in the same area and in the nearby Scheldt estuary (Dauby et al., 1994; Middelburg and Nieuwenhuize, 1998). Regarding the range of values, they are slightly higher than measured before 2000 by Leermakers et al. (2001; December 1996 and July 1997) in the BCZ, yet they are in the range of those measured after water filtration in April 2017 and March 2018 at the same station (between 12 and 15 mg g<sup>-1</sup>; Gaulier et al., 2019). The difference with literature may simply come from different stages of phytoplankton development during the different samplings. Here, the spring bloom started in March 2016 (see the SI) and most likely explains the highest values of particulate C and N concentrations measured in the traps (Boyd and Newton, 1995; Harmelin-Vivien et al., 2008).

During the neap tide, we observed higher POC and PN contents than during the spring tide. Particles suspended in the water column during NT contain more organic material because of their lower densities, while the ones trapped during ST contain more mineral particles (as shown for instance with minimal values of POC/PC ratio during ST). In addition, the size of SPM may play a role as well: strong currents during ST predominantly transport small and big mineral particles resulting in high SPM concentrations and a higher density, while the weak currents recorded during NT allow the trapping of larger organic SPM flocs resulting in low SPM concentrations and lower densities (Baeye et al., 2011; Fettweis et al., 2006; Maerz et al., 2016; Nolting and Eisma, 1988, Adamopoulou et al., 2020 - *to be published*).

Regarding their potential origin, the range of C/N ratios ( $6 < C/N < 8$ ) in these trapped particles suggests a substantial contribution of fresh organic material to the SPM (Middelburg and Nieuwenhuize, 1998), derived from fresh autochthonous matter like phytoplankton (Hellings et al., 1999). This shows a good link with the occurrence of a spring phytoplankton bloom as seen earlier and might lead to an increasing element adsorption/absorption by phytoplanktonic species. Concurrently, the combination of carbon and nitrogen stable isotope signatures in organic matter are also commonly used to investigate the potential origin of SPM (De Brabandere et al., 2002; Middelburg and Nieuwenhuize, 1998; Raymond and Bauer, 2001). Firstly, the  $\delta^{13}\text{C}$  ratios range between -22.1 and -22.8 ‰ in this study, which is in good agreement with the ratios previously obtained in POC of the North Sea: between -14.0 and -27.4 ‰ in the BCZ (Dauby et al., 1994) and between -20.0 ‰ and -23.1 ‰ at station MOW1 (Gaulier et al., 2019b). Moreover, these ratios are in accordance with those of  $\delta^{13}\text{C}$  and  $\delta^{15}\text{N}$  found at the sea-mouth of the Scheldt Estuary ( $\delta^{13}\text{C} = -20.1$  ‰ and  $\delta^{15}\text{N} = 9.5$  ‰; Middelburg and Nieuwenhuize, 1998), one of the most important freshwater sources to the

studied area. Thus, the values obtained for the C and N stable isotope signatures at MOW1 result from a mixing of riverine and marine sources: this confirms that this offshore station is influenced by the Scheldt, the Meuse and the Rhine river, as well as by flows from the North Sea itself and the English Channel (Baeyens et al., 1998; Lee, 1980). Furthermore, each source of organic SPM does not seem to prevail on the other, as the results remain consistent over a month.

Few differences are observed between the SPM trapped in the top trap and those collected close to the seabed in the bottom trap. For instance, the range of POC and PN contents in SPM is wider in the bottom trap than in the top trap, indicating higher fluctuations in the bottom waters, close to the sediment. The mixing of SPM in the water column is therefore not the same due to stronger mixing forces at the sediment interface. According to Fettweis and Baeye (2015), this vertical gradient is mainly observed in Summer, while the SPM are better mixed along the water column in Winter. In addition, the larger fluctuations observed at the bottom result from sediment resuspension, increasing the contribution of sedimentary particles poor in organic matter, to suspended materials in the water column. Indeed, the sediment rather contains low amounts of POC in the Southern North Sea (Bale and Morris, 1998; Bartholomä et al., 2000; van de Velde et al., 2017, 2016).

Finally, the signature of sedimentary organic matter is generally different than that observed in the water column ( $8 < C/N < 10$  in North Sea sediments studied by van de Velde et al., 2016). Degradation processes induce a progressive enrichment of C in the organic molecules compared to N. Here, the distance between the traps did not allow to observe a significant enrichment. For future monitoring, the deployment of a SPM trap higher in the water column (closer to the surface) should enable such observation.

#### 4.4.2. Major elements

According to the  $\mu$ XRF line scans (fig. 4.2) and the ICP-MS measurements (fig. 4.3), the suspended particles are mainly composed of Ca, Si, Al, Fe, Mn and S forming a group of major inorganic elements and carrier phases, while minor components like Cd, Co, Cr, Cu, Ni and Pb are present in less abundance and constitute a group of trace elements (see 4.4.3). This observation is incidentally in agreement with previous studies on SPM conducted in the North Sea catchment area (Nolting and Eisma, 1988; Turner et al., 1991). The suspended particles are therefore mainly composed of sand, organic matter (OM), oxides, clays, calcium carbonate and to lesser extent sulphate and/or sulphide precipitates. From the  $\mu$ XRF profiles, a negative correlation was observed between the relative abundance of most major elements (Ca, Al, Fe, Mn and S) and Si along the trap. Silicon most likely represents sand particles (Ehlert et al., 2016; Grasse et al., 2017) originating from erosive or sedimentary material. When a large amount of sand is provided to the water column, less OM and metals are measured as a result. In addition, Si is often constitutive of phytoplanktonic matter such as diatoms (Dobbins et al., 2017; Liang et al., 2019) and is therefore frequently observed in the suspended particulate fraction during primary production period.

Calcium comes partly from the erosion of carbonates from the sedimentary rocks in the nearby Straits of Dover (Migné et al., 1998; Nolting and Eisma, 1988; Tribovillard et al., 2012). Moreover, and given the occurrence of a spring bloom during sampling, the measured Ca has, in the same way as Si, a biogenic signature through planktonic groups such as coccolithophores (Nolting and Eisma, 1988; Zondervan, 2007).

The sulfur relative abundance recorded by  $\mu$ XRF must be cautiously interpreted since dissolved sulfate is a major element of the seawater (around  $2 \text{ g L}^{-1}$ ). However, since the main composition of the seawater does not evolve over 1 month and supposing that the water percentage along the trap is quite similar, the dissolved sulphate fraction may approximately be constant. Sulfur is also present in biogenic particles and exudates (average elemental quota of  $1.3 \text{ mol/mol P}$ ; Ho et al., 2003), but this fraction is likely negligible in SPM compared to that of remaining dissolved sulfates. The presence of inorganic precipitates in seawater is due to the resuspension of some reduced sulfur compounds produced during the early diagenesis processes in the surface sediments. The fluctuation of the signal displayed in Figure 4.2 is probably a combination of the temporary remobilizations of sulfidic particles to the water column (Burton et al., 2006; Thamdrup et al., 1994; Ye et al., 2013) and to a lesser extent, variations of water content in the traps.

Finally, and in such coastal environment, the presence and/or formation of Fe and Mn-oxides in the particulate phase is usual (Reckhardt et al., 2017; van de Velde et al., 2018; Zhou et al., 2018). Based on the observed correlations and the literature data, these oxides interact with particulate organic matter (Turner et al., 2004). Thus, a colloidal combinations of Fe- and Mn-oxides with OM (Catrouillet et al., 2016; Dang et al., 2015; Rose and Waite, 2003; Viollier et al., 2000) is very likely to occur. In addition, an uptake of dissolved Fe and/or Mn by coccolithophorid organisms (Hartnett et al., 2012; Shi et al., 2010; Sunda and Huntsman, 2000) and/or sorption processes onto carbonate phases can explain the good correlation observed with carbonates.

#### **4.4.3. Trace metal behavior**

Given the background reference values (Figure 4.3) and the enrichment factor calculated for each metal (Table 4.3), the SPM show a clear contamination by

Cd and Pb for the whole sampling period and by Cr and Mn, only at neap tide. This suggests a significant contribution of anthropogenic sources to the enrichment of Cd and Pb in SPM and, to less extent, of Cr and Mn (Abreu et al., 2016; Barbieri, 2016; García et al., 2008). A similar observation was made for Cd and Pb enrichments along the nearby Scheldt Estuary (*see Chapter 2. Trace metal speciation along the Scheldt Estuary*). Such enrichments in the SPM would most likely need more investigation and monitoring in the future, especially for Cd and Pb which are listed as substances of priority concern by the OSPAR Convention (OSPAR, 2009, 2002). In the same way, trace metal concentrations of Cr, Pb and Fe are comparable with those of industrial coastal environments (Dauby et al., 1994; Laslett, 1995). This reflects the strong influence of riverine inputs in this area, like the Scheldt Estuary which flows across heavily populated and urbanized areas and consequently brings these metals into the BCZ (W. Baeyens et al., 1998; Gaulier et al., 2019b; Speeckaert et al., 2018). For the other trace metals, the low EF indicates that the concentrations measured are mostly the result of natural weathering processes (Abreu et al., 2016; García et al., 2008). A comparison of these results to a recent study carried out at the same sampling point between 2016 and 2018 (Gaulier et al., 2019) shows good agreements for Cd, Pb, Co and Ni, while Cu displays lower concentrations in the SPM traps. As shown with Cd, we would expect lower particulate concentrations than measured in the Scheldt Estuary as a result of dilution processes (*see Chapter 2. Trace metal speciation along the Scheldt Estuary*). However, the concentrations of Pb, Co, Ni and Cu are slightly higher than those measured at the estuarine mouth. Instead, they are in a similar range as the values recorded in the middle and upper estuary. Specifically, the maximum values of all elements (systematically recorded at -12 cm in the bottom trap) are often exceeding the concentrations found in the estuary or in the coastal zone. This finding

suggests that the metal contamination at the marine station MOW1 may be linked to historical pollution of the area (coming at least partly from the Scheldt watershed) and that an excess of metal in SPM may come from the resuspension of contaminated sedimentary particles. This assumption could be experimentally tested through sediment core analyses, in order to trace back the origin of the successive deposit layers (*e.g.* metallic and isotopic contents).

As mentioned in 4.4.1, differences between the SPM collected in the top and the bottom trap are also observed for trace elements. Thus, the trace metal levels as well as their EF are, in average, higher in the bottom trap, in average. As the latter was located closer to the seabed during sampling, sediment resuspension could explain the higher values found at the bottom, especially as the sediments show higher concentrations of trace metals than in the above water column in this area (Hatje, 2003; Robinson et al., 2017; Violintzis et al., 2009). This also indicates that the sediment plays a key role in trace metal transfers and significantly contributes to the water column load in trace metals through SPM, especially at spring tides when the currents are stronger, increasing the remobilization of pollutants. This is also confirmed by the increase of S concentrations in the bottom trap, during the ST: reduced sulfur produced in the surface sediment during the early diagenesis processes (Audry et al., 2007; Goldhaber and Kaplan, 1980; van de Velde et al., 2017) are partly resuspended from the sediment to the water column. Thus, due to sediment resuspension and powerful advective mechanisms near the seabed, the bottom waters are more turbid, variable and more enriched in trace metals (Fettweis et al., 2006; Helali et al., 2016; Jago et al., 2002; Manning et al., 2010; Morris et al., 1986; Velegrakis et al., 1997).

Furthermore, the strong similarity between the profiles of all elements (Figure 4.3) is interesting as it indicates a common behavior and origin, or at least that particulate Cd, Cr, Co, Cu, Fe, Mn, Ni and Pb are driven by similar



biogeochemical cycles in this turbulent area (Remeikaitė-Nikienė et al., 2018). Firstly, it seems that they mainly bind to Fe-oxides, whereas Al (representing clays) shows a weak correlation with Cd, Pb, Cr, Mn, Co, Ni and Cu. This difference in concentration variations could come from the presence of a large diversity of fine suspended particles in the water, including a substantial amount of organic matter (including living organisms) binding trace metals without significant quantities of clays (phytoplankton for instance). Such disparity between Al and trace elements was also noticed in a previous study in the North Sea (Nolting and Eisma, 1988). The poor link between Al and other trace metals eventually questions its use in normalizing trace metal concentrations. Al and Fe both usually show a great suitability for normalizing elements, because they act as good tracers for fine-grained particles and rarely significantly originate from anthropogenic sources (Birch, 2020, 2003; Daskalakis and O'Connor, 1995; Yari et al., 2018). However, Fe is often more reactive than Al in marine environment (redox sensitive element cycling between Fe(II) and Fe(III) species with various solubilities) and consequently often less appealing for the normalization (Birch, 2020). Nevertheless, in our case, Fe would be preferred for the normalization of elements. First, because it shows a strong correlation with the other trace metals and secondly because Fe-oxides seem to be an important sorbent phase for trace metals in the water column. This assumption was supported in earlier studies in North Sea coastal zones (Turner and Millward, 2000; Whalley et al., 1999). An additional possible explanation of this strong correlation Fe-trace metals is linked to the influence of redox changes on iron cycling, close to the water-sediment interface. The repetitive re-oxidations of reduced Fe(II) into Fe(III) during sediment resuspension results in the formation of poorly crystallized iron oxyhydroxides (amorphous and reactive) with a huge specific area, capable of quantitatively scavenging trace elements (Burdige and

Komada, 2020; Liu et al., 2019). This process should therefore progressively shift the equilibrium of sorption processes to iron oxides rather than to clay materials.

However, similar results were obtained between Al- and Fe-based EFs, indicating that both elements eventually give the same information on SPM enrichment for environmental risk assessment purpose.

In the  $\mu$ XRF profiles, the relative abundance of most trace metals does not proportionally vary with Si. Only Ni shows a slight positive relation to Si that may be the result from the binding of Ni onto diatom cells. For the other trace elements, the negative correlation rather indicates a weak affinity for sand particles and other Si biogenic forms. Instead, a correlation between Fe, Mn, Pb, Cr and Ca is revealed by the  $\mu$ XRF scans. This can be explained by the ability of Mn, Pb and Cr to be associated with iron oxides or carbonates (Yang et al., 2018), or because these elements may be used by small algae like coccolithophores which are composed of calcium carbonate scales (Balch, 2018; Johnson et al., 2018). These explanations may also be associated to the common source of Ca and Fe particles that induce a good correlation between these 2 major elements. In addition, and as highlighted in 4.4.2, Fe and Mn-oxides form good carrier phases and impact the scavenging of trace elements, as well as their release when the oxides reduce in the sediment (Reckhardt et al., 2017; Trueman, 2017). For instance, elements like Cd, Cr, Cu and Pb show a good affinity for these oxides, as well as for organic matter (Charriau et al., 2011; Stone and Marsalek, 1996; Turner et al., 2004) with the possibility of forming mixed particles composed of OM and iron oxides associations (Catrouillet et al., 2016; Nolting and Eisma, 1988; Turner et al., 2004). In the

$\mu$ XRF results, Ni seems correlated only with Pb, but the signal is very low, and this result has to be taken carefully.

Conversely to  $\mu$ XRF results, the concentrations of trace metals obtained from the total digestion seem higher during neap tides than during spring tides. However, it does not mean that the suspended particles are necessarily more contaminated, as the calculated EFs remain in the same range of values during the two events for all elements. Indeed, the spring tides likely bring higher amount of particulate trace metals than during NT (particularly due to polluted sediment resuspension close to the seabed), but they probably also carry a non-negligible amount of inert suspended matter (due to the stronger currents), finally diluting the particulate trace metals concentrations. The higher relative abundance of S, Ca and Si during ST supports the latter hypothesis. During neap tides, SPM are therefore mainly composed of fine particles (*e.g.* oxides, clays, phytoplankton) which adsorb trace metals and stay suspended in the water column longer.

Finally, very detailed patterns can be observed using the  $\mu$ XRF scans (Fig. 4.2), which cannot be recovered from the trace metal extraction results (Fig. 4.3). The  $\mu$ XRF scan produces much higher resolution profiles which gives individual fluctuations of elements, compared to the classic measurement of particulate trace metals (slicing the SPM cores and acid digestion of particles) which gives an average of these fluctuations. Moreover, the  $\mu$ XRF method has the great advantage of being a non-destructive technique. However, the  $\mu$ XRF cannot give quantitative data if no comparable reference material is available, like it was the case here. In addition, more disparities between the ST and NT were expected on the  $\mu$ XRF profiles. Instead, only few global variations were observed. In conclusion, the complementary use of both techniques ( $\mu$ XRF and acid digestion of particles) is eventually a relevant approach to the study of cores (SPM, soil or sediment). Here, to deeply understand whether the

numerous fluctuations are linked to recurrent events such as daily tidal cycles or not and to exclude background noises from the signal, wavelet or FFT spectral analyses could be an added value to the study and will constitute the next step of this work (ongoing).

#### **4.5. Conclusion**

The characteristics and pollutant enrichments of SPM in the Belgian Coastal Zone can be traced at the scale of tidal cycles, using different tools. Close to the seabed, higher trace metal enrichments, increasing S concentrations and SPM amount highlighted sediment resuspension at the bottom of the water column. In the same way, the historical contamination of the sediments from the Southern North Sea probably constitutes a significant source of metallic compounds, especially during spring tides when increasing current strength stresses the transfers from sediment to the water column. In addition, particle inputs from the Scheldt Estuary may widely influence the particle and water composition around MOW-1 (see Chapter 2).

The highest metal concentrations coincided with a higher amount of small SPM in size (monitored through Fe and Al reference elements) and higher organic and nitrogen concentrations in SPM, while the provenance of the suspended organic matter does not seem to drastically change, which is a mixture of autochthonous and allochthonous particles. Overall, POM and Fe-, Mn-oxides are the main binding phase for trace metals in the Belgian Coastal Zone. In addition, the calculation of enrichment factors has shown the possible anthropogenic inputs of Cd, Pb. However, the enrichment of suspended particles remains the same during NT and ST. Furthermore, the  $\mu$ XRF scans may provide a better view of the SPM composition fluctuations with detailed information on the monthly tidal cycles, and even perhaps on variations

related to daily tides. To better understand the changes in particulate concentrations of trace elements and the partition mechanisms involved, it would be interesting to measure the dissolved fraction as well. In addition, a comparison of the result obtained in this study with deposited material (grab sample or sediment core) would be necessary, to better understand the role of the seabed as a reservoir and as a source of matter. SPM and trace metal transport over seasons, low or high freshwater discharge influence, dry or stormy weather effects are also other leads for further investigations along the BCZ. Beside the focus on suspended particles and strongly complexed trace metals influenced by tides, it could also be relevant to study the impact of tidal cycles on the distribution of labile trace metals (*i.e.* free metal ions and weakly complexed colloids) which have greater adverse effects on marine ecosystems. Overall, considering the tidal variations when monitoring SPM and particulate metal contaminants could lead to a more integrated environmental management and could surely improve our knowledge on anthropogenic impacts and pollutant fluxes. On a larger scale, this could also help to better model and predict the transport of various pollutant types in marine systems subject to strong tidal currents.

Moreover, and in comparison with Chapter 2, the influence of the Scheldt Estuary on the water composition of the BCZ (here MOW-1) seems considerable and should not be ignored. In addition, within the NewSTHEPS project and in collaboration with the Royal Belgian Institute of Natural Sciences, a pollutant exposure model was developed and based on the hydrodynamic model COHERENS, considering advection, diffusion, adsorption/desorption of pollutants to suspended and bed sediment and drawing the link between river sources (Scheldt, Meuse and Rhine) with the BCZ. This preliminary work is still ongoing, but the first results already gave nice insights on pollutant fluxes in the BCZ. For instance, it has yet

demonstrated that the contribution from each river system to the annual average concentration is important, and that it considerably fluctuate over a year. It also has also yet confirmed the strongest contribution of the Scheldt to the Belgian coast (and by extension MOW-1) and helped to identify zones of concern.

## **Acknowledgement**

The authors would like to thank the Belgian Science Policy Office (BELSPO) for funding the NewSTHEPS project (BR/143/A2/NEWTHEPS) and supporting Gaulier C. In addition, the authors would like to thank VUB SRP2 (Tracing and Modelling of Past & Present Global Changes). The RV Belgica crew members, the scientific vessel of the Belgian government, and the OD Nature team (Royal Belgian Institute of Natural Sciences, Brussels) are thanked for sampling and preliminary analyses. The authors thank the Research Foundation Flanders FWO-Hercules foundation for the acquisition of the  $\mu$ XRF instrument, and VUB Strategic Research. De Winter N. is a Flemish Research Foundation (FWO; 12ZB220N) post-doctoral fellow and is supported by a MSCA Individual Fellowship (H2020-MSCA-IF-2018; 843011 – UNBIAS). Leermakers M., Verstraeten D. and Brion N. are also thanked for their support in the analysis.

#### 4.6. Supplementary information

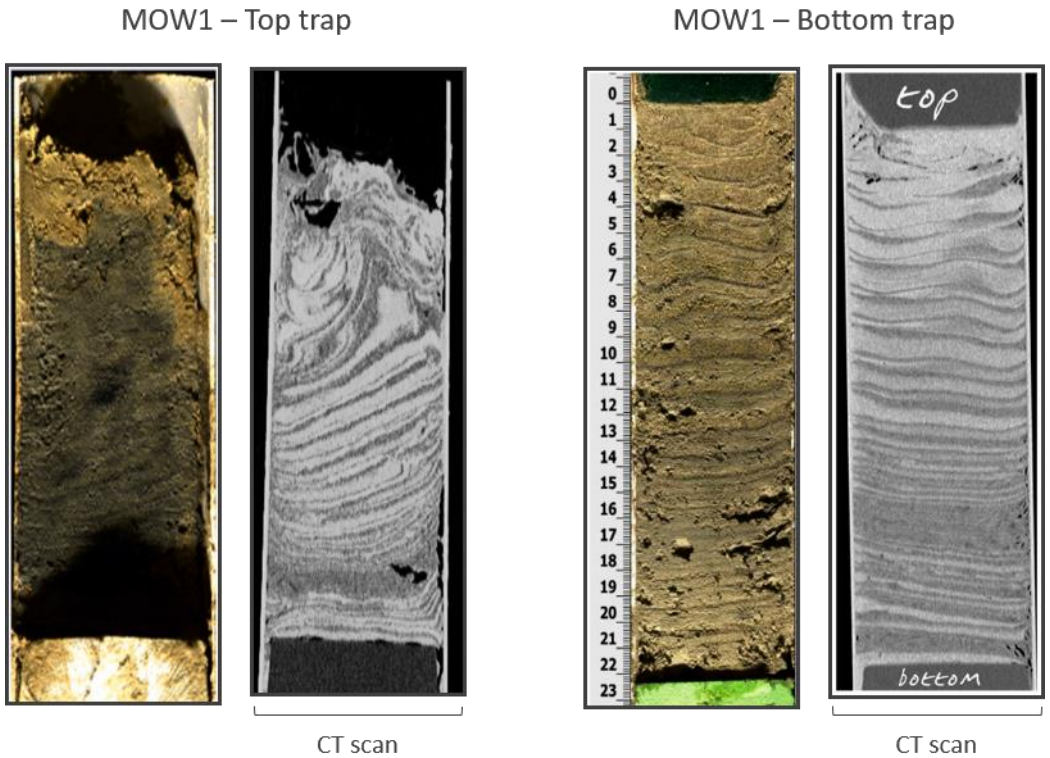


**Figure S4.1:** The CT scans revealed a recurrent pattern of tidal layers. During high currents smaller SPM flocs with higher density (lighter colors on the CT scan) are trapped, and when the currents are decreasing larger SPM flocs with lower density (darker colors on the CT scan) settled and are trapped. Scans retrieved from Adamopoulou et al. (2020 – *to be published*).

---



**Table S4.1:** Correlation and associated p-value matrices from the  $\mu$ XRF measurements.

**Correlation matrix**

	<i>Al</i>	<i>Si</i>	<i>S</i>	<i>Ca</i>	<i>Cr</i>	<i>Mn</i>	<i>Fe</i>	<i>Ni</i>	<i>Cu</i>	<i>Pb</i>
Al	1,00									
Si	-0,37	1,00								
S	-0,14	-0,41	1,00							
Ca	0,08	-0,80	0,03	1,00						
Cr	0,08	-0,14	0,01	0,09	1,00					
Mn	0,11	-0,40	0,03	0,32	0,02	1,00				
Fe	0,47	-0,60	0,03	0,32	0,22	0,39	1,00			
Ni	-0,09	0,18	-0,07	-0,16	0,05	-0,01	-0,09	1,00		
Cu	-0,10	0,01	-0,04	0,07	0,04	0,30	-0,12	0,08	1,00	
Pb	0,04	-0,09	-0,08	0,09	0,04	0,21	0,17	0,26	0,14	1

**p-values**

	<i>Al</i>	<i>Si</i>	<i>S</i>	<i>Ca</i>	<i>Cr</i>	<i>Mn</i>	<i>Fe</i>	<i>Ni</i>	<i>Cu</i>	<i>Pb</i>
Al	0									
Si	0,00	0,00								
S	0,00	0,00	0,00							
Ca	0,06	0,00	0,49	0,00						
Cr	0,04	0,00	0,85	0,04	0,00					
Mn	0,01	0,00	0,47	0,00	0,64	0,00				
Fe	0,00	0,00	0,52	0,00	0,00	0,00	0,00			
Ni	0,04	0,00	0,07	0,00	0,22	0,74	0,02	0,00		
Cu	0,02	0,76	0,30	0,07	0,29	0,00	0,00	0,06	0,00	
Pb	0,33	0,03	0,04	0,03	0,38	0,00	0,00	0,00	0,00	0

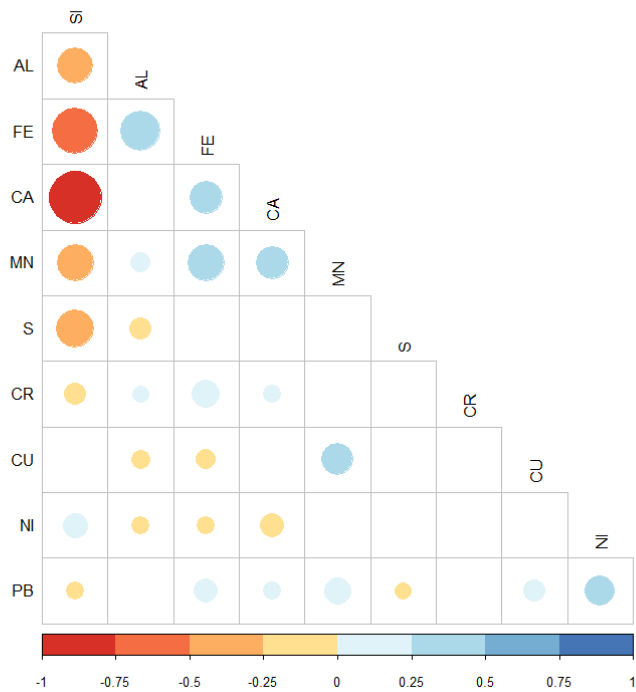


**Figure S4.2:** Correlogram resulting from the  $\mu$ XRF measurements.

---

**Table S4.2:** Correlation and associated p-value matrices for the measurements from the total acid digestion and organic matter characterization

**Correlation matrix**

	<i>PN</i>	<i>POC</i>	<i>D15N</i>	<i>D13C</i>	<i>C.N</i>	<i>C<sub>org</sub>/C<sub>tot</sub></i>	<i>Cd</i>	<i>Pb</i>	<i>Cr</i>	<i>Mn</i>	<i>Fe</i>	<i>Co</i>	<i>Ni</i>	<i>Cu</i>
PN	1.00													
POC	1.00	1.00												
D15N	0.21	0.20	1.00											
D13C	0.50	0.50	0.15	1.00										
C/N	-0.91	-0.89	-0.38	-0.48	1.00									
<i>C<sub>org</sub>/C<sub>tot</sub></i>	0.93	0.94	0.12	0.50	-0.81	1.00								
Cd	0.86	0.87	0.22	0.50	-0.78	0.78	1.00							
Pb	0.88	0.87	0.13	0.63	-0.78	0.75	0.83	1.00						
Cr	0.97	0.97	0.19	0.49	-0.90	0.88	0.89	0.93	1.00					
Mn	0.96	0.95	0.19	0.49	-0.92	0.83	0.85	0.92	0.97	1.00				
Fe	0.96	0.96	0.23	0.43	-0.92	0.86	0.91	0.90	0.99	0.98	1.00			
Co	0.97	0.97	0.24	0.46	-0.91	0.87	0.91	0.90	0.99	0.98	1.00	1.00		
Ni	0.96	0.95	0.23	0.46	-0.92	0.87	0.91	0.89	0.98	0.96	0.99	0.99	1.00	
Cu	0.96	0.96	0.19	0.57	-0.88	0.86	0.92	0.95	0.98	0.97	0.97	0.98	0.98	1.00
Al	0.59	0.60	0.14	-0.13	-0.40	0.61	0.39	0.35	0.54	0.44	0.50	0.50	0.49	0.42

**p-values**

	<i>PN</i>	<i>POC</i>	<i>D15N</i>	<i>D13C</i>	<i>C.N</i>	<i>C<sub>org</sub>/C<sub>tot</sub></i>	<i>Cd</i>	<i>Pb</i>	<i>Cr</i>	<i>Mn</i>	<i>Fe</i>	<i>Co</i>	<i>Ni</i>	<i>Cu</i>
PN														
POC	0.00													
D15N	0.50	0.52												
D13C	0.10	0.10	0.64											
C.N	0.00	0.00	0.23	0.11										
<i>C<sub>org</sub>/C<sub>tot</sub></i>	0.00	0.00	0.72	0.10	0.00									
Cd	0.00	0.00	0.49	0.10	0.00	0.00								
Pb	0.00	0.00	0.69	0.03	0.00	0.00	0.00							
Cr	0.00	0.00	0.56	0.11	0.00	0.00	0.00	0.00						
Mn	0.00	0.00	0.56	0.10	0.00	0.00	0.00	0.00	0.00					
Fe	0.00	0.00	0.47	0.16	0.00	0.00	0.00	0.00	0.00	0.00				
Co	0.00	0.00	0.45	0.13	0.00	0.00	0.00	0.00	0.00	0.00	0.00			
Ni	0.00	0.00	0.47	0.14	0.00	0.00	0.00	0.00	0.00	0.00	0.00	0.00		
Cu	0.00	0.00	0.56	0.05	0.00	0.00	0.00	0.00	0.00	0.00	0.00	0.00	0.00	
Al	0.05	0.04	0.67	0.68	0.20	0.04	0.21	0.26	0.07	0.15	0.10	0.10	0.11	0.18

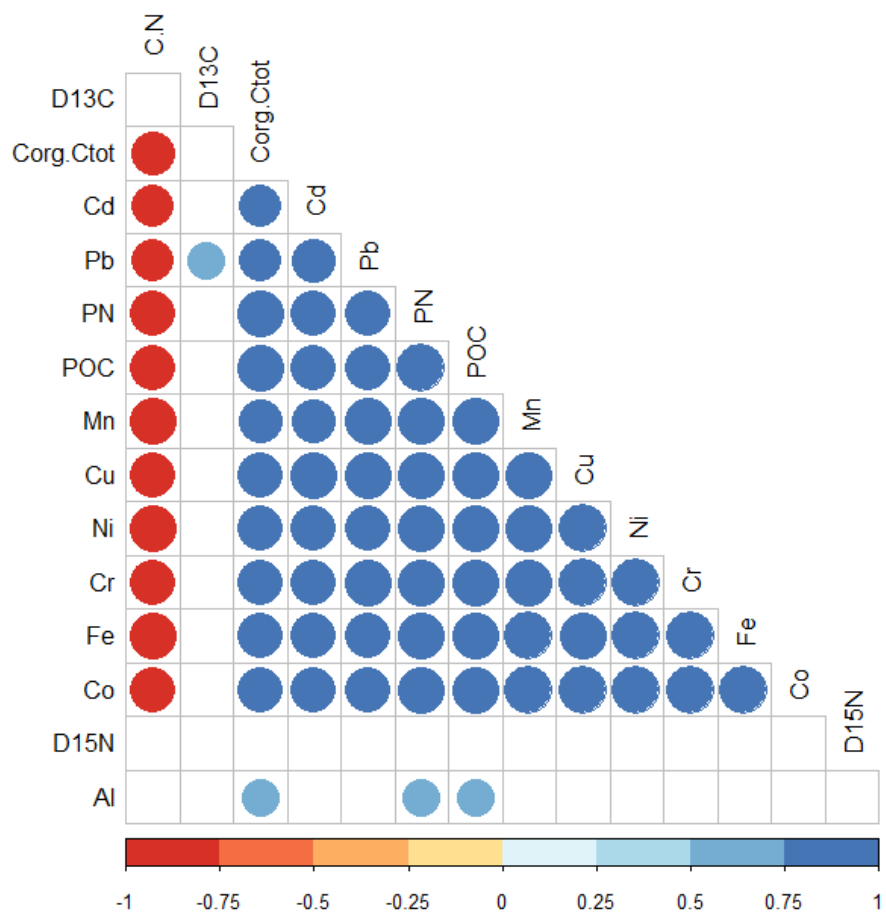


**Figure S4.3:** Correlogram resulting from the total acid digestion and organic matter characterization

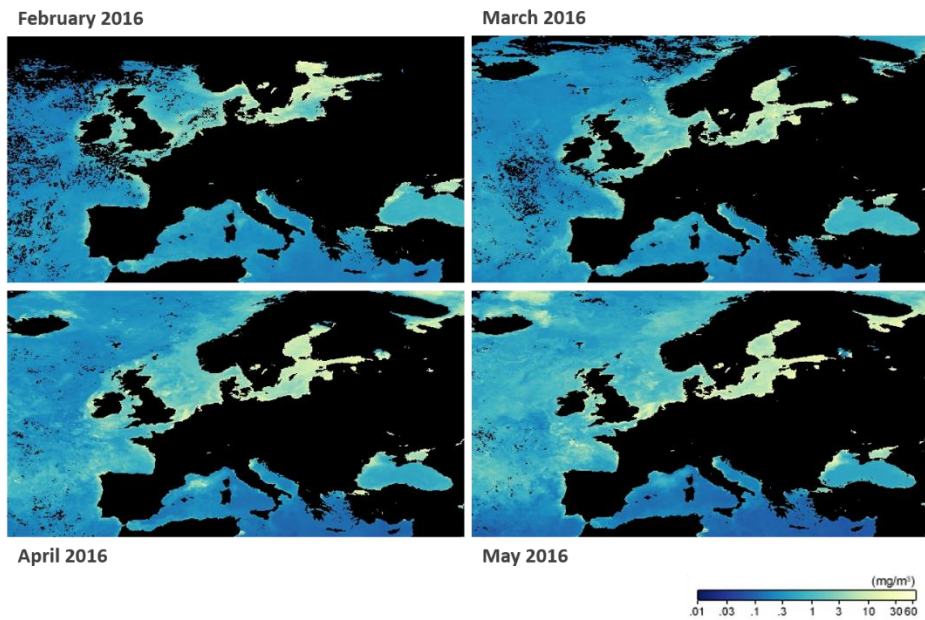
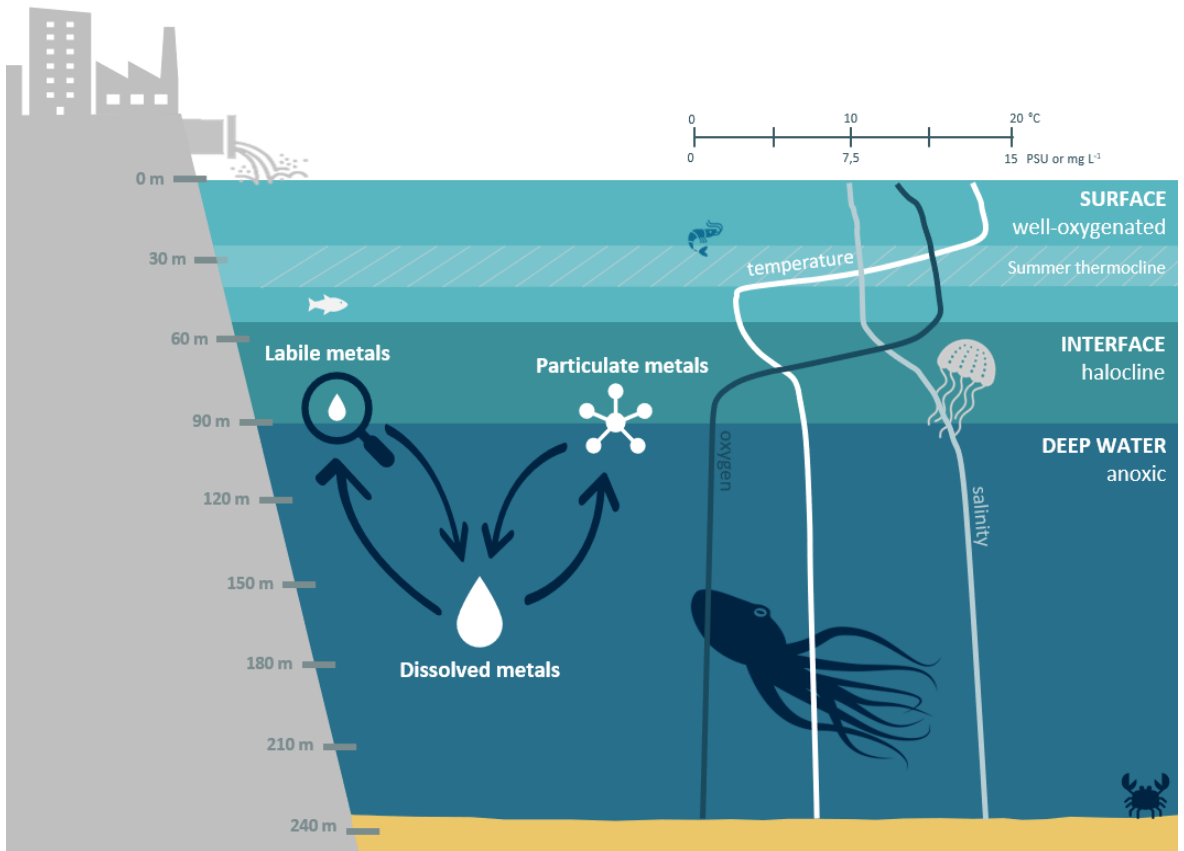


**Figure S4.4:** The evolution of chlorophyll concentration from February to May 2016 (retrieved from (NASA Earth Observations, 2020))

---

# Chapter 5

## Trace metal vertical distribution and speciation in Baltic Sea waters



## Trace metal vertical distribution and speciation in Baltic Sea waters

*Gaulier C., Zhou C., AbdulBur-Alfakhory E., Leermakers M., Superville P.-J., Billon G., Baeyens W., Gao Y. In preparation for Science of the Total Environment.*

### Abstract

Ever since Scandinavia has been populated, the Baltic Sea has served as a path to connect the Northern Europe countries and as a source of human livelihood. Today, metallic pollution associated with rapid coastal development is of specific concern in the Gotland Basin. Because of hypoxia and long water residence time, large variations of physicochemical parameters from the surface waters to the bottom were recorded in the deep basin, influencing trace element distribution. Here, the vertical gradients of labile, dissolved and particulate trace metals as well as the biogeochemistry of nutrients were investigated in both Western and Eastern Gotland Basin, from surface-oxygenated waters to deep-anoxic ones. Labile trace metals were measured using DGT passive samplers, while the dissolved and particulate trace metal concentrations were assessed using classic active sampling techniques. This combination of techniques allows to unravel the link between trace metal concentrations, their possible bioavailability and biogeochemical features of the basin. Overall, the distribution of elements in the water column is mainly related to the water depth, the organic matter mineralization and the resulting oxygen availability which influence biogeochemical reactions. In the deepest waters, the strong euxinia leads to the precipitation of most trace metals with sulfide forming sulfidic colloids, Cu being the most insoluble element. Fe- and Mn-oxides originating from natural sedimentation processes or from a shelf-to-basin shuttle are strongly reduced in the anoxic zone, releasing carrying elements such as dissolved Co and, to a lesser extent, dissolved Pb. Slow release of dissolved Fe and Mn from the sediment might occur as well. Vertical transport of Cd, Cr, Cu and Ni is likely to involve various processes such as releases from Fe- and Mn-oxides, or from other organic/inorganic particles. Dissolved non-labile species are dominant all along the water column, yet labile fractions measured with DGT of Co, Fe, Ni and Mn show a substantial contribution in the anoxic zone. Data from this investigation were also compared with previous studies, carried out before and after the Major Baltic Inflow of 2015.

**Keywords:** Trace metals, Speciation, Baltic Sea, Biogeochemistry, Anoxia



## 5.1. Introduction

Since time immemorial, coastal areas have been a key spot for civilization and society settlement and development (Erlandson and Fitzpatrick, 2006). They have allowed human and countries to connect, but also, they have provided and still ensure nowadays a secure source of food, and various ecological and economic services. Alongside increasing population densities, agricultural and industrial pressures, eutrophication, landscape alterations, sea level rise and climate change, concern has been raised all over the world, looking for an alternative and sustainable management of coastal environments (Anthony, 2014; D'Elia et al., 2019; Heiskanen et al., 2019). As a response, various environmental policies started to take shape. The Baltic Marine Environment Protection Commission - Helsinki Commission (HELCOM) is a good example of such initiatives, supported by countries bordering the Baltic Sea (HELCOM, 2018). Over the past 100 years, the Baltic Sea has indeed degraded dramatically, stressed by industrial activities, busy traffic and fertilizer runoff (Osvath et al., 2001). Indeed, this northern sea is relatively isolated from other seas and oceans and is widely influenced by freshwater inflows, and thus, forms one of the largest brackish inland seas (Leppäranta and Myrberg, 2009): this side-lining and low salinity level have most likely accentuated the impact of anthropogenic activities on the complex ecosystems that it shelters (Korpinen et al., 2012). Despite a rather small surface area (400 000km<sup>2</sup>) and an overall shallowness (average depth of 55m; Leppäranta and Myrberg, 2009), the Baltic Sea shows great variations in depth and sinks to a maximum of -459m in its deepest places (Western Gotland Basin). In addition, the slow and limited water exchange with the North Sea - through the narrow Danish Straits - results in a long water residence time, of around 30 years (Stigebrandt, 2001). Moreover, a quarter of the Baltic Sea is episodically an hypoxic zone, showing oxygen concentrations lower than 2

mg L<sup>-1</sup> (usually below 150m, in the central region of the Baltic Sea; Pohl and Hennings, 2008). Since the last natural reoxygenation event of 2015 (the so-called Major Baltic Inflow), the deepest waters of the Baltic Sea remained under a constant anoxia, without any record of significant oxygenation below the halocline (Artamonova et al., 2019; Hansson et al., 2018). The more saline and therefore denser waters stay at the bottom and are isolated from surface waters and from the atmosphere, consequently limiting oxygen exchanges and stratifying the water column. At those depths, only bacteria can thrive and prosper, feeding on organic matter and producing H<sub>2</sub>S (Conley et al., 2009; HELCOM, 2018).

Metal discharges originating from diffuse sources (wastewater discharge, leaching, etc.) and atmospheric deposition have increased the torments of the Baltic Sea (Furman et al., 2013). Once entering the aquatic environments, trace metals are indeed not easily degraded and will slowly aggregate as suspended matter in the water column, and further accumulate in the sediment, whereas their dissolved phases can be assimilated by the biota and might be enriched along the food chain, which can cause adverse effects on living organisms (Ho et al., 2010; Kennish, 1994; Rheinheimer, 1998). Moreover, the stagnant conditions causing anoxia, water stratification and long residence time intensify trace metal accumulation (HELCOM, 2018; Korpinen et al., 2012). Thus, trace metal distribution and biogeochemical cycles in these zones are mainly driven by vertical stratifying gradients and processes (Pohl and Hennings, 2008). Understanding their speciation and lability in such uncommon environment is decisive to interpret their fate and behavior, even more precisely than simply assess their total concentration (Allen and Hansen, 1996; National Research Council (U.S.), 1977; Sierra et al., 2017).

In this study, an exploration into the biogeochemical behavior of trace metals in the Baltic Sea is conducted, using a combination of passive and active

sampling techniques. The interaction between vertical variations of physicochemical parameters and concentration gradients of labile, dissolved and particulate trace metals was investigated from surface-oxygenated water layers to deep-anoxic ones, in the Gotland Basin. The main objectives were (i) to understand changes in trace metal concentrations along the water column, (ii) to assess their speciation as a function of depth and to study the influence of changing environmental conditions (oxic/anoxic) on their biogeochemical behavior and (iii) to provide advanced information on bioavailable metal fractions in this specific basin.

## **5.2. Material and methods**

### **5.2.1. Chemicals and materials**

For the material cleaning and preparation (Glass, PE and Teflon bottles, Teflon and glass plates), nitric acid (HNO<sub>3</sub>; Fisher, Trace Metal Grade, 65%), distilled nitric acid (distilled in the laboratory), Milli Q water (Millipore) were used. For the sample preparation and treatments, zinc acetate (ZnAc; Merck, pro analysi), glacial acetic acid (CH<sub>3</sub>COOH; Fisher, Trace Metal Grade, >99%), sodium sulfide (Na<sub>2</sub>S·9H<sub>2</sub>O; ThermoFisher, Alfa Aesar, ACS, >98%), degassed Milli Q water, (Millipore; flushed with N<sub>2</sub> gas), HCl (Fisher, Trace Metal Grade, 37%), ferric chloride (FeCl<sub>3</sub>·6H<sub>2</sub>O; Acros Organics, extra pure, >99%), N,N-dimethyl-p-phenylenediamine sulfate (Merck, pro analysi), orthophthaldialdehyde (OPA), N-(1-Naphthyl)ethylenediamine dihydrochloride (NEDD; p.a., Merck, 0.2%), sulfanilamide (p.a., Merck, 2%), ascorbic acid (VWR, >99%, analytical grade), molybdate solution.

For DGT preparation, Chelex<sup>®</sup>-100 (Bio-Rad, 200-400 mesh size), cross-linker (DGT Research, Lancaster), acrylamide (40%, Merck), ammonium persulfate (APS; Merck), tetramethylethylenediamine (TEMED; Merck,

>99%), DGT pistons (caps and bases, DGT research, Lancaster), 0.45 µm-pore size filter membranes (Merck Millipore, Durapore®, 0.45 µm PVDF Membrane, HVLP grade) and NaCl (Merck, Suprapur) were used. For DGT treatment, 1M HNO<sub>3</sub> was prepared by diluting 63 mL HNO<sub>3</sub> (Fisher, Trace Metal Grade, 65%) into 937 mL Milli Q water. For dissolved and particulate trace metal measurements, distilled nitric acid (HNO<sub>3</sub>; Fisher, Trace Metal Grade, 65%; distilled in the laboratory), Milli Q water (Millipore), 0.45 µm-pore size filter membranes (Merck Millipore, Durapore®, 0.45 µm PVDF Membrane, HVLP grade), nitric acid (HNO<sub>3</sub>; Fisher, Trace Metal Grade, 65%), HCl (Fisher, Trace Metal Grade, 37%), HF (Fisher, Trace Metal Grade, 40%) and H<sub>3</sub>BO<sub>3</sub> (Fisher, Trace Metal Grade, 4% w/v) were used.

### **5.2.2. Study sites**

This study was conducted in the Western (WGB) and Eastern (EGB) Gotland Basin, respectively located in Swedish and Latvian waters, as shown in Figure 5.1. The Gotland Basin is a wide area in the central Baltic Sea and is characterized by marked bathymetry discontinuities: at the bottom, steep escarpments create sudden increases in depth, finally forming smaller sub-basins (Stigebrandt, 2001). Notably, the deepest point (-459 m) of the sea is located in the Landsort Deep basin (WGB) while another relatively deep one (-249 m) is found in the Gotland Deep basin (EGB) (Leppäranta and Myrberg, 2009). Besides geographic and bathymetric features, the WGB and the EGB are also ranked by the HELCOM (2018) with the worst environmental grade. The EGB is even indicated as one of the most contaminated area of the Baltic Sea, regarding hazardous substances. Particularly, Cd and Pb are two compounds of concern in both basins, as they exceed the threshold values defined for hazardous substances in biota and in sediments of the Baltic Sea (no water data was provided for the WGB; HELCOM, 2018).

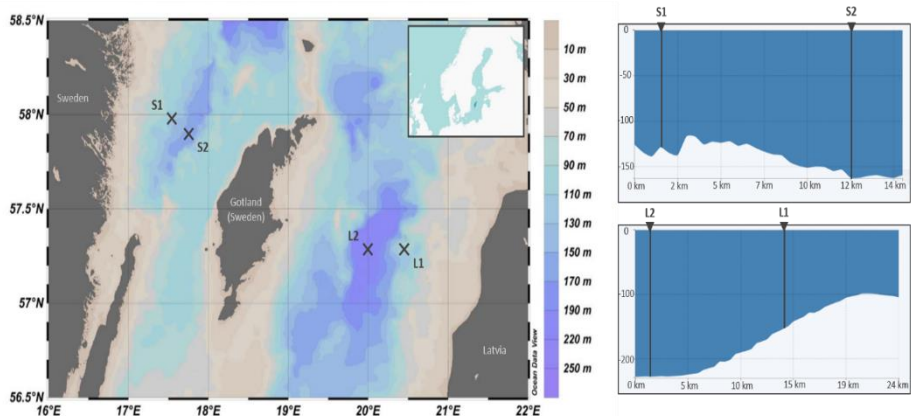


**Figure 5.1:** Location of the sampling sites in the Gotland Basin (adapted from Baltic Sea Hydrographic Commission, 2013).

The sampling campaign was carried out onboard the R.V. Belgica in June 2018. Four stations have been selected based on their maximal depth (Figure 5.1): two in the WGB, S1 (- 127 m) and S2 (- 171 m); two in the EGB, L1 (- 159 m) and L2 (- 249 m). At each station, direct measurements of a set of physicochemical parameters, active sampling and passive sampling were performed, as depicted in the Supplementary Information (SI).

### 5.2.3. Vertical hydrography

At each station, temperature, salinity and dissolved oxygen ( $O_2$ ) were measured *in situ* along a vertical profile in the water column, using a pre-calibrated Seabird SCTD (SBE19plus with OBS-3+ and PAR sensor).

In addition, seawater samples were taken for the assessment of dissolved sulfide [S(-II)], dissolved inorganic nutrients (ammonium  $NH_4^+$ , nitrite  $NO_2^-$ , phosphate  $PO_4^{3-}$ ), Particulate Organic Carbon (POC), Particulate Nitrogen (PN) and trace metals, using a CTD Rosette sampler equipped with a set of 12 Niskin bottles (10 L). The sampled depths are indicated in the SI.

### 5.2.3.1. Particulate organic carbon and nitrogen

At each sampled depth, 500 mL of water sample was collected and filtered using 0.70  $\mu\text{m}$  pre-treated (*i.e.* heated at 500 °C for 2 hours) and pre-weighted glass-microfiber filters (Sartorius Stedim Biotech, GF/F). The filtered samples were later treated for the analyses of dissolved chemical compounds (see 5.2.3.2 and 5.2.3.3). After filtration, the glass-microfiber filters were dried in the oven at 50°C overnight and weighted again. A subsample of each filter was placed for 24 hours in an acid-fume chamber (HCl fumes) to remove the carbonate fraction, then dried again and enclosed in tin cups. Five procedural blank filters were treated in the same way as the samples. The amount of POC and PN on the filters were determined using an Elemental Analyzer (EA-IRMS instrument, Flash EA112, Delta V Plus, Thermo Scientific). The certified reference material IAEA-CH<sub>6</sub> sucrose and IAEA-N<sub>2</sub> ammonium sulfate were used as internal standard respectively for carbon and nitrogen measurements. Limits of detection (LOD) were 1.31  $\mu\text{M}$  for POC and 0.35  $\mu\text{M}$  for PN. The Relative Standard Deviation (RSD) of the measurements was below 17 % for POC and 20 % for PN.

### 5.2.3.2. Dissolved inorganic nutrients

Another aliquot (240 mL) of each filtered seawater sample was prepared in Schott bottles (3x 80 mL) for measuring dissolved inorganic nutrients (ammonium NH<sub>4</sub><sup>+</sup>, nitrite NO<sub>2</sub><sup>-</sup>, phosphate PO<sub>4</sub><sup>3-</sup>) by spectrophotometry using an Ocean Optics, TORUS spectrometer. The reagent preparation is described in the Supplementary Information (SI). From each sample, 500  $\mu\text{L}$  was added to 4.5 mL Milli Q water.

In the solutions intended for the ammonium analyses, 1.25mL of OPA reagent was added and the measurements were performed at 428 nm after 3 hours waiting.

In the solutions intended for the nitrite analyses, 125  $\mu\text{L}$  of NEDD and 125  $\mu\text{L}$  of sulfanilamide were added and the measurements were performed at 550 nm after 20 minutes waiting.

In the solutions intended for the phosphate analyses, 125  $\mu\text{L}$  of acidified ascorbic acid solution and 125  $\mu\text{L}$  of molybdate solution were added and the measurements were performed at 880 nm after 20 minutes waiting.

The concentrations of  $\text{NH}_4^+$ ,  $\text{NO}_2^-$ ,  $\text{PO}_4^{3-}$  were then determined by comparing the field sample results with those of external calibration curves. The LOD were around 0.15  $\mu\text{M}$  for  $\text{NH}_4^+$ , 0.18  $\mu\text{M}$  for  $\text{NO}_2^-$ , 0.01  $\mu\text{M}$  for  $\text{PO}_4^{3-}$ .

### **5.2.3.3. Dissolved sulfide**

An aliquot (80 mL) of each filtered seawater sample was prepared for measuring dissolved sulfides, according to the colorimetric method developed by Cline (1969). The reagent preparation is described in the Supplementary Information (SI). First, the sample was stabilized with 5% ZnAc solution (for 1 mL sample, 100  $\mu\text{l}$  of 5% ZnAc). In the dark, 500  $\mu\text{L}$  of each solution was then treated by addition of 1500  $\mu\text{L}$  Milli Q water and 120  $\mu\text{L}$  of diamine reagent which gave its color to the solution. After 20 minutes waiting, the absorbance measurements were performed by spectrophotometry (Ocean Optics, USB 2000+ UV-VIS spectrometer) at 670 nm. The sulfide concentration was then determined by comparing the absorbance results with those of an external calibration curve. The LOD of this technique was 0.2  $\mu\text{M}$ .

### **5.2.4. Trace metals in the surface waters**

The speciation approach allows to differentiate several types of metal species, mainly based on the particle size (Stumm and Bilinski, 1973): a first separation between the particulate and the dissolved phases of trace metals can be done using a 0.45 $\mu\text{m}$  filtration. Furthermore, another focus is made on

two phases co-existing within the dissolved fraction: a separation between labile and non-labile species, using the DGT technique

#### **5.2.4.1. DGT sampling and treatments**

The DGT technique relies on a controlled diffusive transport of analytes which pass a diffusive gel (pore size 10nm) and are bound on a resin gel. The concentration gradient built during the deployment makes it possible to assess time integrated concentrations of labile trace metal fractions. The DGT passive sampler is composed of a round plastic molding (a cap and a piston base, both assembled), holding together three successive layers, which are: a membrane filter (0.45  $\mu\text{m}$  pore size cellulose acetate – 0.125 mm thick), a diffusive hydrogel (polyacrylamide hydrogel – 0.8 mm thick) backed up by a resin gel (binding Chelex®-100 resin – 0.4 mm thick). The diffusive hydrogel, the resin gel and DGT pistons were prepared according to the method reported by Zhang and Davison (1995) and described in detail in Gaulier et al. (2019).

During the expedition, DGT pistons were deployed in 20 L clean plastic containers filled with seawater of each sampled depth. Each container contained 6 DGT pistons. The deployment duration of DGT, and the water temperatures at deployment and recovery were recorded and further used for the DGT-labile concentration calculations. After deployment, trace metals accumulated on the resin gel were eluted in 1 mL of 1M  $\text{HNO}_3$  for at least 24 hours. The eluents were then diluted five times with MQ-water, prior to their analysis (see 5.2.4.3). From the total mass of the accumulated metal, the time average metal concentration was calculated based on Fick's first law, as described in Gaulier et al. (2019). The LOD of DGT technique was calculated based on 6 DGT blank analysis.



### **5.2.4.2. Sampling and sample treatment for dissolved and particulate metals**

#### **5.2.4.2.1. Dissolved trace metals**

500 mL of seawater collected by the CTD Rosette sampler were filtered using 0.45  $\mu\text{m}$  pre-weighted filter membranes. The filtrate was acidified with 0.2% distilled  $\text{HNO}_3$  and then stored in clean Teflon<sup>®</sup> bottles. Then the acidified filtrates were finally diluted 10 times with MQ water, prior to analysis, while the filter membranes were later treated for the analysis of particulate compounds.

#### **5.2.4.2.2. Particulate trace metals**

The filters used for seawater sample filtration were dried under a laminar flow hood for 2 days and weighted again. The mass difference of the filters was recorded for the calculation of particulate metal concentrations and for the determination of the Suspended Particulate Matter (SPM) amount. The dry filters were then introduced into clean Teflon<sup>®</sup> tubes where 3mL of concentrated HF (40%), 3mL of concentrated HCl (37%) and 1mL of concentrated  $\text{HNO}_3$  (65%) were added. The solution was heated at 70°C overnight and finally after cooling down, 20 mL of  $\text{H}_3\text{BO}_3$  (4%) were added to the Teflon<sup>®</sup> bottles. This solution was then heated at 70°C for three hours. Once the solution cooled down again, it was transferred to PE vessels and further diluted (10 times) before analysis.

#### **5.2.4.3. Trace metal analysis and validation**

Trace metals (Cd, Co, Cr, Cu, Fe, Mn, Ni, Pb and Al) in the prepared solutions were determined using a High Resolution-Inductively Coupled Plasma Mass Spectrometer instrument (HR-ICP-MS, Thermo Finnigan Element II). The calibration was carried out with appropriate dilutions of an acidified multi-element stock solution (Merck, ICP-MS standard XIII). Indium was used as

an internal standard. The LODs were 4.0 ng L<sup>-1</sup> for Cd, 5 ng L<sup>-1</sup> for Co, 0.01 µg L<sup>-1</sup> for Cr, 0.07 µg L<sup>-1</sup> for Cu, 0.47 µg L<sup>-1</sup> for Fe, 0.02 µg L<sup>-1</sup> for Mn, 0.07 µg L<sup>-1</sup> for Ni, 0.01 µg L<sup>-1</sup> for Pb and 12 µg L<sup>-1</sup> for Al. The RSD was lower than 9% for all metal species.

### **5.2.5. Statistical analysis**

Statistical analyses were performed based on a Principal Component Analysis (PCA) and a Hierarchical Ascending Classification method (HAC) using the R data processing software ([www.r-project.org](http://www.r-project.org)). Two packages were used in this study: *corrplot* and *FactoMineR*.

## **5.3. Results**

### **5.3.1. Physicochemical parameters**

The temperature does not vary from one station to another but fluctuates between 3.0 to 17.2 °C depending on the depth (Figure 5.2a). At the surface (< 20 m depth), the temperature shows its highest values (~ 13.9 °C on average) whatever the site. It progressively decreases down to 3.2°C at around 60 m deep before rising again to reach a plateau at 6.5 °C on average, around 100 m deep.

The salinity shows similar values at every station, but ranges between 6.6 to 13.3 PSU as a function of depth (Fig. 5.2b). In the Gotland Basin, it is a typical phenomenon that salinity gradually increases with the depth (Schneider and Otto, 2019; Ulfsbo et al., 2011): here, the most significant increase (factor 1.4 on average) occurs between 60 and 90 m, in the water column.

Compared to salinity, dissolved oxygen (Fig. 5.2c) shows a reverse vertical profile, displaying the highest concentrations in the surface waters (around 9 mg L<sup>-1</sup>) and the lowest ones at the bottom (below 0.1 mg L<sup>-1</sup>). It rather remains

stable in the first 60 meters with a slight maximum around 20 m depth, before decreasing sharply until the seabed.

The SPM amount (Fig. 5.2d) ranges between 0.6 to 2.5 mg L<sup>-1</sup> in the studied zones and shows similar patterns at each station: high values in the surface waters, then a steep decrease until 40 - 60 m deep, and then an increase towards the seabed for all the stations except L2 where the SPM concentrations remain rather stable after -60 m.

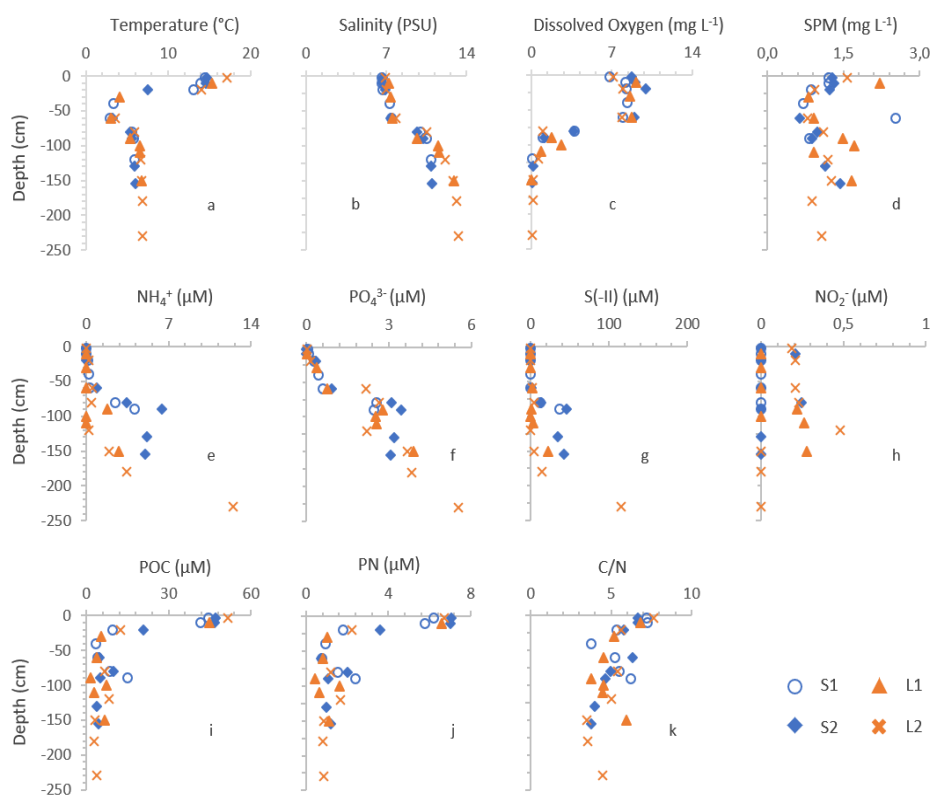


**Figure 5.2:** Vertical profiles of: (a) temperature, (b) salinity and (c) dissolved oxygen, (d) SPM amount, (e, f, h) dissolved nutrient and (g) sulfide concentrations, (i) POC, (j) PN contents and related (k) C/N ratio are given at the four sampling sites: at S1 (blue empty circles) and S2 (blue closed diamonds) in the Western Gotland Basin (WGB) and at L1 (orange closed triangles) and L2 (orange crosses) in the Eastern Gotland Basin (EGB).

### **5.3.2. Dissolved inorganic nutrients and sulfide**

Dissolved  $\text{NH}_4^+$ ,  $\text{PO}_4^{3-}$  and S(-II) display similar increasing trends with depth at all stations (Fig. 5.2e, f, g). Overall, the values vary from  $< 0.15$  to  $12.50 \mu\text{M}$  for  $\text{NH}_4^+$ , from  $< 0.01$  to  $5.53 \mu\text{M}$  for  $\text{PO}_4^{3-}$  and from  $< 0.2$  to  $115 \mu\text{M}$  for S(-II). In the first 60 meters, the levels of  $\text{NH}_4^+$ ,  $\text{PO}_4^{3-}$  and dissolved sulfide are very low, then an increase is generally observed with a first sudden peak appearing around -90 m deep at all stations. Maximum values of these three elements are recorded at station L2 at -230 m, right above the seabed.

Nitrite concentrations are low and fluctuate, but most of them are below the LOD of  $0.8 \mu\text{M}$  (Fig. 5.2h).

### **5.3.3. Particulate organic carbon and nitrogen**

The POC and PN contents of the SPM have similar variations along the depth at all the stations. They vary from  $1.6$  to  $51.5 \mu\text{M}$  and from  $0.4$  to  $7.1 \mu\text{M}$ , respectively (Fig. 5.2i, j). The highest values (around  $47.1 \mu\text{mol L}^{-1}$  for POC and  $6.6 \mu\text{mol L}^{-1}$  for PN) are found at the surface. Then, the values sharply decline at 60 m deep by a factor 9 on average. In addition, the C/N ratio decreases from 7.0 at the surface to 4.6 close to the bottom (Fig. 5.2k).

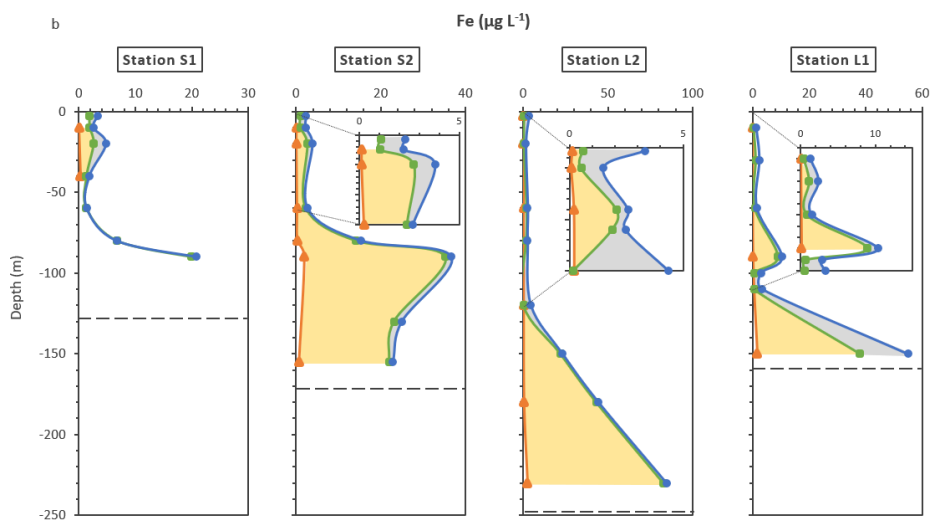
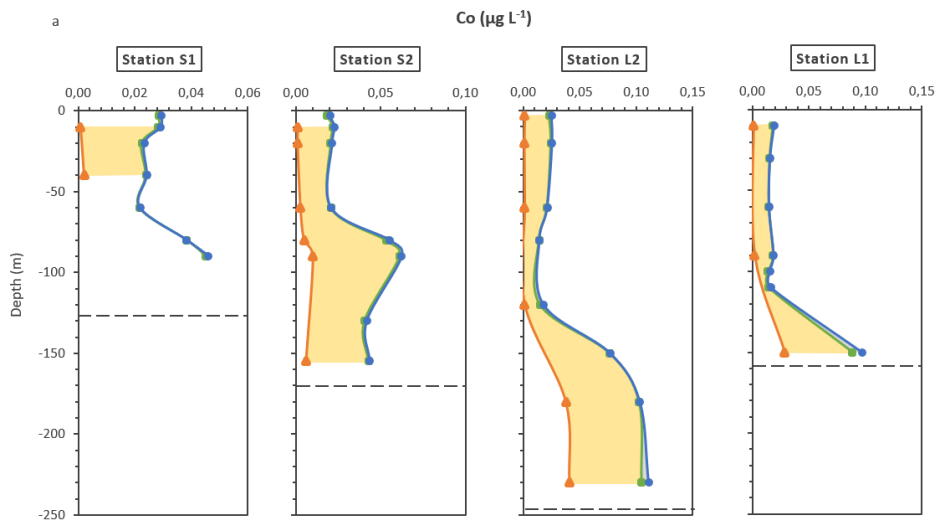
### **5.3.4. Biogeochemical cycling of trace metals**

#### **5.3.4.1. Manganese, iron and cobalt**

The oxygen sensitive elements Co, Fe and Mn display very similar trends along the water column (Figure 5.3a, b, c). Their total (dissolved and particulate) concentrations remain rather low and stable at the surface and then individually increase at different depths for each station. They range from  $0.01$  to  $0.11 \mu\text{g L}^{-1}$  for Co (Fig. 5.3a),  $1.3$  to  $85 \mu\text{g L}^{-1}$  for Fe (Fig. 5.3b) and  $0.94$

to  $1700 \mu\text{g L}^{-1}$  for Mn (Fig. 5.3c). On average, the highest values are measured in the EGB. Moreover, the total concentrations of Co, Fe and Mn keep increasing until the seabed in the EGB and at station S1, while they reach a maximum around -90 m at station S2 and then decrease again near the bottom. The same patterns are observed for dissolved Co, Fe and Mn (dCo, dMn and dFe) with elevated concentrations near the seafloor, as well as for their labile forms (lCo, lFe and lMn) obtained by the DGT technique, which show increasing levels with depth. The particulate concentrations of Co (pCo) are negligible at all stations. Regarding particulate Fe and Mn (pFe and pMn), these concentrations account for a significant fraction at some stations, especially in the upper part of the water column and sometimes in the bottom zone. Overall, the maximum particulate concentrations are  $8.5 \mu\text{g L}^{-1}$  for Co,  $17.1 \mu\text{g L}^{-1}$  for Fe and  $8.1 \mu\text{g L}^{-1}$  for Mn.

Regarding the speciation of Co, Fe and Mn, their dissolved species are in majority, especially near the seabed where they respectively reach an average contribution of 70, 77 and 69% of the total content. Near the surface, the main species of Fe and Mn are in the particulate phase, which respectively represents 53% and 74% of their total content. In addition, significant contributions of pFe are noticed near the bottom, but only at station S2 and L1. Labile Co, Fe and Mn have a low contribution at the surface with average values of 4.2, 4.1 and 16.8% of the total content, respectively, while they reach a contribution of 26% (lCo) and 31% (lMn) close to the bottom. Finally, and in most cases, the dissolved non-labile fractions account for most of the distribution of these three elements.



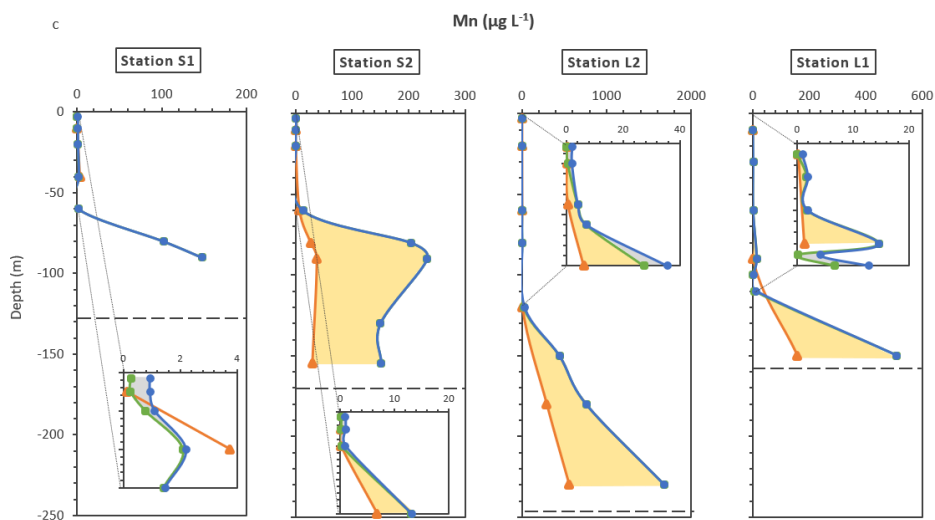


**Figure 5.3:** Vertical speciation profiles of Co (a), Fe (b) and Mn (c) in the WGB (station S1 and S2) and the EGB (station L1 and L2). Total concentrations are given in blue (circle sign; resulting from the addition of dissolved and particulate concentrations brought back to  $\mu\text{g L}^{-1}$ ), dissolved ones in green (square sign) and labile ones in orange (triangle sign). The grey areas indicate the particulate fraction, while the yellow ones give the dissolved non-labile fraction (resulting from the subtraction between dissolved and dissolved labile concentrations). The black dash-lines indicate the maximum depth of each sampling stations.

#### 5.3.4.2. Nickel and Chromium

Ni and to a lesser extent Cr, show little variations with the depth (Figure 5.4a, b): their total concentrations remain in a narrow range of values, whatever the station nor the depth (from 0.66 to 0.89  $\mu\text{g L}^{-1}$  for Ni and from 0.05 to 0.20  $\mu\text{g L}^{-1}$  for Cr). However, Ni is mostly found as a dissolved element, while Cr is mainly particulate. In both cases, the non-labile concentration account for the main dissolved fraction, especially for Cr where the values range between 64 and 95%. The Ni labile species are much more notable than Cr labile species:

especially in station L2, where labile Ni (INi) accounts for more than 50% of total concentrations.

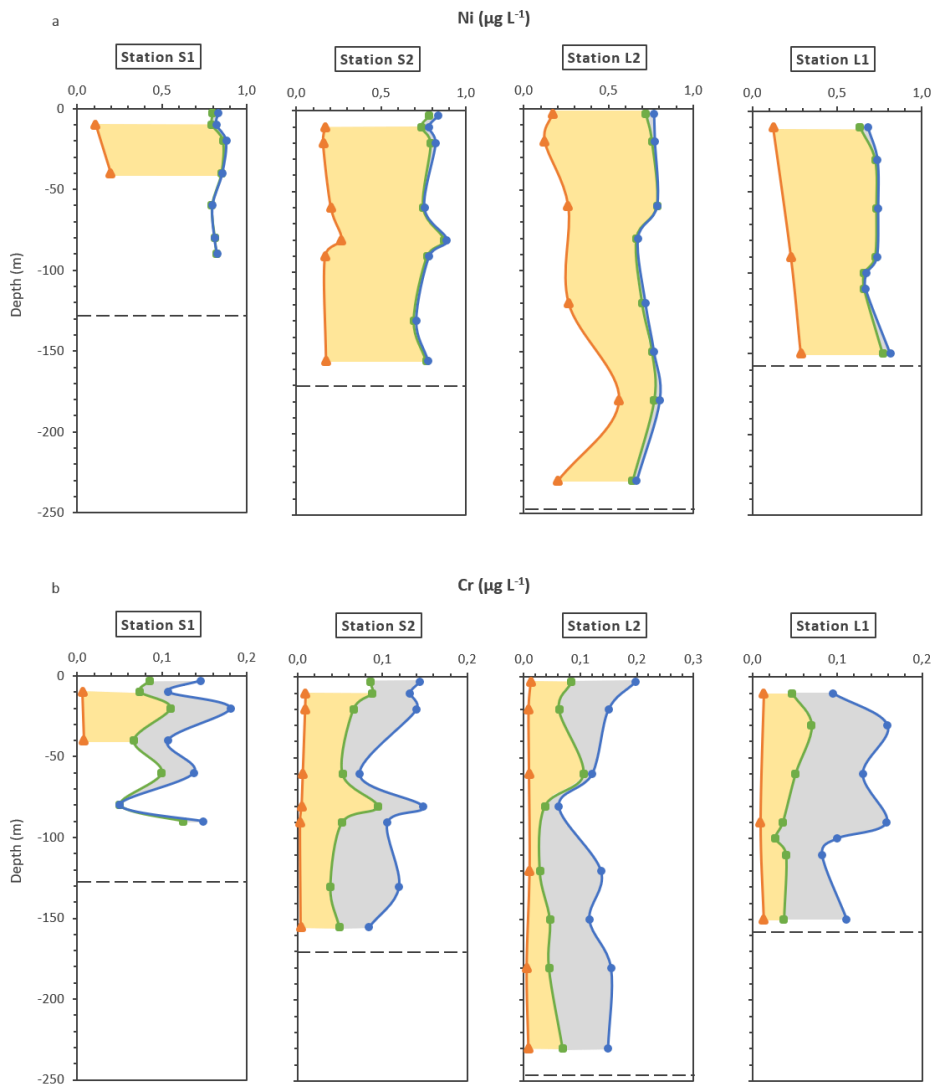


**Figure 5.4:** Vertical speciation profiles of Ni (a) and Cr (b) in the WGB (station S1 and S2) and the EGB (station L1 and L2). Total concentrations are given in blue (circle sign; resulting from the addition of dissolved and particulate concentrations brought back to  $\mu\text{g L}^{-1}$ ), dissolved ones in green (square sign) and labile ones in orange (triangle sign). The grey areas indicate



the particulate fraction, while the yellow ones give the dissolved non-labile fraction (resulting from the subtraction between dissolved and dissolved labile concentrations). The black dash-lines indicate the maximum depth of each sampling stations.

---

#### **5.3.4.3. Copper**

Total Cu concentrations range from 0.29 to 1.26  $\mu\text{g L}^{-1}$  in the investigated zones (Figure 5.5) with maximal concentrations observed at the upper part of the profiles. More precisely, total Cu concentrations rapidly increase in the first meters below the surface (< 20-30 m) and then, gradually decreases until the junction between the halocline and the anoxic zone (around -90 m). In the same way as Cr, labile Cu (lCu) shows very low concentrations (0.01 and 0.08  $\mu\text{g L}^{-1}$ ) compared to the other fractions and most of the dissolved concentration is composed of non-labile species (>75 % of the total dissolved content). The particulate fraction is also very low and account for only 10% of the total Cu concentration, on average. While the lCu fraction does not show any variation due to very low values, the contribution of pCu seems to slightly increase with the depth.

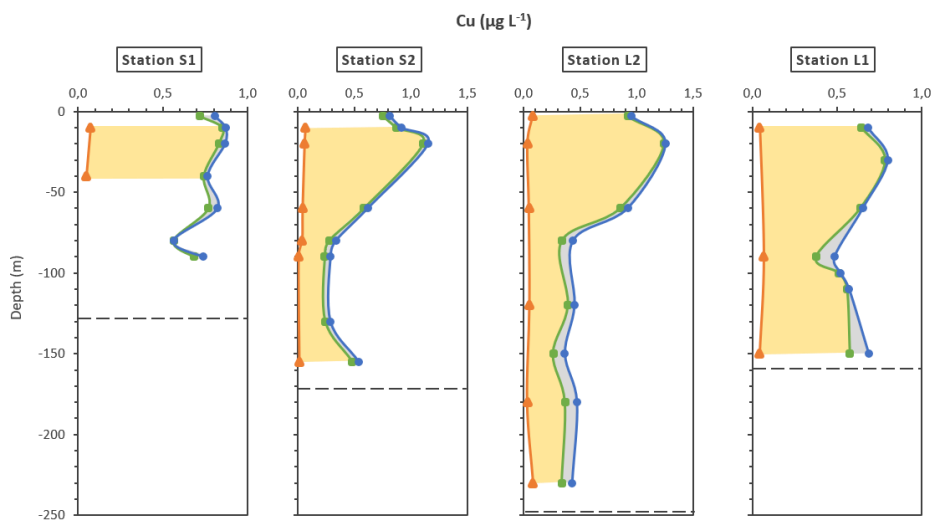


**Figure 5.5:** Vertical speciation profiles of Cu in the WGB (station S1 and S2) and the EGB (station L1 and L2). Total concentrations are given blue (circle sign; resulting from the addition of dissolved and particulate concentrations brought back to  $\mu\text{g L}^{-1}$ ), dissolved ones in green (square sign) and labile ones in orange (triangle sign). The grey areas indicate the particulate fraction, while the yellow ones give the dissolved non-labile fraction (resulting from the subtraction between dissolved and dissolved labile concentrations). The black dash-lines indicate the maximum depth of each sampling stations.

#### 5.3.4.4. Lead

The total concentration of Pb varies from 0.015 to 0.115  $\mu\text{g L}^{-1}$  (Figure 5.6) and is, on average, higher in the EGB (34  $\text{ng L}^{-1}$ ) than in the WGB (22  $\text{ng L}^{-1}$ ). The profiles of total Pb concentrations differ a lot from one station to another. A maximum value is found close to the sea surface at station S1, L1 and to a lesser extent S2. At station L2, a sharp increase is rather observed close to the bottom, below -180 m. A significant decline of total Pb concentration is noticed in the halocline zone at station S1, S2 and L1. As observed for Co, Cr and Cu, the non-labile fraction of Pb accounts for the

main dissolved fraction (mean value of 72%) and the particulate fraction is generally negligible, excepted close to the bottom in station L1.

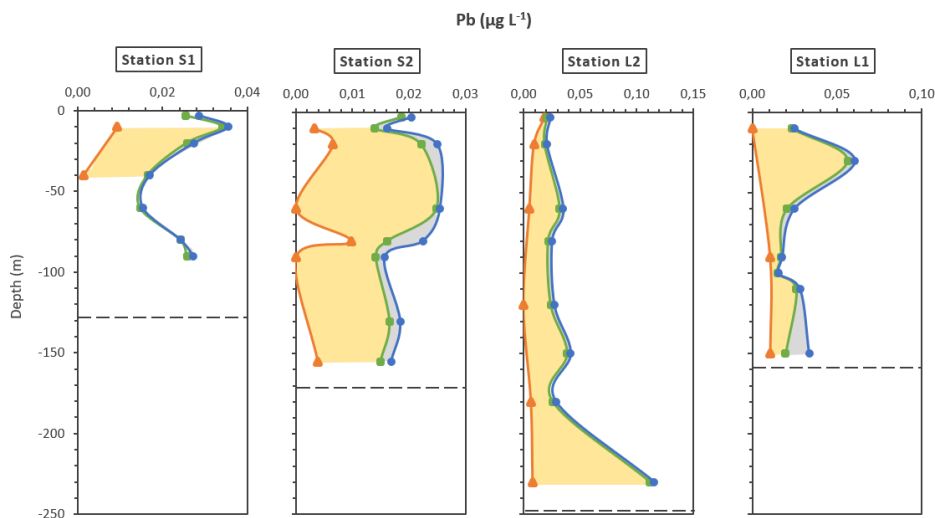


**Figure 5.6:** Vertical speciation profiles of Pb in the WGB (station S1 and S2) and the EGB (station L1 and L2). Total concentrations are given in blue (circle sign; resulting from the addition of dissolved and particulate concentrations brought back to  $\mu\text{g L}^{-1}$ ), dissolved ones in green (square sign) and labile ones in orange (triangle sign). The grey areas indicate the particulate fraction, while the yellow ones give the dissolved non-labile fraction (resulting from the subtraction between dissolved and dissolved labile concentrations). The black dash-lines indicate the maximum depth of each sampling stations.

#### 5.3.4.5. Cadmium

Total Cd concentration varies from 0.011 to 0.043  $\mu\text{g L}^{-1}$  (Figure 5.7) and stay rather stable through the water column. However, one can observe a small trend of decrease at station S1 and of increase at stations L1 and L2. The total concentrations are higher in the EGB (0.026  $\mu\text{g L}^{-1}$ ) than in the WGB (0.016  $\mu\text{g L}^{-1}$ ), on average. The particulate fraction is negligible as shown on Figure

5.7 and the values of labile concentrations have not been robust enough to be displayed in the paper due to a high variability in the replicates.

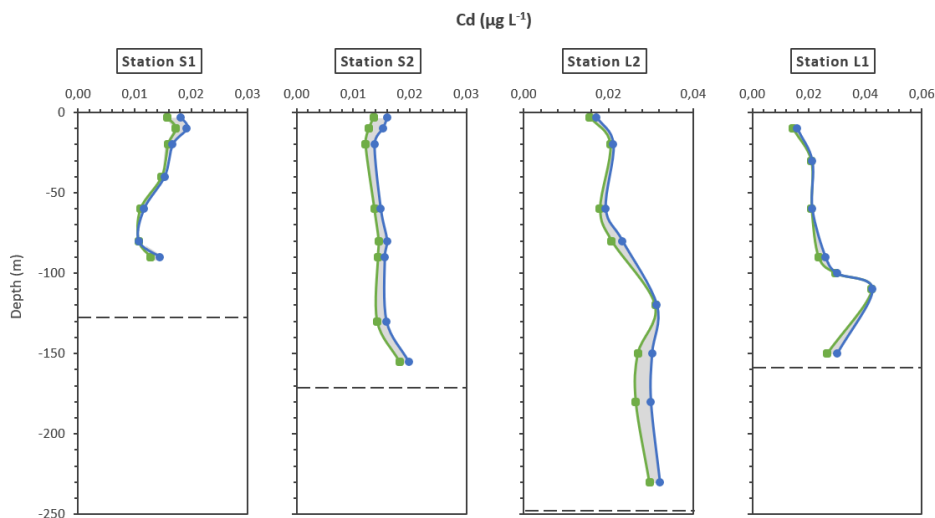


**Figure 5.7:** Vertical speciation profiles of Cd in the Western Gotland Basin (WGB; station S1 and S2) and the Eastern Gotland Basin (EGB; station L1 and L2). Total concentrations are given in blue (circle sign; resulting from the addition of dissolved and particulate concentrations brought back to  $\mu\text{g L}^{-1}$ ), and dissolved ones in green (square sign). The grey areas indicate the particulate fraction. The black dash-lines indicate the maximum depth of each sampling stations.

### 5.3.5. Multivariate statistical data analysis

Figure 5.8 shows the correlations between all the measured parameters. According to the corresponding p-values (detailed information given in the SI), only the significant correlations are shown and described here. The Principal Component Analysis (PCA) coupled to the Hierarchical Ascending Classification (HAC) (Figure 5.9a, b) further completes the information obtained from the correlogram by statistically gathering similar samples and

parameter variations. The HAC plots (Fig. 5.9b) distributes the sampling sites in three clusters.

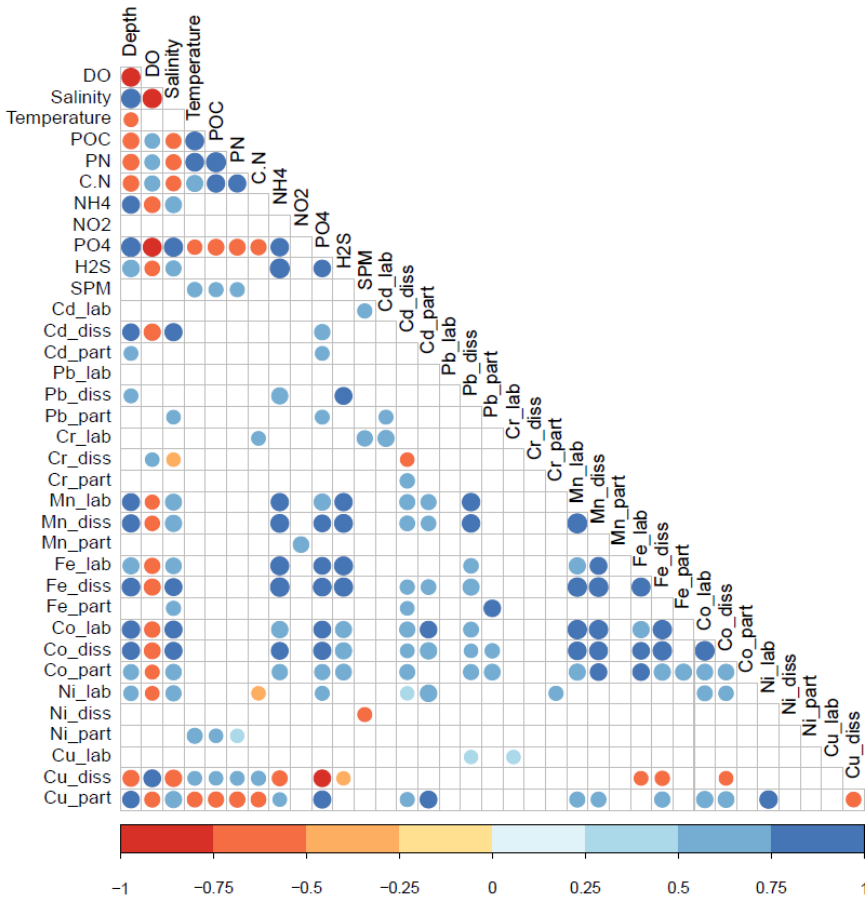


**Figure 5.8:** Correlogram of all the measured parameters. The blue circles indicate positive correlations; the red circles indicate negative correlations. The size of the circles and the intensity of their color are proportional to the strength of the correlation. The legend indicates the link between colors and coefficients. Only the significant correlations are displayed here (*i.e.*  $p$ -value  $< 0.05$ ; see the SI for the detailed values).

First, the stratification of the water column is widely confirmed: the dissolved oxygen, the water temperature and the POC and PN contents are negatively correlated with the depth (respective correlation factors of -0.88, -0.52, -0.68 and -0.69;  $p < 0.05$ ). Conversely, the salinity and the concentration of  $\text{NH}_4^+$ ,  $\text{PO}_4^{2-}$  and S(-II) are positively correlated with the depth (respective correlation factors of 0.95, 0.80, 0.94 and 0.75;  $p < 0.001$ ). Thus, the first cluster (Figure 5.9a, b) gathers all the surface measurements. These samples are characterized by higher oxygenation, higher temperatures and higher concentrations of POC, PN, C/N and dCu. On the other hand, they are linked to lower salinity and lower concentrations of  $\text{PO}_4^{3-}$ ,  $\text{NH}_4^+$ , pCu and INi. A second group is composed of the samples from transitional depths, mainly located between -40 and -155 m, while the last group includes samples from the bottom areas of the stations. Cluster 2 is defined by lower temperatures, but also lower concentrations of POC, PN, C/N and pNi. Finally, the samples from group 3 are characterized by low oxygenation, high salinity and high concentrations of S(-II),  $\text{NH}_4^+$ ,  $\text{PO}_4^{3-}$  and of various trace metals (Co, Fe, dMn, d- and pCd, d- and p-Pb, INi and pCu).

In the same way, several dissolved trace metals dCd, dPb, dMn, dFe, dCo and INi are positively correlated with the increasing depths and salinity (correlation factor of between 0.38 and 0.86;  $p < 0.05$ ; SI). A similar trend is also observed for a few particulate trace metals (pCd, pCo and pCu), but with lower correlation factor (0.52, 0.62 and 0.75, respectively;  $p < 0.05$ ). dCu is eventually the only metal fraction which is negatively correlated with the depth. Besides the depth, a strong positive correlation is also observed between Co, Fe and Mn (correlation factor  $> 0.71$ ;  $p < 0.001$ ). In the same way, dCd and dPb are positively correlated with dCo, dFe and dMn (correlation factors  $> 0.50$ ;  $p < 0.05$ ).

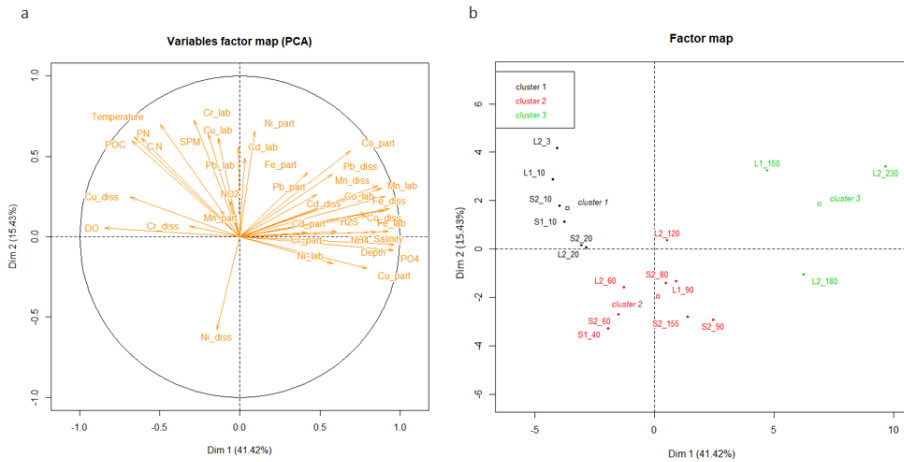


**Figure 5.9:** PCA plots for the parameters (a) and for the sampling locations (b) coupled with a HAC.

## 5.4. Discussion

### 5.4.1. Environmental forces and gradients

All physicochemical parameters (others than trace metals) show strong concentration vertical gradients. Available oxygen, POC and PN are strongly correlated with the water depth and decrease from the surface to the seabed, whilst the salinity and the concentrations of S(-II),  $\text{NH}_4^+$ ,  $\text{PO}_4^{3-}$  are also strongly correlated with water depth, but gradually increase downward. These vertical physicochemical distributions result in a clear stratification of the water column and are supported by the multivariate statistical analysis (Fig. 5.9). Three main zones appear and are in agreement with the literature (see the references hereinafter): (i) close to the surface, in the first  $\sim 60$  m, the environment is well oxygenated, highly productive, but the salinity is low (Piwosz and Pernthaler, 2010; Pohl and Hennings, 2005; Ulfsbo et al., 2011). Between -20 m and -60 m and depending on the season, the temperature tends to decrease and forms a summer thermocline: it constitutes a temporary layer,

creating an interface between a relatively warm upper layer and colder deeper waters (Fennel et al., 1991; Leppäranta and Myrberg, 2009; Stepanova, 2017).

(ii) From -60 to -90 m, the halocline layer constitutes a transition zone over 30 meters, in which the salinity and the temperature increase whereas oxygen sharply disappears (Neretin et al., 2003; Pohl and Hennings, 2005; Schneider and Müller, 2018).

(iii) Below -90 m, the disappearance of oxygen marks the start of an anoxic zone, which can also be described as an euxinic zone given the appearance of high dissolved S(-II) levels (Hermans et al., 2019; Scholz et al., 2018; van de Velde et al., 2020). In this zone, the temperature and salinity stabilize around 8°C and 14 PSU respectively. The ammonium increases together with the appearance of anoxia as well as with the rising concentrations of S(-II) and  $\text{PO}_4^{3-}$ , indicating a strong mineralization of OM with depth or within the sediment, releasing the ammonium back to the water column (Klawonn et al., 2019; Zhu et al., 2019). Following the same vertical pattern,  $\text{PO}_4^{3-}$  is consumed by phytoplankton in the oxygenated layer, resulting in low concentrations at the surface but higher ones in the anoxic waters (Neretin et al., 2003). At around -80m (the oxic-anoxic interface), the level of  $\text{PO}_4^{3-}$  increases faster due to the reduction and dissolution of sinking Fe- and Mn-oxides and the simultaneous release of phosphates (Neretin et al., 2003). In addition, the reduction of Fe-oxides in the anoxic sediment might also lead to the release of phosphates which are then diffused back into the water column (Sudheesh et al., 2017; Sulu-Gambari et al., 2016). Regarding nitrite, its concentration is very low at all the sampling sites and is only detectable in the upper layer of L2 and S2 and deeper layer of L1, limiting its toxicity for the organisms. Close to the surface, the presence of oxygen can hamper the stability of nitrite, but its detection results probably from the oxidation of  $\text{NH}_4^+$  by bacteria (*Nitrosomonas*) (Happel et al., 2018; Jäntti et al., 2018). Deeper in the anoxic zone for example in L1, the previously formed  $\text{NO}_2^-$  is rapidly



consumed through denitrification processes and/or anaerobic ammonium oxidations, known as anammox reaction (Conley et al., 2009).

The vertical profiles of SPM exhibit two maxima: one close to the surface (above -20 m) where a summer phytoplankton biomass may increase the amount of particles, and another one at the oxic-anoxic interface (~ -90m) which may result from particulate matter produced by surface phytoplankton that then ages in the deeper layer, and is commonly recorded (Ivanov and Oguz, 1998; Neretin et al., 2003; Winogradow et al., 2019). Note further that the vertical profiles of SPM, phosphates, ammonia and nitrite are very similar to those obtain by Neretin et al. (2003), recorded in November 2000 when the basin was permanently anoxic.

At the surface, the C/N ratio (6.6 on average) fits well into the Redfield ratio ranging from 6 to 8 and is similar to those of active growing cells like primary producers (Laws et al., 2001). This indicates that the POM is mostly made of autochthonous fresh organic material derived from phytoplankton (Lara et al., 2010). This also highlights the high primary production going on at the surface, linked with environments enriched in oxygen and nutrients (Svedén et al., 2016). However, in the deeper water column, this ratio often reaches values below 6, indicating a reduced contribution of phytoplankton-based POM with depth. According to several studies (Crawford et al., 2015; Goldman et al., 1987), this change in POM composition could reveal the appearance of a bacterial biomass, which can typically reach C/N ratios as low as 4. Specifically, the results suggest a transition with depth, from an autotrophic to a heterotrophic system (Crawford, 2015) or chemolithotrophic system (Conley et al., 2009; Hermans et al., 2019). This change is probably induced by light-limitation and anoxia appearing with depth (Laws et al., 2001).

Considering the biogeochemical cycle of trace elements in the Gotland basin and previous studies (Middelburg et al., 1993; Ulfsbo et al., 2011), the distribution of elements is clearly linked to the stratification of the water column in terms of oxygen availability, temperature and salinity that influence organic matter mineralization and biogeochemical reactions (Fig. 5.9).

#### **5.4.2. Trace metal speciation along the depth of the Gotland Basin**

At the surface of all stations where the water is well oxygenated, Fe shows low total concentrations in general and a good affinity for particles as it forms Fe-oxides. In the dissolved fraction, it is also not much labile, and probably bound to organic matter, various colloids, including nanoplankton (Beghoura et al., 2019; Jilbert et al., 2017). On the other hand, when the oxygen decreases, the total Fe concentration increases strongly, especially in the dissolved fraction. If this sudden enrichment of iron in the dissolved pool can partially be explained by a low release of Fe(II) from bottom sediments (*i.e.* diffusion mechanisms; Helmond et al., 2019; van de Velde et al., 2020), a large part of it probably comes from the shelf. Indeed, this “shelf-to-basin shuttle” phenomenon has often been described in the Baltic Sea as well as in the Black Sea (Lenstra et al., 2019; Lyons and Severmann, 2006; Reed et al., 2016; Scholz et al., 2019, 2013; van de Velde et al., 2020) tends to magnify Fe concentrations in deep anoxic environments. Briefly, particles from the shore slowly progress at the water-sediment interface from the oxic shelf to the anoxic basin. This phenomenon requires resuspension which releases Fe(II) previously produced in the porewaters. In oxic water column, Fe(II) is rapidly re-oxidized and settles again further down in deeper layers (*i.e.* offshore). Conversely, when it reaches the anoxic waters, Fe(II) is stabilized

and is able to react with sulfides for instance, to form complexes, clusters, colloids and precipitates such as pyrite. It seems to be the case at stations L1 and S2 because of pFe increase and was also previously reported (Fehr et al., 2010; Shen et al., 2002; Sternbeck et al., 1999). Two different processes are therefore involved in the Fe cycle: the total Fe concentrations increase due to the shelf-to-basin shuttle, and the dissolved fraction increases due to the oxygen decrease (lower redox conditions).

Concurrently, Mn might also follow a similar shelf-to-basin shuttle like observed for Fe in the Gotland Basin, given the strong correlations between their biogeochemical behavior and as previously evidenced (Jilbert and Slomp, 2013; Lenstra et al., 2020; Scholz et al., 2013; van de Velde et al., 2020). Mn is also more labile than Fe in marine systems as previously shown (Hutchins and Bruland, 1995; Turner and Olsen, 2000) and the oxidation of Mn(II) is less quick than that of Fe(II), resulting in higher concentrations of dMn compared to dFe (on average by a factor 20).

In addition to these processes, Fe and Mn accumulation in the Gotland Basin is generally observed at the redoxcline of the halocline (~ -90m). In this zone, the redox cycles of Fe and Mn are well described in Busigny et al. (2016) and called the “iron and manganese wheels”, and result in increased dissolved Fe and Mn concentrations (Busigny et al., 2016).

Alongside the water column, Co strongly correlates with Fe and Mn biogeochemical cycles as mentioned above. Its vertical transport is therefore mainly regulated by the coprecipitation with or adsorption onto Fe- and Mn-oxides regarding downward fluxes, and by the concurrent diffusion upwards (Kremling, 1983; Pempkowiak et al., 2000; van de Velde et al., 2020). Moreover, ICo, IFe and IMn strongly correlate with depth, the salinity and the

concentrations of  $\text{NH}_4^+$ , S(-II) and  $\text{PO}_4^{3-}$ , as they mainly undergo reduction mechanisms in this basin.

Regarding the other elements and in both studied regions of the Gotland Basin, Cu is not very labile overall, due to its strong affinity to organic matter (Hume et al., 2018; Yin et al., 2002). The input of Cu to the water column rather comes from the surface in a dissolved non-labile form. At around -20 m in all stations, an enrichment of the dissolved phase is especially observed, most likely linked to the presence of phytoplankton reducing Cu or to its release during remineralization increasing dCu contribution (Gelting, 2009). With the depth, a significant decrease of the dCu concentrations is observed at station S2 and L2 and is not entirely balanced by the particulate fraction. In these areas, Cu is strongly eliminated along the water column, and quickly settles down from the halocline zone on. After the halocline layer, Cu may also form CuS complexes in the anoxic zone, enhancing its precipitation and storage into the sediment. As a result, Cu becomes highly insoluble after -80m which means that the water column is impoverished of Cu with time and with the continuous euxinia (Brumsack, 2006). Similar vertical gradients were observed in Baltic Sea by other studies (Kremling, 1983; Magnusson and Westerlund, 1980; Pempkowiak et al., 2000). At station S1 and L1, despite the anoxia and the presence of sulfide at high depths, only little evolution of Cu is observed. Thus, it seems that the non-labile complexes are rather stable, most likely due to the formation of colloids and/or clusters of Cu-sulphides (Luther and Rickard, 2005).

Cr, Ni and to a lesser extent Cd, display globally a conservative behavior as their total concentration and speciation do not show any strong trend as a function of depth. While all the elements display a more pronounced dissolved phase, Cr shows a significant particulate fraction compared to its total concentration. As observed as well in oxygen deficient waters (Moos et al.,

2020), particulate Cr progressively settles and is finally stored in the sediment. Here Cr(III) might be dominant given its strong affinity to SPM and forms strong Cr(III)-oxides which are only slightly oxidized from the surface to the halocline by the available oxygen, especially at station S2 and L2 (Geisler and Schmidt, 1991; Gustafsson et al., 2014; Pađan et al., 2019; Sternbeck et al., 1999). The dissolved fraction may be constituted of Cr(IV) which shows a higher toxicity than Cr(III), and forms stable dissolved oxo-complexes (Pađan et al., 2019). However, this fraction contributes less to the total content than the particulate one. The labile fraction remains low here, because only Cr(III) binds onto the DGT resin gels (Ernstberger et al., 2002).

Ni appears to be the most labile element among all the studied ones, meaning that its residence time in the water column is probably higher than the other trace metals (Turner et al., 1998). However, in the dissolved phase, a strong positive correlation was recorded between INi, the depth, the salinity and the concentration of  $\text{PO}_4^{3-}$ , indicating that the slight increase of INi along the water column is probably due to the mineralization of organic matter. Note further that the reduction of iron and manganese oxo-hydroxides and the production of sulfides in the bottom does not impact the solubility of Ni, which was reported by other studies as well (van de Velde et al., 2020; Vijayaraghavan et al., 2005).

Cd is known to form dissolved chloro- or sulfato-complexes with increasing salinity, explaining the dominance of dCd in the water column (Bingham et al., 1984; Lefèvre et al., 2009; Pempkowiak et al., 2000). In addition, dCd likely binds to low-molecular-weight organic ligands at higher depths (Waeles et al., 2008).

Finally, Pb behavior diverges from one station to another. pPb correlates well with pFe, meaning its vertical particulate flux might result from sorption

processes onto Fe-oxides in the upper part of the water column (Eslamikhah et al., 2017; Trueman, 2017). At the bottom of station L1, Pb might efficiently precipitate with free sulfides and to a lesser extent with pyrite (Morse and Luther, 1999; Oueslati et al., 2018; Sternbeck et al., 1999). At station L2, Pb exhibits a different pattern: given the increase of dPb around the seabed, a release of Pb from the sediment is suggested. As the non-labile fraction is clearly dominant and the sulfide concentrations are the highest, sulfidic ligands (for instance polysulfides) and/or Pb-S clusters may promote the stability of Pb in this anoxic environment (Luther and Rickard, 2005). Finally, at station S2, around -80 m, the same peak of concentration is observed for IPb and INi, which might be related with scavenging processes observed earlier on Fe- and Mn-oxides and indicate a change in adsorption capacity and most likely a release of these elements during the manganese and iron wheels.

#### **5.4.3. Temporal and spatial variability**

Based on Environmental Quality Standards (EQS, annual average) for water which have been defined under the Water Framework Directive (WFD) for priority substances (European Commission, 2013, 2010), the total concentrations of Cd, Ni and Pb in the water column are all below the recommended threshold values of 0.2, 8.6 and 1.3  $\mu\text{g L}^{-1}$ , respectively. In the same way, Cd, Cu and Pb are all below the Acute Water Quality Criteria (AWQC; Durán and Beiras, 2013), although the total concentration of Cu in the surface waters of station S2 and L2 (-20 m) is relatively close to the recommended probabilistic value of 1.39  $\mu\text{g L}^{-1}$ . Particulate levels of Cd are above the natural median levels found in earth's crust. The same is observed for Cu (in the surface and halocline layer of S1, in the halocline and deep waters of L1 and L2), Cr (at the surface of L1, in the deep waters of L2) and

Mn (in the deep waters of L1, in the surface and deep layer of L2). Regarding Cu, elevated concentrations in the Baltic Sea caused by an increasing use of copper-based antifouling paint on boats have been particularly pointed out by many recent studies (Bighiu et al., 2017b, 2017a; Eklund and Watermann, 2018; Ytreberg et al., 2016).

The Baltic Sea environment has been presented as very stratified, with little exchange with the North Sea causing stagnancy, pollutant accumulation and anoxia in the deep basins. Although this system can remain stable over several years, random ephemeral re-oxygenation events of the whole water column are likely to occur at any time (Höfllich et al., 2017; Mohrholz, 2018). The Major Baltic Inflow (MBI) recorded in 2015 in the Gotland Basin contributed to the natural oxygenation of the deep waters after 10 years under anoxic conditions and had a remarkable effect on trace element biogeochemistry. It also provided highly saline waters from the North Sea and enhanced fluxes from and to the sediment (Dellwig et al., 2018; Hermans et al., 2019; Liblik et al., 2018; Mohrholz et al., 2015; van de Velde et al., 2020) and its influence was eventually detected until 2016. Post-MBI, these studies reveal a net release of dMn from the sediment back to the water column (Dellwig et al., 2018; van de Velde et al., 2020), while Fe and Co were partially kept in the sediment, reducing the water column inventory of these elements. Back to complete anoxic conditions, the production of sulfide at high depths (below the halocline) may have increased the burial of Cd, Cu, and Pb in the sediment (Pohl and Hennings, 2005). Overall, the vertical profiles of Co, Cu, Mn and Pb in the water column did not show any pronounced differences compared to previous years (before the MBI of 2015) (Neretin et al., 2003; Pohl and Hennings, 2005). However, according to the same study (data from July 2000; Pohl and Hennings, 2005), Cd behaves in a similar way as Cu along the depth gradient, which was not observed in this study (i.e. only little variations of

dCd and pCd). While dPb and pPb, pCd and pNi are in good agreement with measurements described in the literature (before the MBI of 2015; Pempkowiak et al., 2000; Pohl and Hennings, 2005), dCd, dCu and pCu, dMn and pMn show slightly higher concentrations than observed earlier (Neretin et al., 2003; Pempkowiak et al., 2000; Pohl and Hennings, 2005). The dissolved profiles of Cd, Fe, Ni and Mn are also in concordance with the most recent study (van de Velde et al., 2020).

Regarding the stratification of the water column, the sampling sites have similar temperature, oxygen and salinity. However, a higher variability is observed for trace metals. First, higher values are often found in the EGB than in the WGB: this is the case for Co, Fe, Mn, Cd, Pb. Only Cu and Ni show a reverse trend. If the trace element distribution is often similar at the surface, it seems to differ much more downward. An explanation to this could be that the EGB and the WGB indeed have different near-bottom current circulations, thus differently influencing trace metal spread below the halocline (Neretin et al., 2003). Moreover, the influences from freshwater inflow or groundwater inputs might also be more important on the Eastern part of the basin (Szymczycha et al., 2014, 2012).

## **5.5. Conclusion**

In the deep basins of the Baltic Sea, a strong stratification of the water column is triggered by established and stagnant anoxic conditions and very limited vertical exchanges. As a result, the surface is well-oxygenated, highly productive, yet the environment suffers from strong anoxia and euxinia below the halocline. Thus, the fluxes of trace metals in the water column are mainly regulated by a variety of vertical gradients and reactions. In the anoxic zone, most elements precipitate with dissolved sulfide: Cu shows the lowest



solubility and might form strong CuS complexes, as it is strongly removed from the water column to be buried in the sediments. Vertical fluxes of Fe and Mn in the water column is controlled by Fe- and Mn-oxides sinking from the oxic layers (shelf-to-basin shuttle and natural sedimentation of particles) and being reduced in anoxic conditions, and, with less intensity, by slow diffusion mechanisms from the seabed. Co and, to a lesser extent, Pb showed a quite strong affinity for Fe- and Mn-oxides, as they tend to follow the same biogeochemical cycle. For elements such as Cd, Cu, Pb and Co, their vertical transport involves many processes such as for example their adsorption onto Fe- and Mn-oxides, or organic/inorganic particles or their diffusion. Ni and Cr seemed to be controlled by other transport mechanisms. From a general point of view, the particulate phase of trace metals only constitutes a small fraction of the total concentration (compared to the dissolved one) for all elements, except for Cr. The highest particulate metal concentrations are found either at the very surface, most likely related to their biological uptake by phytoplankton (Paquin et al., 2003). Or they are found close to the seabed for certain trace metals, indicating coprecipitation processes near the bottom. Dissolved species remain dominant all along the water column, and non-labile elements are often more important than labile ones. Nevertheless, the DGT technique was successfully applied and highlights that the labile fraction of Co, Fe, Mn and Ni is of greater importance in the anoxic zone.

Nowadays, concern is rising regarding the extent of anoxia since the last decades (Lehmann et al., 2014; Lenz et al., 2015; Savchuk, 2013). This will most likely influence the present biogeochemical cycling of trace metals and perhaps increase their lability in the upper zones. Thus, future studies should assess the degree of impact that increasing anoxic zones could have. Moreover, even if the long-term existing anoxia is the main factor controlling trace element cycling in the Gotland Basin, the MBI events can often be the

source of great discussions as well, because of the possible resuspension and transfer of hazardous compounds to the surface layers (Broclawik et al., 2018; Kuss et al., 2017) which could occur during such phenomenon, even if it remains transient.

## **Acknowledgement**

The authors would like to thank the Belgian Science Policy Office (BELSPO) for funding the NewSTHEPS project (BR/143/A2/NEWTHEPS) and supporting Gaulier C. (FOD-12). The RV Belgica crew members, the scientific vessel of the Belgian government, are thanked for the sampling campaign.

## 5.6. Supplementary Information

### 5.6.1. Material and Methods

**Table S5.1:** Overview of the sampling strategy.

Station	Sampling depth (m)	DGT deployment	Grab sampling	CTD records	Dissolved nutrients, sulfides
S1 <i>(57°58.80'N; 17°33.00'E)</i>	-3		X	X	X
	-10	X	X	X	X
	-20		X	X	X
	-40	X	X	X	X
	-60		X	X	X
	-80		X	X	X
	-90		X	X	X
	-120			X	
S2 <i>(57°54.00'N; 17°45.00'E)</i>	-3		X	X	X
	-10	X	X	X	X
	-20	X	X	X	X
	-60	X	X	X	X
	-80	X	X	X	X
	-90	X	X	X	X
	-130		X	X	X
	-155	X	X	X	X
L1 <i>(57°17.26'N; 20°27.00'E)</i>	-10	X	X	X	X
	-30		X	X	X
	-60		X	X	X
	-90	X	X	X	X
	-100		X	X	X
	-110		X	X	X
	-150	X	X	X	X
L2 <i>(57°17.26'N; 20°13.50'E)</i>	-3	X	X	X	X
	-20	X	X	X	X
	-60	X	X	X	X
	-80		X	X	X
	-120	X	X	X	X
	-150		X	X	X
	-180	X	X	X	X
	-230	X	X	X	X

**Table S5.2:** Reagent preparation for dissolved sulfide measurements

Stock ( $\approx$ 60 samples)	End vol (ml)	Recipe
5% ZnAc	100	5 g ZnAc in 100 ml MQ + 100 $\mu$ L glacial acetic acid
6 N HCl	500	250 mL 37% HCl + 250 ml MQ
10 mM Na <sub>2</sub> S stock 1	50	0.12 g Na <sub>2</sub> S $\cdot$ 9H <sub>2</sub> O in 50 ml degassed MQ + 50 $\mu$ L 6N HCl
Diamine reagent	500	2g N,N-dimethyl-p-phenylenediamine sulfate + 3 g FeCl <sub>3</sub> $\cdot$ 6H <sub>2</sub> O in 500 mL 6N HCl

**Table S5.3:** Reagent preparation for dissolved inorganic nutrient measurements

Reagent	End vol (ml)	Recipe
OPA	XX	XX
NEDD (0.2%)	100	100 mg N-1-naphthylethylenediamine dihydrochloride in 100 mL MQ
Sulfanilamide (2%)	100	2 g sulfanilamide in 100 mL 10% (v/v) HCl.
Acidified acid ascorbic	50	10g ascorbic acid C <sub>6</sub> H <sub>8</sub> O <sub>6</sub> in 50mL MQ + 9N H <sub>2</sub> SO <sub>4</sub>
Molybdate solution	495	12.5g ammonium heptamolybdate tetrahydrate in 125mL MQ + 350 mL 9N H <sub>2</sub> SO <sub>4</sub> + 0.5 g potassium antimony tartrate in 20mL MQ

### 5.6.2. Results

**Table S5.4:** Correlation matrix

	Depth	DO	Sal.	Temp.	POC	PN	C.N	NH4	NO2	PO4	S(-II)	SPM	Cd_lab	Cd_diss	Cd_part	Pb_lab	Pb_diss	Pb_part	Cr_lab	Cr_diss	Cr_part	Mn_lab	Mn_diss	Mn_part	Fe_lab	Fe_diss	Fe_part	
Depth	1																											
DO	-0,88	1																										
Sal.	0,95	-0,9	1																									
Temp.	-0,52	0,4	-0,4	1																								
POC	-0,68	0,59	-0,6	0,88	1																							
PN	-0,69	0,61	-0,6	0,87	0,99	1																						
C.N	-0,66	0,63	-0,6	0,71	0,83	0,81	1																					
NH4	0,80	-0,7	0,69	-0,33	-0,46	-0,5	-0,5	1																				
NO2	-0,01	-0,2	0,17	0,05	-0,02	0	0,09	-0,29	1																			
PO4	0,94	-0,9	0,92	-0,57	-0,68	-0,7	-0,6	0,84	0,04	1																		
S(-II)	0,75	-0,6	0,62	-0,23	-0,36	-0,4	-0,4	0,98	-0,26	0,52	0,28	-0,11	0,55	1														
SPM	-0,14	0	0	0,57	0,55	0,54	0,38	-0,14	0,12	-0,15	-0,08	1																
Cd_lab	-0,03	0,02	0,12	0,15	0,2	0,21	0,31	-0,14	0,36	0,03	-0,11	0,55	1															
Cd_diss	0,75	-0,7	0,81	-0,19	-0,45	-0,5	-0,4	0,41	0,41	0,65	0,41	0,03	0,15	1														
Cd_part	0,52	-0,4	0,47	-0,2	-0,23	-0,3	-0,3	0,38	-0,26	0,52	0,28	-0,22	-0,15	0,3	1													
Pb_lab	-0,04	-0,1	0	0,37	0,25	0,2	0,24	0,01	0,21	0,04	0	0,22	0,2	0,14	0,19	1												
Pb_diss	0,53	-0,2	0,38	-0,06	-0,13	-0,2	-0,1	0,71	-0,22	0,48	0,78	-0,1	0,05	0,47	0,28	0,1	1											
Pb_part	0,41	-0,4	0,51	-0,23	-0,25	-0,2	0	0,26	0,4	0,53	0,22	0,02	0,53	0,31	0,32	0,34	0,1	1										
Cr_lab	-0,28	0,27	-0,2	0,44	0,46	0,44	0,52	-0,39	0,42	-0,32	-0,28	0,64	0,7	0,15	-0,28	0,25	0,03	0,14	1									
Cr_diss	-0,40	0,5	-0,5	0,17	0,38	0,39	0,33	-0,08	-0,05	-0,26	-0,05	-0,28	-0,02	-0,5	0	0,29	0,11	0,12	-0,08	1								
Cr_part	0,36	-0,4	0,44	-0,03	-0,34	-0,4	-0,4	0,18	0,22	0,3	0,09	-0,23	-0,07	0,57	0,31	0,26	0,11	0,02	-0,1	-0,35	1							
Mn_lab	0,79	-0,5	0,7	-0,17	-0,33	-0,3	-0,3	0,82	-0,24	0,73	0,82	-0,1	0,03	0,62	0,62	0,13	0,84	0,32	-0,1	-0,11	0,38	1						
Mn_diss	0,81	-0,6	0,72	-0,19	-0,35	-0,4	-0,4	0,87	-0,22	0,77	0,87	-0,1	0,04	0,6	0,58	0,13	0,84	0,36	-0,13	-0,09	0,34	0,99	1					
Mn_part	-0,01	-0,1	0,14	0,13	0,05	0,06	0,09	-0,27	0,67	-0,13	-0,22	0,05	0,19	0,44	-0,45	-0,18	-0,06	-0,08	0,26	-0,33	0,33	-0,18	-0,19	1				
Fe_lab	0,70	-0,6	0,67	-0,3	-0,41	-0,4	-0,3	0,89	-0,2	0,77	0,89	-0,08	-0,02	0,39	0,29	-0,03	0,58	0,41	-0,19	-0,17	0,09	0,72	0,78	-0,22	1			
Fe_diss	0,86	-0,7	0,79	-0,28	-0,44	-0,5	-0,4	0,93	-0,26	0,86	0,91	-0,09	-0,03	0,55	0,59	0,09	0,7	0,4	-0,25	-0,18	0,3	0,93	0,96	-0,28	0,89	1		
Fe_part	0,40	-0,5	0,55	-0,1	-0,2	-0,2	0,04	0,13	0,44	0,4	0,14	0,26	0,46	0,51	0,16	0,24	0,01	0,75	0,42	-0,38	0,1	0,25	0,27	0,16	0,45	0,34	1	
Co_lab	0,83	-0,7	0,8	-0,22	-0,39	-0,4	-0,4	0,73	-0,2	0,78	0,7	-0,08	0,07	0,63	0,75	0,15	0,61	0,47	-0,11	-0,24	0,42	0,93	0,92	-0,23	0,72	0,92	0,46	
Co_diss	0,81	-0,7	0,79	-0,24	-0,41	-0,4	-0,4	0,77	-0,22	0,81	0,72	-0,11	0,04	0,52	0,73	0,17	0,5	0,57	-0,26	-0,16	0,36	0,86	0,87	-0,31	0,77	0,93	0,46	
Co_part	0,62	-0,5	0,66	-0,09	-0,23	-0,3	0	0,64	0,25	0,63	0,68	0,11	0,38	0,61	0,2	0,24	0,63	0,68	0,24	-0,14	0,18	0,71	0,75	0,11	0,75	0,72	0,7	
Ni_lab	0,58	-0,5	0,63	-0,41	-0,45	-0,5	-0,5	0,16	0,12	0,53	0,03	-0,26	0,07	0,49	0,74	0,04	0	0,38	-0,2	-0,21	0,54	0,41	0,37	-0,01	0,08	0,37	0,26	
Ni_diss	-0,19	0,14	-0,2	-0,39	-0,26	-0,2	-0,2	-0,24	-0,04	-0,09	-0,33	-0,53	-0,24	-0,39	0,05	0,09	-0,48	0,28	-0,48	0,36	-0,08	-0,36	-0,33	-0,27	-0,21	-0,25	-0,03	
Ni_part	0,02	0	0,12	0,62	0,5	0,49	0,38	-0,02	0	-0,07	0	0,28	0,16	0,15	0,48	0,36	0,1	0,19	0,23	0	0,37	0,34	0,29	0,07	0,03	0,22	0,25	
Cu_lab	-0,17	0,28	-0,2	0,36	0,45	0,42	0,4	-0,08	0,15	-0,21	0,01	0,19	0,13	0,15	0,03	0,47	0,49	-0,1	0,5	0,28	0,05	0,21	0,18	0,12	-0,14	-0,03	-0,04	
Cu_diss	-0,7	0,78	-0,7	0,52	0,51	0,52	0,55	-0,62	-0,01	-0,77	-0,49	0,04	0,06	-0,4	-0,3	0,25	-0,19	-0,22	0,38	0,39	-0,17	-0,41	-0,45	0,01	-0,52	-0,56	-0,17	
Cu_part	0,75	-0,6	0,72	-0,61	-0,63	-0,6	-0,6	0,51	0,03	0,8	0,39	-0,33	0,02	0,54	0,78	0,01	0,32	0,42	-0,27	-0,13	0,4	0,62	0,6	-0,21	0,42	0,64	0,23	

	Co_lab	Co_diss	Co_part	Ni_lab	Ni_diss	Ni_part	Cu_lab	Cu_diss	Cu_part
Co_lab	1								
Co_diss	0,96	1							
Co_part	0,68	0,67	1						
Ni_lab	0,61	0,57	0,11	1					
Ni_diss	-0,21	-0,04	-0,29	0,16	1				
Ni_part	0,42	0,39	0,25	0,3	-0,23	1			
Cu_lab	0,01	-0,15	0,22	-0,2	-0,33	0,29	1		
Cu_diss	-0,46	-0,52	-0,33	-0,45	0,1	0,17	0,28	1	
Cu_part	0,72	0,68	0,3	0,84	0,02	0,03	-0,12	-0,59	1

**Table S5.5: P-value matrix**

Depth	DO	Sal.	Temp.	POC	PN	C.N	NH4	NO2	PO4	S(-II)	SPM	Cd_lab	Cd_diss	Cd_part	Pb_lab	Pb_diss	Pb_part	Cr_lab	Cr_diss	Cr_part	Mn_lab	Mn_diss	Mn_part	Fe_lab	Fe_diss	Fe_part
Depth	0,00																									
DO	0,00																									
Sal.	0,00	0,00																								
Temp.	0,03	0,12	0,07																							
POC	0,00	0,01	0,01	0,00																						
PN	0,00	0,01	0,01	0,00	0,00																					
C.N	0,00	0,01	0,01	0,00	0,00	0,00																				
NH4	0,00	0,00	0,00	0,20	0,06	0,06	0,05																			
NO2	0,98	0,43	0,50	0,86	0,95	0,97	0,73	0,26																		
PO4	0,00	0,00	0,00	0,02	0,00	0,00	0,01	0,00	0,88																	
S(-II)	0,00	0,01	0,01	0,37	0,16	0,15	0,15	0,00	0,24	0,00																
SPM	0,60	0,91	0,95	0,02	0,02	0,02	0,14	0,58	0,65	0,56	0,77															
Cd_lab	0,92	0,93	0,66	0,56	0,43	0,41	0,23	0,58	0,15	0,91	0,68	0,02														
Cd_diss	0,00	0,00	0,00	0,46	0,07	0,06	0,11	0,10	0,10	0,01	0,11	0,92	0,57													
Cd_part	0,03	0,16	0,06	0,45	0,37	0,34	0,33	0,14	0,31	0,03	0,27	0,40	0,56	0,24												
Pb_lab	0,88	0,78	0,98	0,14	0,33	0,44	0,35	0,98	0,41	0,88	1,00	0,40	0,44	0,60	0,46											
Pb_diss	0,03	0,37	0,14	0,81	0,62	0,57	0,76	0,00	0,39	0,05	0,00	0,70	0,85	0,05	0,27	0,70										
Pb_part	0,11	0,11	0,04	0,37	0,34	0,35	0,92	0,32	0,11	0,03	0,40	0,93	0,03	0,22	0,21	0,19	0,71									
Cr_lab	0,27	0,30	0,51	0,07	0,06	0,07	0,03	0,12	0,09	0,21	0,27	0,01	0,00	0,58	0,27	0,32	0,92	0,60								
Cr_diss	0,12	0,04	0,04	0,51	0,14	0,12	0,19	0,75	0,86	0,32	0,84	0,28	0,93	0,04	0,99	0,27	0,67	0,65	0,76							
Cr_part	0,16	0,09	0,08	0,90	0,19	0,17	0,08	0,49	0,40	0,24	0,72	0,38	0,80	0,02	0,23	0,32	0,66	0,93	0,70	0,16						
Mn_lab	0,00	0,02	0,00	0,52	0,20	0,18	0,18	0,00	0,36	0,00	0,00	0,69	0,89	0,01	0,01	0,61	0,00	0,21	0,71	0,69	0,13					
Mn_diss	0,00	0,01	0,00	0,46	0,17	0,15	0,17	0,00	0,39	0,00	0,00	0,70	0,87	0,01	0,01	0,61	0,00	0,15	0,62	0,73	0,18	0,00				
Mn_part	0,97	0,62	0,59	0,63	0,85	0,83	0,72	0,30	0,00	0,61	0,40	0,85	0,47	0,08	0,07	0,50	0,81	0,75	0,31	0,20	0,19	0,49	0,46			
Fe_lab	0,00	0,01	0,00	0,24	0,10	0,08	0,23	0,00	0,45	0,00	0,00	0,75	0,93	0,12	0,25	0,91	0,01	0,11	0,46	0,50	0,74	0,00	0,00	0,40		
Fe_diss	0,00	0,00	0,00	0,28	0,08	0,07	0,08	0,00	0,31	0,00	0,00	0,73	0,91	0,02	0,01	0,72	0,00	0,11	0,33	0,49	0,24	0,00	0,00	0,28	0,00	
Fe_part	0,12	0,05	0,02	0,70	0,45	0,40	0,87	0,62	0,08	0,11	0,58	0,32	0,07	0,04	0,53	0,36	0,96	0,00	0,09	0,14	0,71	0,33	0,29	0,54	0,07	0,18
Co_lab	0,00	0,00	0,00	0,39	0,12	0,10	0,13	0,00	0,45	0,00	0,00	0,77	0,78	0,01	0,00	0,58	0,01	0,06	0,67	0,36	0,09	0,00	0,00	0,37	0,00	0,00
Co_diss	0,00	0,00	0,00	0,35	0,11	0,09	0,12	0,00	0,41	0,00	0,00	0,66	0,89	0,03	0,00	0,51	0,04	0,02	0,31	0,55	0,16	0,00	0,00	0,22	0,00	0,00
Co_part	0,01	0,03	0,00	0,74	0,37	0,34	0,89	0,01	0,32	0,01	0,00	0,66	0,13	0,01	0,45	0,34	0,01	0,00	0,35	0,59	0,48	0,00	0,00	0,66	0,00	0,00
Ni_lab	0,02	0,04	0,01	0,11	0,07	0,07	0,04	0,54	0,64	0,03	0,91	0,31	0,79	0,05	0,00	0,89	0,99	0,13	0,45	0,42	0,02	0,10	0,15	0,98	0,75	0,14
Ni_diss	0,46	0,60	0,47	0,12	0,32	0,36	0,40	0,35	0,89	0,74	0,20	0,03	0,36	0,12	0,84	0,74	0,05	0,28	0,05	0,15	0,77	0,16	0,19	0,29	0,41	0,33
Ni_part	0,95	0,96	0,66	0,01	0,04	0,04	0,13	0,94	0,99	0,79	0,99	0,28	0,53	0,57	0,05	0,16	0,69	0,46	0,38	1,00	0,15	0,18	0,25	0,80	0,92	0,40
Cu_lab	0,51	0,28	0,41	0,15	0,07	0,09	0,11	0,76	0,57	0,42	0,96	0,47	0,63	0,57	0,90	0,06	0,05	0,69	0,04	0,27	0,83	0,41	0,50	0,66	0,59	0,91
Cu_diss	0,00	0,00	0,00	0,03	0,04	0,03	0,02	0,01	0,96	0,00	0,05	0,87	0,82	0,11	0,24	0,34	0,46	0,39	0,14	0,12	0,52	0,11	0,07	0,97	0,03	0,02
Cu_part	0,00	0,01	0,00	0,01	0,01	0,01	0,04	0,92	0,00	0,13	0,20	0,95	0,03	0,00	0,96	0,21	0,10	0,30	0,62	0,11	0,01	0,01	0,42	0,10	0,01	0,38





# Chapter 6

## General conclusions and perspectives



## **6.1. Highlights and new insights**

This research was done in the framework of the NewSTHEPS project and beyond, given the opportunity of missions and collaborations which appeared over these three years of PhD thesis. Following NewSTHEPS' main objective to develop integrated approaches and novel procedures for comprehensive environmental monitoring and risk assessment of a broad set of both priority and emerging contaminants in the marine environment, this doctoral thesis specifically aimed to:

(i) apply a unique combination of field and laboratory chemical techniques to study trace metal dynamics and speciation, unraveling their lability along horizontal and vertical transects and filling the research gap on labile trace elements;

(ii) develop and evaluate a framework and toolbox for monitoring the chemical anthropogenic pressures on coastal ecosystems, which should be integrated, efficient, cost-effective and scientifically relevant;

(iii) develop innovative and comprehensive multi-method approaches to monitor and screen a broad range of waterborne trace metals in the Belgian coastal waters, Scheldt Estuary and Baltic Sea.

A detailed focus has been made on estuarine and coastal areas, because of their high economic, touristic and ecological values. They constitute a great source of food and income for human beings and are the place of intense merchant shipping. Especially as the world population and urbanized areas increase, more and more industries and populations settle by the sea, along coasts and estuaries: crucial and central points of international exchanges. However, the rapid development of the coastal regions results in more and more severe environmental pollution problems, including uncontrolled discharge to the water system, boat painting and oil leaking, overfishing, etc. Today, it

therefore becomes ethically and legally necessary to maintain, not only their economic contribution, but also their good ecological status (described by their biological and physicochemical quality).

The coastal areas of this research are of great interest in studies on metal pollution, given their industrial history and their current utility. First, the Scheldt historically constitutes one of the most polluted estuaries in Europe. Despite the numerous efforts made from national and European levels to reduce the discharge of metals into the estuary, traces of historical and present contamination are still visible today. Following the estuary, our work also naturally turned towards the behavior of metals along the Belgian coasts: in two main industrial harbors and further off the coasts, in the plume let by the estuary discharge. These two Chapters (2 and 3), together with Chapter 4 (specifically headed towards particulate trace metals, SPM and influence of tides), gave us a first glimpse of the horizontal fluxes and speciation of trace metals in Belgian surface waters. Subsequently, the work in Chapter 5 focused on a survey and description of trace metal vertical distribution and speciation in the Baltic Sea. The Baltic Sea is a small and isolated marine system strongly influenced by fresh water and severe hypoxia. Unlike the Southern North Sea, it shows very large variation of depths inducing great physicochemical changes along the water column. At the heart of Scandinavian countries, the Baltic Sea behaves as a collection basin accumulating trace metal discharges from surrounding rivers and was therefore another relevant area for the study of trace metal biogeochemical behaviors.

From these expeditions, we emphasized the dynamic and speciation of trace metals which are strongly affected by important environmental features and gradients (salinity, oxygenation, tides, shape of the estuarine/seabed, etc.). For instance, the biogeochemical cycles of trace metals were recorded in the Scheldt Estuary and resulted in non-conservative behavior of elements

influenced by salinity, and strong mixing mechanisms. In the same way, in the Baltic Sea, trace metal cycling seemed widely affected by euxinia and reduction processes. In addition, a good continuum of concentration ranges was measured from the Scheldt Estuary, to the coastal zone and further offshore, while several temporal and local variabilities were highlighted (seasonally, monthly, year after year by comparisons with literature data). In terms of speciation, a dominance of dissolved species (non-labile and labile) was generally observed in the marine waters (relative contribution to the total concentration), while higher particulate fractions occur in the freshwaters of the upper Scheldt Estuary. Concurrently, the role of SPM in trapping and storing trace metals was also observed, which certainly decreases the direct impact of dissolved metals on marine organisms. However, this big reservoir may also become a source of pollution when trace metal resuspension and solubilization happen due to increasing salinity, pH changes, strong tides, human activities like trawling and dredging, etc.

Trace metal speciation is the main key to explain and predict bioavailability and potential toxicity of trace metals to the marine fauna and flora. In practice, both classic active sampling and passive sampling for trace metals were carried out in this study. The passive sampling technique of DGT was successfully used for the *in-situ* measurement of labile metals and eventually constitutes a good surrogate to the biomonitoring of trace elements, usually using mussels, algae, etc. The results from trace metal accumulation on the DGT and in living organisms (soft body, shell) can be, in this sense and under certain conditions, easily compared. This combination of techniques has permit to generate a unique set of knowledge and data, required to fulfill international regulatory requirements (WFD, MSFD) and commitments (OSPAR, HELCOM). In the future, a specific attention must therefore be paid to the use of DGT as a valuable tool for monitoring the bioavailability of trace

metals in fresh and marine waters. Besides the DGT approach, we would also recommend a systematic measurement of physicochemical parameters such as pH, salinity, oxygenation and temperature, on fieldwork. These latter are indispensable elements for understanding behavior and speciation changes of trace elements. Additionally, a detailed focus on SPM with the measurements of carbon and nitrogen stable isotope ratios has shown a good interest for tracing the origin of SPM, giving us supplementary information on particulate trace metal sources (rather marine or terrestrial) and SPM organic composition. Such additional approach to pollutant monitoring is eventually very interesting to, for instance, improve our knowledge on SPM and trace metals transports in coastal environments, and to help building stronger predictive environmental model of pollutant transfer and pathways.

Finally, this extensive approach including the use of passive samplers like DGT has the potential to be part of a new standard and legal framework for future environmental monitoring.

## **6.2. Research prospects**

The great diversity of existing aquatic ecosystems, both ecologically and physico-chemically, makes them fascinating environments to study. The Scheldt Estuary, the North Sea and the Baltic Sea are three typical examples of this variety, and studies in the same vein as this one could also be carried out along many coastal areas in the world, impacted by metal pollution of anthropogenic origin. To go even further, many questions around the biogeochemical cycling of trace metals in marine environments remain unsolved, and many leads still need to be explored. Below, I tried to draw up several key tracks for continuation of the presented research, practical considerations for future monitoring and other research possibilities.

As introduced in the first chapter, the measurement of dissolved trace metals (including labile elements) in seawater is, after all, not such an easy task due to several reasons mentioned in Chapter 1. Therefore, techniques in analytical chemistry endeavored to develop instruments with higher precision lowering detection limits and/or isolating the species of interest and preconcentrating them. As many techniques exist, it often becomes a maze to select the most appropriate one. Here, we chose the DGT technique for the measurement of labile trace metals, but electrochemical methods must be considered for future analytical comparison. These very sensitive methods show great suitability for dissolved trace metal measurements in seawater, as well as for labile trace metal measurements and determination of complexing capacity. Moreover, yet this alternative biological approach was not applied here, the monitoring of trace metals directly accumulated in the biota from either naturally occurring or transplanted species is often carried out. Despite several advantages (especially for measuring the intricate and exact metallic uptake by organisms), this technique hardly overcomes the issue brought by the great variability of uptake between species but also individuals from a same species. However, the results from both approaches (DGT and biomonitoring) may be used in a complementary way.

If the use of DGT *in situ* in the field is clearly a great advantage, naturally turbulent environments can often cause troubles for the deployment of such type of passive samplers. Thus, practical considerations must be taken beforehand. In very tumultuous environments, suitable fastening and protecting system must be used (buoy, weight, plastic cage, etc.), in order to avoid any loss of material. In addition, specific attention must be paid to the assessment of the Diffusive Boundary Layer (DBL) existing between the DGT piston surface and the adjacent water column (partly influenced by the turbulence of the studied environment), since thicker DBL will result in bigger

under-estimation of the labile concentrations. Concerning more advanced studies in open ocean, the deployment of a Sea-glider mounted with DGT samplers has been tested and allowed the measurement of ultra-trace level of metals (nanomole) over long distance and period. In future, the development of very sensitive electrochemical sensors which could be for instance combined with a Sea-glider to measure ultra-trace metals could be a meaningful and cutting-edge research approach.

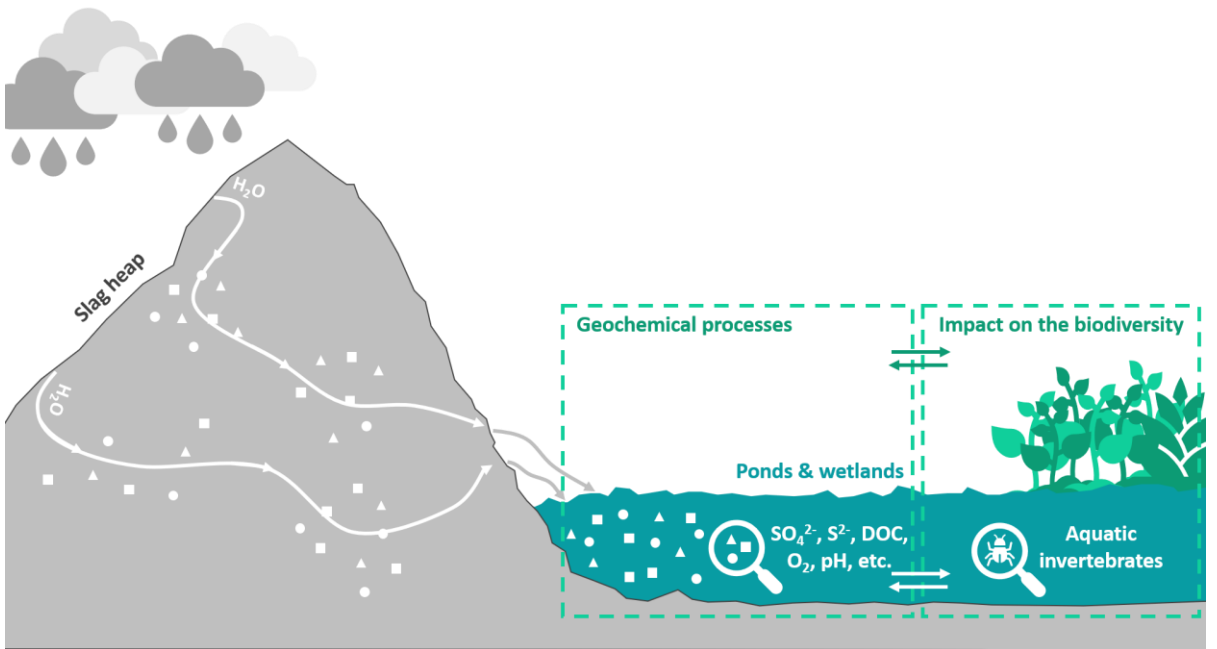
In a larger scale, this research has revealed the importance of using innovative tools and procedures for the further development of a sustainable integrated management of estuarine and coastal ecosystems and their aquatic resources. This type of study is in line with other projects, such as the Monitool project, and ultimately may allow to address the European Directive requirements for the assessment of transitional and coastal water status. Thus, the collected data and the use of passive sampling devices such as DGT will serve as a robust base for future guidelines implemented by governments and improve the implementation of the WFD by adapting the existing EQS. Such speciation approach in metal contamination studies will, undoubtedly, be incorporated in future regulations. Furthermore, as foreseen within the NewSTHEPS project's objectives, the dataset resulting from this research will be further used in an integrated model to predict accumulation and chemical speciation in given coastal areas, and to identify zones of concern. A preliminary work carried out in collaboration with the Royal Belgian Institute of Natural Sciences already gave nice insights on pollutant fluxes in the Belgian Coastal Zone.

Finally, temporal variability has only been a little addressed in this work, yet its understanding is of crucial importance for future monitoring. Indeed, daily phenomena such as daily tides can first impact the biogeochemical cycling of trace metals. Tidal cycles are ubiquitous components of estuarine and coastal areas but are too often ignored or deliberately omitted from scientists. Future

monitoring could focus on an in-depth investigation of tides effect on trace metal distribution and lability in the Scheldt Estuary and further in the BCZ, either during 13-hours or monthly cycles. To do so, high-frequency measurements are needed and could be performed by online monitoring tools (*e.g.* direct measurement using voltammetry) or continuous sample preconcentration using a Sea-fast system. In addition, the deployment of SPM traps coupled with  $\mu$ XRF methods as suggested in Chapter 4 seem to provide a good description of the SPM composition fluctuations over time (monthly variations induced by tides). Furthermore, if we widen the time scale, seasonal and long-term variations (*e.g.* climate change) can also play a key role in trace metal behavior and bioavailability. This was slightly approached in Chapter 3 which has shown variations of trace metal speciation over seasons, and over a years-scale in Chapter 2 and 5 through literature comparisons. Climate change and its effect on trace metal biogeochemical cycles could also be one of the most crucial research axes of the coming years. Marine waters act as a natural carbon sink but increasing amount of CO<sub>2</sub> in the atmosphere leads to more and more CO<sub>2</sub> trappings in the seawaters. Therefore, the sea becomes more and more acidic, most likely affecting protective structure made of calcium carbonates (*e.g.* corals, shellfish) as well as the solubilization of pollutants like trace metals (increasing their bioavailability and toxicity). In addition, the rising seawaters might increase erosion processes and cause the resuspension of hazardous elements from soil which could not be reached by any water before. In this sense, assessing the variability of trace metal speciation over flood events compared to dryer seasons might be relevant. To keep a close watch on such seasonal and long-term influences, monitoring campaign several times a year, over several years needs to be steadily conducted, using a combination of several sampling and analytical tools.



# Annexes



Adapted from Gaulier C., Billon G., Lesven L., Falantin C., Superville P.-J., Baeyens W., Gao Y. (2020). Leaching of two northern France slag heaps: Influence on the surrounding aquatic environment. *Environmental Pollution* 257, 113601.

---

The following work results from a study which I conducted together with the University of Lille and the North Department Council of France during my master thesis, in 2016, on the influence of slag heap leaching (i.e. old artificial hills built by accumulation of mining residue) on aquatic environments. Slightly different from the research work that have been proposed in the previous chapters (trace metals in marine environments), this study focused on the biogeochemical cycle of sulfur and major elements in freshwater ecosystems. Juggling between two approaches, one physicochemical, the other ecological, this project was intended to assess vast wetlands and small ponds surrounding massive slag heaps, rather neglected after the exploitation of coal mines. As a large-scale project and after obtaining my master's degree, it mattered to me to continue and especially finalize this study, in parallel with my own thesis project. This work has been nicely highlighted in the form of a scientific article, published in the journal *Environmental Pollution* in February 2020. And I have the great pleasure to share a version with you today.

Briefly, the main highlights of this work were:

- (i) Wetlands are widely enriched in sulphates, caused by slag heap leaching.
- (ii) Impact of leaching on wetlands was assessed using chemical & biological approaches.
- (iii) The water composition reveals a typical example of a neutralized acid mine drainage.
- (iv) Combination of high  $S^{2-}$ , low  $O_2$  and pH may lead to a loss of biodiversity.
- (v) Variations in DOC and lixivate composition induce spatio-temporal changes.

## **Leaching of two Northern France slag heaps: influence on the surrounding aquatic environment**

### **Abstract**

After the exploitation of coal mines in the 19<sup>th</sup> and 20<sup>th</sup> centuries in northern France, many mining slag heaps (SH) were left without any particular management or monitoring. Currently, the influence of these SHs on the quality of surrounding wetlands is hardly known. The purpose of this work is to determine the water quality in the neighbourhood of two SHs located near the city of Douai and its influence on the distribution of aquatic invertebrates in local wetlands. Our approach involves (1) the spatial and temporal characterization of the water composition (anions, major elements, sulphide, DOC and alkalinity) and of the biological diversity (aquatic invertebrates) and (2), based on this chemical and biological screening, the establishment of relationships between water quality and biodiversity distribution through multivariate data analysis. The results clearly indicate that substantial leaching from the slag heaps occurs, given the very high concentrations of dissolved sulphates (in the range of 2 g L<sup>-1</sup>). While the pH remains weakly basic, indicating that the leaching water has been neutralized by the highly carbonated regional substratum, high levels of biodegradable organic matter and sulphate contents have been noticed. They sporadically cause significant drops in dissolved oxygen and the occurrence of dissolved sulphides that massively reduce biodiversity, qualitatively and quantitatively. In Summer, oxygen saturation is generally lower due to the higher rate of organic matter degradation, and the risk of anoxic episodes therefore increases. Finally, as wetlands are vulnerable environments, these preliminary results suggest that monitoring and management of these sites must be attempted quickly to avoid the degradation of those valuable habitats.

**Keywords:** Slag heap, Wetland, Acid Mine Drainage, Water quality, Biodiversity.

## **1. Introduction**

The Hauts-de-France region faced huge changes between the 17<sup>th</sup> and the 20<sup>th</sup> century with the appearance of coal mining which has accelerated its industrial and economic development, but has also transformed its landscape (Foucher et al., 2012). Indeed, the traces left behind by former mining sites are still visible today. They take the shape of hills, called slag heaps (SH), resulting from a long accumulation of mine tailings (mainly black schist and sandstones) (Apourceau-Poly and Bertram, 2016). During this industrial period, the slag heaps were the property of the mining company, Charbonnage de France. However, when the coal extraction stopped, SHs have been rapidly abandoned, leaving in the northern landscape huge piles of natural mining material. Of anthropogenic origin, some of these slag heaps have gradually become green spaces due to a natural return of the vegetation (CPIE Chaîne des terrils et al., 2014). On their slopes and at their feet, they now shelter remarkable but fragile ecosystems. They host unique habitats, thanks to abnormally high temperatures resulting from the lower albedo of the black schist (Denimal, 2001). Hence, they allow rare and protected species to survive in the region and constitute a shelter and/or a feeding place for many others. However, they are highly sensitive to erosion, landslide and leaching. In the early years of this century, these sites have therefore been re-evaluated as Sensitive Natural Areas and have been purchased by the North Department Council, because of their value as biodiversity hotspots (Sader, 2018). Further on, the slag heaps became UNESCO World Heritage in 2012 and are now part of the biodiversity wealth of the region (Apourceau-Poly and Bertram, 2016; Gilbert, 2012). While these slag heaps were thus fostered for their biodiversity wealth, vast wetlands (and more specifically peatlands) spread out in the same area were damaged by the erection of these slag heaps. This created an important environmental problem especially since wetland areas are

becoming a worldwide environmental concern: wetland destruction including habitat fragmentation and degradation is increasing while climate change increases the pressure on the wetland ecosystem (Holland et al., 1995; Davis and Froend, 1999; Gibbs, 2000). They are nowadays facing a strong decline, while they have a proven added value for biodiversity and therefore a need to be protected (Gibbs, 1993; Mitsch and Gosselink, 2000). Wetlands host complex ecosystems including both aquatic and terrestrial biotopes. Moreover, the various habitats, with permanently to temporary water zones, are related to different chemical properties of the water and the soil (Akcil and Koldas, 2006). The story of the slag heaps is thus one with two faces: slag heaps offer a unique environment for many rare species, but their erection has caused habitat fragmentation and degradation of already existing environments.

As mentioned, the SH soils are particularly sensitive to erosion and leaching, either by rainwater or by the oscillation of underground water reservoirs (Figure 1). After such phenomena, the leaching water carries dissolved species and suspended matter from the mining hill into the surrounding wetland and therefore potentially influences this ecosystem (Duffaut, 2001). Slag heap leaching in the Hauts-de-France mine region was initially studied to investigate the impact on groundwater quality (Denimal, 2001). More general studies on post-mining issues included studies on trace metal leaching (Allan, 1995), on Acid Mine Drainage (AMD) issues (Akcil and Koldas, 2006) or on nutrient levels and litter decomposition and their impact on the ecosystem (Lee and Bukaveckas, 2002). The AMD is a common effect of SH leaching which results from the oxidation of pyrite ( $\text{FeS}_2$ ) and produces an acidic leachate source for the environment (Rose and Cravotta III, 1998). Its consequences on aquatic environments such as wetlands are today still poorly studied, specifically in the Hauts-de-France mining area. Moreover, there is a

lack of knowledge on the link existing between biodiversity of these wetlands and the leaching inputs of the SHs into them.

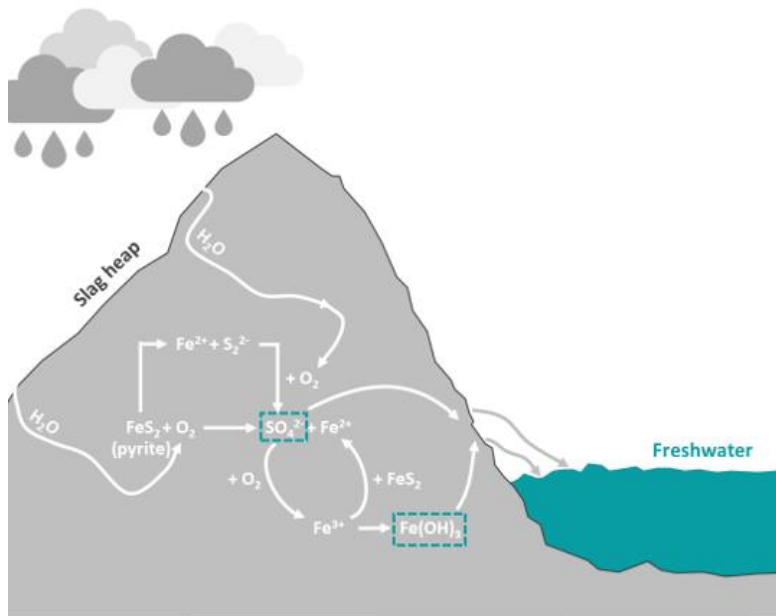


**Figure 2:** Overview of the slagheap leaching process (after Thompson, 2015)

Therefore, more studies must be carried out to better understand the diverse influences of SHs on surrounding wetlands and ponds. Invertebrates occupy a central place in aquatic ecosystems since they are ranked at the lower trophic levels of the food chain and they have a role both as consumer (phytoplankton, etc...) and food source (especially for fish and aquatic birds) (Benoit-Chabot, 2014). Information on their nature and quantity is therefore essential for assessing the ecological quality of wetlands at the bottom of slag heaps. Thus, the objectives of the present study are: (i) to establish a state of the art of the

physicochemical and biological composition of these atypical environments; (ii) to assess the possible influence of slag heap leaching on the surrounding aquatic ecosystem composition and distribution; and finally (iii) to investigate potential variation of these processes in time and in space.

## **2. Material and methods**

### **2.1. Study site**

Two slag heaps have been selected in agreement with the Northern France Department Council that had noticed recurrent patches of water leaching into the surrounding wetlands. They are both located close to the city of Douai and are called hereafter SH I and SH II (Figure 2). Both have the same tabular shape, but SH I was formed from 1958 to 1984 having a 97-ha surface, while the other one was formed between 1912 and 1975 having a surface of 140 ha (North Department Council, internal communication). The soil surrounding both SHs is mainly occupied by vegetation (agricultural land, woods and meadows) and by water bodies (waterways, ponds and wetlands). The water levels in the ponds and wetlands are relatively stable throughout the year, although they pass through seasonal low and high-water periods. Both SHs are surrounded by a complex network of ponds and wetlands which are fed by the outflow from the slag heaps (enriched in elements from the SH, *i.e.* leaching phenomena) by rainwater and groundwater.

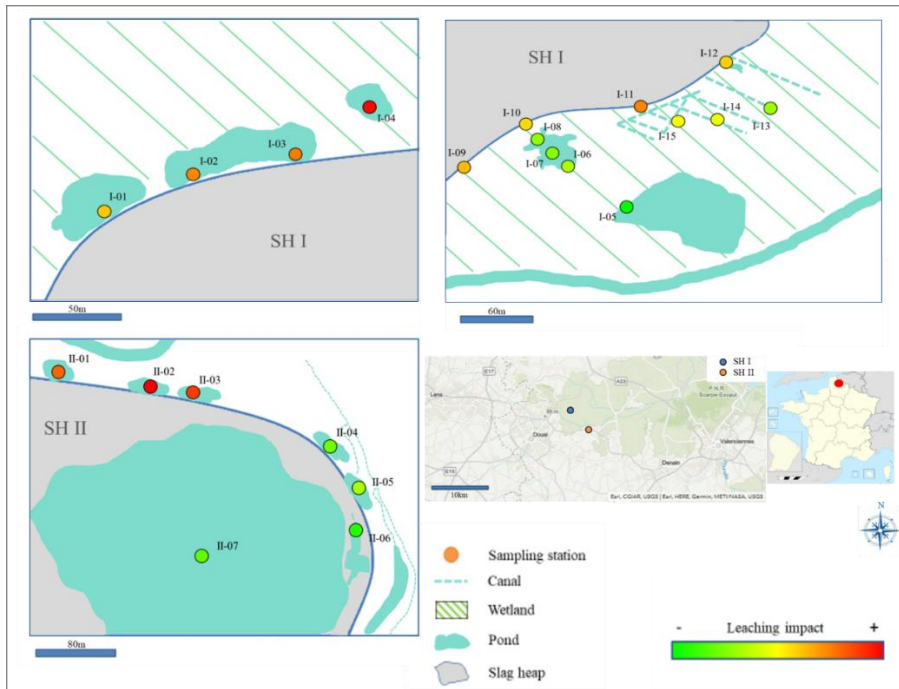


**Figure 2:** Sampling map for the two slag heaps: SH I and SH II, both close to the city of Douai. SH I is split into 2 distinct zones, which are separated by a significant distance: sampling points I-01 to I-04 are located on the West side of SH I, while points I-05 to I-15 are located on the East side. For confidentiality reasons, the name and aerial views of both slag heaps are not shown here.

Four very shallow and narrow ponds were sampled at the foot of the SH I (I-01 to I-04) and of the SH II (II-01 to II-06). At the foot of SH II, a deeper and bigger pond (24.5 hectares, 2m deep in average) is also present. Twenty stations were chosen in this pond, but since the results between those stations were not significantly different, only the average of the results is reported in this paper and referred to as station II-07. Finally, a screening of a wetland located in the southern part of SH I was also performed (I-05 to I-15), in order to investigate potential concentration gradients (Figure 2).



Close to a third SH (SH III), a non-impacted reference station, that is recurrently monitored by the Ecology service of the North Department Council, has also been chosen: reference point III-01. According to the internal reports of the Ecology service, the wetland close to SH III is protected from the leaching waters by a clay horizon, resulting in good water quality and good biodiversity indicators (nesting and feeding sites, presence of reed bed, helophytes, hydrophytes, clear water) (North Department Council, 2012). Note further that all GPS coordinates of the sampling points are listed in the supplementary information section.

Two sampling campaigns have been carried out, in order to study possible temporal changes occurring in the environment around the SHs. Each sampling campaign lasted less than 24 h, in order to avoid any influences from weather (rain, drought, etc.) or changes in groundwater levels. A first sampling campaign took place by the end of March 2016 at all 42 stations, including the reference point (III-01). A second one took place by the beginning of July 2016 but only at a few specific stations close to SH I (I-01 to I-04, I-09 to I-12). The second campaign was reduced compared to the first one mostly due to unforeseen events: hunting season and inaccessibility of the sites.

## **2.2. Sampling, *in situ* measurements and sample pre-treatments**

Temperature, pH, dissolved oxygen saturation and conductivity were measured *in situ* at each station using electrodes previously calibrated [pH: combined glass and Ag/AgCl/KCl electrodes (Metter-Toledo), dissolved oxygen saturation: Clark sensor (WTW, Oxi 340) and conductivity (WTW: ProfiLine Cond 3110)]. For the other parameters (alkalinity, anions, major elements, dissolved organic carbon and characterization of organic matter), water was sampled in a clean PFA bottle at about 20 cm depth (when possible)

below the surface. A first part of the sample remained unfiltered prior to the biological analysis and was kept at 5°C in an icebox. Back in the laboratory, the aquatic invertebrates were removed from the unfiltered water samples, using a 0.5 mm sieve; aquatic invertebrates were then placed into clean glass flasks, and 70% isopropyl alcohol was added to prevent organisms from decomposing and to avoid predation by higher trophic organisms. The second part of the sample was filtered immediately in the field through 0.45 µm pore size filters (cellulose acetate membranes, Sartorius) for the determination of all parameters, except organic matter. Three aliquots were subsequently prepared for measuring: (i) major elements by addition of 400 µl ultrapure HNO<sub>3</sub> (Fisher Scientific, Optima™); (ii) sulphides by addition of 10 µL of 2N zinc acetate [guaranteed AGR (Analytical Grade Reagents)] and 10 µL of 10<sup>-2</sup> M NaOH (AGR) solution in 10 mL of the sample to stabilize the analyte; and (iii) anions and alkalinity without any treatment but kept at 4°C in an icebox. The third part of the sample was filtered on a glass fibre filter (0.7 µm, Whatmann) previously pyrolyzed at 450°C for 24 hours. This aliquot was kept in the icebox for subsequent analyses of the organic carbon content.

## **2.3. Chemical analysis**

### **2.3.1. Sulphides**

The solution prepared in the field for sulphide measurements was treated by addition of ferric chloride and N,N-dimethyl-p-phenylenediamine oxalate solution to form the methylene blue complex. In order to eliminate the colour due to the presence of ferric ion in the solution, ammonium phosphate dibasic solution, used as a buffer, is added after 5 min to the last solution (Expertise Center in Environmental Analysis of Quebec, 2015). All the reagents were of analytical grade (AGR). The measurements were performed by spectrophotometry (Varian, Cary 300 Scan UV-Visible) at 664 nm. The

sulphide concentration was then determined by comparing the field sample result with that of a calibration curve, made in the same conditions as the field sample. The S(-II) standard mother solution was prepared under nitrogen atmosphere from  $\text{Na}_2\text{S}\cdot 9\text{H}_2\text{O}$  (Aldrich) and titrated before use by potentiometry with a  $\text{Cd}^{2+}$  standard solution, using a sulphide ion selective electrode (Orion) and a  $\text{Hg}/\text{Hg}_2\text{SO}_4$  reference electrode. The limit of detection of this technique was  $0.2 \text{ mg L}^{-1}$  and the relative standard deviation carried out on triplicates from several samples was better than 5 %.

### **2.3.2. Anions**

Sulphate, nitrate, chloride, phosphate and fluoride concentrations were assessed with ionic chromatography (Dionex, column Ion Pac AS18,  $4 \times 250 \text{ mm}$ ). The MagIC Net 3.1 software was used to process and calibrate the analysis. Limit of detections (LOD) were  $0.05 \text{ mg L}^{-1}$  for sulphate,  $0.01 \text{ mg L}^{-1}$  for nitrate,  $0.02 \text{ mg L}^{-1}$  for chloride,  $0.04 \text{ mg L}^{-1}$  for phosphate and  $0.01 \text{ mg L}^{-1}$  for fluoride. The relative standard deviation (RSD) carried out on several triplicate measurements was better than 10 % for all species.

### **2.3.3. Major Elements**

Elemental analyses of Ca, Fe, P, Mn, Mg, Na, Sr, K, Si and B were performed in the water samples by Inductively Coupled Plasma Atomic Emission Spectroscopy (ICP-AES, Varian, Vista Pro, axial view) after multi-elemental External calibrations. Limits of detections (LOD) were  $0.1 \text{ mg L}^{-1}$  for Ca,  $0.06 \text{ mg L}^{-1}$  for Fe,  $0.2 \text{ mg L}^{-1}$  for P,  $0.01 \text{ mg L}^{-1}$  for Mn,  $0.03 \text{ mg L}^{-1}$  for Mg,  $0.06 \text{ mg L}^{-1}$  for Na,  $0.01 \text{ mg L}^{-1}$  for Sr and  $0.1 \text{ mg L}^{-1}$  for K. The relative standard deviation (RSD) carried out on triplicates was better than 5% for all species.

#### **2.3.4. Alkalinity**

Automatic pH-metric titrations using 0.05 M HCl were carried out (Metrohm, model 848 Titrino Plus) to determine the alkalinity in our samples assuming that, according to pH values (between 6.9 and 8.5) and the other ions present (sulphate, chloride) in the solution, the measured alkalinity is related to the concentration of  $\text{HCO}_3^-$ . Indeed, at neutral pH,  $\text{HCO}_3^-$  is the dominant carbonate species and significant contributions of  $\text{CO}_3^{2-}$  and  $\text{H}_2\text{CO}_3$  only appear at pH levels greater than 9.0 or lower than 6.0, respectively (Tarvainen et al., 2005). The LOD of this technique is estimated at  $0.1 \text{ mg L}^{-1}$  (based on a sample volume of 10 mL, a titrant HCl solution at 0.05 M and 50  $\mu\text{L}$  stepwise acid additions) with a relative standard deviation of 5%.

#### **2.3.5. Dissolved Organic Carbon (DOC)**

DOC content was analysed using a TOC-meter (Shimadzu, TOC-VCSH), using the NPOC method (Non Purgeable Organic Carbon). An external calibration curve, using potassium hydrogenphthalate, was previously assessed. The LOD is  $0.2 \text{ mg C L}^{-1}$  with a RSD calculated on several triplicates, lower than 5 %.

#### **2.4. Biological analysis**

Two biological indicators (number of aquatic invertebrate taxa and total abundance of aquatic invertebrates) were determined at each station, using 1 L water samples. The aquatic invertebrates have been sorted and then identified through a binocular microscope, using the sight hunting method and determination keys to classify them in a taxonomic family (Tachet et al., 2010). The number of taxa is defined as a group of living beings (here, aquatic invertebrates) from the same family. The abundance was equal to the total number of aquatic invertebrates listed at each sampling station including all taxa.

## 2.5. Statistical procedures

Principal Component Analysis (PCA) were performed with the R data processing software ([www.R-project.org](http://www.R-project.org)) using two packages: Corrplot and FactoMineR. The analysis of the statistical distributions of the data showed that some parameters were not normally distributed (*i.e.* not following a Gaussian distribution). Spearman correlation and PCA on ranked data were then performed to improve the robustness of the statistical analysis.

## 2.6. External data

As the groundwaters were not sampled, external data were provided by the French Water Agency from the piezometers 903641, 902687 and 901551 located respectively in Marchiennes, Pecquencourt and Somain (see the Supplementary Information section for the GPS coordinates). These piezometers were selected, because of their proximity to the studied areas.

## 3. Results and discussions

### 3.1. General description

***pH and conductivity*** — pH values range from 6.9 to 8.5, including the reference station III-01 with a rather narrow distribution (see Table 1 and Supplementary Information for all data). The conductivity varies from 1.2 to 5.0 mS cm<sup>-1</sup> with a median value at 4 mS cm<sup>-1</sup> showing a large range of variations. These values, including III-01 (lowest value at 1.2 mS cm<sup>-1</sup>), are higher than those observed in the surrounding rivers (0.93 mS cm<sup>-1</sup> in average) and the groundwaters (0.88 mS cm<sup>-1</sup> in average) (Artois-Picardie Water Agency, 2017). This could be due to leaching processes which will be discussed later. But also, as indicated by the value of III-01, this could be due to the higher salt concentrations since evaporation occurs in these small ponds.

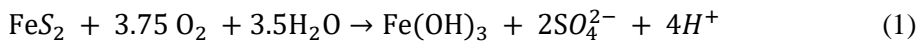
As no threshold values of good status for wetlands have been defined in the European Water Framework Directive, the criteria applied to rivers and ponds (Legifrance, 2015; Official Journal of the European Communities, 2000) was used in this study. Only six sampling points (I-05, II-07, II-04 II-05, II-06 and III-01) have a conductivity value below the threshold value of  $3\text{mS cm}^{-1}$  indicating that most of the waters are enriched in dissolved salts provided by the SH leaching.

**Table 1:** Overview of the water composition for the first campaign (March 2016)

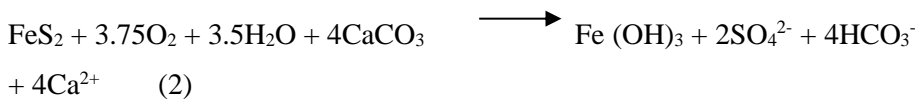
	min.	max.	mean	reference site III-01	groundwater
<i>In situ measurements</i>					
pH	6.9 (I-04)	8.5 (I-13)	7.7	7.7	7
Conductivity (mS cm <sup>-1</sup> )	1.2 (III-01)	5.0 (I-04)	3.6	1.2	0.88
Dissolved oxygen saturation (%)	9 (II-02)	140 (I-01)	75	98	25
<i>Alkalinity (mmol L<sup>-1</sup>)</i>					
Alkalinity	1.51 (II-06)	24.2 (I-10)	13.7	2.76	5.06
<i>Sulphides (mg L<sup>-1</sup>)</i>					
Sulphide	< 0.2	30 (II-01)	3.3	< 0.2	-
<i>Dissolved organic matter</i>					
DOC (mg C L <sup>-1</sup> )	1.6 (I-04, I-09)	25.1 (I-05)	8.6	7.5	1.6
<i>Major elements (mg L<sup>-1</sup>)</i>					
Ca	47 (I-05)	350 (II-03)	169	189	147
Mg	49 (I-05)	240 (II-03)	131	60	15
K	13 (I-05)	39 (II-03)	21	2.5	6
Sr	0.5 (I-05)	6.1 (II-02)	2.4	1.1	-
Mn	0.02 (II-06)	1.03 (II-03)	0.29	0.03	0.01
Fe	< 0.06	0.32 (II-04)	0.09	< 0.06	0.03
P	< 0.2	0.93 (II-02)	0.26	< 0.2	-
Na	41 (II-04)	480 (I-04)	307	55	25
<i>Anions (mg L<sup>-1</sup>)</i>					
NO <sub>3</sub> <sup>-</sup>	< 0.50 (I-12, II-06)	0.95 (II-05)	0.68	< 0.50	5
PO <sub>4</sub> <sup>3-</sup>	< 0.10	1.17 (II-01)	0.26	0.80	0.03
F <sup>-</sup>	< 0.01	0.31 (II-05)	0.13	0.21	0.17
SO <sub>4</sub> <sup>2-</sup>	899 (I-05)	2693 (II-03)	1732	979	128
Cl <sup>-</sup>	8.1 (I-09)	26.6 (I-05)	15.0	27.1	27.1

**Sulphates, cations and alkalinity** — Concentrations of sulphate are diverse and range between 900 and 2690 mg L<sup>-1</sup> exceeding significantly the bad-status threshold of the WFD (250 mg L<sup>-1</sup>). These concentrations were also compared to surrounding groundwaters with an average value of 128 mg L<sup>-1</sup> (Artois-Picardie Water Agency 2017) (no available data for rivers surrounding). At stations I-01, I-02, I-04, II-01, II-02 and II-03, the sulphate content exceeds 2000 mg L<sup>-1</sup>, while only at the reference station (III-01) and at the most remote station of SH I (I-05) sulphate concentrations are below 1000 mg L<sup>-1</sup>.

High sulphate levels are a typical characteristic of SH leaching due to the oxidation of several sulphide minerals like pyrite (Rose and Cravotta III, 1998). When rainwater (oxygenated and with a slightly acidic pH around 5-6) or eventually water from a superficial aquifer encounters the iron sulphide minerals present in the SH, oxidation processes take place allowing the release of H<sup>+</sup>, sulphates and Fe (III). The complete oxidation reaction involved is shown in Equation 1 (Denimal, 2001):



In our case, pH values remain quite neutral and dissolved iron concentrations are low. Indeed, iron levels range from < 0.06 (LOD) to 0.32 mg L<sup>-1</sup>. This differs from a classic Acid Mine Drainage (AMD) and is called a neutralized AMD (nAMD) (Rose and Cravotta III, 1998). The neutral pH results from the presence of carbonate compounds in the soils (*i.e.* chalks) that buffer the leaching water (*e.g.* calcium carbonate in Equation 2).

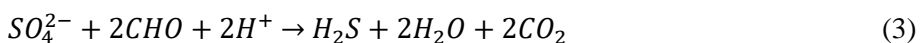


Concentrations of calcium, magnesium, potassium, strontium, manganese and sodium vary from 47 to 350 mg L<sup>-1</sup> (Ca), 49 to 240 mg L<sup>-1</sup> (Mg), 13 to 39 mg L<sup>-1</sup> (K), 0.50 to 6.1 mg L<sup>-1</sup> (Sr), 0.02 to 1.0 mg L<sup>-1</sup> (Mn) and 41 to 480 mg L<sup>-1</sup>



(Na), showing a wide range of variation and with several values exceeding largely those found at the reference site and in the surrounding groundwater, see Table 1 (no available data for the surrounding rivers). High concentrations of these elements can also be due to slag heap leaching followed by carbonate buffering (nAMD) (Monterroso and Macias, 1998).

A large range of alkalinity values, from 1.51 (II-06) to 24.2 mmol L<sup>-1</sup> (I-10), are observed with several values exceeding largely those found at the reference site III-01 (2.76 mmol L<sup>-1</sup>) and in the surrounding groundwater (5.06 mmol L<sup>-1</sup> in average) (no available data for the surrounding rivers). Besides carbonates at circumneutral pH, alkalinity can also include other chemical species such as bisulphide, silicates, borates and phosphates. After quantification of phosphates, of total Si and of B, it is justified to say that, except for station II-01 where sulphides are found at high concentrations (0.9 mmol of sulphides for 2.2 mmol of alkalinity), alkalinity is primarily composed of hydrogen carbonates. Hydrogen carbonate concentration could result from the neutralisation of the AMD, especially at SH II where a significant correlation is observed between alkalinity, sulphate and major cations coming from the leaching (Figure 3). However, for SH I, alkalinity is not correlated with the released species, which can be due to several reasons. Firstly, Rose and Cravotta III (1998) described several neutralisation processes without affecting alkalinity. The acidity can indeed be neutralised by dissolution of FeCO<sub>3</sub> or silicate minerals in which case alkalinity is not affected. Secondly, in SH I and to lesser extent in SH II, the reduction of sulphates by Sulphate Reducing Bacteria (SRB) will consume protons and simultaneously produce gaseous H<sub>2</sub>S (Equation 3; Wu et al., 2013).



As the dissolved organic carbon concentrations are generally higher in SH I

than in SH II, the bio-reduction of the sulphates may be favoured at SH I, with, as a consequence, the increase in alkalinity and a poorer correlation between alkalinity and the other slag heap leaching markers. Thirdly, the non-correlation between alkalinity and the released species may also be linked to other phenomena like photosynthesis and aerobic respiration, consuming either  $\text{NO}_3^-$  or  $\text{NH}_4^+$  (Stumm and Morgan, 1996). Precipitation of various solid phases, such as metal sulphides or evaporation when the water level is low, can cause alkalinity changes too.

**Anions and DOC** — Nutrient concentrations ( $\text{NO}_3^-$  and  $\text{PO}_4^{3-}$ ) are possible eutrophication indicators in aquatic environments. Nitrate levels range from  $< 0.01$  to  $0.95 \text{ mg L}^{-1}$ , which is low compared to the surrounding waterbody averages ( $5 \text{ mg L}^{-1}$  for groundwaters,  $31 \text{ mg L}^{-1}$  for rivers) and to the WFD threshold value of  $10 \text{ mg L}^{-1}$ , definition for a “very good state of water”. Phosphate exhibits very low concentration levels, mostly under the detection limit of  $0.04 \text{ mg L}^{-1}$ . Except for a few stations, most of them display phosphate levels below the detection limit. Overall, the impact of urban and agriculture activities on our study sites are limited and do not favour eutrophication processes in the ponds and wetlands.

Fluorides and chlorides can have adverse effects on terrestrial aquatic ecosystems when present at high concentrations (Elphick et al., 2011; United States Geological Survey, 2009).  $\text{F}^-$  levels range from  $< 0.01$  to  $0.31 \text{ mg L}^{-1}$ , which comply with the average content of the surrounding groundwater ( $0.17 \text{ mg L}^{-1}$ ) and are below the threshold value of  $0.5 \text{ mg L}^{-1}$  above which  $\text{F}^-$  has been shown to affect aquatic organisms (Camargo, 2003).  $\text{Cl}^-$  concentrations are low (between  $8.1$  and  $26.6 \text{ mg L}^{-1}$ ) and below the groundwater and III-1 levels ( $27.1 \text{ mg L}^{-1}$ ) and the WFD threshold value of  $50 \text{ mg L}^{-1}$  (Official Journal of the European Communities, 2000).

DOC concentrations range from 1.6 to 25.1 mg C L<sup>-1</sup> with the lowest values at stations I-04 and I-09 and all stations of SH II. At the other SH I stations and at the reference station III-01 (7.5 mg C L<sup>-1</sup>), the threshold value as defined by the WFD (5 mg C L<sup>-1</sup>) is exceeded. However, the WFD threshold value for DOC must be handled with caution, because these reference values were originally determined to qualify the state of a water mass (lake, river, etc.), while we are here dealing with wetlands which are, by definition, rich in vegetation and thus in DOC. In a wetland, the WFD threshold value of DOC can be easily exceeded. The highest DOC concentrations were recorded at I-05, I-08 and I-13 with values above 15 mg C L<sup>-1</sup>, corresponding to a bad status of water bodies. As SH II is far less vegetated than SH I, it is not surprising to find lower DOC values in SH II. This observation can mainly be explained by the difference in age and maturity of both systems. In addition, vegetation maintenance is better in SH II than in SH I where vegetation overgrowth creates obstacles in the water runoff. Finally, as reported by Lee and Bukaveckas (2002), wetlands impacted by mine drainage usually show slower decomposition rates and lower nutrient levels in comparison to wetlands found in predominantly agricultural areas (Lee and Bukaveckas, 2002).

***Oxygen, sulphides and total P*** — Dissolved oxygen saturation ranged from 9 to 140% with an average of about 75%. There is, therefore, a wide range of variation with very high values at some locations (I-01, 02, 03, 05, 09, 12, II-03, 05, 06 and III-01 > 90%) and very low at the surface, even anoxic at the bottom, of others (I-01, 04, II-02 < 30%). Sulphide concentrations were only detected in these three anoxic stations. Total dissolved phosphorus concentrations also seemed to be linked to dissolved oxygen concentration. Varying from < 0.2 to 0.93 mg/L, the variation in phosphate was negatively correlated to that in O<sub>2</sub>. It has been observed that in hypoxic or anoxic conditions, the reduction of iron oxides can lead to the release of phosphates

in the water that were previously trapped in these oxides (Patrick and Khalid, 1974).

**Biological analysis** — The biological inventory highlighted the presence of several aquatic invertebrate families. Sixteen families of species, spread over all sampling stations, have been identified and quantified (Table 2), with as the most important, *Cyclops sp*, *Chydoridae* and *Daphniidae*.

The poorest biodiversity levels were observed at SH II stations II-01 and II-02 (respectively, 0 and 1 for the taxon, 0 and 13 for the abundance), where oxygen levels were low and sulphide concentrations high, exceeding 24 mg L<sup>-1</sup>. Station II-03 showed the highest biodiversity level with 3 taxa and an abundance of 39 individuals. At this station oxygen levels were high, sulphide was not detected, and the highest levels of Ca, K, Mg, Mn and sulphates were observed.

At SH I, the biodiversity wealth seems higher than at SH II: the total number of taxa is 8 (I-01) and the total abundance 288 (I-08). However, large differences between the sampling stations can be observed. The lowest biodiversity levels are observed at stations I-04 and I-05 (respectively, 0 and 2 for the taxon, 0 and 14 for the abundance), the highest levels at I-01 and I-08.

**Table 2:** Overview of the biological diversity in the water samples. The number of aquatic invertebrates collected in 1 L of water is shown.

Taxonomic group	SH I															SH II					SH III		
	01	02	03	04	05	06	07	08	09	10	11	12	13	14	15	01	02	03	04	05	06	01	
<i>Cyclops sp</i>	69	61	35		13		8	65	28	13	62	12	10	16	7		13	20	19			8	
<i>Diaptomus sp</i>																						10	
<i>Orthocladinae</i>						2		3															
<i>Chironominae</i>	1		2																	3			
<i>Ceratopogonidae</i>	3					3																	
<i>Culicidae</i>					1																		
<i>Chydoridae</i>	30	8						30	15	11	21	12	40	30	11		8		10	6	5		
<i>Daphniidae</i>	62	165	88			80	140	181	33	15	40		61	40	24		11			10	6		
Nematode																				3			
<i>Cyphon sp</i>								1															
<i>Hydrophilus sp</i>												1											
<i>Graptodytes sp</i>	2																						
Collembola	1																						
<i>Rotifera</i>											6												
Ostracode						1		8	2	2	2			7									
<i>Driops sp</i>	1																						
Total taxon	8	3	3	0	2	4	2	6	4	4	5	3	3	4	3	0	1	3	1	3	3	3	
Total abundance	169	234	125	0	14	86	148	288	78	41	131	25	111	93	42	0	13	39	19	16	26	19	

Aquatic invertebrate species, also those found here, can be used as bio-indicators of their environment (e.g. Health Monitoring Institute, 2004; Hodgkinson and Jackson, 2005). For instance, *Cyclops sp* (found at all stations except I-04, 06, II-01, 05, 06) and *Diatomus sp* (found only at II-06) are invertebrate species known for their tolerance to wastewater but also to eutrophication processes. More specifically, *Chironominae* (stations I-01, 03 and II-05), *Ceratopogonidae* (stations I-01 and I-06), *Culicidae* (I-05) and *Nematode* (II-05) are bio-indicators of organic or chemical polluted waters as they are tolerant to such environmental conditions. On the contrary, *Hydrophilus sp* (only found at station I-12) is a species which is sensitive to water pollution by organic matter and chemicals. *Rotifera* (I-11) is sensitive to salinity, while *Ostracode* (stations I-06, 08, 09, 10, 11, 14) can tolerate salinity but it is sensitive to organic matter, industrial and metal-mining pollution (David M. Rosenberg and Resh, 1993). The salinity resistance of the *Ostracode* family as well as the high alkalinity and the relatively low leaching impact at stations I-06, 08, 09, 10, 11, 14, allowed them to develop there.

### **3.2. Lixiviation influence**

When looking at the results from the PCA (see Fig. 3 – A and C), the first axis with the most variance (PC1 with almost 50% of the data variability) fits well with the lixiviation process. For both sites taken separately, sulphates, major cations, conductivity are close on the right side of PC1. On the opposite side of the PC1 axis, the chlorides are found for both sampling sites (Fig. 3 – A and C) and the DOC is found only at SH I (Fig. 3 – A). These elements are both indicators of non-impacted waters (or less impacted) from the slag heap. A gradient of these two sources is indicated in Figure 3: the first principal component represents the mixing of lixiviates (positive part) and lake water (negative part). The distribution of the points on Fig. 3B gives the relative

importance of the two sources for each station. We notice that the “cleanest” stations are in the lakes (I-05 and II-07) and several nearby stations.

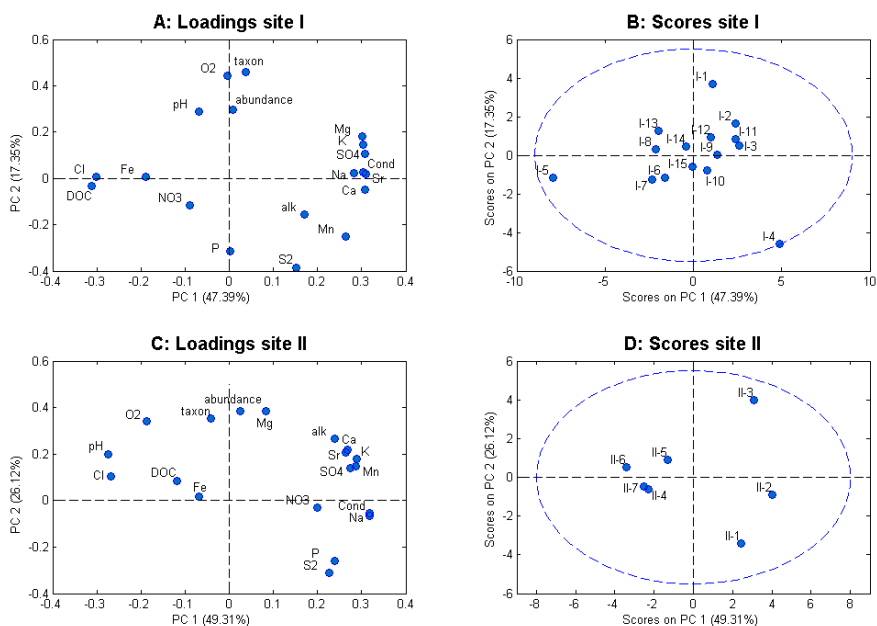


**Figure 3:** PCA results for site I (A and B) and site II (C and D). Samplings performed in March 2016. On site I: A, loadings on the 2 first components and B, scores of the different stations on the same axes. On site II: C and D, same as for site I. S2 represents the sulphides.

The leaching of the slags influences the water composition at the foot of the two SHs. Indeed, sulphates, Ca, Sr, Mg, Na and to a lesser extent alkalinity are correlated at both sites, indicating that all these elements are probably solubilised simultaneously during the leaching process. However, the average composition of the leaching solution after normalization by the sulphate concentration varies between the 2 SHs as indicated in Table 3. From this

table, it is clear that there exists a supplementary mineral phase supplying dissolved sodium and carbonate during the leaching or neutralization process at site I. However, at site II, a slight increase in the amounts of calcium and strontium can be noticed. The two sites being only 2 km apart, such a difference was surprising. However, it appears that the two slag heaps have different histories. SH I is a relatively recent “washing slag heap”, which was build up between 1950 and 1984 and contains fine particles. SH II is a more historical one (1912-1975), containing a lot of coal and a larger size of slags. In 1975, the remaining coal was extracted from these slags with a washing process and the residues were thereafter redeposited at the same place. Since the mineral composition of the soil between the two sites is different, the lixiviates composition varies as well. It may explain why for SH II, most dissolvable salts, *e.g.* the sodium carbonate phase, may already have been leached.

**Table 3:** Sulphate-normalised average concentrations of total dissolved Ca, K, Mg, Na, Sr and alkalinity. \* and \*\* indicates the significance of the ratio difference between site I and site II with a 5% and 1% error respectively.

	SH I	SH II	
Sulphates	1	1	
Ca	0.21	0.26	*
Alkalinity	1.1	0.21	**
K	0.031	0.029	
Mg	0.29	0.33	
Na	1.0	0.26	**
Sr	0.0013	0.0019	**



### 3.3. Hypoxia

Hypoxia or even anoxia has been observed at several sampling sites. This could be due to a complete consumption of dissolved oxygen for the oxidation of organic matter in the small ponds, which are full of vegetal debris. It is also possible that some water leaching from the SH was yet anoxic as all the oxygen was used for pyrite re-oxidation. This is partly supported by the fact that only stations very close to the SH were found with low O<sub>2</sub> concentration and sulphides.

When all oxygen is consumed, anaerobic respiration leads to the reduction of iron oxides and concomitantly the release of P and the reduction of sulphates. The pH also slightly decreases due to the release of CO<sub>2</sub> from oxidised organic matter (Seybold et al., 2002). On the PCA in SH I (Fig. 3A), O<sub>2</sub> and pH are close to each other on the positive part of PC2, but opposite to P and sulphides on the same axis. This is mainly true for SH I. If for SH II the opposition between pH / O<sub>2</sub> and P / sulphides is still visible, it is not as clear as on the second principal component PC2. This lack of complete orthogonality could be the sign of a link between hypoxia and lixiviation on SH II (*e.g.* anoxic lixiviates).

### 3.4. Chemistry and biodiversity

It seems that for SH I, as it is indicated on Fig. 3.A, lixiviation from the SH and the biological diversity are unrelated. No decrease of the taxon and of the abundance is found along the lixiviation gradient. Lixiviation and aquatic invertebrate diversity and abundance seem orthogonal. Hypoxia seems to influence the invertebrate distribution much more ( $R = 0.61$  and  $0.55$  respectively for O<sub>2</sub> vs taxon and for O<sub>2</sub> vs abundance for all campaigns). The lack of oxygen is very damaging, as it goes pair with the emerging sulphides.

The toxicity of sulphides depends on the species, the exposure time and its concentration. Sulphides mainly interfere with respiration metabolism: levels reaching  $\mu\text{g L}^{-1}$  levels will affect the whole aquatic organism, but concentrations at the  $\text{ng L}^{-1}$  level are, for instance, enough to impact enzyme functioning like the cytochrome c oxidase which is a transmembrane protein complex and part of the respiratory electron transport chain of eukaryotes including aquatic invertebrates (Castresana et al. 1994). As a competitive inhibitor of the cytochrome c oxidase enzyme, excessive levels of sulphide can lead to cell asphyxia (Grieshaber and Völkel, 1998; Nicholls et al., 2013). Overall, the appearance of sulphides was shown to amplify hypoxia effects (Bagarinao, 1993). The impact and diffusion of sulphide through a cell is also directly proportional to the  $\text{H}_2\text{S}$  concentration in the solution. Indeed,  $\text{H}_2\text{S}$  can easily cross membranes, whereas the hydrogen sulphide  $\text{HS}^-$  may be electrically excluded. Nevertheless,  $\text{HS}^-$  can still contribute to toxicity at high concentration (Beauchamp et al., 1984).

For SH II, the quality also depends strongly on the dissolved oxygen concentration ( $R= 0.90$  and  $0.77$  respectively for  $\text{O}_2$  vs taxon and for  $\text{O}_2$  vs abundance). However, as it has been seen before for this site, hypoxia and lixiviation may not be as independent as it is observed for SH I. Lixiviation from the heap may be indirectly responsible for the lack of invertebrates.

### **3.5. Temporal variability**

In July 2016, eight stations from the first campaign were sampled again: I-01, 02, 03, 04, 09, 10, 11 and 12. Figure 4 compares these results to the ones obtained in March showing the change in wetland composition between these two seasons.

The concentrations of Ca, K, Mg, Mn, Na and Sr drastically decreased for all stations between March and July: a 30% to 70% decrease is systematically recorded (Mg and Sr behaviour is the same as Ca; see Supplementary Information for complete data set). As previously mentioned, these elements are usually carried together with sulphate during the leaching process. However, sulphate concentrations do not really change with time. Complex geochemical processes such as dissolution of gypsum, precipitation reactions of alkaline earth elements with a high amount of carbonates, water exchange between overlying and groundwater must have been involved.

These phenomena must have been induced by a lack of precipitation, leaching, temperature increase or water evaporation in the small ponds.

A general decrease of dissolved oxygen saturation and pH, coupled to an increase of alkalinity, was noted. This could indicate that the respiration process exceeded the primary production in these ponds. Indeed, the low water level, the high amount of sediments and particulate organic matter from the microphytes and tree leaves (based on field observations) seem to accelerate the degradation process when the temperature raises. In parallel, the sulphide concentrations increased at station I-03 and I-12 and decreased at stations I-04 and I-10. We therefore suppose that the reduction of sulphates into sulphides has not been intensified by the increase in temperature and the pluviometry decline. Regarding biodiversity, the number of taxa decreased except at I-09, as well as the abundance except at I-09, I-10 and I-11. Therefore, it seems that the decrease of the biodiversity is linked to degradation processes of organic matter caused by the activity of micro-organisms. These processes reduce the dissolved oxygen concentration and may produce micro-niches of high dissolved sulphide concentrations. This biogeochemical evolution could therefore lead rapidly to an eutrophication of the water system (Science for Environment Policy, 2015).

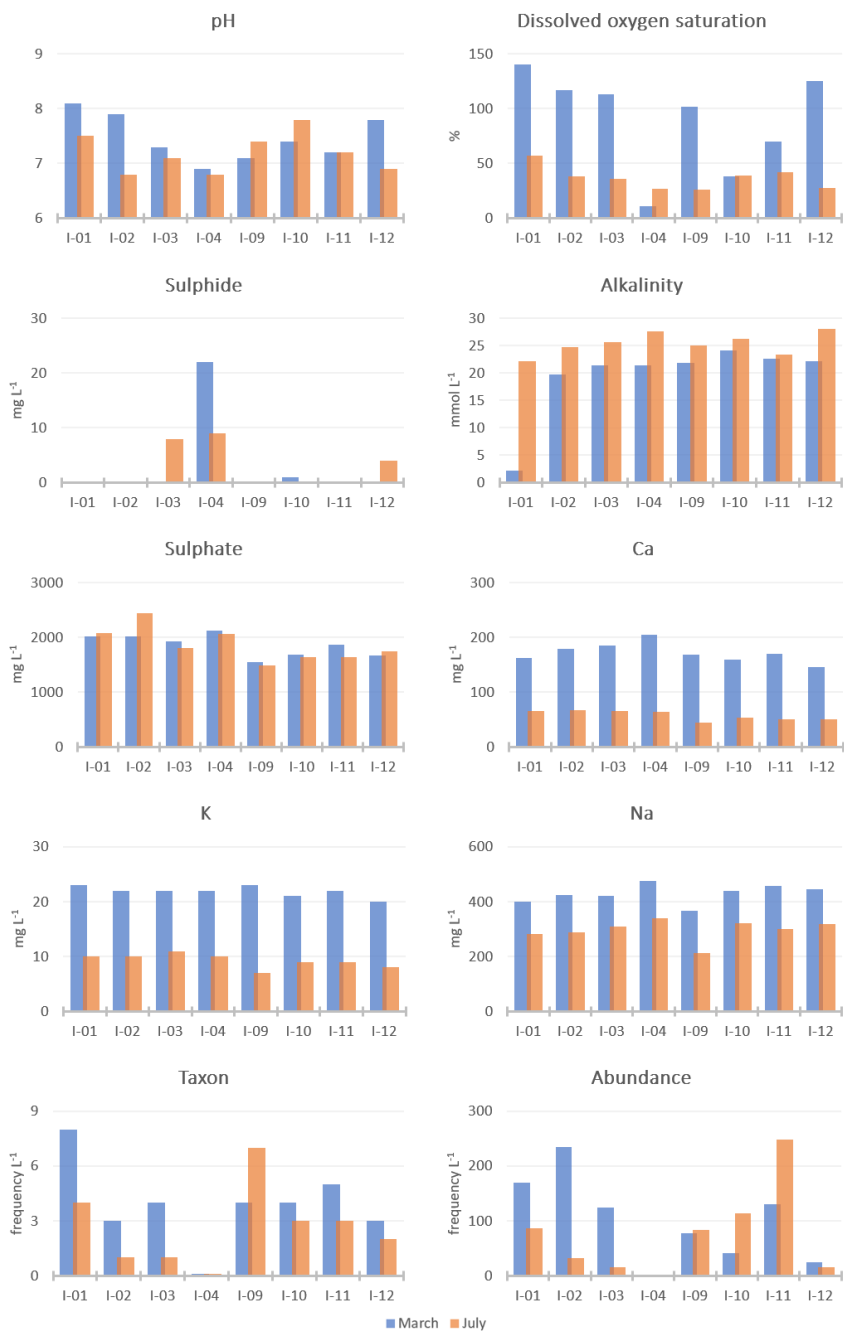


**Figure 4:** Temporal evolution of the wetland composition between March and July 2016.

#### 4. Conclusion

This study was conducted with the aim of assessing the potential influence of slag heap leaching on the surrounding aquatic environment, in the Hauts-de-France region. We endeavoured to determine the existence or the absence of a link between the chemical composition of surface waters and the biodiversity distribution of each studied zone. One of the main findings relates to the presence of sulphates, which are the first indicators of a mining waste leaching. These sulphate concentrations, which are far above the surrounding background concentrations, are the results of pyrite oxidation contained in the slag heaps soil. Most of the studied areas are enriched in dissolved salts provided by the SH leaching. More precisely, the composition of the water around the two slag heaps reveals a typical example of a neutralized acid mine drainage, with a clear neutral pH and low Fe levels. This was especially confirmed by the presence of carbonate compounds from the soils, high enough to buffer the leaching waters, and by the high concentrations of many typical sub-products of such SH leaching (Ca, Mg, K, Mn, Na). At three sampling stations, located very close to the SH, a reduction of sulphate to sulphide coupled with anoxia and with phosphate release has been evidenced. This phenomenon might be amplified in the case of high amounts of organic matter. According to our results, this has led to a decrease in composition and distribution of aquatic invertebrates, thus in biodiversity. Most likely, the appearance of sulphides (partially under  $H_2S$ ) intensifies the impact of hypoxia in such ecosystems. Nevertheless, it is difficult to predict whether the ecological imbalance observed at these sampling stations constitutes an isolated case or if it is an indication of what would happen in future on a larger scale in the rest of the wetlands. Despite these three cases, the invertebrate inventories generally reveal a good biodiversity richness at most of the studied areas: this was mainly linked to good oxygenation conditions of the aquatic

environment and to the absence of sulphide. At these stations no influence from SH lixiviation was noticed. From March to July, increasing temperatures coupled with a pluviometry decline do not seem to promote sulphate reduction into sulphide. Even though dissolved oxygen and pH tend to be lower in Summer. Furthermore, loss of biodiversity in July seems only to be related to low dissolved oxygen levels, resulting from higher degradation rates of organic matter by micro-organisms. However, the latter processes may cause, if not controlled and managed, rapid eutrophication of the ecosystem. Finally, the same leaching signature (high sulphate levels, nAMD) is observed in the aquatic environments surrounding both SHs. However, due to a difference in age and maturity between the two SH systems and, to a lesser extent, to a difference in vegetation maintenance, some variations were highlighted, especially regarding DOC levels and the lixivate composition (explained by an historical difference in the SH treatment process).

In future, it would be crucial to continue a scrutiny and scientific monitoring of these very particular and fragile wetlands (including sediments and micro-organisms), especially to better understand their evolution over time during low and high-water periods and during seasonal changes. In addition, monitoring the water fraction migrating to groundwater reserves located beneath the slag heaps would be welcomed as a complementary research approach. Finally, from an operational point of view, it would be necessary to propose remediation actions to prevent possible harmful effects on these wetlands. For instance, more vegetation maintenance around the area and/or the use of pumps could be interesting levers, in order to guarantee a better water circulation, as it was the case in the past during the exploitation of the coalmines.

### **Acknowledgments**

The North Department Council (France) is warmly acknowledged for the funding of this study. We greatly appreciated the collaboration with Virginie Callipel (belonging to the North Department Council) and the Artois-Picardie French Water Agency for access to their databases. Justine Stourbe is also thanked very much for her work on the invertebrates counting, as well as Véronique Alaimo and David Dumoulin for their technical support.

## 5. Supplementary Information

### 5.1. Material and methods

#### 5.1.1. Study site

**Table S1:** GPS coordinates of the sampling points

Sampling code	GPS Coordinates	
	Latitude	Longitude
<b>I-01</b>	N 50.39439°	E 003.19151°
<b>I-02</b>	N 50.39467°	E 003.19230°
<b>I-03</b>	N 50.39486°	E 003.19319°
<b>I-04</b>	N 50.39519°	E 003.19366°
<b>I-05</b>	N 50.39048°	E 003.20417°
<b>I-06</b>	N 50.38940°	E 003.20069°
<b>I-07</b>	N 50.38957°	E 003.20047°
<b>I-08</b>	N 50.38962°	E 003.20028°
<b>I-09</b>	N 50.39050°	E 003.20316°
<b>I-10</b>	N 50.39028°	E 003.20272°
<b>I-11</b>	N 50.39003°	E 003.20162°
<b>I-12</b>	N 50.39044°	E 003.20306°
<b>I-13</b>	N 50.38996°	E 003.20390°
<b>I-14</b>	N 50.38994°	E 003.20295°
<b>I-15</b>	N 50.38985°	E 003.20285°
<b>II-01</b>	N 50.38683°	E 003.24150°
<b>II-02</b>	N 50.38626°	E 003.24454°
<b>II-03</b>	N 50.38600°	E 003.24605°
<b>II-04</b>	N 50.38461°	E 003.25169°
<b>II-05</b>	N 50.383550°	E 003.25289°
<b>II-06</b>	N 50.38294°	E 003.25260°
<b>II-07</b>		
<b>II-07-01</b>	N 50.38171°	E 003.24990°
<b>II-07-02</b>	N 50.38396°	E 003.24387°
<b>II-07-03</b>	N 50.38417°	E 003.24553°
<b>II-07-04</b>	N 50.38414°	E 003.24681°



<b>II-07-05</b>	N 50.38512°	E 003.24878°
<b>II-07-06</b>	N 50.38497°	E 003.25063°
<b>II-07-07</b>	N 50.38412°	E 003.25157°
<b>II-07-08</b>	N 50.38318°	E 003.25241°
<b>II-07-09</b>	N 50.38206°	E 003.25223°
<b>II-07-10</b>	N 50.38113°	E 003.25257°
<b>II-07-11</b>	N 50.38040°	E 003.25199°
<b>II-07-12</b>	N 50.37934°	E 003.25121°
<b>II-07-13</b>	N 50.37870°	E 003.24980°
<b>II-07-14</b>	N 50.37860°	E 003.24820°
<b>II-07-15</b>	N 50.37939°	E 003.24708°
<b>II-07-16</b>	N 50.38095°	E 003.24733°
<b>II-07-17</b>	N 50.38141°	E 003.24751°
<b>II-07-18</b>	N 50.38160°	E 003.24693°
<b>II-07-19</b>	N 50.38210°	E 003.24543°
<b>II-07-20</b>	N 50.38326°	E 003.24370°
<b>III-01</b>	N 50.402926°	E 003.116132°

### 5.1.2. External data

**Table S2:** GPS coordinates of the piezometers

<b>Piezometers</b>		
<b>903641</b>	50°25'12.6592" N	3°17'4.9369" E
<b>902687</b>	50°23'22.9132" N	3°12'44.2760" E
<b>901551</b>	50°22'36.9037" N	3°17'1.8204" E

## 5.2. Results and discussions

### 5.2.1. General description

**Table S3:** Dataset from the first campaign

Station	pH	Diss. oxygen sat.	Conductivity	Sulphide	Nitrate	Phosphate	Fluoride	Chloride	Sulphate	Alkalinity	Diss. Org. Carbon
-	%		<i>mS cm<sup>-1</sup></i>	<i>mg L<sup>-1</sup></i>	<i>mg L<sup>-1</sup></i>	<i>mg L<sup>-1</sup></i>	<i>mg L<sup>-1</sup></i>	<i>mg L<sup>-1</sup></i>	<i>mg L<sup>-1</sup></i>	<i>mmol L<sup>-1</sup></i>	<i>mg C L<sup>-1</sup></i>
I-01	8.1	140	4.1	<LOD	0.83	<LOD	<LOD	16.7	2018	2.2	7.5
I-02	7.9	117	4.3	<LOD	0.84	<LOD	<LOD	10.1	2013	19.7	6.1
I-03	7.3	113	4.5	<LOD	0.85	<LOD	<LOD	10.2	1925	21.4	5.8
I-04	6.9	11	5.0	22	0.84	<LOD	<LOD	9.8	2119	21.4	4.8
I-05	7	94	1.8	<LOD	0.92	0.84	0.25	26.6	899	2.6	25.1
I-06	7.9	40	3.6	<LOD	0.89	0.68	0.28	17.7	1470	21.8	14.0
I-07	8	42	3.6	<LOD	0.78	0.92	0.18	14.9	1293	16.3	14.4
I-08	8.1	57	3.5	<LOD	0.83	0.82	0.30	18.0	1419	20.5	16.6
I-09	7.1	102	3.9	0.1	0.77	<LOD	0.20	8.1	1547	21.8	4.2
I-10	7.4	38	3.8	0.6	0.75	<LOD	<LOD	12.3	1688	24.2	8.5
I-11	7.2	70	4.1	<LOD	0.10	<LOD	<LOD	11.3	1861	22.6	7.6
I-12	7.8	125	4.4	<LOD	<LOD	<LOD	<LOD	11.1	1662	22.1	11.0
I-13	8.5	98	4.2	<LOD	0.77	<LOD	<LOD	16.3	1604	20.3	18.8
I-14	8.1	65	4.0	<LOD	0.76	<LOD	<LOD	15.1	1648	20.4	13.3
I-15	8	42	4.1	<LOD	0.76	<LOD	<LOD	14.5	1501	23.3	12.2
II-01	7	20	4.5	30	0.89	1.17	<LOD	10.4	2277	2.2	1.6
II-02	7.3	9	4.4	24	0.84	0.73	0.30	10.8	2117	8.6	3.7
II-03	7.6	103	4.0	<LOD	0.84	<LOD	0.24	12.9	2693	10.8	2.6
II-04	7.8	66	2.2	<LOD	0.77	<LOD	0.28	18.2	1866	3.5	2.7
II-05	7.8	98	2.9	<LOD	0.95	<LOD	0.31	18.7	1847	3.4	2.4
II-06	8.3	94	2.1	<LOD	<LOD	<LOD	0.20	14.9	1579	1.5	4.1
II-07	8.1	82	2.1	<LOD	0.56	<LOD	0.22	18.1	1811	3.0	3.9
III-01	7.7	98	1.2	<LOD	<LOD	0.80	0.21	27.1	979	2.8	7.6

**Table S3:** Dataset from the first campaign (continued)

Station	Ca	Fe	K	Mg	Mn	Na	P	Sr	Taxon	Abundance
	<i>mg L<sup>-1</sup></i>	<i>mg L<sup>-1</sup></i>	<i>mg L<sup>-1</sup></i>	<i>mg L<sup>-1</sup></i>	<i>mg L<sup>-1</sup></i>	<i>mg L<sup>-1</sup></i>	<i>mg L<sup>-1</sup></i>	<i>mg L<sup>-1</sup></i>	<i>in 1 L of water</i>	<i>in 1 L of water</i>
I-01	162	0.10	22.9	148	0.23	401	<LOD	2.5	8	169
I-02	179	<LOD	22.2	135	0.21	423	<LOD	2.7	3	234
I-03	185	0.07	21.7	129	0.38	420	0.23	2.8	4	125
I-04	204	<LOD	22.2	137	0.66	477	0.48	2.8	0	0
I-05	47	0.10	13.1	49	0.02	225	<LOD	0.5	2	14
I-06	140	0.12	19.5	104	0.15	378	0.69	1.7	3	86
I-07	133	0.13	17.3	97	0.15	355	0.73	1.6	2	148
I-08	115	0.10	19.4	106	0.13	367	0.62	1.4	4	288
I-09	168	0.12	22.7	142	0.30	366	0.37	2.1	4	78
I-10	160	0.09	21.4	115	0.19	439	0.38	2.1	4	41
I-11	170	<LOD	21.9	142	0.23	456	0.22	2.2	5	131
I-12	145	0.08	20.0	127	0.21	444	<LOD	1.9	3	25
I-13	67	0.10	19.6	116	0.05	432	<LOD	1.0	3	111
I-14	132	0.10	20.4	122	0.14	428	0.27	1.7	4	93
I-15	147	0.12	21.0	125	0.19	434	0.35	1.9	3	42
II-01	182	<LOD	25.4	135	0.55	246	0.65	2.8	0	0
II-02	329	0.08	34.0	150	0.89	281	0.93	6.1	1	13
II-03	346	0.08	38.5	240	1.03	214	<LOD	6.0	3	39
II-04	161	0.32	13.7	126	0.40	41	<LOD	2.4	1	19
II-05	188	0.11	21.7	185	0.58	66	<LOD	3.0	3	16
II-06	157	<LOD	18.0	150	0.02	49	<LOD	2.5	3	26
II-07	184	<LOD	20.9	176	0.04	56	<LOD	2.9	<i>nd</i>	<i>nd</i>
III-01	189	<LOD	2.5	60	0.03	55	<LOD	1.1	3	19

## 5.2.2. Temporal variability

**Table S4:** Dataset from the second campaign

Station	pH	Dissolved oxygen saturation	Conductivity	Sulphide	Nitrate	Phosphate	Fluoride	Chloride	Sulphate	Alkalinity	Dissolved Organic Carbon
-	-	%	$mS\ cm^{-1}$	$mg\ L^{-1}$	$mg\ L^{-1}$	$mg\ L^{-1}$	$mg\ L^{-1}$	$mg\ L^{-1}$	$mg\ L^{-1}$	$mmol\ L^{-1}$	$mg\ C\ L^{-1}$
I-01	7.5	57	4.6	<LOD	0.8	<LOD	0.3	10.1	2084	22.1	6
I-02	6.8	38	4.7	<LOD	0.9	1	0.3	10	2445	24.7	5
I-03	7.1	36	4.7	8	0.8	1.1	0.3	10	1805	25.6	4
I-04	6.8	27	5.2	9	0.9	<LOD	0.4	9.5	2057	27.6	4
I-09	7.4	26	3	<LOD	0.8	1.3	0.4	9	1483	25.0	5
I-10	7.8	39	1.8	<LOD	0.8	1	0.3	11	1641	26.2	8
I-11	7.2	42	4.6	<LOD	0.8	0.9	0.3	10.1	1639	23.4	9
I-12	6.9	28	5.1	4	0.8	0.9	0.3	10.2	1739	28.0	8

Station	Ca	Fe	K	Mg	Mn	Na	P	Sr	Taxon	Abundance
	$mg\ L^{-1}$	$mg\ L^{-1}$	$mg\ L^{-1}$	$mg\ L^{-1}$	$mg\ L^{-1}$	$mg\ L^{-1}$	$mg\ L^{-1}$	$mg\ L^{-1}$	in 1 L of water	in 1 L of water
I-01	66	<LOD	10	60	0.2	281	0.3	0.8	4	86
I-02	67	<LOD	10	56	0.2	289	0.3	0.8	1	32
I-03	66	<LOD	11	55	0.2	310	0.4	0.9	1	15
I-04	64	<LOD	10	55	0.2	339	0.4	0.8	0	0
I-09	45	<LOD	7	46	0.1	213	0.4	0.6	7	83
I-10	54	<LOD	9	48	0.1	322	0.3	0.6	3	113
I-11	50	<LOD	9	53	0.1	301	0.3	0.6	3	248
I-12	50	<LOD	8	51	0.1	317	0.3	0.6	2	16

# References

- Abbasse, G., Ouddane, B., Fischer, J.C., 2003. Determination of Trace Metal Complexes by Natural Organic and Inorganic Ligands in Coastal Seawater. *Analytical Sciences* 19, 529–535. <https://doi.org/10.2116/analsci.19.529>
- Abreu, I.M., Cordeiro, R.C., Soares-Gomes, A., Abessa, D.M.S., Maranhão, L.A., Santelli, R.E., 2016. Ecological risk evaluation of sediment metals in a tropical Eutrophic Bay, Guanabara Bay, Southeast Atlantic. *Marine Pollution Bulletin* 109, 435–445. <https://doi.org/10.1016/j.marpolbul.2016.05.030>
- Achterberg, E.P., Braungardt, C., 1999. Stripping voltammetry for the determination of trace metal speciation and in-situ measurements of trace metal distributions in marine waters. *Analytica Chimica Acta* 400, 381–397. [https://doi.org/10.1016/S0003-2670\(99\)00619-4](https://doi.org/10.1016/S0003-2670(99)00619-4)
- Adriaens, R., Zeelmaekers, E., Fettweis, M., Vanlierde, E., Vanlede, J., Stassen, P., Elsen, J., Śródoń, J., Vandenberghe, N., 2018. Quantitative clay mineralogy as provenance indicator for recent muds in the southern North Sea. *Marine Geology* 398, 48–58. <https://doi.org/10.1016/j.margeo.2017.12.011>
- Agency for Toxic Substances and Disease Registry, 2019. Toxicological Profiles.
- Akçay, H., Oğuz, A., Karapire, C., 2003. Study of heavy metal pollution and speciation in Buyak Menderes and Gediz river sediments. *Water Research* 37, 813–822. [https://doi.org/10.1016/S0043-1354\(02\)00392-5](https://doi.org/10.1016/S0043-1354(02)00392-5)
- Akcil, A., Koldas, S., 2006. Acid Mine Drainage (AMD): causes, treatment and case studies. *Journal of Cleaner Production* 14, 1139–1145. <https://doi.org/10.1016/j.jclepro.2004.09.006>
- Aldana, G., Hernández, M., Cram, S., Arellano, O., Morton, O., León, C.P. de, 2018. Trace metal speciation in a wastewater wetland and its bioaccumulation in tilapia *Oreochromis niloticus*. *Chemical Speciation & Bioavailability* 30, 23–32. <https://doi.org/10.1080/09542299.2018.1452635>
- Ali, H., Khan, E., Ilahi, I., 2019. Environmental Chemistry and Ecotoxicology of Hazardous Heavy Metals: Environmental Persistence, Toxicity, and Bioaccumulation [WWW Document]. *Journal of Chemistry*. <https://doi.org/10.1155/2019/6730305>
- Ali, I., Aboul-Enein, H.Y., 2006. *Instrumental Methods in Metal Ion Speciation*. CRC Press.
- Allan, R.J., 1995. Impact of Mining Activities on the Terrestrial and Aquatic Environment with Emphasis on Mitigation and Remedial Measures, in: Förstner, U., Salomons, W., Mader, P. (Eds.), *Heavy Metals: Problems and Solutions*, Environmental Science. Springer Berlin Heidelberg, Berlin, Heidelberg, pp. 119–140. [https://doi.org/10.1007/978-3-642-79316-5\\_8](https://doi.org/10.1007/978-3-642-79316-5_8)
- Allen, H.E., Hansen, D.J., 1996. The Importance of Trace Metal Speciation to Water Quality Criteria. *Water Environment Research* 68, 42–54.
- AlSuhaimi, A.O., AlRadaddi, S.M., Al-Sheikh Ali, A.K., Shraim, A.M., AlRadaddi, T.S., 2019. Silica-based chelating resin bearing dual 8-Hydroxyquinoline

- moieties and its applications for solid phase extraction of trace metals from seawater prior to their analysis by ICP-MS. *Arabian Journal of Chemistry* 12, 360–369. <https://doi.org/10.1016/j.arabjc.2017.10.006>
- Amato, E.D., Covaci, A., Town, R.M., Hereijgers, J., Bellekens, B., Giacometti, V., Breugelmans, T., Weyn, M., Dardenne, F., Bervoets, L., Blust, R., 2018. A novel active-passive sampling approach for measuring time-averaged concentrations of pollutants in water. *Chemosphere* 209, 363–372. <https://doi.org/10.1016/j.chemosphere.2018.06.079>
- Aminot, A., Kérouel, R., 2004. *Hydrologie des écosystèmes marins: paramètres et analyses*. Editions Quae.
- Andersen, J.H., Al-Hamdani, Z., Harvey, E.T., Kallenbach, E., Murray, C., Stock, A., 2020. Relative impacts of multiple human stressors in estuaries and coastal waters in the North Sea–Baltic Sea transition zone. *Science of The Total Environment* 704, 135316. <https://doi.org/10.1016/j.scitotenv.2019.135316>
- Andreini, C., Bertini, I., Cavallaro, G., Holliday, G.L., Thornton, J.M., 2008. Metal ions in biological catalysis: from enzyme databases to general principles. *J Biol Inorg Chem* 13, 1205–1218. <https://doi.org/10.1007/s00775-008-0404-5>
- Anthony, E.J., 2014. The Human influence on the Mediterranean coast over the last 200 years: a brief appraisal from a geomorphological perspective. *Géomorphologie : relief, processus, environnement* 20, 219–226. <https://doi.org/10.4000/geomorphologie.10654>
- Aparicio-González, A., Duarte, C.M., Tovar-Sánchez, A., 2012. Trace metals in deep ocean waters: A review. *Journal of Marine Systems* 100–101, 26–33. <https://doi.org/10.1016/j.jmarsys.2012.03.008>
- Apourceau-Poly, C., Bertram, C., 2016. *Les cahiers techniques de la mission bassin minier. Les paysages du Bassin minier Nord-Pas de Calais*.
- Arslan, Z., Oymak, T., White, J., 2018. Triethylamine-assisted Mg(OH)<sub>2</sub> coprecipitation/preconcentration for determination of trace metals and rare earth elements in seawater by inductively coupled plasma mass spectrometry (ICP-MS). *Analytica Chimica Acta* 1008, 18–28. <https://doi.org/10.1016/j.aca.2018.01.017>
- Artamonova, K.V., Demidov, A.N., Zuev, O.A., 2019. Suboxic and Anoxic Conditions of Deep Waters in the Gdansk Basin of the Baltic Sea. *Oceanology* 59, 639–647. <https://doi.org/10.1134/S0001437019050011>
- Audry, S., Blanc, G., Schäfer, J., Robert, S., 2007. Effect of estuarine sediment resuspension on early diagenesis, sulfide oxidation and dissolved molybdenum and uranium distribution in the Gironde estuary, France. *Chemical Geology* 238, 149–167. <https://doi.org/10.1016/j.chemgeo.2006.11.006>
- Bade, R., Oh, S., Shin, W.S., 2012. Diffusive gradients in thin films (DGT) for the prediction of bioavailability of heavy metals in contaminated soils to earthworm (*Eisenia foetida*) and oral bioavailable concentrations. *Science of The Total Environment* 416, 127–136. <https://doi.org/10.1016/j.scitotenv.2011.11.007>

- Baeye, M., Fettweis, M., Voulgaris, G., Van Lancker, V., 2011. Sediment mobility in response to tidal and wind-driven flows along the Belgian inner shelf, southern North Sea. *Ocean Dynamics* 61, 611–622. <https://doi.org/10.1007/s10236-010-0370-7>
- Baeyens, W., 1998. Trace metals in the Westerschelde estuary: A case-study of a polluted, partially anoxic estuary, *Developments in Hydrobiology*. Kluwer Academic Publishers, Dordrecht.
- Baeyens, W., 1997. Evolution of trace metal concentrations in the Scheldt estuary (1978–1995). A comparison with estuarine and ocean levels. *Hydrobiologia* 366, 157–167. <https://doi.org/10.1023/A:1003136613574>
- Baeyens, W., Bowie, A.R., Buesseler, K., Elskens, M., Gao, Y., Lamborg, C., Leermakers, M., Remenyi, T., Zhang, H., 2011. Size-fractionated labile trace elements in the Northwest Pacific and Southern Oceans. *Marine Chemistry* 126, 108–113. <https://doi.org/10.1016/j.marchem.2011.04.004>
- Baeyens, W., Elskens, M., Van Ryssen, R., Leermakers, M., 1998. The impact of the Scheldt input on the trace metal distribution in the Belgian Coastal area (results of 1981-1983 and 1995-1996). *Hydrobiologia*, Kluwer Academic Publishers 366, 91–108.
- Baeyens, W., Gao, Y., Davison, W., Galceran, J., Leermakers, M., Puy, J., Superville, P.-J., Beguery, L., 2018a. In situ measurements of micronutrient dynamics in open seawater show that complex dissociation rates may limit diatom growth. *Scientific Reports* 8, 16125. <https://doi.org/10.1038/s41598-018-34465-w>
- Baeyens, W., Gao, Y., Davison, W., Galceran, J., Leermakers, M., Puy, J., Superville, P.-J., Beguery, L., 2018b. In situ measurements of micronutrient dynamics in open seawater show that complex dissociation rates may limit diatom growth. *Scientific Reports* 8. <https://doi.org/10.1038/s41598-018-34465-w>
- Baeyens, W., Gillain, G., Decadt, G., Elskens, I., 1987. Trace metals in the eastern part of the North Sea. I : Analyses and short-term distributions. *Oceanologica Acta* 10, 169–179.
- Baeyens, W., Leermakers, M., Gieter, M.De., Nguyen, H.L., Parmentier, K., Panutrakul, S., Elskens, M., 2005. Overview of trace metal contamination in the Scheldt estuary and effect of regulatory measures. *Hydrobiologia* 540, 141–154. <https://doi.org/10.1007/s10750-004-7129-4>
- Baeyens, Willy, van Eck, B., Lambert, C., Wollast, R., Goeyens, L., 1998. General description of the Scheldt Estuary. *Hydrobiologia*, Kluwer Academic Publishers *Trace Metals in the Westerschelde Estuary*, 1–14.
- Baeyens, W.F.J. (Ed.), 1998. *Trace metals in the Westerschelde Estuary: a case-study of a polluted, partially anoxic estuary*, *Developments in hydrobiology*. Kluwer Academic Publishers, Dordrecht ; Boston.
- Bagarinao, T.U., 1993. Sulfide as a toxicant in aquatic habitats. *SEAFDEC Asian Aquaculture* XV, 2–4.
- Balch, J., Guéguen, C., 2015. Effects of molecular weight on the diffusion coefficient of aquatic dissolved organic matter and humic substances.

- Chemosphere 119, 498–503.  
<https://doi.org/10.1016/j.chemosphere.2014.07.013>
- Balch, W.M., 2018. The Ecology, Biogeochemistry, and Optical Properties of Coccolithophores. *Annual Review of Marine Science* 10, 71–98.  
<https://doi.org/10.1146/annurev-marine-121916-063319>
- Bale, A.J., Morris, A.W., 1998. Organic carbon in suspended particulate material in the North Sea: Effect of mixing resuspended and background particles. *Continental Shelf Research* 18, 1333–1345. [https://doi.org/10.1016/S0278-4343\(98\)00046-6](https://doi.org/10.1016/S0278-4343(98)00046-6)
- Balls, P.W., 1988. The control of trace metal concentrations in coastal seawater through partition onto suspended particulate matter. *Netherlands Journal of Sea Research* 22, 213–218. [https://doi.org/10.1016/0077-7579\(88\)90025-7](https://doi.org/10.1016/0077-7579(88)90025-7)
- Baltic Marine Environment Protection Commission, 2019. HELCOM [WWW Document]. URL <http://www.helcom.fi/> (accessed 7.15.19).
- Baltic Sea Hydrographic Commission, 2013. Baltic Sea Bathymetry Database version 0.9.3. Downloaded from <http://data.bshc.pro/> on 28/02/2020.
- Barbieri, M., 2016. The Importance of Enrichment Factor (EF) and Geoaccumulation Index (Igeo) to Evaluate the Soil Contamination. *Geology & Geophysics* 5, 237. <https://doi.org/10.4172/2381-8719.100023>
- Barletta, M., Lima, A.R.A., Costa, M.F., 2019. Distribution, sources and consequences of nutrients, persistent organic pollutants, metals and microplastics in South American estuaries. *Science of The Total Environment* 651, 1199–1218.  
<https://doi.org/10.1016/j.scitotenv.2018.09.276>
- Barrett, P.M., Resing, J.A., Grand, M.M., Measures, C.I., Landing, W.M., 2018. Trace element composition of suspended particulate matter along three meridional CLIVAR sections in the Indian and Southern Oceans: Impact of scavenging on Al distributions. *Chemical Geology* 502, 15–28.  
<https://doi.org/10.1016/j.chemgeo.2018.06.015>
- Bartholomä, A., Flemming, B.W., Delafontaine, M.T., 2000. Mass balancing the seasonal turnover of mud and sand in the vicinity of an intertidal mussel bank in the Wadden Sea (southern North Sea), in: Flemming, B.W., Delafontaine, M.T., Liebezeit, G. (Eds.), *Proceedings in Marine Science, Muddy Coast Dynamics and Resource Management*. Elsevier, pp. 85–106.  
[https://doi.org/10.1016/S1568-2692\(00\)80008-X](https://doi.org/10.1016/S1568-2692(00)80008-X)
- Barwick, M., Maher, W., 2003. Biotransference and biomagnification of selenium copper, cadmium, zinc, arsenic and lead in a temperate seagrass ecosystem from Lake Macquarie Estuary, NSW, Australia. *Mar. Environ. Res.* 56, 471–502. [https://doi.org/10.1016/S0141-1136\(03\)00028-X](https://doi.org/10.1016/S0141-1136(03)00028-X)
- Bass, J.A.B., Blust, R., Clarke, R.T., Corbin, T.A., Davison, W., de Schamphelaere, K.A.C., Janssen, C.R., Kalis, E.J.J., Kelly, M.G., Kneebone, N.T., Lawlor, A.J., Lofts, S., Temminghoff, E.J.M., Thacker, S.A., Tipping, E., Vincent, C.D., Wamken, K.W., Zhang, H., 2008. Using science to create a better place, *Environmental Quality Standards for trace metals in the aquatic environment* (Scientific Report No. SC030194). Environment Agency, Bristol.



- Batley, G.E., Gardner, D., 1977. Sampling and storage of natural waters for trace metal analysis. *Water Research* 11, 745–756. [https://doi.org/10.1016/0043-1354\(77\)90042-2](https://doi.org/10.1016/0043-1354(77)90042-2)
- Beauchamp, R.O., Bus, J.S., Popp, J.A., Boreiko, C.J., Andjelkovich, D.A., Leber, P., 1984. A Critical Review of the Literature on Hydrogen Sulfide Toxicity. *CRC Critical Reviews in Toxicology* 13, 25–97. <https://doi.org/10.3109/10408448409029321>
- Bedioui, F., 1999. Voltampérométrie. Théorie et mise en oeuvre expérimentale. Ed. Techniques Ingénieur.
- Beghoura, H., Gorgues, T., Aumont, O., Planquette, H.F., Tagliabue, A., Auger, P.-A., 2019. Impact of Inorganic Particles of Sedimentary Origin on Global Dissolved Iron and Phytoplankton Distribution. *Journal of Geophysical Research: Oceans* 124, 8626–8646. <https://doi.org/10.1029/2019JC015119>
- Belgian Federal Science Policy Office, 2018. Marine pollution [WWW Document]. Belgian Platform on Earth Observation. URL <https://eo.belspo.be/en/marine-pollution> (accessed 6.20.19).
- Benjamin, M.M., 2014. *Water Chemistry: Second Edition*. Waveland Press.
- Benoit-Chabot, V., 2014. Les facteurs de sélection des bio-indicateurs de la qualité des écosystèmes aquatiques : élaboration d'un outil d'aide à la décision (Master thesis). Centre universitaire de formation en environnement et développement durable.
- Bhurtun, P., 2018. Dynamique de la qualité des masses d'eau dans le bassin Artois-Picardie : Compréhension des mécanismes actuels et prévision des évolutions dans un contexte de changement climatique (Doctoral Thesis). Lille University.
- Bianchi, T.S., 2007. *Biogeochemistry of Estuaries*. Oxford University Press, USA.
- Bibby, R.L., Webster-Brown, J.G., 2006. Trace metal adsorption onto urban stream suspended particulate matter (Auckland region, New Zealand). *Applied Geochemistry* 21, 1135–1151. <https://doi.org/10.1016/j.apgeochem.2006.03.014>
- Bighiu, M.A., Eriksson-Wiklund, A.-K., Eklund, B., 2017a. Biofouling of leisure boats as a source of metal pollution. *Environ Sci Pollut Res* 24, 997–1006. <https://doi.org/10.1007/s11356-016-7883-7>
- Bighiu, M.A., Gorokhova, E., Carney Almroth, B., Eriksson Wiklund, A.-K., 2017b. Metal contamination in harbours impacts life-history traits and metallothionein levels in snails. *PLoS One* 12. <https://doi.org/10.1371/journal.pone.0180157>
- Bingham, F.T., Sposito, G., Strong, J.E., 1984. The Effect of Chloride on the Availability of Cadmium I. *Journal of Environment Quality* 13, 71. <https://doi.org/10.2134/jeq1984.00472425001300010013x>
- Birch, G.F., 2020. An assessment of aluminum and iron in normalisation and enrichment procedures for environmental assessment of marine sediment. *Science of The Total Environment* 138123. <https://doi.org/10.1016/j.scitotenv.2020.138123>

- Birch, G.F., 2003. A test of normalization methods for marine sediment, including a new post-extraction normalization (PEN) technique. *Hydrobiologia* 492, 5–13. <https://doi.org/10.1023/A:1024844629087>
- Blackford, J.C., Gilbert, F.J., 2007. pH variability and CO<sub>2</sub> induced acidification in the North Sea. *Journal of Marine Systems* 64, 229–241. <https://doi.org/10.1016/j.jmarsys.2006.03.016>
- Bockelmann, F.-D., Puls, W., Kleeberg, U., Müller, D., Emeis, K.-C., 2018. Mapping mud content and median grain-size of North Sea sediments – A geostatistical approach. *Marine Geology* 397, 60–71. <https://doi.org/10.1016/j.margeo.2017.11.003>
- Boyd, P., Newton, P., 1995. Evidence of the potential influence of planktonic community structure on the interannual variability of particulate organic carbon flux. *Deep Sea Research Part I: Oceanographic Research Papers* 42, 619–639. [https://doi.org/10.1016/0967-0637\(95\)00017-Z](https://doi.org/10.1016/0967-0637(95)00017-Z)
- Brack, W., Dulio, V., Ågerstrand, M., Allan, I., Altenburger, R., Brinkmann, M., Bunke, D., Burgess, R.M., Cousins, I., Escher, B.I., Hernández, F.J., Hewitt, L.M., Hilscherová, K., Hollender, J., Hollert, H., Kase, R., Klauer, B., Lindim, C., Herráez, D.L., Miège, C., Munthe, J., O’Toole, S., Posthuma, L., Rüdell, H., Schäfer, R.B., Sengl, M., Smedes, F., van de Meent, D., van den Brink, P.J., van Gils, J., van Wezel, A.P., Vethaak, A.D., Vermeirssen, E., von der Ohe, P.C., Vrana, B., 2017. Towards the review of the European Union Water Framework Directive: Recommendations for more efficient assessment and management of chemical contamination in European surface water resources. *Science of The Total Environment* 576, 720–737. <https://doi.org/10.1016/j.scitotenv.2016.10.104>
- Brand, E., 2019. Intertidal beach morphodynamics of a macro-tidal sandy coast (Belgium) (Doctoral Thesis). Vrije Universiteit Brussel, Brussels.
- Braungardt, C.B., Howell, K.A., Tappin, A.D., Achterberg, E.P., 2011. Temporal variability in dynamic and colloidal metal fractions determined by high resolution in situ measurements in a UK estuary. *Chemosphere* 84, 423–431. <https://doi.org/10.1016/j.chemosphere.2011.03.050>
- Broclawik, O., Łukawska-Matuszewska, K., Bolalek, J., 2018. Impact of the 2014 Major Baltic Inflow on benthic fluxes of ferrous iron and phosphate below the permanent halocline in the southern Baltic Sea. *Oceanological and Hydrobiological Studies* 47, 275–287. <https://doi.org/10.1515/ohs-2018-0026>
- Bruland, K.W., Coale, K.H., Mart, L., 1985. Analysis of seawater for dissolved cadmium, copper and lead: An intercomparison of voltammetric and atomic absorption methods. *Marine Chemistry* 17, 285–300. [https://doi.org/10.1016/0304-4203\(85\)90002-7](https://doi.org/10.1016/0304-4203(85)90002-7)
- Brumbaugh, W.G., Petty, J.D., Huckins, J.N., Manahan, S.E., 2002. Stabilized Liquid Membrane Device (SLMD) for the Passive, Integrative Sampling of Labile Metals in Water. *Water, Air, & Soil Pollution* 133, 109–119. <https://doi.org/10.1023/A:1012923529742>

- Brumsack, H.-J., 2006. The trace metal content of recent organic carbon-rich sediments: Implications for Cretaceous black shale formation. *Palaeogeography, Palaeoclimatology, Palaeoecology* 232, 344–361. <https://doi.org/10.1016/j.palaeo.2005.05.011>
- Bukaveckas, P.A., Katarzyte, M., Schlegel, A., Spuriene, R., Egerton, T., Vaiciute, D., 2019. Composition and settling properties of suspended particulate matter in estuaries of the Chesapeake Bay and Baltic Sea regions. *J Soils Sediments* 19, 2580–2593. <https://doi.org/10.1007/s11368-018-02224-z>
- Burdige, D.J., Komada, T., 2020. Iron redox cycling, sediment resuspension and the role of sediments in low oxygen environments as sources of iron to the water column. *Marine Chemistry* 223, 103793. <https://doi.org/10.1016/j.marchem.2020.103793>
- Burton, E.D., Bush, R.T., Sullivan, L.A., 2006. Acid-Volatile Sulfide Oxidation in Coastal Flood Plain Drains: Iron–Sulfur Cycling and Effects on Water Quality. *Environ. Sci. Technol.* 40, 1217–1222. <https://doi.org/10.1021/es0520058>
- Busigny, V., Jézéquel, D., Cosmidis, J., Viollier, E., Benzerara, K., Planavsky, N.J., Albéric, P., Lebeau, O., Sarazin, G., Michard, G., 2016. The Iron Wheel in Lac Pavin: Interaction with Phosphorus Cycle, in: Sime-Ngando, T., Boivin, P., Chapron, E., Jezequel, D., Meybeck, M. (Eds.), *Lake Pavin: History, Geology, Biogeochemistry, and Sedimentology of a Deep Meromictic Maar Lake*. Springer International Publishing, Cham, pp. 205–220. [https://doi.org/10.1007/978-3-319-39961-4\\_12](https://doi.org/10.1007/978-3-319-39961-4_12)
- Byrne, R.H., Kump, L.R., Cantrell, K.J., 1988. The influence of temperature and pH on trace metal speciation in seawater. *Marine Chemistry* 25, 163–181. [https://doi.org/10.1016/0304-4203\(88\)90062-X](https://doi.org/10.1016/0304-4203(88)90062-X)
- Camargo, J.A., 2003. Fluoride toxicity to aquatic organisms: a review. *Chemosphere* 50, 251–264. [https://doi.org/10.1016/S0045-6535\(02\)00498-8](https://doi.org/10.1016/S0045-6535(02)00498-8)
- Caruso, J.A., Montes-Bayon, M., 2003. Elemental speciation studies—new directions for trace metal analysis. *Ecotoxicology and Environmental Safety, Special Issue on Methodologies for Assessing Exposures to Metals: Speciation, Bioaccessibility and Bioavailability in the Environment, Food and Feed* 56, 148–163. [https://doi.org/10.1016/S0147-6513\(03\)00058-7](https://doi.org/10.1016/S0147-6513(03)00058-7)
- Carvalho, L., Mackay, E.B., Cardoso, A.C., Baatrup-Pedersen, A., Birk, S., Blackstock, K.L., Borics, G., Borja, A., Feld, C.K., Ferreira, M.T., Globevnik, L., Grizzetti, B., Hendry, S., Hering, D., Kelly, M., Langaas, S., Meissner, K., Panagopoulos, Y., Penning, E., Rouillard, J., Sabater, S., Schmedtje, U., Spears, B.M., Venohr, M., van de Bund, W., Solheim, A.L., 2019. Protecting and restoring Europe’s waters: An analysis of the future development needs of the Water Framework Directive. *Science of The Total Environment* 658, 1228–1238. <https://doi.org/10.1016/j.scitotenv.2018.12.255>
- Catrouillet, C., Davranche, M., Dia, A., Bouhnik-Le Coz, M., Demangeat, E., Gruau, G., 2016. Does As(III) interact with Fe(II), Fe(III) and organic matter through ternary complexes? *Journal of Colloid and Interface Science* 470, 153–161. <https://doi.org/10.1016/j.jcis.2016.02.047>

- Chapalain, M., Verney, R., Fettweis, M., Jacquet, M., Le Berre, D., Le Hir, P., 2019. Investigating suspended particulate matter in coastal waters using the fractal theory. *Ocean Dynamics* 69, 59–81. <https://doi.org/10.1007/s10236-018-1229-6>
- Charriau, A., Lesven, L., Gao, Y., Leermakers, M., Baeyens, W., Ouddane, B., Billon, G., 2011. Trace metal behaviour in riverine sediments: Role of organic matter and sulfides. *Applied Geochemistry* 26, 80–90. <https://doi.org/10.1016/j.apgeochem.2010.11.005>
- Charriau, A., Lissalde, S., Poulier, G., Mazzella, N., Buzier, R., Guibaud, G., 2016. Overview of the Chemcatcher® for the passive sampling of various pollutants in aquatic environments Part A: Principles, calibration, preparation and analysis of the sampler. *Talanta* 148, 556–571. <https://doi.org/10.1016/j.talanta.2015.06.064>
- Chester, R., 1990. *Marine Geochemistry*. Springer Netherlands, Dordrecht. <https://doi.org/10.1007/978-94-010-9488-7>
- Clark, R.B., Frid, C., Attrill, M., 1997. *Marine pollution*, 4th ed. ed. Oxford [England]; New York : Oxford University Press.
- Cline, J.D., 1969. SPECTROPHOTOMETRIC DETERMINATION OF HYDROGEN SULFIDE IN NATURAL WATERS. *Limnology and Oceanography* 14, 454–458. <https://doi.org/10.4319/lo.1969.14.3.0454>
- Cloern, J.E., 1996. Phytoplankton bloom dynamics in coastal ecosystems: A review with some general lessons from sustained investigation of San Francisco Bay, California. *Reviews of Geophysics* 34, 127–168. <https://doi.org/10.1029/96RG00986>
- Cloern, J.E., Abreu, P.C., Carstensen, J., Chauvaud, L., Elmgren, R., Grall, J., Greening, H., Johansson, J.O.R., Kahru, M., Sherwood, E.T., Xu, J., Yin, K., 2016. Human activities and climate variability drive fast-paced change across the world's estuarine–coastal ecosystems. *Global Change Biology* 22, 513–529. <https://doi.org/10.1111/gcb.13059>
- Colombo, C., van den Berg, C.M.G., 1997. Simultaneous determination of several trace metals in seawater using cathodic stripping voltammetry with mixed ligands. *Analytica Chimica Acta* 337, 29–40. [https://doi.org/10.1016/S0003-2670\(96\)00401-1](https://doi.org/10.1016/S0003-2670(96)00401-1)
- Colombo, M., Rogalla, B., Myers, P.G., Allen, S.E., Orians, K.J., 2019. Tracing Dissolved Lead Sources in the Canadian Arctic: Insights from the Canadian GEOTRACES Program. *ACS Earth and Space Chemistry* 3, 1302–1314. <https://doi.org/10.1021/acsearthspacechem.9b00083>
- Companys, E., Galceran, J., Pinheiro, J.P., Puy, J., Salaün, P., 2017. A review on electrochemical methods for trace metal speciation in environmental media. *Current Opinion in Electrochemistry* 3, 144–162. <https://doi.org/10.1016/j.coelec.2017.09.007>
- Conley, D.J., Björck, S., Bonsdorff, E., Carstensen, J., Destouni, G., Gustafsson, B.G., Hietanen, S., Kortekaas, M., Kuosa, H., Markus Meier, H.E., Müller-Karulis, B., Nordberg, K., Norkko, A., Nürnberg, G., Pitkänen, H., Rabalais, N.N., Rosenberg, R., Savchuk, O.P., Slomp, C.P., Voss, M., Wulff, F., Zillén, L., 2009. Hypoxia-Related Processes in the Baltic Sea.

- Environmental Science & Technology 43, 3412–3420.  
<https://doi.org/10.1021/es802762a>
- CPIE Chaîne des terrils, Mission Bassin Minier Nord-Pas de Calais, Bassin Minier Nord-Pas de Calais UNESCO, 2014. Les terrils du Nord-Pas de Calais : Glossaire de la base de données “Access” des terrils du Nord et du Pas-de-Calais (glossaire).
- Crawford, D.W., Wyatt, S.N., Wrohan, I.A., Cefarelli, A.O., Giesbrecht, K.E., Kelly, B., Varela, D.E., 2015. Low particulate carbon to nitrogen ratios in marine surface waters of the Arctic. *Global Biogeochemical Cycles* 29, 2021–2033. <https://doi.org/10.1002/2015GB005200>
- da Silva, G.S., Gloaguen, T.V., Couto, C.F., Motta, P.N.S.D., 2017. Persistence and mobility of metals in an estuarine environment 25 years after closure of a lead smelter, Bahia State, Brazil. *Environmental Earth Sciences* 76. <https://doi.org/10.1007/s12665-017-6886-0>
- Dang, D.H., Lenoble, V., Durrieu, G., Omanović, D., Mullot, J.-U., Mounier, S., Garnier, C., 2015. Seasonal variations of coastal sedimentary trace metals cycling: Insight on the effect of manganese and iron (oxy)hydroxides, sulphide and organic matter. *Marine Pollution Bulletin* 92, 113–124. <https://doi.org/10.1016/j.marpolbul.2014.12.048>
- Danielsson, L.G., 1982. On the use of filters for distinguishing between dissolved and particulate fractions in natural waters. *Water Research* 16, 179–182. [https://doi.org/10.1016/0043-1354\(82\)90108-7](https://doi.org/10.1016/0043-1354(82)90108-7)
- Daskalakis, K.D., O’Connor, T.P., 1995. Normalization and Elemental Sediment Contamination in the Coastal United States. *Environ. Sci. Technol.* 29, 470–477. <https://doi.org/10.1021/es00002a024>
- Dauby, P., Frankignoulle, M., Gobert, S., Bouqueneau, J.-M., 1994. Distribution of POC, PON, and particulate Al, Cd, Cr, Cu, Pb, Ti, Zn and  $\delta^{13}\text{C}$  in the English Channel and adjacent areas. *Oceanologica Acta* 17, 643–657.
- David M. Rosenberg, Resh, V.H., 1993. *Freshwater Biomonitoring and Benthic Macroinvertebrates*. Springer US.
- Davison, W., 2016a. *Diffusive gradients in thin-films for environmental measurements*, Cambridge environmental chemistry series. Cambridge University Press, Cambridge.
- Davison, W., 2016b. *Diffusive Gradients in Thin-Films for Environmental Measurements*. Cambridge University Press, Cambridge. <https://doi.org/10.1017/CBO9781316442654>
- De Brabandere, L., Dehairs, F., Van Damme, S., Brion, N., Meire, P., Daro, N., 2002.  $\delta^{15}\text{N}$  and  $\delta^{13}\text{C}$  dynamics of suspended organic matter in freshwater and brackish waters of the Scheldt estuary. *Journal of Sea Research* 48, 1–15. [https://doi.org/10.1016/S1385-1101\(02\)00132-6](https://doi.org/10.1016/S1385-1101(02)00132-6)
- de Souza Machado, A.A., Spencer, K., Kloas, W., Toffolon, M., Zarfl, C., 2016. Metal fate and effects in estuaries: A review and conceptual model for better understanding of toxicity. *Science of The Total Environment* 541, 268–281. <https://doi.org/10.1016/j.scitotenv.2015.09.045>
- de Winter, N.J., Claeys, P., 2017. Micro X-ray fluorescence ( $\mu\text{XRF}$ ) line scanning on Cretaceous rudist bivalves: A new method for reproducible trace

- element profiles in bivalve calcite. *Sedimentology* 64, 231–251.  
<https://doi.org/10.1111/sed.12299>
- de Winter, N.J., Sinnesael, M., Makarona, C., Vansteenberge, S., Claeys, P., 2017. Trace element analyses of carbonates using portable and micro-X-ray fluorescence: performance and optimization of measurement parameters and strategies. *J. Anal. At. Spectrom.* 32, 1211–1223.  
<https://doi.org/10.1039/C6JA00361C>
- De Wolf, H., Bäckeljau, T., Blust, R., 2000. Heavy metal accumulation in the periwinkle *Littorina littorea*, along a pollution gradient in the Scheldt estuary. *Science of The Total Environment* 262, 111–121.  
[https://doi.org/10.1016/S0048-9697\(00\)00601-X](https://doi.org/10.1016/S0048-9697(00)00601-X)
- Dehairs, F., Baeyens, W., Van Gansbeke, D., 1989. Tight coupling between enrichment of iron and manganese in North Sea suspended matter and sedimentary redox processes: Evidence for seasonal variability. *Estuarine, Coastal and Shelf Science* 29, 457–471. [https://doi.org/10.1016/0272-7714\(89\)90080-2](https://doi.org/10.1016/0272-7714(89)90080-2)
- D’Elia, C.F., Bidjerano, M., Wheeler, T.B., 2019. Chapter 17 - Population Growth, Nutrient Enrichment, and Science-Based Policy in the Chesapeake Bay Watershed, in: Wolanski, E., Day, J.W., Elliott, M., Ramachandran, R. (Eds.), *Coasts and Estuaries*. Elsevier, pp. 293–310.  
<https://doi.org/10.1016/B978-0-12-814003-1.00017-4>
- Dellwig, O., Schnetger, B., Meyer, D., Pollehne, F., Häusler, K., Arz, H.W., 2018. Impact of the Major Baltic Inflow in 2014 on Manganese Cycling in the Gotland Deep (Baltic Sea). *Front. Mar. Sci.* 5.  
<https://doi.org/10.3389/fmars.2018.00248>
- Denimal, S., 2001. Impact des terrils houillers du bassin minier Nord-Pas-de-Calais sur la qualité des eaux de la nappe de la Craie. Université des Sciences et Technologies de Lille, Lille, France.
- Deycard, V.N., Schäfer, J., Blanc, G., Coynel, A., Petit, J.C.J., Lancelleur, L., Dutruch, L., Bossy, C., Ventura, A., 2014. Contributions and potential impacts of seven priority substances (As, Cd, Cu, Cr, Ni, Pb, and Zn) to a major European Estuary (Gironde Estuary, France) from urban wastewater. *Marine Chemistry, Estuarine Biogeochemistry* 167, 123–134.  
<https://doi.org/10.1016/j.marchem.2014.05.005>
- Dierssen, H., Balzer, W., Landing, W.M., 2001. Simplified synthesis of an 8-hydroxyquinoline chelating resin and a study of trace metal profiles from Jellyfish Lake, Palau. *Marine Chemistry* 73, 173–192.  
[https://doi.org/10.1016/S0304-4203\(00\)00107-9](https://doi.org/10.1016/S0304-4203(00)00107-9)
- Diop, C., Dewaelé, D., Diop, M., Touré, A., Cabral, M., Cazier, F., Fall, M., Diouf, A., Ouddane, B., 2014. Assessment of contamination, distribution and chemical speciation of trace metals in water column in the Dakar coast and the Saint Louis estuary from Senegal, West Africa. *Marine Pollution Bulletin* 86, 539–546. <https://doi.org/10.1016/j.marpolbul.2014.06.051>
- Dobbins, W., Krause, J.W., Agustí, S., Duarte, C.M., Schulz, I.K., Winding, M., Rowe, K.A., Sejr, M., 2017. The Role of Silicon Limitation in

- Phytoplankton Phenology in a Sub-Arctic Fjord System. AGU Fall Meeting Abstracts 21.
- dos Passos, A.S., Tonon, G.F., Nakadi, F.V., Mangrich, A.S., Andrade, J.B. de, Welz, B., Vale, M.G.R., 2018. Determination of Cr, Cu and Pb in industrial waste of oil shale using high-resolution continuum source graphite furnace atomic absorption spectrometry and direct solid sample analysis. *Anal. Methods* 10, 3645–3653. <https://doi.org/10.1039/C8AY01270A>
- Drexler, J., Fisher, N., Henningsen, G., Lanno, R., McGeer, J., Sappington, K., Beringer, M., 2003. Issue Paper on the bioavailability and bioaccumulation of Metals. U.S. Environmental Protection Agency 120p.
- Driscoll, C.T., Otton, J.K., Iverfeldt, A., 1994. Trace metals speciation and cycling, in: *Biogeochemistry of Small Catchments; a Tool for Environmental Research*. pp. 301–322.
- Du Laing, G., De Vos, R., Vandecasteele, B., Lesage, E., Tack, F.M.G., Verloo, M.G., 2008. Effect of salinity on heavy metal mobility and availability in intertidal sediments of the Scheldt estuary. *Estuarine, Coastal and Shelf Science* 77, 589–602. <https://doi.org/10.1016/j.ecss.2007.10.017>
- Du Laing, G., Meers, E., Dewispelaere, M., Vandecasteele, B., Rinklebe, J., Tack, F.M.G., Verloo, M.G., 2009. Heavy metal mobility in intertidal sediments of the Scheldt estuary: Field monitoring. *Science of The Total Environment* 407, 2919–2930. <https://doi.org/10.1016/j.scitotenv.2008.12.024>
- Duffaut, P., 2001. On stability of volcanoes and other heaps. *Revue Française de Géotechnique* 87–90. <https://doi.org/10.1051/geotech/2001095087>
- Duinker, J.C., Nolting, R.F., Michel, D., 1982. Effects of salinity, pH and redox conditions on the behavior of Cd, Zn, Ni and Mn in the Scheldt Estuary. *Thalass. Jugoslav* 191–202.
- Dundar, M.S., Altundag, H., 2018. Distribution of some major and trace elements in the lower Sakarya River by using ICP-MS. *Journal of Chemical Metrology* 12, 128–139. <https://doi.org/10.25135/jcm.22.18.11.1073>
- Dupré, B., Viers, J., Dandurand, J.-L., Polve, M., Bénézech, P., Vervier, P., Braun, J.-J., 1999. Major and trace elements associated with colloids in organic-rich river waters: ultrafiltration of natural and spiked solutions. *Chemical Geology* 160, 63–80. [https://doi.org/10.1016/S0009-2541\(99\)00060-1](https://doi.org/10.1016/S0009-2541(99)00060-1)
- Durán, I., Beiras, R., 2013. Ecotoxicologically based marine acute water quality criteria for metals intended for protection of coastal areas. *Science of The Total Environment* 463–464, 446–453. <https://doi.org/10.1016/j.scitotenv.2013.05.077>
- Ebling, A.M., Landing, W.M., 2015. Sampling and analysis of the sea surface microlayer for dissolved and particulate trace elements. *Marine Chemistry, Biogeochemistry of trace elements and their isotopes* 177, 134–142. <https://doi.org/10.1016/j.marchem.2015.03.012>
- Ehlert, C., Reckhardt, A., Greskowiak, J., Liguori, B.T.P., Böning, P., Paffrath, R., Brumsack, H.-J., Pahnke, K., 2016. Transformation of silicon in a sandy beach ecosystem: Insights from stable silicon isotopes from fresh and saline groundwaters. *Chemical Geology* 440, 207–218. <https://doi.org/10.1016/j.chemgeo.2016.07.015>

- Eisma, D., Irion, G., 1988. Suspended Matter and Sediment Transport, in: Salomons, W., Bayne, B.L., Duursma, E.K., Förstner, U. (Eds.), *Pollution of the North Sea: An Assessment*. Springer, Berlin, Heidelberg, pp. 20–35. [https://doi.org/10.1007/978-3-642-73709-1\\_2](https://doi.org/10.1007/978-3-642-73709-1_2)
- Eklund, B., Watermann, B., 2018. Persistence of TBT and copper in excess on leisure boat hulls around the Baltic Sea. *Environ Sci Pollut Res* 25, 14595–14605. <https://doi.org/10.1007/s11356-018-1614-1>
- Elderfield, H., Holland, H.D., Elderfield, Henry, Turekian, K.K., 2006. *The Oceans and Marine Geochemistry*. Elsevier.
- Elliott, M., Day, J.W., Ramachandran, R., Wolanski, E., 2019. Chapter 1 - A Synthesis: What Is the Future for Coasts, Estuaries, Deltas and Other Transitional Habitats in 2050 and Beyond?, in: Wolanski, E., Day, J.W., Elliott, M., Ramachandran, R. (Eds.), *Coasts and Estuaries*. Elsevier, pp. 1–28. <https://doi.org/10.1016/B978-0-12-814003-1.00001-0>
- Elliott, M., Hemingway, K., 2002. *Fishes in Estuaries*. John Wiley & Sons, Ltd. <https://doi.org/10.1002/9780470995228.fmatter>
- Elphick, J.R.F., Bergh, K.D., Bailey, H.C., 2011. Chronic toxicity of chloride to freshwater species: Effects of hardness and implications for water quality guidelines. *Environmental Toxicology and Chemistry* 30, 239–246. <https://doi.org/10.1002/etc.365>
- Elskens, M., Gourgue, O., Baeyens, W., Chou, L., Deleersnijder, E., Leermakers, M., de Brauwere, A., 2014. Modelling metal speciation in the Scheldt Estuary: Combining a flexible-resolution transport model with empirical functions. *Science of The Total Environment* 476–477, 346–358. <https://doi.org/10.1016/j.scitotenv.2013.12.047>
- Erlandson, J.M., Fitzpatrick, S.M., 2006. Oceans, Islands, and Coasts: Current Perspectives on the Role of the Sea in Human Prehistory. *The Journal of Island and Coastal Archaeology* 1, 5–32. <https://doi.org/10.1080/15564890600639504>
- Ernstberger, H., Zhang, H., Davison, W., 2002. Determination of chromium speciation in natural systems using DGT. *Anal Bioanal Chem* 373, 873–879. <https://doi.org/10.1007/s00216-002-1370-3>
- Eslamikhah, Z., Guggenberger, G., Carstens, J.F., 2017. Adsorption of Pb on iron oxide colloids as a function of DOM concentration. Presented at the Jahrestagung der DBG 2017: Horizonte des Bodens, Göttingen.
- Estrada, E.S., Juhel, G., Han, P., Kelly, B.C., Lee, W.K., Bayen, S., 2017. Multi-tool assessment of trace metals in mangroves combining sediment and clam sampling, DGT passive samplers and caged mussels. *Science of The Total Environment* 574, 847–857. <https://doi.org/10.1016/j.scitotenv.2016.09.055>
- European Commission, 2013. Directive 2013/39/EU of the European Parliament and of the Council of 12 August 2013 amending Directives 2000/60/EC and 2008/105/EC as regards priority substances in the field of water policy. *Official Journal of the European Union* 17.
- European Commission, 2010. Commission Decision of 1 September 2010 on criteria and methodological standards on good environmental status of marine waters (2010/477/EU). *Official Journal of the European Union* 11.



- European Environment Agency (Ed.), 2013. Balancing the future of Europe's coasts: knowledge base for integrated management, EEA Report. European Environment Agency [u.a.], Copenhagen.
- European Environment Agency, 2008. Côtes et mers.
- European Parliament and of the Council, 2008. Directive 2008/105/CE du Parlement européen et du Conseil du 16 décembre 2008 établissant des normes de qualité environnementale dans le domaine de l'eau, modifiant et abrogeant les directives du Conseil 82/176/CEE, 83/513/CEE, 84/156/CEE, 84/491/CEE, 86/280/CEE et modifiant la directive 2000/60/CE, 348.
- European Parliament and of the Council, 2000. Directive 2000/60/EC of the European Parliament and of the Council of 23 October 2000 establishing a framework for Community action in the field of water policy, 327.
- Expertise Center in Environmental Analysis of Quebec, 2015. Détermination des sulfures : méthode colorimétrique avec le chlorure ferrique et l'oxalate de N,N-diméthylep-phénylènediamine (Protocole No. MA. 300 – S 1.2, rev. 3). Ministère du Développement durable, de l'Environnement et de la Lutte contre les changements climatiques du Québec..
- Fairbrother, A., Wenstel, R., Sappington, K., Wood, W., 2007. Framework for Metals Risk Assessment. *Ecotoxicology and Environmental Safety* 68, 145–227. <https://doi.org/10.1016/j.ecoenv.2007.03.015>
- Farghaly, O.A., Hameed, R.S.A., Abu-Nawwas, A.-A.H., 2014. Analytical Application Using Modern Electrochemical Techniques. *International Journal Electrochemical Science* 9, 3287–3318.
- Fehr, M.A., Andersson, P.S., Hålenius, U., Gustafsson, Ö., Mörth, C.-M., 2010. Iron enrichments and Fe isotopic compositions of surface sediments from the Gotland Deep, Baltic Sea. *Chemical Geology* 277, 310–322. <https://doi.org/10.1016/j.chemgeo.2010.08.014>
- Fennel, W., Seifert, T., Kayser, B., 1991. Rossby radii and phase speeds in the Baltic Sea. *Continental Shelf Research* 11, 23–36. [https://doi.org/10.1016/0278-4343\(91\)90032-2](https://doi.org/10.1016/0278-4343(91)90032-2)
- Fettweis, M., Baeye, M., 2015. Seasonal variation in concentration, size, and settling velocity of muddy marine flocs in the benthic boundary layer. *Journal of Geophysical Research: Oceans* 120, 5648–5667. <https://doi.org/10.1002/2014JC010644>
- Fettweis, M., Baeye, M., Lee, B.J., Chen, P., Yu, J.C.S., 2012. Hydro-meteorological influences and multimodal suspended particle size distributions in the Belgian nearshore area (southern North Sea). *Geo-Mar Lett* 32, 123–137. <https://doi.org/10.1007/s00367-011-0266-7>
- Fettweis, M., Francken, F., Pison, V., Van den Eynde, D., 2006. Suspended particulate matter dynamics and aggregate sizes in a high turbidity area. *Marine Geology* 235, 63–74. <https://doi.org/10.1016/j.margeo.2006.10.005>
- Fettweis, M., Lee, B., 2017. Spatial and Seasonal Variation of Biomineral Suspended Particulate Matter Properties in High-Turbid Nearshore and Low-Turbid Offshore Zones. *Water* 9, 694. <https://doi.org/10.3390/w9090694>

- Fettweis, M., Riethmüller, R., Verney, R., Becker, M., Backers, J., Baeye, M., Chapalain, M., Claeys, S., Claus, J., Cox, T., Deloffre, J., Depreiter, D., Druine, F., Flöser, G., Grünler, S., Jourdin, F., Lafite, R., Nauw, J., Nechad, B., Röttgers, R., Sottolichio, A., Van Engeland, T., Vanhaverbeke, W., Vereecken, H., 2019. Uncertainties associated with in situ high-frequency long-term observations of suspended particulate matter concentration using optical and acoustic sensors. *Progress in Oceanography* 178, 102162. <https://doi.org/10.1016/j.pocean.2019.102162>
- Fick, S.S., Nakadi, F.V., Fujiwara, F., Smichowski, P., Vale, M.G.R., Welz, B., Andrade, J.B. de, 2018. Investigation of spectral interference in the determination of Pb in road dust using high-resolution continuum source graphite furnace atomic absorption spectrometry and direct solid sample analysis. *J. Anal. At. Spectrom.* 33, 593–602. <https://doi.org/10.1039/C7JA00405B>
- Folens, K., Du Laing, G., 2017. Dispersion and solubility of In, Tl, Ta and Nb in the aquatic environment and intertidal sediments of the Scheldt estuary (Flanders, Belgium). *Chemosphere* 183, 401–409. <https://doi.org/10.1016/j.chemosphere.2017.05.076>
- Förstner, U., Salomons, W., 1980. Trace metal analysis on polluted sediments. *Environmental Technology Letters* 1, 494–505. <https://doi.org/10.1080/09593338009384006>
- Förstner, U., Wittmann, G.T.W., 2012. *Metal Pollution in the Aquatic Environment*. Springer Science & Business Media.
- Foucher, J.-L., Bodenez, P., Ben Slimane, K., 2012. *Après-Mine en France. Congrès International sur la gestion des rejets miniers et l'après mine (GESRIM)* 8.
- Frank, M., 2011. Chemical twins, separated. *Nature Geoscience* 4, 220.
- Furman, E., Pihlajamäki, M., Välipakka, P., Myrberg, K., 2013. *The Baltic Sea: Environment and Ecology*.
- Gaillardet, J., Viers, J., Dupré, B., 2003. Trace Elements in River Waters, in: *Treatise on Geochemistry*. Elsevier, pp. 225–272. <https://doi.org/10.1016/B0-08-043751-6/05165-3>
- Gao, L., Gao, B., Xu, D., Liu, L., 2020. DGT: A promising technology for in-situ measurement of metal speciation in the environment. *Science of The Total Environment* 715, 136810. <https://doi.org/10.1016/j.scitotenv.2020.136810>
- Gao, Y., de Brauwere, A., Elskens, M., Croes, K., Baeyens, W., Leermakers, M., 2013. Evolution of trace metal and organic pollutant concentrations in the Scheldt River Basin and the Belgian Coastal Zone over the last three decades. *Journal of Marine Systems* 128, 52–61. <https://doi.org/10.1016/j.jmarsys.2012.04.002>
- Gao, Y., Leermakers, M., Gabelle, C., Divis, P., Billon, G., Ouddane, B., Fischer, J.-C., Wartel, M., Baeyens, W., 2006. High-resolution profiles of trace metals in the pore waters of riverine sediment assessed by DET and DGT. *Sci. Total Environ.* 362, 266–277. <https://doi.org/10.1016/j.scitotenv.2005.11.023>
- Gao, Y., van de Velde, S., Williams, P.N., Baeyens, W., Zhang, H., 2015. Two-dimensional images of dissolved sulfide and metals in anoxic sediments by

- a novel diffusive gradients in thin film probe and optical scanning techniques. *TrAC Trends in Analytical Chemistry* 66, 63–71.  
<https://doi.org/10.1016/j.trac.2014.11.012>
- Gao, Y., Zhou, C., Gaulier, C., Bratkic, A., Galceran, J., Puy, J., Zhang, H., Leermakers, M., Baeyens, W., 2019. Labile trace metal concentration measurements in marine environments: From coastal to open ocean areas. *TrAC Trends in Analytical Chemistry* 116, 92–101.  
<https://doi.org/10.1016/j.trac.2019.04.027>
- García, E.M., Cruz-Motta, J.J., Farina, O., Bastidas, C., 2008. Anthropogenic influences on heavy metals across marine habitats in the western coast of Venezuela. *Continental Shelf Research* 28, 2757–2766.  
<https://doi.org/10.1016/j.csr.2008.09.020>
- Garg, U., Smith, L.D., 2017. *Biomarkers in Inborn Errors of Metabolism: Clinical Aspects and Laboratory Determination*, Elsevier. ed, 1.
- Garneau, C., Sauvage, S., Sánchez-Pérez, J.-M., Lofts, S., Brito, D., Neves, R., Probst, A., 2017. Modelling trace metal transfer in large rivers under dynamic hydrology: A coupled hydrodynamic and chemical equilibrium model. *Environmental Modelling & Software* 89, 77–96.  
<https://doi.org/10.1016/j.envsoft.2016.11.018>
- Gaulier, C., Zhou, C., Guo, W., Bratkic, A., Superville, P.-J., Billon, G., Baeyens, W., Gao, Y., 2019a. Trace metal speciation in North Sea coastal waters. *Science of The Total Environment*.  
<https://doi.org/10.1016/j.scitotenv.2019.07.314>
- Gaulier, C., Zhou, C., Guo, W., Bratkic, A., Superville, P.-J., Billon, G., Baeyens, W., Gao, Y., 2019b. Trace metal speciation in North Sea coastal waters. *Science of The Total Environment* 692, 701–712.  
<https://doi.org/10.1016/j.scitotenv.2019.07.314>
- Geisler, C.-D., Schmidt, D., 1991. An overview of chromium in the marine environment. *Deutsche Hydrographische Zeitschrift* 44, 185–196.  
<https://doi.org/10.1007/BF02226462>
- Gelting, J., 2009. *Speciation of trace metals in the Baltic Sea with focus on the Euphotic zone (Doctoral Thesis)*. Luleå tekniska universitet, Luleå.
- Gelting, J., 2006. *Trace Metal Speciation in the Baltic Sea (Master Thesis)*. Luleå tekniska universitet.
- Giakisikli, G., Zachariadis, P., Kila, I., Teshima, N., Anthemidis, A., 2016. Flow Injection Solid Phase Extraction for Trace Metal Determination Using a Chelating Resin and Flame Atomic Absorption Spectrometry Detection. *Analytical Letters* 49, 929–942.  
<https://doi.org/10.1080/00032719.2015.1038547>
- Gilbert, D., 2012. Coal slag heaps join pyramids on World Heritage list. CNN.
- Gillain, G., Ooyckaerts, G., Disteche, A., 1979. The determination of trace metals in sea water and suspended matter by classical anodic stripping (Zn, Cd, Pb, Cu) or differential pulse anodic stripping voltammetry with a hanging mercury drop electrode (Zn, Cd, Pb, Cu, Sb and Bi). An approach to speciation. 59, 11.

- Goldhaber, M.B., Kaplan, I.R., 1980. Mechanisms of sulfur incorporation and isotope fractionation during early diagenesis in sediments of the gulf of California. *Marine Chemistry* 9, 95–143. [https://doi.org/10.1016/0304-4203\(80\)90063-8](https://doi.org/10.1016/0304-4203(80)90063-8)
- Goldman, J.C., Caron, D.A., Dennett, M.R., 1987. Regulation of gross growth efficiency and ammonium regeneration in bacteria by substrate C: N ratio 1: Ammonium regeneration by bacteria. *Limnology and Oceanography* 32, 1239–1252. <https://doi.org/10.4319/lo.1987.32.6.1239>
- Gonzalez, J.-L., Thouvenin, B., Dange, C., 2007. The role of particles in the behavior and speciation of trace metals: the cadmium example. *La Houille Blanche* 56–62. <https://doi.org/10.1051/lhb:2007047>
- Gorbi, G., Corradi, M.G., Invidia, M., Bassi, M., 2001. Light Intensity Influences Chromium Bioaccumulation and Toxicity in *Scenedesmus acutus* (Chlorophyceae). *Ecotoxicology and Environmental Safety* 48, 36–42. <https://doi.org/10.1006/eesa.2000.2000>
- Górecki, T., Namieśnik, J., 2002. Passive sampling. *TrAC Trends in Analytical Chemistry* 21, 276–291. [https://doi.org/10.1016/S0165-9936\(02\)00407-7](https://doi.org/10.1016/S0165-9936(02)00407-7)
- Granado-Castro, M.D., Casanueva-Marengo, M.J., Galindo-Riaño, M.D., El Mai, H., Díaz-de-Alba, M., 2018. A separation and preconcentration process for metal speciation using a liquid membrane: A case study for iron speciation in seawater. *Marine Chemistry* 198, 56–63. <https://doi.org/10.1016/j.marchem.2017.11.009>
- Grasse, P., Brzezinski, M.A., Cardinal, D., Souza, G.F. de, Andersson, P., Closset, I., Cao, Z., Dai, M., Ehlert, C., Estrade, N., François, R., Frank, M., Jiang, G., Jones, J.L., Kooijman, E., Liu, Q., Lu, D., Pahnke, K., Ponzevera, E., Schmitt, M., Sun, X., Sutton, J.N., Thil, F., Weis, D., Wetzel, F., Zhang, A., Zhang, J., Zhang, Z., 2017. GEOTRACES inter-calibration of the stable silicon isotope composition of dissolved silicic acid in seawater. *J. Anal. At. Spectrom.* 32, 562–578. <https://doi.org/10.1039/C6JA00302H>
- Green, N., 2003. Hazardous substances in the European marine environment: trends in metals and persistent organic pollutants, Topic report / European Environment Agency. Office for Official Publications of the European Communities ; Bernan Associates [distributor], Luxembourg : Lanham, Md.
- Grimwood, M.J., Dixon, E., 1997. Assessment of risks posed by List II metals to Sensitive Marine Areas (SMAs) and adequacy of existing environmental quality standards (EQSs) for SMA protection (No. WRc Report CO 4278/10435-0 to English Nature). UK Marine SAC Project, Life.
- Gustafsson, J.P., Persson, I., Oromieh, A.G., van Schaik, J.W.J., Sjöstedt, C., Kleja, D.B., 2014. Chromium(III) Complexation to Natural Organic Matter: Mechanisms and Modeling. *Environ. Sci. Technol.* 48, 1753–1761. <https://doi.org/10.1021/es404557e>
- Hansson, M., Viktorsson, L., Andersson, L., 2018. Oxygen Survey in the Baltic Sea 2018 - Extent of Anoxia and Hypoxia, 1960-2018.
- Happel, E., Bartl, I., Voss, M., Riemann, L., 2018. Extensive nitrification and active ammonia oxidizers in two contrasting coastal systems of the Baltic Sea.

- Environmental Microbiology 20, 2913–2926. <https://doi.org/10.1111/1462-2920.14293>
- Hargreaves, A.J., Vale, P., Whelan, J., Constantino, C., Dotro, G., Campo, P., Cartmell, E., 2017. Distribution of trace metals (Cu, Pb, Ni, Zn) between particulate, colloidal and truly dissolved fractions in wastewater treatment. *Chemosphere* 175, 239–246. <https://doi.org/10.1016/j.chemosphere.2017.02.034>
- Harmelin-Vivien, M., Loizeau, V., Mellon, C., Beker, B., Arlhac, D., Bodiguel, X., Ferraton, F., Hermand, R., Philippon, X., Salen-Picard, C., 2008. Comparison of C and N stable isotope ratios between surface particulate organic matter and microphytoplankton in the Gulf of Lions (NW Mediterranean). *Continental Shelf Research, Sediment Dynamics in the Gulf of Lions; the Impact of Extreme Events* 28, 1911–1919. <https://doi.org/10.1016/j.csr.2008.03.002>
- Hartnett, A., Böttger, L.H., Matzanke, B.F., Carrano, C.J., 2012. Iron transport and storage in the coccolithophore: *Emiliana huxleyi*. *Metallomics* 4, 1160–1166. <https://doi.org/10.1039/C2MT20144E>
- Hatje, V., 2003. Particulate trace metal and major element distributions over consecutive tidal cycles in Port Jackson Estuary, Australia. *Env Geol* 44, 231–239. <https://doi.org/10.1007/s00254-002-0750-5>
- He, M., Huang, L., Zhao, B., Chen, B., Hu, B., 2017. Advanced functional materials in solid phase extraction for ICP-MS determination of trace elements and their species - A review. *Analytica Chimica Acta* 973, 1–24. <https://doi.org/10.1016/j.aca.2017.03.047>
- Health Monitoring Institute, 2004. Utilisation des bio-indicateurs pour la surveillance des émissions et des risques. Institut de Veille Sanitaire.
- Heiskanen, A.-S., Bonsdorff, E., Joas, M., 2019. Chapter 20 - Baltic Sea: A Recovering Future From Decades of Eutrophication, in: Wolanski, E., Day, J.W., Elliott, M., Ramachandran, R. (Eds.), *Coasts and Estuaries*. Elsevier, pp. 343–362. <https://doi.org/10.1016/B978-0-12-814003-1.00020-4>
- Helali, M.A., Zaaboub, N., Oueslati, W., Added, A., Aleya, L., 2016. Suspended particulate matter fluxes along with their associated metals, organic matter and carbonates in a coastal Mediterranean area affected by mining activities. *Marine Pollution Bulletin* 104, 171–181. <https://doi.org/10.1016/j.marpolbul.2016.01.041>
- HELCOM, 2018. State of the Baltic Sea – Second HELCOM holistic assessment 2011-2016. *Baltic Sea Environment Proceedings*.
- Helgen, S.O., Moore, J.N., 1996. Natural Background Determination and Impact Quantification in Trace Metal-Contaminated River Sediments. *Environ. Sci. Technol.* 30, 129–135. <https://doi.org/10.1021/es950192b>
- Hellings, L., Dehairs, F., Tackx, M., Keppens, E., Baeyens, W., 1999. Origin and fate of organic carbon in the freshwater part of the Scheldt Estuary as traced by stable carbon isotope composition. *Biogeochemistry* 47, 167–186. <https://doi.org/10.1007/BF00994921>
- Helmond, N.A.G.M. van, Robertson, E.K., Conley, D.J., Hermans, M., Humborg, C., Kubeneck, L.J., Lenstra, W.K., Slomp, C.P., 2019. Efficient removal of

- phosphorus and nitrogen in sediments of the eutrophic Stockholm Archipelago, Baltic Sea. *Biogeosciences Discussions* 1–36. <https://doi.org/10.5194/bg-2019-376>
- Hering, D., Borja, A., Carstensen, J., Carvalho, L., Elliott, M., Feld, C.K., Heiskanen, A.-S., Johnson, R.K., Moe, J., Pont, D., Solheim, A.L., de Bund, W. van, 2010. The European Water Framework Directive at the age of 10: A critical review of the achievements with recommendations for the future. *Science of The Total Environment* 408, 4007–4019. <https://doi.org/10.1016/j.scitotenv.2010.05.031>
- Hermans, M., Lenstra, W.K., van Helmond, N.A.G.M., Behrends, T., Egger, M., Séguret, M.J.M., Gustafsson, E., Gustafsson, B.G., Slomp, C.P., 2019. Impact of natural re-oxygenation on the sediment dynamics of manganese, iron and phosphorus in a euxinic Baltic Sea basin. *Geochimica et Cosmochimica Acta* 246, 174–196. <https://doi.org/10.1016/j.gca.2018.11.033>
- Ho, H.H., Swennen, R., Van Damme, A., 2010. DISTRIBUTION AND CONTAMINATION STATUS OF HEAVY METALS IN ESTUARINE SEDIMENTS NEAR CUA ONG HARBOR, HA LONG BAY, VIETNAM. *GEOLOGICA BELGICA* 37–47.
- Ho, T.-Y., Quigg, A., Finkel, Z.V., Milligan, A.J., Wyman, K., Falkowski, P.G., Morel, F.M.M., 2003. The Elemental Composition of Some Marine Phytoplankton. *Journal of Phycology* 39, 1145–1159. <https://doi.org/10.1111/j.0022-3646.2003.03-090.x>
- Hobbie, J.E., 2000. *Estuarine Science: A Synthetic Approach to Research and Practice*. Island Press.
- Hodkinson, I.D., Jackson, J.K., 2005. Terrestrial and Aquatic Invertebrates as Bioindicators for Environmental Monitoring, with Particular Reference to Mountain Ecosystems. *Environmental Management* 35, 649–666. <https://doi.org/10.1007/s00267-004-0211-x>
- Hodson, M.E., 2004. Heavy metals—geochemical bogey men? *Environmental Pollution* 129, 341–343. <https://doi.org/10.1016/j.envpol.2003.11.003>
- Höflich, K., Lehmann, A., Myrberg, K., 2017. Towards an improved mechanistic understanding of major saltwater inflows into the Baltic Sea 19, 18430.
- Holmes, J., Pathirathna, P., Hashemi, P., 2019. Novel frontiers in voltammetric trace metal analysis: Towards real time, on-site, in situ measurements. *TrAC Trends in Analytical Chemistry* 111, 206–219. <https://doi.org/10.1016/j.trac.2018.11.003>
- Howe, P.D., Malcolm, H.M., Dobson, S., 2004. Manganese and its compounds: environmental aspects, Concise international chemical assessment document. World Health Organization, Geneva.
- Hume, S., Caron, F., Siemann, S., 2018. Binding of Cu, Co, and Cs to fluorescent components of natural organic matter (NOM) from three contrasting sites. *Environ Sci Pollut Res* 25, 20141–20153. <https://doi.org/10.1007/s11356-018-2181-1>
- Hutchins, D.A., Bruland, K.W., 1995. Fe, Zn, Mn and N transfer between size classes in a coastal phytoplankton community: Trace metal and major

- nutrient recycling compared [WWW Document].  
<https://doi.org/info:doi/10.1357/0022240953213197>
- Huysman, S., 2019. Development and validation of high-resolution mass spectrometry-based approaches for active and passive sampling of emerging organic micropollutants in the marine environment (Doctoral Thesis). Ghent University, Ghent.
- Iglesias, I., Almeida, C.M.R., Teixeira, C., Mucha, A.P., Magalhães, A., Bio, A., Bastos, L., 2020. Linking contaminant distribution to hydrodynamic patterns in an urban estuary: The Douro estuary test case. *Science of The Total Environment* 707, 135792.  
<https://doi.org/10.1016/j.scitotenv.2019.135792>
- Illuminati, S., Annibaldi, A., Truzzi, C., Tercier-Waeber, M.-L., Noël, S., Braungardt, C.B., Achterberg, E.P., Howell, K.A., Turner, D., Marini, M., Romagnoli, T., Totti, C., Confalonieri, F., Graziottin, F., Buffle, J., Scarponi, G., 2019a. In-situ trace metal (Cd, Pb, Cu) speciation along the Po River plume (Northern Adriatic Sea) using submersible systems. *Marine Chemistry* 212, 47–63. <https://doi.org/10.1016/j.marchem.2019.04.001>
- Illuminati, S., Annibaldi, A., Truzzi, C., Tercier-Waeber, M.-L., Noël, S., Braungardt, C.B., Achterberg, E.P., Howell, K.A., Turner, D., Marini, M., Romagnoli, T., Totti, C., Confalonieri, F., Graziottin, F., Buffle, J., Scarponi, G., 2019b. In-situ trace metal (Cd, Pb, Cu) speciation along the Po River plume (Northern Adriatic Sea) using submersible systems. *Marine Chemistry*. <https://doi.org/10.1016/j.marchem.2019.04.001>
- Ivanov, L.I., Oguz, T., 1998. Ecosystem Modeling as a Management Tool for the Black Sea: [Proceedings of the NATO TU Black Sea Project, Ecosystem Modeling as a Management Tool for the Black Sea, Zori Rossii, Ukraine, 15-19 June, 1997]. Springer Science & Business Media.
- Jacks, G., Nystrand, M., 2019. Speciation of trace elements in groundwater, surface water and sediments: a short review. *Environ Earth Sci* 78, 349.  
<https://doi.org/10.1007/s12665-019-8334-9>
- Jago, C.F., Jones, S.E., Latter, R.J., McCandliss, R.R., Hearn, M.R., Howarth, M.J., 2002. Resuspension of benthic fluff by tidal currents in deep stratified waters, northern North Sea. *Journal of Sea Research, Processes of Vertical Exchange in Shelf Seas (PROVCESS), PART II* 48, 259–269.  
[https://doi.org/10.1016/S1385-1101\(02\)00181-8](https://doi.org/10.1016/S1385-1101(02)00181-8)
- Jakimska, A., Konieczka, P., Skóra, K., Namieśnik, J., 2011. Bioaccumulation of Metals in Tissues of Marine Animals, Part I: the Role and Impact of Heavy Metals on Organisms. *Pol. J. Environ. Stud.* 20, 1117–1125.
- Jäntti, H., Ward, B.B., Dippner, J.W., Hietanen, S., 2018. Nitrification and the ammonia-oxidizing communities in the central Baltic Sea water column. *Estuarine, Coastal and Shelf Science* 202, 280–289.  
<https://doi.org/10.1016/j.ecss.2018.01.019>
- Jilbert, T., Asmala, E., Schröder, C., Tiihonen, R., Myllykangas, J.-P., Virtasalo, J.J., Kotilainen, A., Peltola, P., Ekholm, P., Hietanen, S., 2017. Flocculation of dissolved organic matter controls the distribution of iron in

- boreal estuarine sediments (Discussion Paper). *Biogeosciences Discussions*. <https://doi.org/10.5194/bg-2017-181>
- Jilbert, T., Slomp, C.P., 2013. Iron and manganese shuttles control the formation of authigenic phosphorus minerals in the euxinic basins of the Baltic Sea. *Geochimica et Cosmochimica Acta* 107, 155–169. <https://doi.org/10.1016/j.gca.2013.01.005>
- Johnson, A., Lovenduski, N.S., Krumhardt, K.M., 2018. Coccolithophore calcium carbonate export in an acidified ocean. AGU Fall Meeting Abstracts 41.
- Jones, B., Bolam, T., 2007. Copper speciation survey from UK marinas, harbours and estuaries. *Marine Pollution Bulletin* 54, 1127–1138. <https://doi.org/10.1016/j.marpolbul.2007.04.021>
- Jonnalagadda, S.B., Rao, P.V.V.P., 1993. Toxicity, bioavailability and metal speciation. *Comparative Biochemistry and Physiology Part C: Pharmacology, Toxicology and Endocrinology* 106, 585–595. [https://doi.org/10.1016/0742-8413\(93\)90215-7](https://doi.org/10.1016/0742-8413(93)90215-7)
- Journal Officiel de la République Française, 2018. Décrets, arrêtés, circulaires - Textes généraux du Ministère de la Transition Ecologique et Solidaire (Décrets No. TREL1819388A). Ministère de la Transition Ecologique et Solidaire.
- Kahlon, S.K., Sharma, G., Julka, J.M., Kumar, A., Sharma, S., Stadler, F.J., 2018. Impact of heavy metals and nanoparticles on aquatic biota. *Environ Chem Lett* 16, 919–946. <https://doi.org/10.1007/s10311-018-0737-4>
- Kalaydjian, R., Girard, S., 2017. Données économiques maritimes françaises 2016. Ifremer. <https://doi.org/10.13155/49962>
- Källqvist, T., 2007. PNEC for metals in the marine environment derived from species sensitivity distributions (No. Report SNO 5336-2007, 27053). Norwegian Institute for Water Research.
- Kennish, M.J., 1998. Pollution impacts on marine biotic communities, Marine science series. CRC Press, Boca Raton, Fla.
- Kennish, M.J., 1994. Pollution in Estuaries and Coastal Marine Waters. *Journal of Coastal Research* 27–49.
- Kerr, J.G., Cooke, C.A., 2017. Erosion of the Alberta badlands produces highly variable and elevated heavy metal concentrations in the Red Deer River, Alberta. *Science of The Total Environment* 596–597, 427–436. <https://doi.org/10.1016/j.scitotenv.2017.04.037>
- Kim, J.H., Gibb, H.J., Howe, P., Sheffer, M., 2006. Cobalt and inorganic cobalt compounds, Concise international chemical assessment document. World Health Organization, Geneva.
- Klawonn, I., Bonaglia, S., Whitehouse, M.J., Littmann, S., Tienken, D., Kuypers, M.M.M., Brüchert, V., Ploug, H., 2019. Untangling hidden nutrient dynamics: rapid ammonium cycling and single-cell ammonium assimilation in marine plankton communities. *ISME J* 13, 1960–1974. <https://doi.org/10.1038/s41396-019-0386-z>
- Komjarova, I., 2009. Uptake of Trace Metals in Aquatic Organisms: a Stable Isotopes Experiment (Doctoral Thesis). University of Antwerp, Antwerp.



- Komjarova, I., Blust, R., 2006. Comparison of liquid–liquid extraction, solid-phase extraction and co-precipitation preconcentration methods for the determination of cadmium, copper, nickel, lead and zinc in seawater. *Analytica Chimica Acta* 576, 221–228. <https://doi.org/10.1016/j.aca.2006.06.002>
- Korpinen, S., Meski, L., Andersen, J.H., Laamanen, M., 2012. Human pressures and their potential impact on the Baltic Sea ecosystem. *Ecological Indicators* 15, 105–114. <https://doi.org/10.1016/j.ecolind.2011.09.023>
- Kremling, K., 1983. The behavior of Zn, Cd, Cu, Ni, Co, Fe, and Mn in anoxic baltic waters. *Marine Chemistry* 13, 87–108. [https://doi.org/10.1016/0304-4203\(83\)90019-1](https://doi.org/10.1016/0304-4203(83)90019-1)
- Kummu, M., Moel, H. de, Salvucci, G., Viviroli, D., Ward, P.J., Varis, O., 2016. Over the hills and further away from coast: global geospatial patterns of human and environment over the 20th–21st centuries. *Environ. Res. Lett.* 11, 034010. <https://doi.org/10.1088/1748-9326/11/3/034010>
- Kuss, J., Cordes, F., Mohrholz, V., Nausch, G., Naumann, M., Krüger, S., Schulz-Bull, D.E., 2017. The Impact of the Major Baltic Inflow of December 2014 on the Mercury Species Distribution in the Baltic Sea. *Environ. Sci. Technol.* 51, 11692–11700. <https://doi.org/10.1021/acs.est.7b03011>
- Lagerström, M., Ferreira, J., Ytreberg, E., Eriksson-Wiklund, A.-K., 2020. Flawed risk assessment of antifouling paints leads to exceedance of guideline values in Baltic Sea marinas. *Environmental Science and Pollution Research*. <https://doi.org/10.1007/s11356-020-08973-0>
- Landner, L., Reuther, R., 2004. Metals in society and in the environment: a critical review of current knowledge on fluxes, speciation, bioavailability and risk for adverse effects of copper, chromium, nickel and zinc, *Environmental pollution*. Kluwer Academic Publ, Dordrecht.
- Lara, R.J., Alder, V., Franzosi, C.A., Kattner, G., 2010. Characteristics of suspended particulate organic matter in the southwestern Atlantic: Influence of temperature, nutrient and phytoplankton features on the stable isotope signature. *Journal of Marine Systems* 79, 199–209. <https://doi.org/10.1016/j.jmarsys.2009.09.002>
- Laslett, R.E., 1995. Concentrations of dissolved and suspended particulate Cd, Cu, Mn, Ni, Pb and Zn in surface waters around the coasts of England and Wales and in adjacent seas. *Estuarine, Coastal and Shelf Science* 40, 67–85. [https://doi.org/10.1016/0272-7714\(95\)90014-4](https://doi.org/10.1016/0272-7714(95)90014-4)
- Lau, J.D., Hicks, C.C., Gurney, G.G., Cinner, J.E., 2019. What matters to whom and why? Understanding the importance of coastal ecosystem services in developing coastal communities. *Ecosystem Services* 35, 219–230. <https://doi.org/10.1016/j.ecoser.2018.12.012>
- Lau, W.W.Y., 2013. Beyond carbon: Conceptualizing payments for ecosystem services in blue forests on carbon and other marine and coastal ecosystem services. *Ocean & Coastal Management* 83, 5–14. <https://doi.org/10.1016/j.ocecoaman.2012.03.011>

- Lauvset, S.K., Gruber, N., 2014. Long-term trends in surface ocean pH in the North Atlantic. *Marine Chemistry* 162, 71–76. <https://doi.org/10.1016/j.marchem.2014.03.009>
- Laws, E.A., Popp, B.N., Bidigare, R.R., Riebesell, U., Burkhardt, S., Wakeham, S.G., 2001. Controls on the molecular distribution and carbon isotopic composition of alkenones in certain haptophyte algae. *Geochemistry, Geophysics, Geosystems* 2. <https://doi.org/10.1029/2000GC000057>
- Lee, A.A., Bukaveckas, P.A., 2002. Surface water nutrient concentrations and litter decomposition rates in wetlands impacted by agriculture and mining activities. *Aquatic Botany* 74, 273–285. [https://doi.org/10.1016/S0304-3770\(02\)00128-6](https://doi.org/10.1016/S0304-3770(02)00128-6)
- Lee, A.J., 1980. Chapter 14 North Sea: Physical Oceanography, in: Banner, F.T., Collins, M.B., Massie, K.S. (Eds.), Elsevier Oceanography Series, The North-West European Shelf Seas: The Sea Bed and the Sea in Motion II. Physical and Chemical Oceanography, and Physical Resources. Elsevier, pp. 467–493. [https://doi.org/10.1016/S0422-9894\(08\)71359-X](https://doi.org/10.1016/S0422-9894(08)71359-X)
- Leermakers, M., Galletti, S., De Galan, S., Brion, N., Baeyens, W., 2001. Mercury in the Southern North Sea and Scheldt estuary. *Marine Chemistry* 75, 229–248. [https://doi.org/10.1016/S0304-4203\(01\)00039-1](https://doi.org/10.1016/S0304-4203(01)00039-1)
- Lefèvre, I., Marchal, G., Meerts, P., Corréal, E., Lutts, S., 2009. Chloride salinity reduces cadmium accumulation by the Mediterranean halophyte species *Atriplex halimus* L. *Environmental and Experimental Botany* 65, 142–152. <https://doi.org/10.1016/j.envexpbot.2008.07.005>
- Legifrance, 2015. Arrêté du 27 juillet 2015 modifiant l'arrêté du 25 janvier 2010 relatif aux méthodes et critères d'évaluation de l'état écologique, de l'état chimique et du potentiel écologique des eaux de surface pris en application des articles R. 212-10, R. 212-11 et R. 212-18 du code de l'environnement.
- Lehmann, A., Hinrichsen, H.-H., Getzlaff, K., Myrberg, K., 2014. Quantifying the heterogeneity of hypoxic and anoxic areas in the Baltic Sea by a simplified coupled hydrodynamic-oxygen consumption model approach. *Journal of Marine Systems* 134, 20–28. <https://doi.org/10.1016/j.jmarsys.2014.02.012>
- Lenstra, W.K., Hermans, M., Séguret, M.J.M., Witbaard, R., Behrends, T., Dijkstra, N., van Helmond, N.A.G.M., Kraal, P., Laan, P., Rijkenberg, M.J.A., Severmann, S., Teacă, A., Slomp, C.P., 2019. The shelf-to-basin iron shuttle in the Black Sea revisited. *Chemical Geology* 511, 314–341. <https://doi.org/10.1016/j.chemgeo.2018.10.024>
- Lenstra, W.K., Séguret, M.J.M., Behrends, T., Groeneveld, R.K., Hermans, M., Witbaard, R., Slomp, C.P., 2020. Controls on the shuttling of manganese over the northwestern Black Sea shelf and its fate in the euxinic deep basin. *Geochimica et Cosmochimica Acta* 273, 177–204. <https://doi.org/10.1016/j.gca.2020.01.031>
- Lenz, C., Jilbert, T., Conley, D.J., Wolthers, M., Slomp, C.P., 2015. Are recent changes in sediment manganese sequestration in the euxinic basins of the Baltic Sea linked to the expansion of hypoxia? *Biogeosciences* 12, 4875–4894. <https://doi.org/10.5194/bg-12-4875-2015>

- Leppäranta, M., Myrberg, K., 2009. *Physical Oceanography of the Baltic Sea*. Springer Science & Business Media.
- Lesven, L., 2008. Devenir des éléments traces métalliques au sein du sédiment, un compartiment clé de l'environnement aquatique. Université des Sciences et Technologies de Lille, Lille, France.
- Li, Y., Rothwell, S., Cheng, H., Jones, K.C., Zhang, H., 2019. Bioavailability and metabolism in a soil-crop system compared using DGT and conventional extraction techniques. *Environment International* 130, 104924. <https://doi.org/10.1016/j.envint.2019.104924>
- Liang, P., Liu, Y., Guo, L., Zeng, J., Lu, H., 2004. Multiwalled carbon nanotubes as solid-phase extraction adsorbent for the preconcentration of trace metal ions and their determination by inductively coupled plasma atomic emission spectrometry. *J. Anal. At. Spectrom.* 19, 1489–1492. <https://doi.org/10.1039/B409619C>
- Liang, Y., Zhang, G., Wan, A., Zhao, Z., Wang, S., Liu, Q., 2019. Nutrient-limitation induced diatom-dinoflagellate shift of spring phytoplankton community in an offshore shellfish farming area. *Marine Pollution Bulletin* 141, 1–8. <https://doi.org/10.1016/j.marpolbul.2019.02.009>
- Liblik, T., Naumann, M., Alenius, P., Hansson, M., Lips, U., Nausch, G., Tuomi, L., Wesslander, K., Laanemets, J., Viktorsson, L., 2018. Propagation of Impact of the Recent Major Baltic Inflows From the Eastern Gotland Basin to the Gulf of Finland. *Front. Mar. Sci.* 5. <https://doi.org/10.3389/fmars.2018.00222>
- Linnik, P.N., Zhezherya, V.A., Linnik, R.P., 2018. Lability of Metals in Surface Waters as the Main Characteristics of Their Potential Bioavailability (a Review). *Hydrobiological Journal* 54, 3–26. <https://doi.org/10.1615/HydrobJ.v54.i6.10>
- Liu, J., Song, J., Yuan, H., Li, X., Li, N., Duan, L., 2019. Trace metal comparative analysis of sinking particles and sediments from a coastal environment of the Jiaozhou Bay, North China: Influence from sediment resuspension. *Chemosphere* 232, 315–326. <https://doi.org/10.1016/j.chemosphere.2019.05.090>
- Loring, D.H., Rantala, R.T.T., 1992. Manual for the geochemical analyses of marine sediments and suspended particulate matter. *Earth-Science Reviews* 32, 235–283. [https://doi.org/10.1016/0012-8252\(92\)90001-A](https://doi.org/10.1016/0012-8252(92)90001-A)
- Louis, Y., 2008. Achievement of a characterisation protocol for dissolved natural organic matter (DNOM) / metallic contaminants interactions (Doctoral Thesis). Université du Sud Toulon Var, Toulon.
- Lourino-Cabana, B., Billon, G., Lesven, L., Sabbe, K., Gillan, D.-C., Gao, Y., Leermakers, M., Baeyens, W., 2014. Monthly variation of trace metals in North Sea sediments. From experimental data to modeling calculations. *Marine Pollution Bulletin* 87, 237–246. <https://doi.org/10.1016/j.marpolbul.2014.07.053>
- Luoma, S.N., Rainbow, P.S., 2011. *Metal Contamination in Aquatic Environments: Science and Lateral Management*. Cambridge University Press.

- Luther, G.W., Rickard, D.T., 2005. Metal Sulfide Cluster Complexes and their Biogeochemical Importance in the Environment. *J Nanopart Res* 7, 389–407. <https://doi.org/10.1007/s11051-005-4272-4>
- Lyons, T.W., Severmann, S., 2006. A critical look at iron paleoredox proxies: New insights from modern euxinic marine basins. *Geochimica et Cosmochimica Acta*, A Special Issue Dedicated to Robert A. Berner 70, 5698–5722. <https://doi.org/10.1016/j.gca.2006.08.021>
- Maerz, J., Hofmeister, R., van der Lee, E.M., Gräwe, U., Riethmüller, R., Wirtz, K.W., 2016. Maximum sinking velocities of suspended particulate matter in a coastal transition zone. *Biogeosciences* 13, 4863–4876. <https://doi.org/10.5194/bg-13-4863-2016>
- Magnusson, B., Westerlund, S., 1980. The determination of Cd, Cu, Fe, Ni, Pb and Zn in Baltic Sea water. *Marine Chemistry* 8, 231–244. [https://doi.org/10.1016/0304-4203\(80\)90012-2](https://doi.org/10.1016/0304-4203(80)90012-2)
- Maity, S., Sahu, S.K., Pandit, G.G., 2017. Determination of Traces of Pb, Cu and Cd in Seawater around Thane Creek by Anodic Stripping Voltammetry Method. *Bull Environ Contam Toxicol* 98, 534–538. <https://doi.org/10.1007/s00128-016-2025-y>
- Mangal, V., Zhu, Y., Shi, Y.X., Guéguen, C., 2016. Assessing cadmium and vanadium accumulation using diffusive gradient in thin-films (DGT) and phytoplankton in the Churchill River estuary, Manitoba. *Chemosphere* 163, 90–98. <https://doi.org/10.1016/j.chemosphere.2016.08.008>
- Manning, A.J., Langston, W.J., Jonas, P.J.C., 2010. A review of sediment dynamics in the Severn Estuary: Influence of flocculation. *Marine Pollution Bulletin*, The Severn Estuary and Bristol Channel: A 25 year critical review 61, 37–51. <https://doi.org/10.1016/j.marpolbul.2009.12.012>
- Martínez, M.L., Intralawan, A., Vázquez, G., Pérez-Maqueo, O., Sutton, P., Landgrave, R., 2007. The coasts of our world: Ecological, economic and social importance. *Ecological Economics*, Ecological Economics of Coastal Disasters 63, 254–272. <https://doi.org/10.1016/j.ecolecon.2006.10.022>
- Martino, M., Turner, A., Nimmo, M., 2004. Distribution, speciation and particle-water interactions of nickel in the Mersey Estuary, UK. *Marine Chemistry* 88, 161–177. <https://doi.org/10.1016/j.marchem.2004.03.007>
- Mason, R.P., 2013. Trace Metals in Aquatic Systems. John Wiley & Sons.
- Matthiessen, P., Reed, J., Johnson, M., 1999. Sources and Potential Effects of Copper and Zinc Concentrations in the Estuarine Waters of Essex and Suffolk, United Kingdom. *Marine Pollution Bulletin* 38, 908–920. [https://doi.org/10.1016/S0025-326X\(99\)00090-9](https://doi.org/10.1016/S0025-326X(99)00090-9)
- Maycock, D., Merrington, G., Peters, A., 2011. Proposed EQS for Water Framework Directive Annex VIII substances: copper (saltwater) (For consultation) (No. SC080021/8n). Water Framework Directive - United Kingdom Technical Advisory Group.
- Meire, P., Ysebaert, T., Damme, S.V., Bergh, E.V. den, Maris, T., Struyf, E., 2005. The Scheldt estuary: a description of a changing ecosystem. *Hydrobiologia* 540, 1–11. <https://doi.org/10.1007/s10750-005-0896-8>

- Menegário, A.A., Yabuki, L.N.M., Luko, K.S., Williams, P.N., Blackburn, D.M., 2017. Use of diffusive gradient in thin films for in situ measurements: A review on the progress in chemical fractionation, speciation and bioavailability of metals in waters. *Analytica Chimica Acta* 983, 54–66. <https://doi.org/10.1016/j.aca.2017.06.041>
- Michael, H.A., Mulligan, A.E., Harvey, C.F., 2005. Seasonal oscillations in water exchange between aquifers and the coastal ocean. *Nature* 436, 1145–1148. <https://doi.org/10.1038/nature03935>
- Middelburg, J.J., Nieuwenhuize, J., 1998. Carbon and nitrogen stable isotopes in suspended matter and sediments from the Schelde Estuary. *Marine Chemistry* 60, 217–225. [https://doi.org/10.1016/S0304-4203\(97\)00104-7](https://doi.org/10.1016/S0304-4203(97)00104-7)
- Middelburg, J.J., Vlug, T., Jaco, F., van der Nat, W.A., 1993. Organic matter mineralization in marine systems. *Global and Planetary Change* 8, 47–58. [https://doi.org/10.1016/0921-8181\(93\)90062-S](https://doi.org/10.1016/0921-8181(93)90062-S)
- Migné, A., Davoult, D., Gattuso, J., 1998. Calcium carbonate production of a dense population of the brittle star *Ophiothrix fragilis* (Echinodermata:Ophiuroidea):role in the carbon cycle of a temperate coastal ecosystem. *Marine Ecology Progress Series* 173, 305–308. <https://doi.org/10.3354/meps173305>
- Mills, G., Gravell, A., 2015. Active and Passive Sampling for Pollutants of Emerging Concern.
- Mirzaei, M., Behzadi, M., Abadi, N.M., Beizaei, A., 2011. Simultaneous separation/preconcentration of ultra trace heavy metals in industrial wastewaters by dispersive liquid–liquid microextraction based on solidification of floating organic drop prior to determination by graphite furnace atomic absorption spectrometry. *Journal of Hazardous Materials* 186, 1739–1743. <https://doi.org/10.1016/j.jhazmat.2010.12.080>
- Mohrholz, V., 2018. Major Baltic Inflow Statistics – Revised. *Front. Mar. Sci.* 5. <https://doi.org/10.3389/fmars.2018.00384>
- Mohrholz, V., Naumann, M., Nausch, G., Krüger, S., Gräwe, U., 2015. Fresh oxygen for the Baltic Sea — An exceptional saline inflow after a decade of stagnation. *Journal of Marine Systems* 148, 152–166. <https://doi.org/10.1016/j.jmarsys.2015.03.005>
- Monterroso, C., Macias, F., 1998. Drainage waters affected by pyrite oxidation in a coal mine in Galicia Ž NW Spain. : Composition and mineral stability. *Science of The Total Environment* 121–132.
- Moos, S.B., Boyle, E.A., Altabet, M.A., Bourbonnais, A., 2020. Investigating the cycling of chromium in the oxygen deficient waters of the Eastern Tropical North Pacific Ocean and the Santa Barbara Basin using stable isotopes. *Marine Chemistry* 103756. <https://doi.org/10.1016/j.marchem.2020.103756>
- Morabito, E., Radaelli, M., Corami, F., Turetta, C., Toscano, G., Capodaglio, G., 2018. Temporal evolution of cadmium, copper and lead concentration in the Venice Lagoon water in relation with the speciation and dissolved/particulate partition. *Marine Pollution Bulletin* 129, 884–892. <https://doi.org/10.1016/j.marpolbul.2017.10.043>

- Morel, F.M.M., Price, N.M., 2003. The Biogeochemical Cycles of Trace Metals in the Oceans. *Science* 300, 944–947. <https://doi.org/10.1126/science.1083545>
- Morris, A.W., Bale, A.J., Howland, R.J.M., Millward, G.E., Ackroyd, D.R., Loring, D.H., Rantala, R.T.T., 1986. Sediment Mobility and its Contribution to Trace Metal Cycling and Retention in a Macrotidal Estuary. *Water Sci Technol* 18, 111–119. <https://doi.org/10.2166/wst.1986.0186>
- Morrison, G.M.P., Batley, G.E., Florence, T.M., 1989. Metal Speciation and Toxicity. *Chemistry in Britain* 791–796.
- Morse, J.W., Luther, G.W., 1999. Chemical influences on trace metal-sulfide interactions in anoxic sediments. *Geochimica et Cosmochimica Acta* 63, 3373–3378. [https://doi.org/10.1016/S0016-7037\(99\)00258-6](https://doi.org/10.1016/S0016-7037(99)00258-6)
- Muysen, B.T.A., Brix, K.V., DeForest, D.K., Janssen, C.R., 2004. Nickel essentiality and homeostasis in aquatic organisms. *Environmental Reviews* 12, 113–131. <https://doi.org/10.1139/a04-004>
- Naithani, J., de Brye, B., Buyze, E., Vyverman, W., Legat, V., Deleersnijder, E., 2016. An ecological model for the Scheldt estuary and tidal rivers ecosystem: spatial and temporal variability of plankton. *Hydrobiologia* 775, 51–67. <https://doi.org/10.1007/s10750-016-2710-1>
- Namieśnik, J., Zabiegała, B., Kot-Wasik, A., Partyka, M., Wasik, A., 2005. Passive sampling and/or extraction techniques in environmental analysis: a review. *Analytical and Bioanalytical Chemistry* 381, 279–301. <https://doi.org/10.1007/s00216-004-2830-8>
- NASA Earth Observations, 2020. Chlorophyll Concentration (1 month - Aqua/MODIS) | NASA [WWW Document]. Chlorophyll Concentration (1 month - Aqua/MODIS) | NASA. URL [https://neo.sci.gsfc.nasa.gov/view.php?datasetId=MY1DMM\\_CHLORA&date=2016-03-05](https://neo.sci.gsfc.nasa.gov/view.php?datasetId=MY1DMM_CHLORA&date=2016-03-05) (accessed 4.22.20).
- National Research Council (U.S.), 1977. Fates of Pollutants: Research and Development Needs, Commission on Natural Resources. ed. National Academies.
- National Research Council (US) Commission on Natural Resources, 1977. Fates of Pollutants: Research and Development Needs. National Academies.
- Ndungu, K., Hurst, M.P., Bruland, K.W., 2005. Comparison of Copper Speciation in Estuarine Water Measured Using Analytical Voltammetry and Supported Liquid Membrane Techniques. *Environ. Sci. Technol.* 39, 3166–3175. <https://doi.org/10.1021/es0483948>
- Neretin, L.N., Pohl, C., Jost, G., Leipe, T., Pollehne, F., 2003. Manganese cycling in the Gotland Deep, Baltic Sea. *Marine Chemistry* 82, 125–143. [https://doi.org/10.1016/S0304-4203\(03\)00048-3](https://doi.org/10.1016/S0304-4203(03)00048-3)
- Nieboer, E., Richardson, D.H.S., 1980. The replacement of the nondescript term ‘heavy metals’ by a biologically and chemically significant classification of metal ions. *Environmental Pollution Series B, Chemical and Physical* 1, 3–26. [https://doi.org/10.1016/0143-148X\(80\)90017-8](https://doi.org/10.1016/0143-148X(80)90017-8)
- Nihoul, J.C.J., Hecq, J.H., 1984. Influence of the residual circulation on the physico-chemical characteristics of water masses and the dynamics of ecosystems in

- the Belgian coastal zone. *Continental Shelf Research* 3, 167–174.  
[https://doi.org/10.1016/0278-4343\(84\)90005-0](https://doi.org/10.1016/0278-4343(84)90005-0)
- Nolting, R.F., Eisma, D., 1988. Elementary composition of suspended particulate matter in the North Sea. *Netherlands Journal of Sea Research* 22, 219–236.  
[https://doi.org/10.1016/0077-7579\(88\)90026-9](https://doi.org/10.1016/0077-7579(88)90026-9)
- Nordberg, G.F., 1978. Factors influencing metabolism and toxicity of metals: a consensus report. *Environmental Health Perspectives* 25, 3–41.  
<https://doi.org/10.1289/ehp.25-1637186>
- North Department Council, 2012. Plan de gestion du terril de l’Escarpelle et des Paturelles 2012-2017. Direction de l’Environnement, Service Espaces Naturels Sensibles.
- O’Connor, J.T., 1974. Removal of trace inorganic constituents by conventional water treatment processes. *Proc. 16th Water Qual. Conf., Trace Metal in Water Supplies: Occurrence, Significance and Control* 99–110.
- Official Journal of the European Communities, 2000. Directive 2000/60/EC Of The European Parliament And Of The Council, 2000/60/EC.
- Official Journal of the European Union, 2006. Regulation (EC) No 1907/2006 of the European Parliament and of the Council of 18 December 2006 concerning the Registration, Evaluation, Authorisation and Restriction of Chemicals (REACH), establishing a European Chemicals Agency, amending Directive 1999/45/EC and repealing Council Regulation (EEC) No 793/93 and Commission Regulation (EC) No 1488/94 as well as Council Directive 76/769/EEC and Commission Directives 91/155/EEC, 93/67/EEC, 93/105/EC and 2000/21/EC, OJ L.
- Orians, K.J., Boyle, E.A., 1993. Determination of picomolar concentrations of titanium, gallium and indium in sea water by inductively coupled plasma mass spectrometry following an 8-hydroxyquinoline chelating resin preconcentration. *Analytica Chimica Acta* 282, 63–74.
- OSPAR, 2019. OSPAR Commission | Protecting and conserving the North-East Atlantic and its resources [WWW Document]. OSPAR Commission. URL <https://www.ospar.org/> (accessed 7.15.19).
- OSPAR, 2009. Background document on Lead.
- OSPAR, 2002. Background Document on Cadmium.
- OSPAR, 1996. Report of the Third OSPAR Workshop on Ecotoxicological Assessment Criteria.
- Osvath, I., Samiei, M., Valkunas, L., Zlatnansky, J., 2001. IAEA PROJECTS HELP ASSESS THE SEA’S MARINE ENVIRONMENT. *IAEA BULLETIN* 7.
- Oueslati, W., Helali, M.A., Zaaboub, N., Sebei, A., Added, A., Aleya, L., 2018. Sulfide influence on metal behavior in a polluted southern Mediterranean lagoon: implications for management. *Environ Sci Pollut Res* 25, 2248–2264. <https://doi.org/10.1007/s11356-017-0529-6>
- Pađan, J., Marcinek, S., Cindrić, A.-M., Layglon, N., Lenoble, V., Salaün, P., Garnier, C., Omanović, D., 2019. Improved voltammetric methodology for chromium redox speciation in estuarine waters. *Analytica Chimica Acta* 1089, 40–47. <https://doi.org/10.1016/j.aca.2019.09.014>

- Paller, M.H., Harmon, S.M., Knox, A.S., Kuhne, W.W., Halverson, N.V., 2019. Assessing effects of dissolved organic carbon and water hardness on metal toxicity to *Ceriodaphnia dubia* using diffusive gradients in thin films (DGT). *Science of The Total Environment* 697, 134107. <https://doi.org/10.1016/j.scitotenv.2019.134107>
- Paquin, P.R., Farley, K., Santore, R.C., Kavadas, C.D., Money, C.G., Wu, K.-B., Di Toro, D.M., 2003. Metals in aquatic systems: A review of exposure, bioaccumulation, and toxicity models, SETAC. ed, Metals and the environment series. Society of Environmental Toxicology and Chemistry, Pensacola, FL.
- Parham, H., Pourreza, N., Rahbar, N., 2009. Solid phase extraction of lead and cadmium using solid sulfur as a new metal extractor prior to determination by flame atomic absorption spectrometry. *Journal of Hazardous Materials* 163, 588–592. <https://doi.org/10.1016/j.jhazmat.2008.07.007>
- Park, C., 2007. Definition of Pollutant, in: *A Dictionary of Environment and Conservation*. Oxford University Press.
- Parmentier, K., 2002. Biogeochemical behaviour of trace metals in the Scheldt estuary and the Southern Bight of the North Sea (Marine Sciences). Vrije Universiteit Brussel, Brussels.
- Patrick, W.H., Khalid, R.A., 1974. Phosphate Release and Sorption by Soils and Sediments: Effect of Aerobic and Anaerobic Conditions. *Science* 186, 53–55. <https://doi.org/10.1126/science.186.4158.53>
- Paucot, H., Wollast, R., 1997. Transport and transformation of trace metals in the scheldt estuary. *Marine Chemistry*, 4th International Symposium on the Biogeochemistry of Model Estuaries 58, 229–244. [https://doi.org/10.1016/S0304-4203\(97\)00037-6](https://doi.org/10.1016/S0304-4203(97)00037-6)
- Pelcová, P., Vičarová, P., Dočekalová, H., Poštulková, E., Kopp, R., Mareš, J., Smolíková, V., 2018. The prediction of mercury bioavailability for common carp (*Cyprinus carpio* L.) using the DGT technique in the presence of chloride ions and humic acid. *Chemosphere* 211, 1109–1112. <https://doi.org/10.1016/j.chemosphere.2018.07.202>
- Pempkowiak, J., Chiffolleau, J.-F., Staniszewski, A., 2000. The Vertical and Horizontal Distribution of Selected Trace Metals in the Baltic Sea off Poland. *Estuarine, Coastal and Shelf Science* 51, 115–125. <https://doi.org/10.1006/ecss.2000.0641>
- Penicaud, V., Lacoue-Labarthe, T., Bustamante, P., 2017. Metal bioaccumulation and detoxification processes in cephalopods: A review. *Environmental Research* 155, 123–133. <https://doi.org/10.1016/j.envres.2017.02.003>
- Peres, S., Magalhães, M.C.F., Abreu, M.M., Leitão, S., Santos, A., Cerejeira, M.J., 2016. Interaction of contaminated sediment from a salt marsh with estuarine water: evaluation by leaching and ecotoxicity assays and salts from leachate evaporation. *Journal of Soils and Sediments* 16, 1612–1624. <https://doi.org/10.1007/s11368-016-1355-z>
- Perfus-Barbeoch, L., Leonhardt, N., Vavasseur, A., Forestier, C., 2002. Heavy metal toxicity: cadmium permeates through calcium channels and disturbs the



- plant water status. *The Plant Journal* 32, 539–548.  
<https://doi.org/10.1046/j.1365-313X.2002.01442.x>
- Phillips, D.J.H., 1977. The use of biological indicator organisms to monitor trace metal pollution in marine and estuarine environments—a review. *Environmental Pollution* (1970) 13, 281–317. [https://doi.org/10.1016/0013-9327\(77\)90047-7](https://doi.org/10.1016/0013-9327(77)90047-7)
- Pinedo-Gonzalez, P., West, A.J., Rivera-Duarte, I., Sañudo-Wilhelmy, S.A., 2014. Diel Changes in Trace Metal Concentration and Distribution in Coastal Waters: Catalina Island As a Study Case. *Environ. Sci. Technol.* 48, 7730–7737. <https://doi.org/10.1021/es5019515>
- Piwoz, K., Pernthaler, J., 2010. Seasonal population dynamics and trophic role of planktonic nanoflagellates in coastal surface waters of the Southern Baltic Sea. *Environmental Microbiology* 12, 364–377.  
<https://doi.org/10.1111/j.1462-2920.2009.02074.x>
- Pohl, C., Hennings, U., 2008. Trace Metals in Baltic Seawater, in: Feistel, R., Nausch, G., Wasmund, N. (Eds.), *State and Evolution of the Baltic Sea, 1952–2005*. John Wiley & Sons, Inc., Hoboken, NJ, USA, pp. 367–393.  
<https://doi.org/10.1002/9780470283134.ch13>
- Pohl, C., Hennings, U., 2005. The coupling of long-term trace metal trends to internal trace metal fluxes at the oxic–anoxic interface in the Gotland Basin (57°19,20'N; 20°03,00'E) Baltic Sea. *Journal of Marine Systems* 56, 207–225. <https://doi.org/10.1016/j.jmarsys.2004.10.001>
- Poole, C.F., 2002. Chapter 12 Principles and practice of solid-phase extraction, in: *Comprehensive Analytical Chemistry, Sampling and Sample Preparation for Field and Laboratory*. Elsevier, pp. 341–387.  
[https://doi.org/10.1016/S0166-526X\(02\)80049-6](https://doi.org/10.1016/S0166-526X(02)80049-6)
- Pourabadehei, M., Mulligan, C.N., 2016. Effect of the resuspension technique on distribution of the heavy metals in sediment and suspended particulate matter. *Chemosphere* 153, 58–67.  
<https://doi.org/10.1016/j.chemosphere.2016.03.026>
- Prasad, M.N.V., Sajwan, K.S., Naidu, R., 2005. *Trace Elements in the Environment: Biogeochemistry, Biotechnology, and Bioremediation*. CRC Press.
- Premier, V., de Souza Machado, A.A., Mitchell, S., Zarfl, C., Spencer, K., Toffolon, M., 2019. A Model-Based Analysis of Metal Fate in the Thames Estuary. *Estuaries and Coasts* 42, 1185–1201. <https://doi.org/10.1007/s12237-019-00544-y>
- Rainbow, P.S., 2018. *Trace Metals in the Environment and Living Organisms: The British Isles as a Case Study*, 1st ed. Cambridge University Press.  
<https://doi.org/10.1017/9781108658423>
- Rainbow, P.S., 2002. Trace metal concentrations in aquatic invertebrates: why and so what? *Environmental Pollution* 120, 497–507.  
[https://doi.org/10.1016/S0269-7491\(02\)00238-5](https://doi.org/10.1016/S0269-7491(02)00238-5)
- Raja, P.M.V., Barron, A.R., 2019. *ICP-MS for Trace Metal Analysis*.
- Rao, G.P.C., Veni, S.S., Pratap, K., Rao, Y.K., Seshiah, K., 2006. Solid Phase Extraction of Trace Metals in Seawater Using Morpholine Dithiocarbamate-Loaded Amberlite XAD-4 and Determination by ICP-

- AES. *Analytical Letters* 39, 1009–1021.  
<https://doi.org/10.1080/00032710600614289>
- Ray, S.J., Andrade, F., Gamez, G., McClenathan, D., Rogers, D., Schilling, G., Wetzel, W., Hieftje, G.M., 2004. Plasma-source mass spectrometry for speciation analysis: state-of-the-art. *J Chromatogr A* 1050, 3–34.
- Raymond, P.A., Bauer, J.E., 2001. Use of <sup>14</sup>C and <sup>13</sup>C natural abundances for evaluating riverine, estuarine, and coastal DOC and POC sources and cycling: a review and synthesis. *Organic Geochemistry* 32, 469–485.  
[https://doi.org/10.1016/S0146-6380\(00\)00190-X](https://doi.org/10.1016/S0146-6380(00)00190-X)
- Reckhardt, A., Beck, M., Greskowiak, J., Schnetger, B., Böttcher, M.E., Gehre, M., Brumsack, H.-J., 2017. Cycling of redox-sensitive elements in a sandy subterranean estuary of the southern North Sea. *Marine Chemistry* 188, 6–17. <https://doi.org/10.1016/j.marchem.2016.11.003>
- Reed, D.C., Gustafsson, B.G., Slomp, C.P., 2016. Shelf-to-basin iron shuttling enhances vivianite formation in deep Baltic Sea sediments. *Earth and Planetary Science Letters* 434, 241–251.  
<https://doi.org/10.1016/j.epsl.2015.11.033>
- Regnier, P., Wollast, R., 1993. Distribution of trace metals in suspended matter of the Scheldt estuary. *Marine Chemistry* 43, 3–19.  
[https://doi.org/10.1016/0304-4203\(93\)90212-7](https://doi.org/10.1016/0304-4203(93)90212-7)
- Remeikaitė-Nikienė, N., Garnaga-Budrė, G., Lujanienė, G., Jokšas, K., Stankevičius, A., Malejevas, V., Barisevičiūtė, R., 2018. Distribution of metals and extent of contamination in sediments from the south-eastern Baltic Sea (Lithuanian zone). *Oceanologia* 60, 193–206.  
<https://doi.org/10.1016/j.oceano.2017.11.001>
- Rheinheimer, G., 1998. Pollution in the Baltic Sea. *Naturwissenschaften* 85, 318–329. <https://doi.org/10.1007/s001140050508>
- Richir, J., 2016. Trace Elements in Marine Environments: Occurrence, Threats and Monitoring with Special Focus on the Coastal Mediterranean. *Journal of Environmental & Analytical Toxicology* 06. <https://doi.org/10.4172/2161-0525.1000349>
- Ríos, A.F., Resplandy, L., García-Ibáñez, M.I., Fajar, N.M., Velo, A., Padin, X.A., Wanninkhof, R., Steinfeldt, R., Rosón, G., Pérez, F.F., 2015. Decadal acidification in the water masses of the Atlantic Ocean. *Proc Natl Acad Sci U S A* 112, 9950–9955. <https://doi.org/10.1073/pnas.1504613112>
- Robert, S., Blanc, G., Schäfer, J., Lavaux, G., Abril, G., 2004. Metal mobilization in the Gironde Estuary (France): the role of the soft mud layer in the maximum turbidity zone. *Marine Chemistry* 87, 1–13.  
[https://doi.org/10.1016/S0304-4203\(03\)00088-4](https://doi.org/10.1016/S0304-4203(03)00088-4)
- Roberts, D., Nachttegaal, M., Sparks, D.L., 2005. Speciation of Metals in Soils, in: *Chemical Processes in Soils, SSSA Book Series*. pp. 619–654.
- Robinson, C.D., Webster, L., Martínez-Gómez, C., Burgeot, T., Gubbins, M.J., Thain, J.E., Vethaak, A.D., McIntosh, A.D., Hylland, K., 2017. Assessment of contaminant concentrations in sediments, fish and mussels sampled from the North Atlantic and European regional seas within the ICON project. Marine Environmental Research, The ICON Project (the trans-European

- research project on field studies related to a large-scale sampling and monitoring 124, 21–31. <https://doi.org/10.1016/j.marenvres.2016.04.005>
- Roig, N., Nadal, M., Sierra, J., Ginebreda, A., Schuhmacher, M., Domingo, J.L., 2011. Novel approach for assessing heavy metal pollution and ecotoxicological status of rivers by means of passive sampling methods. *Environment International* 37, 671–677. <https://doi.org/10.1016/j.envint.2011.01.007>
- Rose, A.L., Waite, T.D., 2003. Kinetics of iron complexation by dissolved natural organic matter in coastal waters. *Marine Chemistry* 84, 85–103. [https://doi.org/10.1016/S0304-4203\(03\)00113-0](https://doi.org/10.1016/S0304-4203(03)00113-0)
- Rose, A.W., Cravotta III, C.A., 1998. Geochemistry of coal mine drainage. Coal mine drainage prediction and pollution prevention in Pennsylvania, Pennsylvania Department of Environmental Protection 1, 1–22.
- Rumisha, C., Elskens, M., Leermakers, M., Kochzius, M., 2012. Trace metal pollution and its influence on the community structure of soft bottom molluscs in intertidal areas of the Dar es Salaam coast, Tanzania. *Marine Pollution Bulletin* 64, 521–531. <https://doi.org/10.1016/j.marpolbul.2011.12.025>
- Rumisha, C., Leermakers, M., Mdegela, R.H., Kochzius, M., Elskens, M., 2017. Bioaccumulation and public health implications of trace metals in edible tissues of the crustaceans *Scylla serrata* and *Penaeus monodon* from the Tanzanian coast. *Environmental Monitoring and Assessment* 189. <https://doi.org/10.1007/s10661-017-6248-0>
- Salim, F., Górecki, T., 2019. Theory and modelling approaches to passive sampling. *Environ. Sci.: Processes Impacts* 21, 1618–1641. <https://doi.org/10.1039/C9EM00215D>
- Sandroni, V., Smith, C.M.M., Donovan, A., 2003. Microwave digestion of sediment, soils and urban particulate matter for trace metal analysis. *Talanta* 60, 715–723. [https://doi.org/10.1016/S0039-9140\(03\)00131-0](https://doi.org/10.1016/S0039-9140(03)00131-0)
- Santoro, A., Held, A., Linsinger, T.P.J., Perez, A., Ricci, M., 2017. Comparison of total and aqua regia extractability of heavy metals in sewage sludge: The case study of a certified reference material. *Trends Analyt Chem* 89, 34–40. <https://doi.org/10.1016/j.trac.2017.01.010>
- Santschi, P.H., Adler, D., Amdurer, M., Li, Y.-H., Bell, J.J., 1980. Thorium isotopes as analogues for “particle-reactive” pollutants in coastal marine environments. *Earth and Planetary Science Letters* 47, 327–335. [https://doi.org/10.1016/0012-821X\(80\)90019-9](https://doi.org/10.1016/0012-821X(80)90019-9)
- Savchuk, O.P., 2013. Large-Scale Dynamics of Hypoxia in the Baltic Sea, in: Yakushev, E.V. (Ed.), *Chemical Structure of Pelagic Redox Interfaces: Observation and Modeling*, The Handbook of Environmental Chemistry. Springer, Berlin, Heidelberg, pp. 137–160. [https://doi.org/10.1007/698\\_2010\\_53](https://doi.org/10.1007/698_2010_53)
- Scanes, P., Ferguson, A., Potts, J., 2017. Estuary Form and Function: Implications for Palaeoecological Studies, in: *Applications of Palaeoenvironmental Techniques in Estuarine Studies*. Springer Netherlands, Dordrecht, pp. 9–44. [https://doi.org/10.1007/978-94-024-0990-1\\_2](https://doi.org/10.1007/978-94-024-0990-1_2)

- Schintu, M., Durante, L., Maccioni, A., Meloni, P., Degetto, S., Contu, A., 2008. Measurement of environmental trace-metal levels in Mediterranean coastal areas with transplanted mussels and DGT techniques. *Marine Pollution Bulletin*, 5th International Conference on Marine Pollution and Ecotoxicology 57, 832–837.  
<https://doi.org/10.1016/j.marpolbul.2008.02.038>
- Schneider, B., Müller, J.D., 2018. The Main Hydrographic Characteristics of the Baltic Sea, in: Schneider, B., Müller, J.D. (Eds.), *Biogeochemical Transformations in the Baltic Sea: Observations Through Carbon Dioxide Glasses*, Springer Oceanography. Springer International Publishing, Cham, pp. 35–41. [https://doi.org/10.1007/978-3-319-61699-5\\_3](https://doi.org/10.1007/978-3-319-61699-5_3)
- Schneider, B., Otto, S., 2019. Organic matter mineralization in the deep water of the Gotland Basin (Baltic Sea): Rates and oxidant demand. *Journal of Marine Systems* 195, 20–29. <https://doi.org/10.1016/j.jmarsys.2019.03.006>
- Scholz, F., Baum, M., Siebert, C., Eroglu, S., Dale, A.W., Naumann, M., Sommer, S., 2018. Sedimentary molybdenum cycling in the aftermath of seawater inflow to the intermittently euxinic Gotland Deep, Central Baltic Sea. *Chemical Geology* 491, 27–38.  
<https://doi.org/10.1016/j.chemgeo.2018.04.031>
- Scholz, F., McManus, J., Sommer, S., 2013. The manganese and iron shuttle in a modern euxinic basin and implications for molybdenum cycling at euxinic ocean margins. *Chemical Geology* 355, 56–68.  
<https://doi.org/10.1016/j.chemgeo.2013.07.006>
- Scholz, F., Schmidt, M., Hensen, C., Eroglu, S., Geilert, S., Gutjahr, M., Liebetrau, V., 2019. Shelf-to-basin iron shuttle in the Guaymas Basin, Gulf of California. *Geochimica et Cosmochimica Acta* 261, 76–92.  
<https://doi.org/10.1016/j.gca.2019.07.006>
- Schulz-Baldes, M., Rehm, E., Farke, H., 1983. Field experiments on the fate of lead and chromium in an intertidal benthic mesocosm, the Bremerhaven Caisson. *Mar. Biol.* 75, 307–318. <https://doi.org/10.1007/BF00406017>
- Science for Environment Policy: European Commission DG Environment News Alert Service, n.d. Risks of biodiversity loss posed by nitrogen and phosphorus pollution in European freshwaters. SCU, The University of West England, Bristol 1.
- Scoullou, M.J., Sakellari, A., Giannopoulou, K., Paraskevopoulou, V., Dassenakis, M., 2007. Dissolved and particulate trace metal levels in the Saronikos Gulf, Greece, in 2004. The impact of the primary Wastewater Treatment Plant of Psittalia. *Desalination, Ninth Environmental Science and Technology Symposium* 210, 98–109.  
<https://doi.org/10.1016/j.desal.2006.05.036>
- Sekhar, C.K., Chary, S.N., Tirumala, K.C., Aparna, V., 2003. Determination of trace metals in sea water by ICP-MS after matrix separation. *Acta Chimica Slovenica* 50, 409–418.
- Seybold, C.A., Mersie, W., Huang, J., McNamee, C., 2002. Soil redox, pH, temperature, and water-table patterns of a freshwater tidal wetland.

- Wetlands 22, 149–158. [https://doi.org/10.1672/0277-5212\(2002\)022\[0149:SRPTAW\]2.0.CO;2](https://doi.org/10.1672/0277-5212(2002)022[0149:SRPTAW]2.0.CO;2)
- Shahzad, B., Tanveer, M., Rehman, A., Cheema, S.A., Fahad, S., Rehman, S., Sharma, A., 2018. Nickel; whether toxic or essential for plants and environment - A review. *Plant Physiology and Biochemistry* 132, 641–651. <https://doi.org/10.1016/j.plaphy.2018.10.014>
- Shen, Y., Canfield, D.E., Knoll, A.H., 2002. Middle Proterozoic ocean chemistry: Evidence from the McArthur Basin, northern Australia. *Am J Sci* 302, 81–109. <https://doi.org/10.2475/ajs.302.2.81>
- Shi, D., Xu, Y., Hopkinson, B.M., Morel, F.M.M., 2010. Effect of Ocean Acidification on Iron Availability to Marine Phytoplankton. *Science* 327, 676–679. <https://doi.org/10.1126/science.1183517>
- Sholkovitz, E.R., 1978. The flocculation of dissolved Fe, Mn, Al, Cu, Ni, Co and Cd during estuarine mixing. *Earth and Planetary Science Letters* 41, 77–86. [https://doi.org/10.1016/0012-821X\(78\)90043-2](https://doi.org/10.1016/0012-821X(78)90043-2)
- Sierra, J., Roig, N., Giménez Papiol, G., Pérez-Gallego, E., Schuhmacher, M., 2017. Prediction of the bioavailability of potentially toxic elements in freshwaters. Comparison between speciation models and passive samplers. *Science of The Total Environment* 605–606, 211–218. <https://doi.org/10.1016/j.scitotenv.2017.06.136>
- Sigg, L.M., Behra, P., Stumm, W., 2014. *Chimie des milieux aquatiques: [Cours et exercices corrigés]*. Dunod, Paris.
- Simonsen, A.M.T., Pedersen, K.B., Jensen, P.E., Elberling, B., Bach, L., 2019. Lability of toxic elements in Submarine Tailings Disposal: The relationship between metal fractionation and metal uptake by sandworms (*Alitta virens*). *Science of The Total Environment* 696, 133903. <https://doi.org/10.1016/j.scitotenv.2019.133903>
- Simpson, N.J.K., 2000. *Solid-phase extraction: principles, techniques, and applications*. CRC Press, New York.
- Simpson, S.L., Yverneau, H., Cremazy, A., Jarolimek, C.V., Price, H.L., Jolley, D.F., 2012. DGT-Induced Copper Flux Predicts Bioaccumulation and Toxicity to Bivalves in Sediments with Varying Properties. *Environmental Science & Technology* 46, 9038–9046. <https://doi.org/10.1021/es301225d>
- Slaveykova, V.I., Karadjova, I.B., Karadjov, M., Tsalev, D.L., 2009. Trace metal speciation and bioavailability in surface waters of the Black Sea coastal area evaluated by HF-PLM and DGT. *Environ. Sci. Technol.* 43, 1798–1803.
- Soetaert, K., Middelburg, J.J., Heip, C., Meire, P., Damme, S.V., Maris, T., 2006. Long-term change in dissolved inorganic nutrients in the heterotrophic Scheldt estuary (Belgium, The Netherlands). *Limnology and Oceanography* 51, 409–423. [https://doi.org/10.4319/lo.2006.51.1\\_part\\_2.0409](https://doi.org/10.4319/lo.2006.51.1_part_2.0409)
- Solomon, F., 2008. Impacts of Metals on Aquatic Ecosystems and Human Health. *Environment and Communities* 14–19.
- Soylak, M., 2004. Solid Phase Extraction of Cu(II), Pb(II), Fe(III), Co(II), and Cr(III) on Chelex-100 Column Prior to Their Flame Atomic Absorption

- Spectrometric Determinations. *Analytical Letters* 37, 1203–1217.  
<https://doi.org/10.1081/AL-120034064>
- Speeckaert, G., Borges, A.V., Champenois, W., Royer, C., Gypens, N., 2018. Annual cycle of dimethylsulfoniopropionate (DMSP) and dimethylsulfoxide (DMSO) related to phytoplankton succession in the Southern North Sea. *Science of The Total Environment* 622–623, 362–372.  
<https://doi.org/10.1016/j.scitotenv.2017.11.359>
- Stepanova, N.B., 2017. Vertical structure and seasonal evolution of the cold intermediate layer in the Baltic Proper. *Estuarine, Coastal and Shelf Science, Understanding the Baltic Sea* 195, 34–40.  
<https://doi.org/10.1016/j.ecss.2017.05.011>
- Sterckeman, T., Douay, F., Baize, D., Fourrier, H., Proix, N., 2007. Pedo-geochemical reference system of Nord-Pas de Calais: Methods and main results. *Etude et Gestion des Sols* 19.
- Sternbeck, J., Skei, J., Verta, M., Östlund, P., 1999. Mobilisation of sedimentary trace metals following improved oxygen conditions: an assessment of the impact of lowered primary productivity on trace metal cycling in the marine environment. Nordic Council of Ministers [Nordiska ministerrådet, Copenhagen.
- Stigebrandt, A., 2001. Physical Oceanography of the Baltic Sea, in: Wulff, F.V., Rahm, L.A., Larsson, P. (Eds.), *A Systems Analysis of the Baltic Sea, Ecological Studies*. Springer, Berlin, Heidelberg, pp. 19–74.  
[https://doi.org/10.1007/978-3-662-04453-7\\_2](https://doi.org/10.1007/978-3-662-04453-7_2)
- Stockdale, A., 2005. The Use of Cation -Exchange Resins in Natural Water Trace Metals Research (Master thesis). Lancaster University.
- Stone, M., Marsalek, J., 1996. Trace metal composition and speciation in street sediment: Sault Ste. Marie, Canada. *Water Air Soil Pollut* 87, 149–169.  
<https://doi.org/10.1007/BF00696834>
- Strypsteen, G., Montreuil, A.-L., Rauwoens, P., 2017. Aeolian sand transport at the Belgian coast: field campaigns and first results. *Coastal Dynamics* 11.
- Stumm, W., Bilinski, H., 1973. Trace metals in natural waters: difficulties of interpretation arising from our ignorance on their speciation, in: *Advances in Water Pollution Research*. Elsevier, pp. 39–52.  
<https://doi.org/10.1016/B978-0-08-017005-3.50011-6>
- Stumm, W., Morgan, J.J., 1996. *Aquatic chemistry: chemical equilibria and rates in natural waters*, 3rd ed. ed, Environmental science and technology. Wiley, New York.
- Sudheesh, V., Movitha, M., Hatha, A.A.M., Renjith, K.R., Resmi, P., Rahiman, M., Nair, S.M., 2017. Effects of seasonal anoxia on the distribution of phosphorus fractions in the surface sediments of southeastern Arabian Sea shelf. *Continental Shelf Research* 150, 57–64.  
<https://doi.org/10.1016/j.csr.2017.09.011>
- Sulu-Gambari, F., Seitaj, D., Meysman, F.J.R., Schauer, R., Polerecky, L., Slomp, C.P., 2016. Cable Bacteria Control Iron–Phosphorus Dynamics in Sediments of a Coastal Hypoxic Basin. *Environ. Sci. Technol.* 50, 1227–1233.  
<https://doi.org/10.1021/acs.est.5b04369>

- Sunda, W.G., 2012. Feedback Interactions between Trace Metal Nutrients and Phytoplankton in the Ocean. *Front Microbiol* 3. <https://doi.org/10.3389/fmicb.2012.00204>
- Sunda, W.G., 1989. Trace Metal Interactions with Marine Phytoplankton. *Biological Oceanography* 6, 411–442.
- Sunda, W.G., Huntsman, S.A., 2000. Effect of Zn, Mn, and Fe on Cd accumulation in phytoplankton: Implications for oceanic Cd cycling. *Limnology and Oceanography* 45, 1501–1516. <https://doi.org/10.4319/lo.2000.45.7.1501>
- Supowit, S.D., Roll, I.B., Dang, V.D., Kroll, K.J., Denslow, N.D., Halden, R.U., 2016. Active Sampling Device for Determining Pollutants in Surface and Pore Water – the In Situ Sampler for Biphasic Water Monitoring. *Sci Rep* 6, 9p. <https://doi.org/10.1038/srep21886>
- Svedén, J.B., Walve, J., Larsson, U., Elmgren, R., 2016. The bloom of nitrogen-fixing cyanobacteria in the northern Baltic Proper stimulates summer production. *Journal of Marine Systems* 163, 102–112. <https://doi.org/10.1016/j.jmarsys.2016.07.003>
- Szymczycha, B., Maciejewska, A., Winogradow, A., Pempkowiak, J., 2014. Could submarine groundwater discharge be a significant carbon source to the southern Baltic Sea? The study reports the results obtained within the framework of the following projects: the statutory activities of the Institute of Oceanology Polish Academy of Sciences theme 2.2, research project No. 2012/05/N/ST10/02761 sponsored by the National Science Centre, and AMBER, the BONUS+EU FP6 Project. *Oceanologia* 56, 327–347. <https://doi.org/10.5697/oc.56-2.327>
- Szymczycha, B., Vogler, S., Pempkowiak, J., 2012. Nutrient fluxes via submarine groundwater discharge to the Bay of Puck, southern Baltic Sea. *Science of The Total Environment* 438, 86–93. <https://doi.org/10.1016/j.scitotenv.2012.08.058>
- Tachet, H., Richoux, P., Bournaud, M., Usseglio-Polatera, P., 2010. *Invertébrés d'eau douce : systématique, biologie, écologie*. CNRS Editions.
- Takeda, K., Marumoto, K., Minamikawa, T., Sakugawa, H., Fujiwara, K., 2000. Three-year determination of trace metals and the lead isotope ratio in rain and snow depositions collected in Higashi-Hiroshima, Japan. *Atmospheric Environment* 34, 4525–4535. [https://doi.org/10.1016/S1352-2310\(00\)00103-5](https://doi.org/10.1016/S1352-2310(00)00103-5)
- Taniguchi, M., Burnett, W.C., Cable, J.E., Turner, J.V., 2002. Investigation of submarine groundwater discharge. *Hydrological Processes* 16, 2115–2129. <https://doi.org/10.1002/hyp.1145>
- Tankere, S.P.C., Statham, P.J., 1996. Distribution of dissolved Cd, Cu, Ni and Zn in the Adriatic Sea. *Marine Pollution Bulletin* 32, 623–630. [https://doi.org/10.1016/0025-326X\(96\)00025-2](https://doi.org/10.1016/0025-326X(96)00025-2)
- Tarvainen, T., Salminen, R., Vos, W.D., 2005. *Geochemical atlas of Europe*. Geological Survey of Finland, Espoo.
- Temara, A., Skei, J.M., Gillan, D., Warnau, M., Jangoux, M., Dubois, P., 1998. Validation of the asteroid *Asterias rubens* (Echinodermata) as a bioindicator of spatial and temporal trends of Pb, Cd, and Zn contamination

- in the field. *Marine Environmental Research* 45, 341–356.  
[https://doi.org/10.1016/S0141-1136\(98\)00026-9](https://doi.org/10.1016/S0141-1136(98)00026-9)
- Tessier, A., Turner, D.R., 1995. *Metal Speciation and Bioavailability in Aquatic Systems*, IUPAC Series. Wiley.
- Teuchies, J., Singh, G., Bervoets, L., Meire, P., 2013. Land use changes and metal mobility: Multi-approach study on tidal marsh restoration in a contaminated estuary. *Science of The Total Environment* 449, 174–183.  
<https://doi.org/10.1016/j.scitotenv.2013.01.053>
- Thamdrup, B., Fossing, H., Jørgensen, B.B., 1994. Manganese, iron and sulfur cycling in a coastal marine sediment, Aarhus bay, Denmark. *Geochimica et Cosmochimica Acta* 58, 5115–5129. [https://doi.org/10.1016/0016-7037\(94\)90298-4](https://doi.org/10.1016/0016-7037(94)90298-4)
- Thanh, P.M., Ketheesan, B., Yan, Z., Stuckey, D., 2016. Trace metal speciation and bioavailability in anaerobic digestion: A review. *Biotechnology Advances* 34, 122–136. <https://doi.org/10.1016/j.biotechadv.2015.12.006>
- Thomas, R., 2013. *Practical guide to ICP-MS: a tutorial for beginners*, Third edition. ed, *Practical spectroscopy*. CRC Press, Taylor & Francis Group, Boca Raton.
- Thomas, R., 2004. *Practical guide to ICP-MS, Practical spectroscopy*. M. Dekker, New York, NY.
- Thompson, J.P., 2015. An acid mine drainage explainer, and a curious account of the Gold King circa 1901. Jonathan P. Thompson. URL <http://jonathanpthompson.blogspot.com/2015/08/an-acid-mine-drainage-explainer-and.html> (accessed 5.6.19).
- Thurman, E.M., Mills, M.S., 1998. *Solid-phase extraction: principles and practice*, Chemical analysis. Wiley, New York.
- Tribovillard, N., Sansjofre, P., Ader, M., Trentesaux, A., Averbuch, O., Barbecot, F., 2012. Early diagenetic carbonate bed formation at the sediment–water interface triggered by synsedimentary faults. *Chemical Geology* 300–301, 1–13. <https://doi.org/10.1016/j.chemgeo.2012.01.014>
- Trueman, B.F., 2017. *Controlling Lead Release To Drinking Water: Impacts Of Iron Oxides, Complexing Species, Orthophosphate, And Lead Pipe Replacement* (Doctoral Thesis). Dalhousie University.
- Turetta, C., Capodaglio, G., Cairns, W., Rabar, S., Cescon, P., 2005. Benthic fluxes of trace metals in the lagoon of Venice. *Microchemical Journal*, XI Italian Hungarian Symposium on Spectrochemistry 79, 149–158.  
<https://doi.org/10.1016/j.microc.2004.06.003>
- Türk Çulha, S., Çulha, M., Karayücel, İ., Çelik, M.Y., Işler, Y., 2017. Heavy metals in *Mytilus galloprovincialis*, suspended particulate matter and sediment from offshore submerged longline system, Black Sea. *Int. J. Environ. Sci. Technol.* 14, 385–396. <https://doi.org/10.1007/s13762-016-1158-1>
- Turner, A., Millward, G.E., 2000. Particle Dynamics and Trace Metal Reactivity in Estuarine Plumes. *Estuarine, Coastal and Shelf Science* 50, 761–774.  
<https://doi.org/10.1006/ecss.2000.0589>
- Turner, A., Millward, G.E., Le Roux, S.M., 2004. Significance of oxides and particulate organic matter in controlling trace metal partitioning in a



- contaminated estuary. *Marine Chemistry* 88, 179–192.  
<https://doi.org/10.1016/j.marchem.2004.03.008>
- Turner, A., Millward, G.E., Morris, A.W., 1991. Particulate metals in five major North Sea estuaries. *Estuarine, Coastal and Shelf Science* 32, 325–346.  
[https://doi.org/10.1016/0272-7714\(91\)90047-F](https://doi.org/10.1016/0272-7714(91)90047-F)
- Turner, A., Nimmo, M., Thuresson, K.A., 1998. Speciation and sorptive behaviour of nickel in an organic-rich estuary (Beaulieu, UK). *Marine Chemistry* 63, 105–118. [https://doi.org/10.1016/S0304-4203\(98\)00054-1](https://doi.org/10.1016/S0304-4203(98)00054-1)
- Turner, A., Olsen, Y.S., 2000. Chemical versus Enzymatic Digestion of Contaminated Estuarine Sediment: Relative Importance of Iron and Manganese Oxides in Controlling Trace Metal Bioavailability. *Estuarine, Coastal and Shelf Science* 51, 717–728.  
<https://doi.org/10.1006/ecss.2000.0725>
- Tusseau-Vuillemin, M.-H., Gourlay, C., Lorgeoux, C., Mouchel, J.-M., Buzier, R., Gilbin, R., Seidel, J.-L., Elbaz-Poulichet, F., 2007. Dissolved and bioavailable contaminants in the Seine river basin. *Science of The Total Environment, Human activity and material fluxes in a regional river basin: the Seine River watershed* 375, 244–256.  
<https://doi.org/10.1016/j.scitotenv.2006.12.018>
- Tuzen, M., Soylak, M., Elci, L., 2005. Multi-element pre-concentration of heavy metal ions by solid phase extraction on Chromosorb 108. *Analytica Chimica Acta* 548, 101–108. <https://doi.org/10.1016/j.aca.2005.06.005>
- Uher, E., Besse, J.-P., Delaigue, O., Husson, F., Lebrun, J.D., 2018. Comparison of the metal contamination in water measured by diffusive gradient in thin film (DGT), biomonitoring and total metal dissolved concentration at a national scale. *Applied Geochemistry* 88, 247–257.  
<https://doi.org/10.1016/j.apgeochem.2017.05.003>
- Uher, E., Tusseau-Vuillemin, M.-H., Gourlay-France, C., 2013. DGT measurement in low flow conditions: diffusive boundary layer and lability considerations. *Environmental Science: Processes & Impacts* 15, 1351.  
<https://doi.org/10.1039/c3em00151b>
- Uher, E., Zhang, H., Santos, S., Tusseau-Vuillemin, M.-H., Gourlay-Francé, C., 2012. Impact of Biofouling on Diffusive Gradient in Thin Film Measurements in Water. *Anal. Chem.* 84, 3111–3118.  
<https://doi.org/10.1021/ac2028535>
- Ulfso, A., Hulth, S., Anderson, L.G., 2011. pH and biogeochemical processes in the Gotland Basin of the Baltic Sea. *Marine Chemistry* 127, 20–30.  
<https://doi.org/10.1016/j.marchem.2011.07.004>
- Uncles, R.J., Frickers, P.E., Easton, A.E., Griffiths, M.L., Harris, C., Howland, R.J.M., King, R.S., Morris, A.W., Plummer, D.H., Tappin, A.D., 2000. Concentrations of suspended particulate organic carbon in the tidal Yorkshire Ouse River and Humber Estuary. *Science of The Total Environment* 251–252, 233–242. [https://doi.org/10.1016/S0048-9697\(00\)00386-7](https://doi.org/10.1016/S0048-9697(00)00386-7)
- United States Department of Agriculture, 2018. Determination of Metals by ICP-MS and ICP-OES (Optical Emission Spectrometry) (No. CLG-TM3.06). United

- States Department of Agriculture Food Safety and Inspection Service, Office of Public Health Science.
- United States Geological Survey, 2009. Chloride Found At Levels That Can Harm Aquatic Life In Urban Streams Of Northern US. ScienceDaily.
- Väänänen, K., Leppänen, M.T., Chen, X., Akkanen, J., 2018. Metal bioavailability in ecological risk assessment of freshwater ecosystems: From science to environmental management. *Ecotoxicology and Environmental Safety* 147, 430–446. <https://doi.org/10.1016/j.ecoenv.2017.08.064>
- Valenta, P., Duursma, E.K., Merks, A.G.A., Rützel, H., Nürnberg, H.W., 1986. Distribution of Cd, Pb and Cu between the dissolved and particulate phase in the Eastern Scheldt and Western Scheldt estuary. *Science of The Total Environment* 53, 41–76. [https://doi.org/10.1016/0048-9697\(86\)90092-6](https://doi.org/10.1016/0048-9697(86)90092-6)
- Van Ael, E., Blust, R., Bervoets, L., 2017. Metals in the Scheldt estuary: From environmental concentrations to bioaccumulation. *Environmental Pollution* 228, 82–91. <https://doi.org/10.1016/j.envpol.2017.05.028>
- Van Damme, S., Struyf, E., Maris, T., Ysebaert, T., Dehairs, F., Tackx, M., Heip, C., Meire, P., 2005. Spatial and temporal patterns of water quality along the estuarine salinity gradient of the Scheldt estuary (Belgium and The Netherlands): results of an integrated monitoring approach. *Hydrobiologia* 540, 29–45. <https://doi.org/10.1007/s10750-004-7102-2>
- van de Velde, S., Callebaut, I., Gao, Y., Meysman, F.J.R., 2017. Impact of electrogenic sulfur oxidation on trace metal cycling in a coastal sediment. *Chemical Geology* 452, 9–23. <https://doi.org/10.1016/j.chemgeo.2017.01.028>
- van de Velde, S., Lesven, L., Burdorf, L.D.W., Hidalgo-Martinez, S., Geelhoed, J.S., Van Rijswijk, P., Gao, Y., Meysman, F.J.R., 2016. The impact of electrogenic sulfur oxidation on the biogeochemistry of coastal sediments: A field study. *Geochimica et Cosmochimica Acta* 194, 211–232. <https://doi.org/10.1016/j.gca.2016.08.038>
- van de Velde, S.J., Hylén, A., Kononets, M., Marzocchi, U., Leermakers, M., Choumiline, K., Hall, P.O.J., Meysman, F.J.R., 2020. Elevated sedimentary removal of Fe, Mn, and trace elements following a transient oxygenation event in the Eastern Gotland Basin, central Baltic Sea. *Geochimica et Cosmochimica Acta* 271, 16–32. <https://doi.org/10.1016/j.gca.2019.11.034>
- van der Zee, C., Roelvros, N., Chou, L., 2007. Phosphorus speciation, transformation and retention in the Scheldt estuary (Belgium/The Netherlands) from the freshwater tidal limits to the North Sea. *Marine Chemistry, Special issue: Dedicated to the memory of Professor Roland Wollast* 106, 76–91. <https://doi.org/10.1016/j.marchem.2007.01.003>
- van Leeuwen, H.P., Town, R.M., Buffle, J., Clevén, R.F.M.J., Davison, W., Puy, J., van Riemsdijk, W.H., Sigg, L., 2005. Dynamic Speciation Analysis and Bioavailability of Metals in Aquatic Systems. *Environmental Science & Technology* 39, 8545–8556. <https://doi.org/10.1021/es050404x>
- Vandepitte, L., Decock, W., Mees, J., 2010. Belgian Register of Marine Species, compiled and validated by the VLIZ Belgian Marine Species Consortium. VLIZ Special Publication 78 pp.

- Vázquez-Rodríguez, M., Pérez, F.F., Velo, A., Ríos, A.F., Mercier, H., 2012. Observed acidification trends in North Atlantic water masses. *Biogeosciences* 9, 5217–5230. <https://doi.org/10.5194/bg-9-5217-2012>
- Velegrakis, A.F., Gao, S., Lafite, R., Dupont, J.P., Huault, M.F., Nash, L.A., Collins, M.B., 1997. Resuspension and advection processes affecting suspended particulate matter concentrations in the central English Channel. *Journal of Sea Research* 38, 17–34. [https://doi.org/10.1016/S1385-1101\(97\)00041-5](https://doi.org/10.1016/S1385-1101(97)00041-5)
- Verfaillie, E., Van Lancker, V., Van Meirvenne, M., 2006. Multivariate geostatistics for the predictive modelling of the surficial sand distribution in shelf seas. *Continental Shelf Research* 26, 2454–2468. <https://doi.org/10.1016/j.csr.2006.07.028>
- Vicente-Martorell, J.J., Galindo-Riaño, M.D., García-Vargas, M., Granado-Castro, M.D., 2009. Bioavailability of heavy metals monitoring water, sediments and fish species from a polluted estuary. *Journal of Hazardous Materials* 162, 823–836. <https://doi.org/10.1016/j.jhazmat.2008.05.106>
- Viers, J., Barroux, G., Pinelli, M., Seyler, P., Oliva, P., Dupré, B., Boaventura, G.R., 2005. The influence of the Amazonian floodplain ecosystems on the trace element dynamics of the Amazon River mainstem (Brazil). *Science of The Total Environment* 339, 219–232. <https://doi.org/10.1016/j.scitotenv.2004.07.034>
- Vijayaraghavan, K., Jegan, J., Palanivelu, K., Velan, M., 2005. Biosorption of copper, cobalt and nickel by marine green alga *Ulva reticulata* in a packed column. *Chemosphere* 60, 419–426. <https://doi.org/10.1016/j.chemosphere.2004.12.016>
- Violintzis, C., Arditoglou, A., Voutsas, D., 2009. Elemental composition of suspended particulate matter and sediments in the coastal environment of Thermaikos Bay, Greece: Delineating the impact of inland waters and wastewaters. *Journal of Hazardous Materials* 166, 1250–1260. <https://doi.org/10.1016/j.jhazmat.2008.12.046>
- Viollier, E., Inglett, P.W., Hunter, K., Roychoudhury, A.N., Van Cappellen, P., 2000. The ferrozine method revisited: Fe(II)/Fe(III) determination in natural waters. *Applied Geochemistry* 15, 785–790. [https://doi.org/10.1016/S0883-2927\(99\)00097-9](https://doi.org/10.1016/S0883-2927(99)00097-9)
- Vlaams Instituut voor de Zee, 2012. Zee Worden, Schelde. VLIZ - De Grote Rede 29–33.
- Vlaams-Nederlandse Scheldecommissie, 2018. Research and monitoring: main conclusions of research Agenda for the Future and T2015. *Schelde Magazine* 6–7.
- Voulvoulis, N., Arpon, K.D., Giakoumis, T., 2017. The EU Water Framework Directive: From great expectations to problems with implementation. *Science of The Total Environment* 575, 358–366. <https://doi.org/10.1016/j.scitotenv.2016.09.228>
- Vrana, B., Allan, I.J., Greenwood, R., Mills, G.A., Dominiak, E., Svensson, K., Knutsson, J., Morrison, G., 2005. Passive sampling techniques for

- monitoring pollutants in water. *TrAC Trends in Analytical Chemistry* 24, 845–868. <https://doi.org/10.1016/j.trac.2005.06.006>
- Waeles, M., Riso, R.D., Cabon, J.-Y., Maguer, J.-F., L’Helguen, S., 2009. Speciation of dissolved copper and cadmium in the Loire estuary and over the North Biscay continental shelf in spring. *Estuarine, Coastal and Shelf Science* 84, 139–146. <https://doi.org/10.1016/j.ecss.2009.06.011>
- Waeles, M., Riso, R.D., Le Corre, P., 2005. Seasonal variations of cadmium speciation in the Penzé estuary, NW France. *Estuarine, Coastal and Shelf Science* 65, 143–152. <https://doi.org/10.1016/j.ecss.2005.06.002>
- Waeles, M., Tanguy, V., Lespes, G., Riso, R.D., 2008. Behaviour of colloidal trace metals (Cu, Pb and Cd) in estuarine waters: An approach using frontal ultrafiltration (UF) and stripping chronopotentiometric methods (SCP). *Estuarine, Coastal and Shelf Science* 80, 538–544. <https://doi.org/10.1016/j.ecss.2008.09.010>
- Wang, B.-S., Lee, C.-P., Ho, T.-Y., 2014. Trace metal determination in natural waters by automated solid phase extraction system and ICP-MS: The influence of low level Mg and Ca. *Talanta* 128, 337–344. <https://doi.org/10.1016/j.talanta.2014.04.077>
- Wang, N., Wang, A., Kong, L., He, M., 2018. Calculation and application of Sb toxicity coefficient for potential ecological risk assessment. *Science of The Total Environment* 610–611, 167–174. <https://doi.org/10.1016/j.scitotenv.2017.07.268>
- Wang, W., 1987. Factors affecting metal toxicity to (and accumulation by) aquatic organisms — Overview. *Environment International* 13, 437–457. [https://doi.org/10.1016/0160-4120\(87\)90006-7](https://doi.org/10.1016/0160-4120(87)90006-7)
- Wang, W.-C., Mao, H., Ma, D.-D., Yang, W.-X., 2014. Characteristics, functions, and applications of metallothionein in aquatic vertebrates. *Frontiers in Marine Science* 1. <https://doi.org/10.3389/fmars.2014.00034>
- Warnken, K.W., Gill, G.A., Wen, L.-S., Griffin, L.L., Santschi, P.H., 1999. Trace metal analysis of natural waters by ICP-MS with on-line preconcentration and ultrasonic nebulization. *Journal of Analytical Atomic Spectrometry* 14, 247–252. <https://doi.org/10.1039/a806822d>
- Water Agency Artois-Picardie, 2017a. La surveillance des eaux littorales [WWW Document]. URL <http://www.eau-artois-picardie.fr/la-surveillance-des-eaux-littorales> (accessed 7.31.19).
- Water Agency Artois-Picardie, 2017b. The ecological and chemical status of the watershed and groundwater in the North of France [WWW Document]. Agence de l’Eau Artois-Picardie | l’avenir de l’eau. URL <http://www.eau-artois-picardie.fr/> (accessed 10.9.18).
- Watkinson, A., 2008. Antibiotics and Antibiotic Resistant Bacteria in the Aquatic Environment: A Global Issue, an Australian Perspective (Doctoral Thesis). University of Queensland.
- Wedding, L.M., Reiter, S.M., Verutes, G.M., Hartge, E., Guannel, G., Good, L.H., 2018. Values at the Land-Sea Interface: Mapping Ecosystem Services in the Coastal Environment. *Current: The Journal of Marine Education* 32, 25. <https://doi.org/10.5334/cjme.15>

- Wepener, V., Bervoets, L., Mubiana, V., Blust, R., 2008. Metal exposure and biological responses in resident and transplanted blue mussels (*Mytilus edulis*) from the Scheldt estuary. *Marine Pollution Bulletin*, 5th International Conference on Marine Pollution and Ecotoxicology 57, 624–631. <https://doi.org/10.1016/j.marpolbul.2008.03.030>
- Whalley, C., Rowlatt, S., Bennett, M., Lovell, D., 1999. Total Arsenic in Sediments from the Western North Sea and the Humber Estuary. *Marine Pollution Bulletin* 38, 394–400. [https://doi.org/10.1016/S0025-326X\(98\)00158-1](https://doi.org/10.1016/S0025-326X(98)00158-1)
- Wheatland, J.A.T., Bushby, A.J., Spencer, K.L., 2017. Quantifying the Structure and Composition of Flocculated Suspended Particulate Matter Using Focused Ion Beam Nanotomography. *Environmental Science & Technology* 51, 8917–8925. <https://doi.org/10.1021/acs.est.7b00770>
- Winogradow, A., Mackiewicz, A., Pempkowiak, J., 2019. Seasonal changes in particulate organic matter (POM) concentrations and properties measured from deep areas of the Baltic Sea. *Oceanologia* 61, 505–521. <https://doi.org/10.1016/j.oceano.2019.05.004>
- Wollast, R., 1988. The Scheldt Estuary, in: Salomons, W., Bayne, B.L., Duursma, E.K., Förstner, U. (Eds.), *Pollution of the North Sea: An Assessment*. Springer Berlin Heidelberg, Berlin, Heidelberg, pp. 183–193. [https://doi.org/10.1007/978-3-642-73709-1\\_11](https://doi.org/10.1007/978-3-642-73709-1_11)
- Xing, G., Sardar, M.R., Lin, B., Lin, J.-M., 2019. Analysis of trace metals in water samples using NOBIAS chelate resins by HPLC and ICP-MS. *Talanta* 204, 50–56. <https://doi.org/10.1016/j.talanta.2019.05.041>
- Xu, D., Gao, B., Chen, S., Peng, W., Zhang, M., Qu, X., Gao, L., Li, Y., 2019. Release risk assessment of trace metals in urban soils using in-situ DGT and DIFS model. *Science of The Total Environment* 694, 133624. <https://doi.org/10.1016/j.scitotenv.2019.133624>
- Yang, H., Lu, H., Ruffine, L., 2018. Geochemical characteristics of iron in sediments from the Sea of Marmara. *Deep Sea Research Part II: Topical Studies in Oceanography, Fluids and geochemical processes at the seismically active fault zone in the Sea of Marmara* 153, 121–130. <https://doi.org/10.1016/j.dsr2.2018.01.010>
- Yari, A., Dabrin, A., Coquery, M., 2018. *Recommandations pour l'estimation des tendances temporelles et des distributions spatiales des concentrations de contaminants dans les sédiments (No. Rapport AQUAREF 2017)*.
- Ye, S., Laws, E.A., Gambrell, R., 2013. Trace element remobilization following the resuspension of sediments under controlled redox conditions: City Park Lake, Baton Rouge, LA. *Applied Geochemistry* 28, 91–99. <https://doi.org/10.1016/j.apgeochem.2012.09.008>
- Yeats, P.A., Dalziel, J.A., 1987. ICES intercalibration for metals in suspended particulate matter. *ICES Journal of Marine Science* 43, 272–278. <https://doi.org/10.1093/icesjms/43.3.272>
- Yin, Y., Impellitteri, C.A., You, S.-J., Allen, H.E., 2002. The importance of organic matter distribution and extract soil:solution ratio on the desorption of heavy metals from soils. *Science of The Total Environment* 287, 107–119. [https://doi.org/10.1016/S0048-9697\(01\)01000-2](https://doi.org/10.1016/S0048-9697(01)01000-2)

- Ytreberg, E., Bighiu, M.A., Lundgren, L., Eklund, B., 2016. XRF measurements of tin, copper and zinc in antifouling paints coated on leisure boats. *Environmental Pollution* 213, 594–599. <https://doi.org/10.1016/j.envpol.2016.03.029>
- Zabiegała, B., Kot-Wasik, A., Urbanowicz, M., Namieśnik, J., 2010. Passive sampling as a tool for obtaining reliable analytical information in environmental quality monitoring. *Anal Bioanal Chem* 396, 273–296. <https://doi.org/10.1007/s00216-009-3244-4>
- Zhang, C., Ding, S., Xu, D., Tang, Y., Wong, M.H., 2014. Bioavailability assessment of phosphorus and metals in soils and sediments: a review of diffusive gradients in thin films (DGT). *Environ Monit Assess* 186, 7367–7378. <https://doi.org/10.1007/s10661-014-3933-0>
- Zhang, H., Davison, W., Mortimer, R.J.G., Krom, M.D., Hayes, P.J., Davies, I.M., 2002. Localised remobilization of metals in a marine sediment. *Sci. Total Environ.* 296, 175–187.
- Zhang, Hao., Davison, William., 1995. Performance Characteristics of Diffusion Gradients in Thin Films for the in Situ Measurement of Trace Metals in Aqueous Solution. *Anal. Chem.* 67, 3391–3400. <https://doi.org/10.1021/ac00115a005>
- Zhu, X., Cui, Y., Chang, X., Wang, H., 2016. Selective solid-phase extraction and analysis of trace-level Cr(III), Fe(III), Pb(II), and Mn(II) Ions in wastewater using diethylenetriamine-functionalized carbon nanotubes dispersed in graphene oxide colloids. *Talanta* 146, 358–363. <https://doi.org/10.1016/j.talanta.2015.08.073>
- Zhu, Y., Jin, X., Tang, W., Meng, X., Shan, B., 2019. Comprehensive analysis of nitrogen distributions and ammonia nitrogen release fluxes in the sediments of Baiyangdian Lake, China. *Journal of Environmental Sciences* 76, 319–328. <https://doi.org/10.1016/j.jes.2018.05.024>
- Zitoun, R., 2019. Copper speciation in different marine ecosystems around New Zealand (Thesis). University of Otago.
- Zondervan, I., 2007. The effects of light, macronutrients, trace metals and CO<sub>2</sub> on the production of calcium carbonate and organic carbon in coccolithophores—A review. *Deep Sea Research Part II: Topical Studies in Oceanography, The Role of Marine Organic Carbon and Calcite Fluxes in Driving Global Climate Change, Past and Future* 54, 521–537. <https://doi.org/10.1016/j.dsr2.2006.12.004>
- Zwolsman, J.J.G., Van Eck, G.T.M., 1993. Dissolved and particulate trace metal geochemistry in the Scheldt Estuary, S. W. Netherlands (water column and sediments). *Netherlands Journal of Aquatic Ecology* 27, 287–300. <https://doi.org/10.1007/BF02334792>
- Zwolsman, J.J.G., van Eck, G.T.M., Burger, G., 1996. Spatial and Temporal Distribution of Trace Metals in Sediments from the Scheldt Estuary, South-west Netherlands. *Estuarine, Coastal and Shelf Science* 43, 55–79. <https://doi.org/10.1006/ecss.1996.0057>

# Curriculum Vitae

**Name** Camille Gaulier  
**Date of birth** 8<sup>th</sup> of May 1992  
**Nationality** French  
**E-mail** camille.gaulier@vub.be  
**ORCID** 0000-0003-2118-2061

## EDUCATION

---

**PhD** “Trace metals in coastal waters: emphasis on their dynamic, speciation and bioavailability under various environmental conditions” 2017 - present  
*Joint-PhD between the Vrije Universiteit Brussel (Belgium) & the Lille University (France)*  
Under the supervision of Pr. Dr. Yue Gao and Pr. Dr. Gabriel Billon

**Engineer** Agriculture, Food Sciences, Environment 2012 - 2016  
*Engineer School ISARA - Lyon (France)*  
Specialization in Agriculture, Environment and Natural Resources Management

**Erasmus+** Forestry, Natural Resources and Wildlife Management program 2015  
*Høgskolen i Hedmark (Norway)*  
Nordic ecosystems, wildlife ecology and management, ecology and management of freshwater fisheries

## PROFESSIONAL EXPERIENCE

---

**PhD Student in Environmental Chemistry, Marine Sciences** 2017 - 2020  
*Vrije Universiteit Brussel (Belgium) & Lille University (France)*  
“Trace metals in coastal waters: emphasis on their dynamic, speciation and bioavailability under various environmental conditions”

**Environmental Intern** 2016  
*Département du Nord & Lille University (France)*  
“Leaching of two northern France slag heaps: influence on the surrounding”

aquatic environment”

**Monitoring leader in a sea turtle protection NGO** 2014

*Archelon (Greece)*

Volunteer for a sea turtle conservation and habitat restoration program

**Intern in a farm** 2013

*Monts du Lyonnais (France)*

Farm management (fruit and vegetable growing and livestock farming)

**Several student jobs** 2012 - 2015

Saleswoman in a pastry and chocolate factory, cashier in a supermarket, order-picker, general assistant in a fast-food restaurant

## RESEARCH OUTPUTS

---

### PUBLICATION (published)

---

**Leaching of two Northern France slag heaps: influence on the surrounding aquatic environment** 2020

Gaulier C., Billon G., Lesven L., Falantin C., Superville P-J., Baeyens W., & Gao Y.

In: *Environmental Pollution*. 257, 113601. doi: 10.1016/j.envpol.2019.113601

**Trace metal speciation in North Sea coastal waters** 2019

Gaulier C., Zhou C., Guo W., Bratkič A., Superville P-J., Billon G., Baeyens W., Gao Y.

In: *Science of the Total Environment*. 692, 701-712. doi: 10.1016/j.scitotenv.2019.07.314

**Labile trace metal concentration measurements in marine environments: From coastal to open ocean areas** 2019

Gao Y., Zhou C., Gaulier C., Bratkič A., Galceran J., Puy J., Zhang H., Leermakers M., Baeyens W.

In: *Trends in Analytical Chemistry*. 116, 92-101. doi: 10.1016/j.trac.2019.04.027

### PUBLICATION (submitted)



---

**Advances in understanding mobilization processes of trace metals in marine sediments** 2020  
 Zhou, C., Gaulier C., Luo, M., Zhang X., Bratkič A. Baeyens W., Davison W., Gao Y.  
 In: *Environmental Science & Technology*.

**PARTICIPATION TO CONFERENCES**

---

**ORGANIZATION OF CONFERENCES**

---

**PhD Student Day 2019 (Local Organizing Committee)** 2019  
 Lille, France

**YES SETAC 2019 (Local Organizing Committee)** 2019  
 Ghent, Belgium

**PRESENTATION AT CONFERENCES (oral)**

---

**The geochemical behavior of trace metals in the Eastern Gotland Basin: a speciation study from oxic and anoxic waters** 2019  
 DGT Conference, Vienna, Austria

**The geochemical behavior of trace metals along the Belgian Coasts: What can we learn from the use of diffusive gradient in thin-films?** 2018  
 Goldschmidt, Boston, USA

**The leaching of two northern France slag heaps: diagnosis of the surrounding aquatic environment and impact assessment** 2018  
 JNOEJC, Lille, France

**Insight into trace metal behaviors in a macro-tidal environment** 2018  
 VLIZ Marine Science Day, Bredene, Belgium

**The geochemical behavior of trace metals in the Belgian Coastal Zone: insight into the suspended particulate matter in a macro-tidal environment** 2018  
 ChemCYS, Blankenberge, Belgium

## **PRESENTATION AT CONFERENCES (poster)**

---

- Trace metal speciation in anoxic waters: stunning diving in the depths of the Baltic Sea** 2020  
ChemCYS, Blankenberge, Belgium
- Insight into trace metal behaviors in a macro-tidal environment** 2018  
JNOEJC, Lille, France
- The geochemical behavior of trace metals in the water column of the Belgian Coastal Zone** 2017  
Goldschmidt, Paris, France
- Study of the biogeochemical behavior of pollutants in the Belgian coastal environment** 2017  
VLIZ Marine Science Day, Bruges, Belgium

## **DOCTORAL TRAINING AND ACTIVITIES**

---

### **DOMAIN-SPECIFIC SKILLS**

---

- Fieldwork onboard of the RV Belgica and Zeetijger** 2017 - 2020  
In the Southern North Sea, along the Scheldt Estuary, in the Baltic Sea
- Biotalent e-learning course** 2019  
“Biodiversity in a changing climate”  
40 learning hours, 4 ECVET (European Credit system for Vocational Education and Training)
- Introduction to R: an open-source statistical toolbox** 2018  
DS NSE, Vrije Universiteit Brussel

### **TRANSFERABLE SKILLS**

---

- Presenting with impact** 2019  
DS NSE, Vrije Universiteit Brussel
- The development of a digital identity and the use of virtual social networks** 2019  
ED SMRE, University of Lille
- How to improve your chances of being published?** 2018

ED SMRE, University of Lille

**Strategies for job hunting** 2018  
ED SMRE, University of Lille

**How to apply for a job abroad (CV and cover letter)?** 2018  
ED SMRE, University of Lille

**Publishing your Article in a Scientific Journal** 2017  
DS NSE, Vrije Universiteit Brussel

### EDUCATIONAL SUPPORT

---

**Supervision of Master thesis** 2019  
Tianhui Ma  
*"Biogeochemical behavior of trace metals and organic nutrients in Belgian coastal areas"*

**Supervision of Bachelor thesis** 2019  
Kevin Vanbrusselen  
*"Bioavailability of trace metals from the Scheldt Estuary to the Belgian coasts"*

**Supervision of Bachelor students** 2017 - 2018  
Bachelor Projectwerk (5 weeks)

### AWARD AND GRANTS

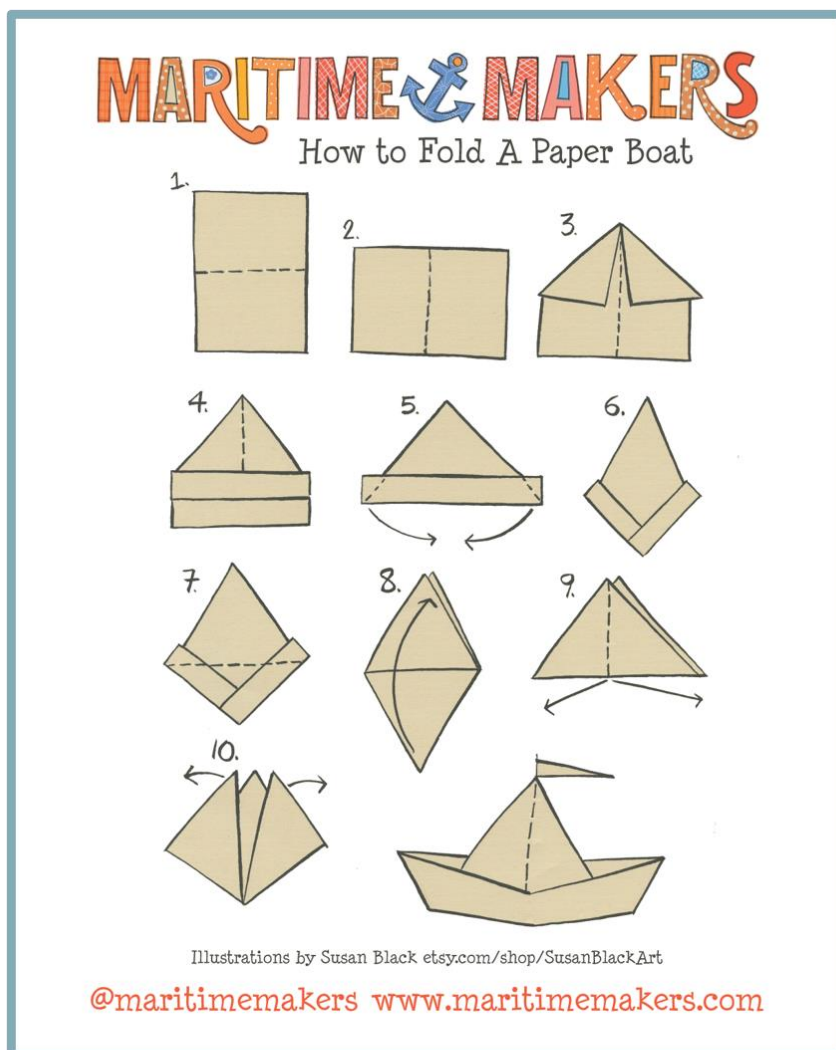
---

**EAG Student Sponsorship** 2020  
Travel grant, European Association of Geochemistry

**Award for best oral presentation** 2018  
Société Chimique de France  
JNOEJC, Lille, France  
*"The leaching of two northern France slag heaps: diagnosis of the surrounding aquatic environment and impact assessment"*

PhD defenses can be long and very boring (be brave!)... in case of deadly boredom, you have 1h30 minutes (at least) to learn how to make a perfect replica of the R.V. Belgica, aka. the very famous Belgian research vessel!

Enjoy,



P.S. 1: I have left the next page empty on purpose, for you to practice your new paper-folding skills.

P.S. 2: you're very welcome!

